THE METAL COMPLEX CATALYSED HYDROLYSIS

OF

ORGANOPHOSPHORUS ESTERS

A Thesis

submitted for the degree of

DOCTOR OF PHILOSOPHY

in the Faculty of Science of the

University of St. Andrews

by

Norman Govan B.Sc., M.Sc.

United College of St. Salvator

and St. Leonards College

May 1991

To

Mum, Dad and Gail

in gratitude and with love.

DECLARATION

I, Norman Govan, hereby certify that this thesis has been composed by myself, that it is a record of my own work, and that it has not been accepted in partial or complete fulfilment of any other degree or professional qualification.

I was admitted to the Faculty of Science of the University of St. Andrews under Ordinance No. 12 in October, 1988.

Signed May 1991

CERTIFICATION

I hereby certify that the candidate has fulfilled the conditions of the Resolution and Regulations appropriate to the degree of Ph.D.

Signed May 1991

COPYRIGHT

ACKNOWLEDGEMENTS

I wish to thank Professor R.W. Hay for introducing me to the many facets of coordination chemistry and his supervision and encouragement throughout this and other studies. I also sincerely thank, Dr. P.R. Norman for his supervision and assistance during the course of this work.

I thank the Chemistry Departments of St. Andrews University, Stirling University and C.D.E. (Porton Down) for providing research facilities, and the M.O.D. for providing financial support.

I warmly thank the technical staff (unsung heroes, past and present) in the Chemistry Departments of Stirling University and St. Andrews University for their diligent service. Many thanks go to my fellow researchers for their friendship, happy memories and "a wee drap moral support". I thank also Dr. A.D. Lloyd and Dr. W. Bell for further "moral support" and their assistance in the presentation of this manuscript.

Finally, and most importantly, I wish to thank my parents, brothers and sisters for their backing and encouragement throughout my academic career, and Gail for her loyal support and hard work in the typing of this thesis.

CONTENTS

ABBREVIATIONS

The following abbreviations are used for convenient nomenclature of the various ligands.

[9]aneN$_3$	1,4,7-triaza-cyclononane
[15]aneN$_5$	1,4,7,10,13-pentaaza-cyclopentadecane
bipy	2,2'-bipyridyl
cyclen	1,4,7,10-tetra-azacyclodecane
dpa	2,2'-dipyridylamine
glygly	glycylglycine
imid	imidazole
tmen	N,N,N',N'-tetramethylethylenediamine
trimen	N,N,N'-trimethylethylenediamine
tmten	N,N,N'-trimethyl-N'-tetradecylethylenediamine
tren	2,2',2"-triaminoethylamine
trpn	3,3',3"-triaminopropylamine

ABSTRACT

The hydrolysis of the phosphate triesters 4-nitrophenyldiethyl phosphate (PNPDEP), 2,4-dinitrophenyldiethyl phosphate (DNPDEP) and the phosphonate ester 2,4-dinitrophenylethyl methylphosphonate (DNPEMP), have been examined by both stop-flow spectrophotometeric and pH-stat techniques and their water and base hydrolysis rates reported. These reactions have also been studied in the presence of various nucleophiles including simple non-labile mono-aqua metal complexes. Comparison of reaction rates for the metal complexes with sterically hindered organic nucleophiles indicates that such metal complexes function predominately as general base catalysts. Bronsted B values of 0.39 and 0.52 have been determined for DNPDEP and DNPEMP respectively with a variety of bases.

A number of copper(II) complexes have been prepared and investigated as potential catalysts for the hydrolysis of DNPDEP. The complexes have the general structure $Cu(L)(OH_2)_2$ in solution where L is a bidentate, bi-monodentate or tridentate ligand. The activities of the complexes as catalysts of DNPDEP hydrolysis in neutral water varied in the order : $Cu(dpa)(OH)_2$ > $Cu(tmen)(OH_2)_2$ > $Cu(trimen)(OH_2)$ > $Cu(imid)_2(OH_2)_2$ > $Cu([9]aneN_3)(OH_2)_2$

> $Cu(bipy)(OH_2)_2$ > $Cu(glygly)(OH_2)$. At pH 7 with a catalyst concentration of 2.5×10^{-3} mol dm^{-3} a rate enhancement of ca. 10^4 fold is observed for the copper(II)-tmen system. The pH dependence of the catalysis is consistent with the hydroxoaqua complex being the active species in solution. This view is supported by speciation calculations which show a correlation between the rate of hydrolysis and the concentration of the monohydroxo chelate $[Cu(L)(OH)(OH_2)]^+$. The greater kinetic effectiveness of this weak base, compared with hydroxide ion on a molar basis indicates a bifunctional mechanism in which bound hydroxide acts as a nucleophile, in conjunction with electrophilic catalysis by copper at the phosphoryl oxygen. The reactions are truly catalytic and exhibit turnover.

The efficiencies of three cis-aquohydroxotetraazacobalt(III) complexes $[Co(cyclen)(OH)(OH_2)]^{2+}$, $[Co(tren)(OH)(OH_2)]^{2+}$ and $[Co(trpn)(OH)(OH_2)]^{2+}$ in prompting the hydrolysis of DNPDEP and DNPEMP have been compared. The marked dependence of the activity of the cobalt(III) complex on the structure of the "spectator" tetraamine ligand is discussed.

A metallomicelle based on the long chain copper(II) complex of N,N,N'-trimethyl-N'-tetradecylethylenediamine is shown to be an excellent catalyst for the hydrolysis of neutral phosphorus esters. At pH 8 using a metallomicelle concentration of 1.75×10^{-4} M 10^4 fold hydrolysis rates are observed.

A lanthanum macrocycle is shown to be an effective catalyst in the hydrolysis of the phosphate triester DNPDEP and the reaction also displays turnover.

CHAPTER ONE

GENERAL INTRODUCTION

1.1 INTRODUCTION

Phosphoryl and nucleotidyl transfer enzymes are extremely important and wide spread in biology. They have in common the catalysis of nucleophilic reactions of phosphorus esters, and the general requirement for divalent metal ions, particularly Mg^{2+}, for activity. This requirement has stimulated considerable interest in the catalytic roles of metal ions in phosphate ester hydrolysis chemistry[1-4]. However, the importance of this class of compounds extends beyond natural biological systems to man made chemicals that are employed as insecticides for pest control and as toxic compounds used in chemical weapons.

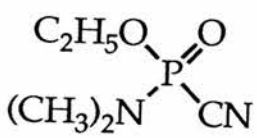

GA (Tabun)

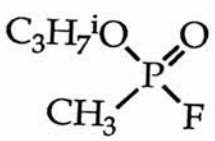

GB (Sarin)

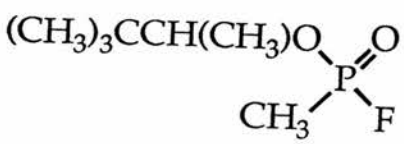

GB (Soman)

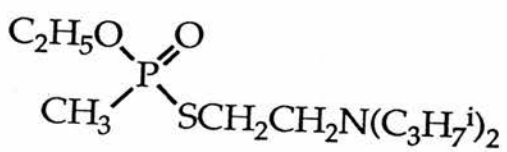

VX

The development of chemical weapons is a complex and emotive subject. The range of chemical agents is vast and

produce a variety of physiological effects depending on their chemical nature[5]. By far the most lethal class of compounds is the nerve poisoning compounds (the G- and V-agents, shown below) which are all organic esters of substitutued phosphoric acid.

While these toxic chemical agents remain, personnel must be adequately protected from the hazard. In practice this means protective suits and respirators[6]. The main method of detoxification of these compounds from an antidotal and defence view point is by hydrolysis[7]. The hydrolysis of phosphonate esters is, however, slow at neutral pH but increases substantially when the solution is made progressively more alkaline. Hence, the main practical decontamination procedures involve the use of concentrated alkali. Although this method is very effective, reagents of this type are too aggressive to be used for treating contaminated personnel and sensitive materials such as aluminium airframes and plastics.

In the search for milder decontaminants capable of more general applications attention is being given to the use of metal ion ligand complexes as catalysts for the destruction of chemical agents. A number of metal complexes have been shown to offer usable reactivity, for example; copper and more interestingly zinc complexes[8]; the environmental applicability of the latter element makes it particularly suitable for use in large scale decontamination. A novel

zinc complex [1.1] of the macrocyclic ligand 1,4,7,10-tetra-

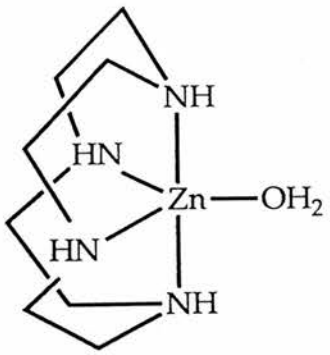

$[Zn(cyclen)(OH_2)]^{2+}$

[1.1]

azacyclodecane which contains a co-ordinated water molecule has been shown to function as a general base catalyst for the hydrolysis of simulant agent with a significant rate enhancement. In this complex, the ligand functions by binding to the metal and increasing the polarisation of the water molecule bonded directly to the metal enabling it to function as a catalyst near neutral pH. Clearly, metal-ligand catalytic systems are a viable alternative to the highly corrosive methods currently employed for decontamination, since they act by creating a high concentration of bound hydroxide around neutral pH.

Despite the numerous publications that demonstrate the ability of metal ions and metal complexes to promote hydrolysis reactions at neutral tetrahedral phosphorus(V) centres, the mechanism(s) by which these reactions proceed is not fully understood. In view of the potential that

metal complexes posses to catalytically degrade such toxic materials, the work described herein was undertaken to elucidate the interactions of metal ions and phosphorus esters. The development of more effective metal complex catalysed systems was approached by means of three general criteria.

(a) Choice of suitable metal.

(b) Choice of suitable ligand.

(c) Choice of side group substituents on the ligands chosen.

1.2 REFERENCES

1. T.C. Bruice and S.J. Benkovic, 'Bioorganic Mechanisms', Benjamin, New York, 1966, vol. 2, chaps. 5, 6 and 7.
2. J.R. Cox and O.B. Ramsay, Chem.Rev., 64, 317, (1964).
3. C.A. Bunton, J.Chem.Educ., 45, 21, (1964).
4. R.W. Hay, Comp.Coord.Chem., 6, 443, (1987).
5. R.M. Black and D.G. Upshall, Chem.Britian, 24, 659, (1988).
6. R.J. Powel, Chem.Britian, 24, 665, (1988).
7. B.C. Barrass, Chem.Britian, 24, 667, (1988).
8. P.R. Norman, A. Tate and P. Rich, Inorg.Chim.Acta., 150, 227, (1988).
9. See references (1-7) in Chapter 3.

CHAPTER TWO

SIMULANT PHOSPHORUS ESTERS AND THEIR RATES OF BASE HYDROLYSIS

2.1 INTRODUCTION

In view of the experimental hazards and difficulties of working with C.W. agents themselves these studies have been carried out using agent simulants incorporating the 4-nitro and 2,4-dinitrophenate anions. The substrate esters employed were the phosphate esters 4-nitrophenyl diethylphosphate (PNPDEP) [2.1], 2,4-dinitrophenyl diethylphosphate (DNPDEP) [2.2] and the phosphonate ester 2,4-dinitrophenylethyl methylphosphonate DNPEMP [2.3].

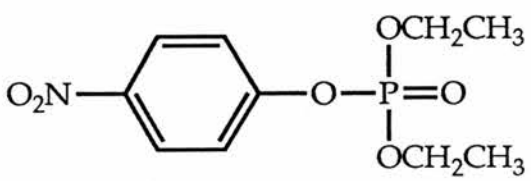

[2.1]

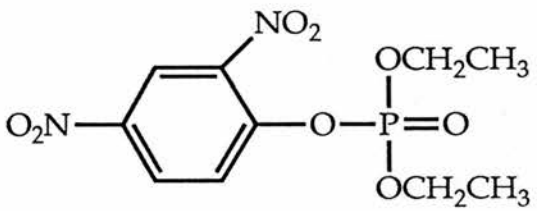

[2.2]

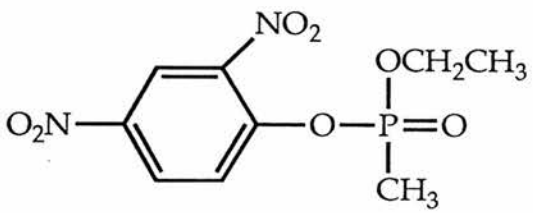

[2.3]

These esters are water soluble and have the added advantage that their hydrolysis reactions can be readily monitored spectrophotomerically.

Prior to any catalytic studies a knowledge of the base hydrolysis rates and appropriate activation parameters of the substrate esters is required. In this section the synthesis and characterisation of the substrate esters together with their rates of base hydrolysis are reported.

2.2 SYNTHESIS OF SUBSTRATE ESTERS

CAUTION: THE PHOSPHORUS ESTERS DESCRIBED EXHIBIT POTENT ANTICHOLINESTERASE ACTIVITY. GREAT CARE SHOULD BE EXERCISED IN THERE HANDLING AND USE.

2.2.1 4-nitrophenyl diethylphosphate, (PNPDEP)

Pure PNPDEP was commercially available from Aldrich as "Paraoxon".

2.2.2 4-nitrophenyl diphenylphosphate, (PNPDPP)

The compound was prepared by a modification of the method of Gulick[1]. A white crystalline product was obtained with melting point 49-50°C (lit 49-51°C). Anal. Calcd. for $C_{18}H_{14}NO_6P$: C, 58.23; H, 3.80; N, 3.77. Found: C, 57.72; H, 3.86; N, 3.75%

2.2.3 2,4-dinitrophenyl diethylphosphate,(DNPDEP)

Diethylchlorophosphate (63.0g, 0.366 mol) was added dropwise to a stirred suspension of dry sodium 2,4-dinitrophenoxide (75.4g, 0.366 mol) in 450 ml of dry toluene. On completion of the addition, the mixutre was

refluxed for five hours, cooled, washed with ice water (150 ml), cold 5% sodium carbonate (150 ml) and ice water (150 ml). The toluene layer was dried over $MgSO_4$ and concentrated in a vacuo to give crude DNPDEP in 60% yield. The crude product was kept in the deep freeze and aliquots purified immediately prior to use as described below.

Anal. Calcd. for $C_{10}H_{13}N_2O_8P$: C, 37.51; H, 4.09; N, 7.74. Found: C, 36.88; H, 4.06; N, 8.23%. ^{13}C NMR; ($CDCl_3$,TMS): 16.3; 65.8; 121.6(CH); 123.6(CH); 129.1(CH); 140.7(C-X); 143.8(C-X); 148.4(C-X). IR; 1540 (NO_2); 1350 (P=O); 1032 (P-O-alkyl); 1270 (P-O-aryl) cm^{-1}.

2.2.4 **2,4-dinitrophenylethyl methylphosphonate, (DNPEMP)**

Ethyl methylphosphonchloridate (28.8g, 0.2 mol) was added dropwise to a stirred suspension of sodium 2,4-dinitrophenate (41.2g, 0.2 mol) in dry toluene (200 ml). On completion of the addition the mixture was refluxed for four hours, cooled, filtered and concentrated in vacuo to give crude DNPEMP in 70% yield. Purification immediately before use was carried out as described below.

Anal. Calcd. for $C_9H_{11}N_2O_7P$: C, 37.25; H, 3.82; N, 9.65. Found: C, 34.67; H, 408; N, 8.21%. ^{13}C NMR; ($CDCl_3$,TMS) : 7.2(CH_3); 16.2(CH_3); 63.0(CH_2); 121.5(CH); 124.5(CH); 128.1(CH); 141.3(C-X); 143.6(C-X); 148.7(C-X);

IR; 1540(NO_2); 1250 (P=O); 1040 (P-O-alkyl); 1250(P-O-arlyl) cm^{-1}. Purity was checked by HPLC. Measurements were preformed on a Hypersil ODS column (Michrom) at 30°C. Products were monitored spectrophotomerically at 270 nm or over the wavelength range 190-370 nm using an LKB 2140 Rapid Spectral Detector. The mobile phase was 50mM H_3PO_4/CH_3CN(3:2 v/v). HPLC gave a purity of >98% for the phosphonate ester.

2.2.5 **Purification of Phosphorus esters prior to use:**

Immediately prior to use 1.0g of ester was dissolved in 20 ml of ice cold chloroform, and the solution shaken in a separating funnel with 25 ml of ice cold 5% $NaHCO_3$, 25 ml of ice cold water, 25 ml of ice cold 0.1M HCl and 2 x 25 ml aliquots of ice cold water. The organic layer was kept over Na_2SO_4 for several hours and finally the solvent was removed at 40°C under vacuum. The phosphate residue was then used for kinetic experiments.

2.3 MATERIALS AND METHODS

All reagents used were the purest availabale with non-commercial compounds being synthesised and purified as described. Standard sodium hydroxide solutions were made from BDH "Convol" ampoules adjusted to the desired concentration and standardised against potassium hydrogen phthalate immediately before use.

^{13}C NMR spectra were run on a Jeol FX 60 FT instrument. Samples were dissolved in $CDC1_3$ and chemical shifts measured versus TMS. IR spectra were run on a Perkin Elmer 1750 FT IR spectrophotometer. Interval scan spectra were determined with a Perkin Elmer Lambda 5 uv/vis spectrophotometer. Microanalysis were carried out on a Carlo-Erba CHN analyser. HPLC measurements were performed on a Hypersil ODS column (Michrom) at $30^{o}C$. Products were monitored spectrophotometerically at 270 nm and the mobile phase was 50mM H_3PO_4/CH_3CN (3:2 v/v).

Difficulty was experienced in obtaining precise microanalytical data for the phosphorus esters studied. In these cases other means were utilised to assay structure and purity. In all cases IR and NMR data are consistent with the structures given, while purity was assessed as follows. For 2,4-DNPEMP purity was assayed by HPLC (>97%) and by complete hydrolysis, based on $E_{400nm} = 1.130 \times 10^4$ this gave

a purity of better than 98%.

pH was measured by a Radiometer PHM64 meter fitted with a Croning micro combination electrode and standardised with appropriate NBS buffers.

Experiments described in this section employ stock solutions of PNPDEP at 5×10^{-3} mol dm^{-3} and those of DNPDEP and DNPEMP are both 2×10^{-2} mol dm^{-3} all being made up in dry acetonitrile.

2.4 KINETIC METHODS

The kinetics of the base hydrolysis of the substrate esters was followed spectrophotometrically by monitoring release of the appropriate phenoxide ion. The hydrolysis of 4-nitrophenyl ester was monitored at 400 nm and both the 2,4-dinitrophenyl esters at 360 nm except in the case of stopped flow measurements where for convenience, the visual absorption at 400 nm was used. A typical interval scan spectrum of the base hydrolysis of PNPDEP is shown in Figure 2.1 and that of DNPDEP is shown in Figure 2.2.

2.4.1 DETERMINATION OF RATE CONSTANTS FOR THE BASE HYDROLYSIS OF PNPDEP BY SPECTROPHOTOMETRY

Kinetic monitoring of the base hydrolysis of PNPDEP was carried out on a Gifford 2400S spectrophotometer interfaced to an Apple II computing system. The cell block was maintained at the desired temperature $\pm 0.1^{o}C$ by a circulating water thermostat. Reactions were initiated by syringing 50 µl (Hamilton microsyringe) into the spectrophotometer cell (total vol = 2.8 ml) containing the reaction medium (I = 0.1 M, KNO_3) previously equilibrated at the appropriate temperature. The solution was then rapidly stirred and the absorbance change monitoried at 400 nm. In every case the final concentration of the ester was

Figure 2.1 Interval scan absorption spectrum for PNPDEP in 0.1M NaOH at 25°C. Time interval 30s.

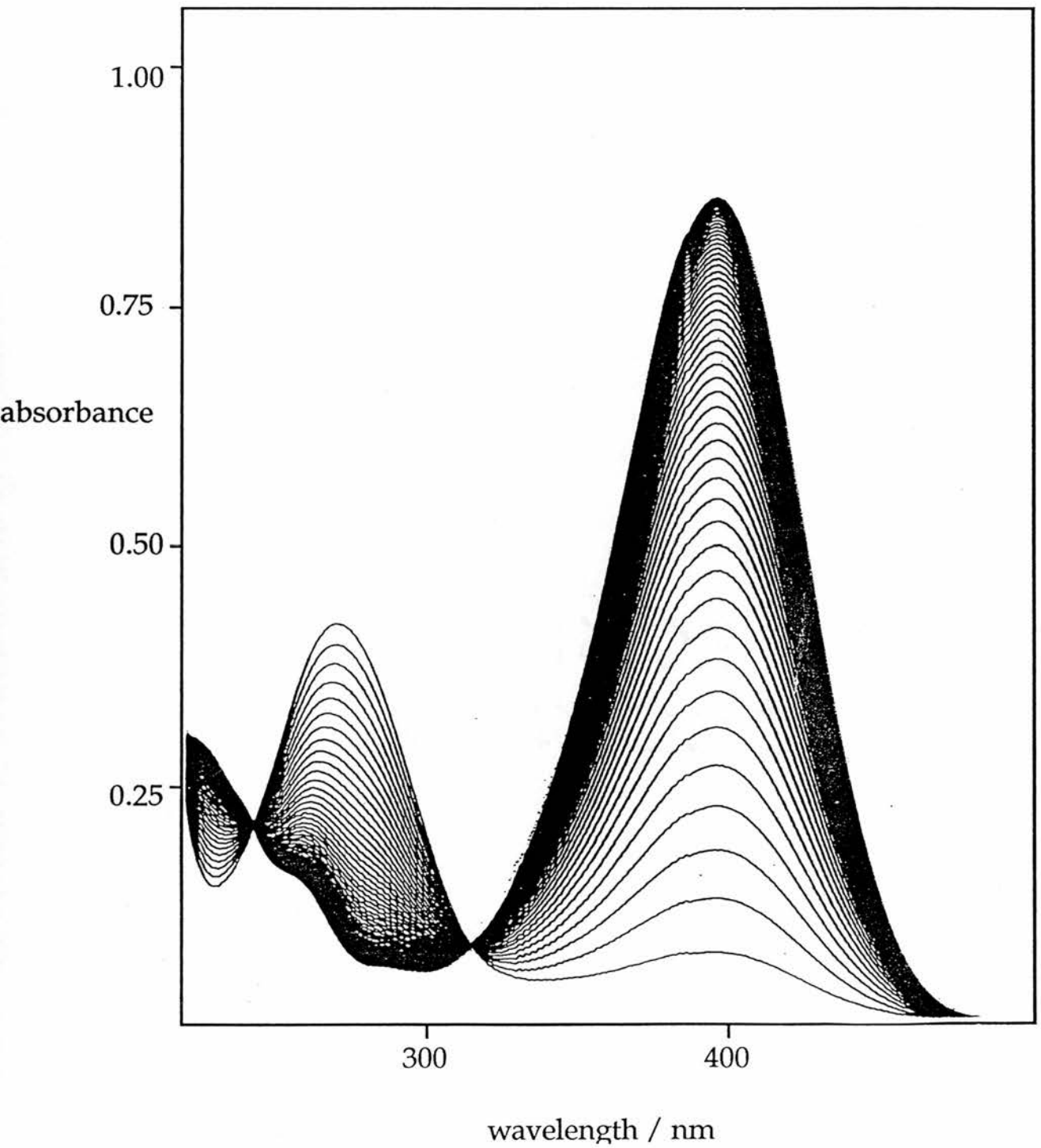

Figure 2.2 Interval scan absorption spectrum for DNPDEP in 0.01M NaOH at 25°C. Time interval 20s.

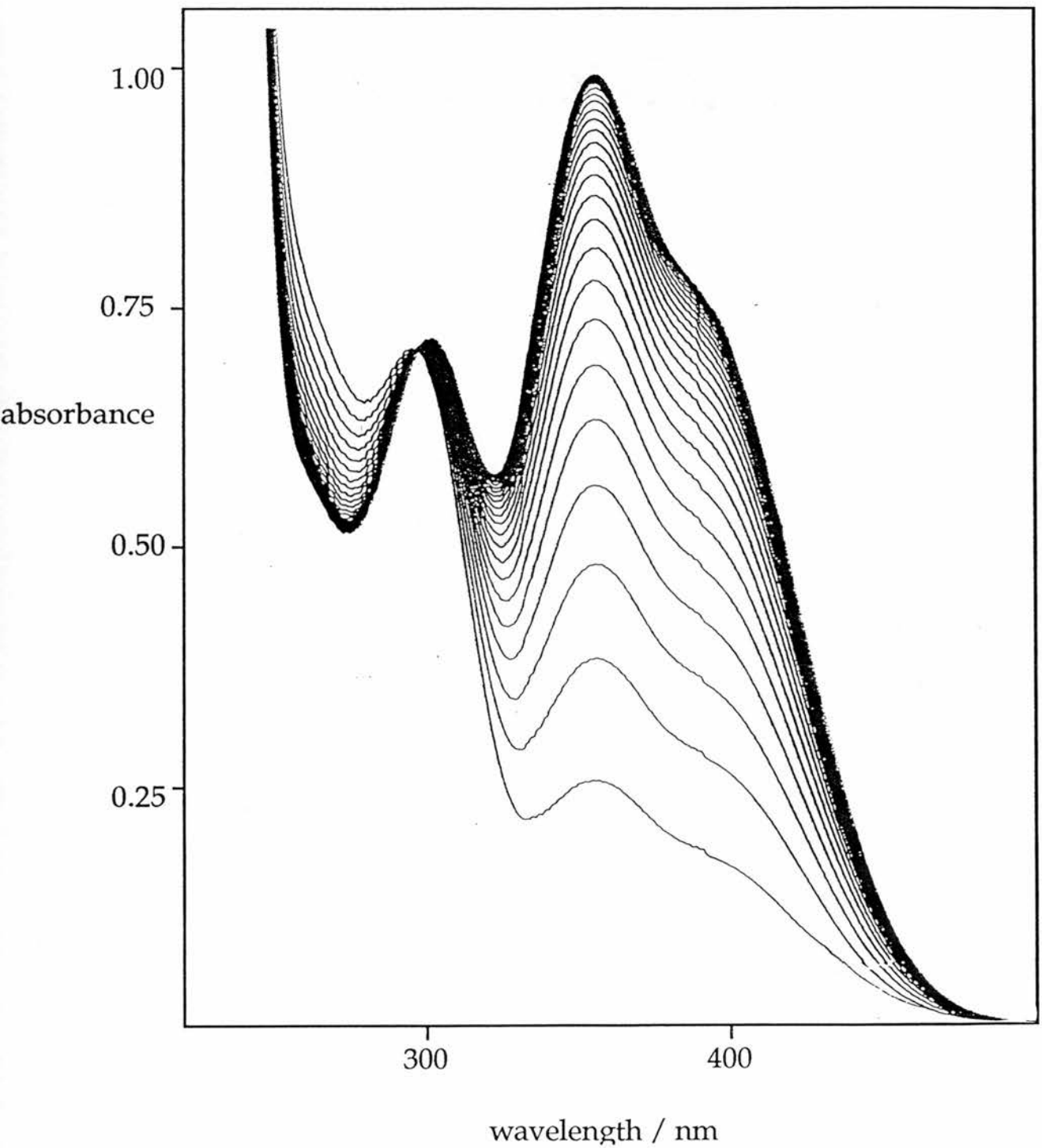

in the range 3 x 10^{-5} - 4 x 10^{-5} mol dm^{-3} Plots of ln (A_∞ - A_t) versus time were linear at least 4 half-lives. All experiments were run in triplicate and tabulated data represent the average of these experiments.

2.4.2 DETERMINATION FOR RATE CONSTANT BY pH-STAT TECHNIQUE (DNPDEP AND DNPEMP).

The apparatus used in these procedures is shown schematically in (Figure 2.3).

The reaction medium (15 cm^3) containing a known concentration of the nucleophile and sufficient KNO_3 to maintain the ionic strength at 0.1 mol dm^{-3} was added to the reaction vessel and maintained with constant stirring at the desired temperature by a circulating water thermostat. The pH of the solution was then adjusted and maintained throughout the reaction to a pH value sufficient to ensure complete dissociation of the nucleophile (for >95% dissociation, pH = pK + 1.4). The pH stat consisted of a Radiometer PHM64 pH meter attached to an Orion "Ross" type 8103 semimicro combination electrode containing KNO_3 (1.0 M) in its salt bridge. The PHM64 meter controlled a Radiometer ABU 13 autoburette (via a TTT60 controller) which delivered 0.1M NaOH to the reaction vessel from a 0.25 cm^3 capacity syringe. The mixture was then pumped by means of Gilson "Minipulse" peristaltic pumps via capillary teflon tubing through a 1 cm flow cell contained in an LKB 4050

Figure 2.3 Schematic diagram of pH-stat assembly.

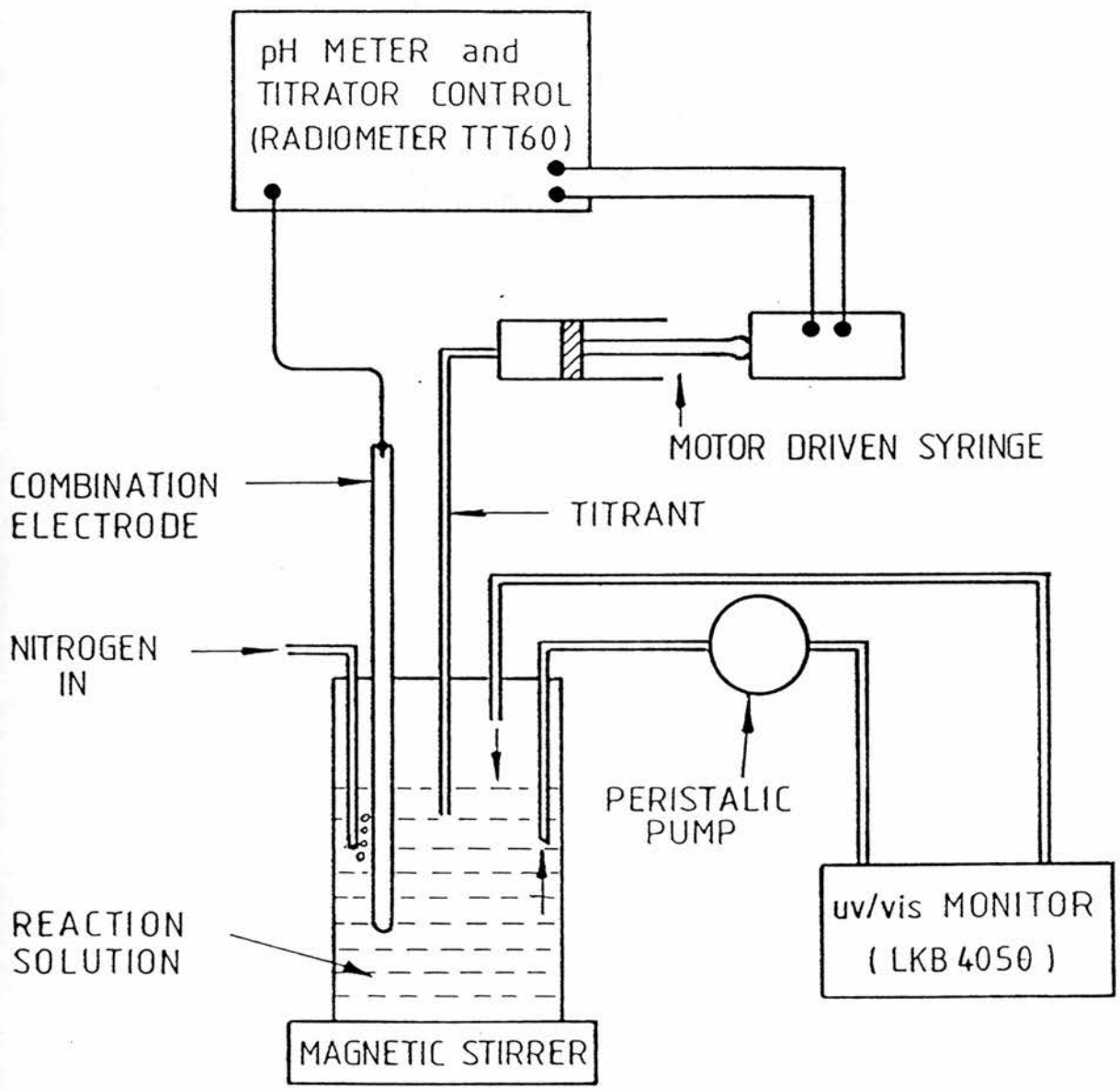

uv/visible spectrophotometer and the effluent was passed back into the reaction vessel. Runs were initiated by injecting 100 µl of the stock phosphorus ester solution to the reaction vessel. Rates were calculated from a linear regression analysis (unweighted) of plots of ln (A_{∞} - At) versus time. Plots were linear for at least 3 half-lives.

2.4.3 DETERMINATION OF RATE CONSTANTS BY STOP-FLOW SPECTROPHOTOMETRY (DNPDEP AND DNPEMP).

The stop-flow system is shown diagramatically in (Figure 2.4).

The system consists of a High-Tec Scientific Sample Handling Unit (SHU) fitted with a grating monochromator, tungsten-halogen light source and EMI 9798QB 11 stage end window photomultiplier to monitor absorbance changes. The output from the PM tube is fed into an Infotek AD 2000 Analog to Digital converter (high-speed) and then via a Hewlett-Packard 98622 GP10 16-BIT parallel interface into an HP-310 micro computer where curve fitting routines based on the algorithm Gampp[2] were used to calculate the desired rate constants. A total of 400 data points were collected during each run, irrespective of the time base used. Reaction was achieved by loading the sample syringes with (i) 0.02 -0.10 mol dm^3 solutions of the nucleophile under investigation dissolved in I=0.1 (KNO_3). (ii) 150 µl of the stock phosphorus ester in 10 ml of 0.1M KNO_3. The apparatus

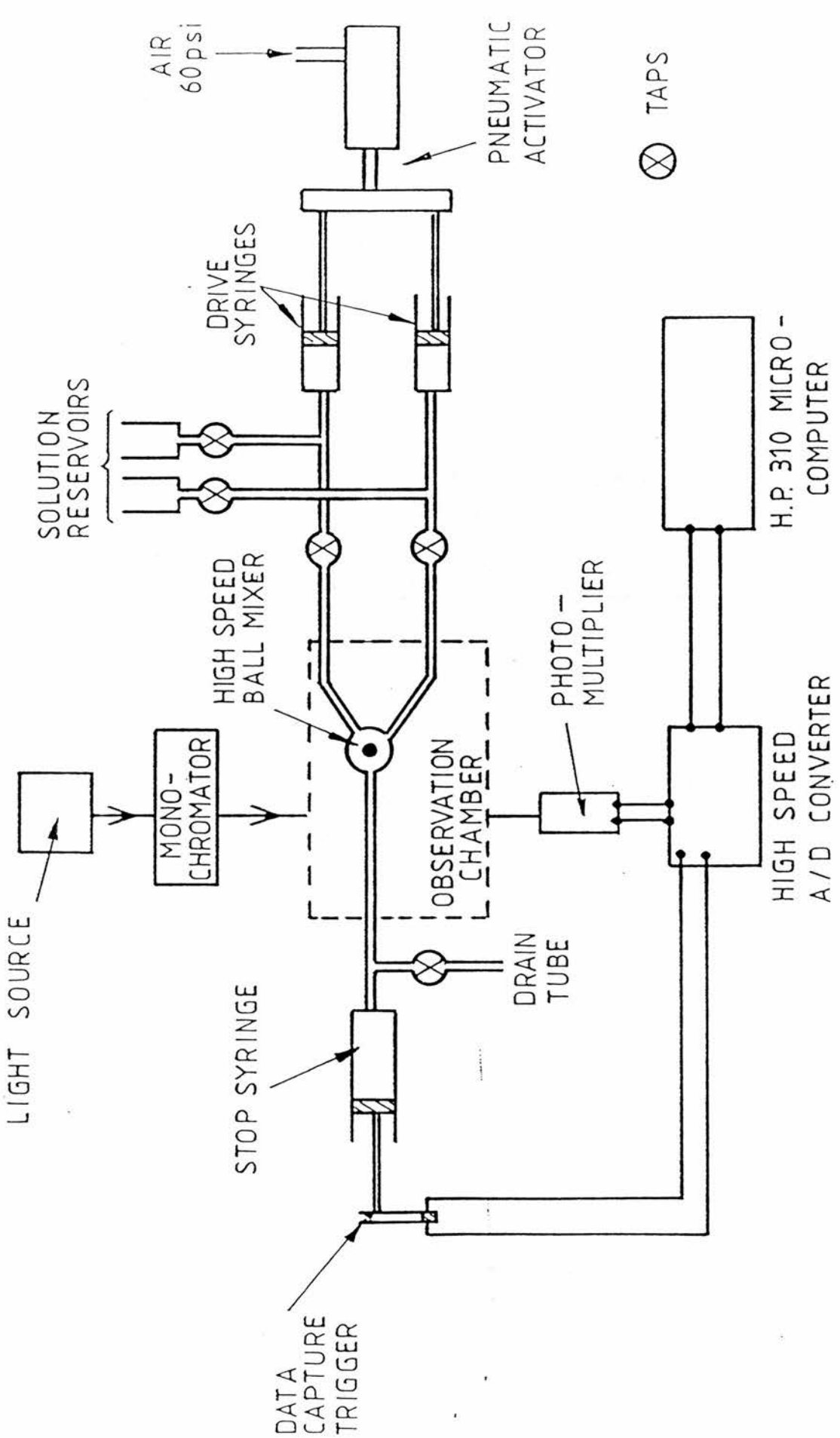

Figure 2.4 Schematic diagram of stopped-flow assembly.

was thermostated at the desired temperature (LKB 2219 II circulator) and reaction initiated by pneumatically injecting 100 µl of each reactant into the mixing observation chamber (Figure 2.4). The effluent from the chamber was used to operate a stopping syringe which in turn, activated the trigger for data collection. Typically, a pressure of 60 psi on the activating ram yielded a dead time of 2 milliseconds.

2.5 RESULTS

2.5.1 SIMULANT SELECTION

Preliminary investigations were carried out using the readily prepared simulant, 4-nitrophenyl diphenylphosphate [2.4].

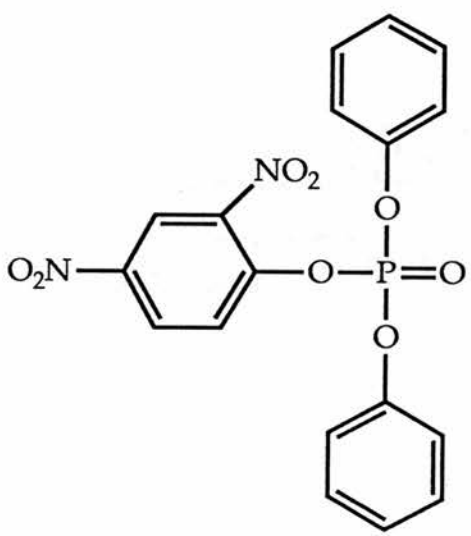

[2.4]

This substrate has been used by other workers[3] in hydrolysis studies but was found to be unsuitable for various reasons.

a) The compound was very insoluble in aqueous systems and required the use of mixed solvents. This is

to be avoided in such a fundamental study as it complicates the analysis of kinetic data.

b) Reaction times at neutral pH's were very slow (typically, $t_{0.5}$ at pH7 and 40°C is about 5 hours), making collection of large amounts of kinetic data tedious.

c) The similarity of the pK's of p-nitrophenol ($\sim$ 7.1) and phenol ($\sim$10) meant that appreciable hydrolysis of phenoxide occured concurrently with 4-nitrophenoxide, as determined by HPLC, which also complicated the interpretation of the kinetic data.

d) The liberated 4-nitrophenoxide ion was sufficiently highly coloured only above its pK of 7.1 and direct observation of reactions at lower pH was impracticable.

The use of the 2,4-dinitro simulants [2.2] and [2.3] overcame many of the problems. The ethyl substituents considerably enhanced water solubility and were much poorer leaving groups than phenol so that only one reaction course was observed. The 2,4-dinitrophenoxide leaving group has a much lower pK than 4-nitrophenoxide and reactions were directly observable at all pH's above 4.1. The low pK meant that reactions were also much more rapid than those with 4-nitrophenoxide as a leaving group, typically $t_{0.5}$ at 40°C and pH7 for 2,4-dinitrophenoxide esters was approximately 30 minutes.

The pK of 2,4-dinitrophenol (ca. 4.1) is similar to that of HF (ca. 3.5). Since rates of reaction of phosphate esters are dependent on the pK of the leaving group,[4] this makes 2,4-dinitrophenoxide a much better analogue for F^- than is 4-nitrophenoxide. Experimentally, 2,4-dinitrophenoxide was also found to have two significant absorption maxima at 360 and 400 nm, which enabled the monitoring wavelength to be changed when absorption by metal complex interfered.

2.5.2 WATER AND HYDROXIDE HYDROLYSIS RATES OF SIMULANT PHOSPHORUS ESTERS

Since hydrogen ion terms are negligible at the pH values used for the experiments, the kinetic course of the reactions can be described with sufficient accuracy by the following equation;

$$k_{obs} = k_{aq} + k_{OH}[OH^-] + k_{nuc}[Nuc^-] \qquad eq2.1$$

where,

k_{obs} = experimentally observed rate constant

k_{aq} = spontaneous first order reaction rate with water

k_{OH} = second order rate constant for the reaction with hydroxide ion

k_{nuc} = second order rate constant for the reaction with other nucleophiles present

PNPDEP hydrolysis rates

For the phosphorus ester PNPDEP the spontaneous aquation rate was insignificant and with no other nucleophile present and sodium hydroxide in large excess, the reaction is first order in ester

$$\text{Rate} = k_{obs}\,[\text{ester}]$$

TABLE 2.1 **Rate constants k_{OH} for the base hydrolysis of PNPDEP over the temperature range 25-40°C at I = 0.1 (KNO_3)**

TEMP /°C	$[OH^-]$ /mol dm^{-3}	$10^4 k_{obs}$ /s^{-1}	$10^2 k_{OH}$ /$M^{-1}s^{-1}$
25.0	0.0238	2.52	1.06
	0.0505	5.22	1.03
	0.772	8.15	1.06
	0.1024	10.85	1.06
30.0	0.0238	3.07	1.56
	0.0505	7.77	1.54
	0.0772	11.49	1.52
	0.1024	15.13	1.54
35.0	0.0238	5.08	2.13
	0.0505	10.80	2.13
	0.0772	16.17	2.09
	0.1024	21.81	2.13
40.0	0.0238	7.09	2.98
	0.0505	14.75	2.92
	0.0772	21.80	3.02
	0.1024	29.80	2.91

[PNPDEP] = 3.2 x 10^{-5}M. Reaction monitored at 400 nm.

TABLE 2.2 Activation Parameters for the base hydrolysis of PNPDEP at I = 0.1 (KNO_3)

TEMP /^oC ($\pm$0.1^oC)	$10^2 k_{OH}$ (obs) /s^{-1}	$10^2 k_{OH}$ (calc) /s^{-1}
25.0	1.05	1.06
30.0	1.54	1.51
35.0	2.12	2.13
40.0	2.96	2.97

Values of k_{OH} calculated on the basis of the activation parameters $\Delta H^{\neq}$ = 50.63 K J mol^{-1} and $\Delta S^{\neq}_{298}$ = - 112.9 JK^{-1} obtained from the experimental constants. The Eyring plot has a correlation coefficient of 0.9996.

Values of k_{obs} show a linear dependence upon the hydroxide ion concentration so that

$$\text{Rate} = k_{OH}\,[\text{ester}][OH^-]$$

and values of k_{OH} where obtained from the relationship.

$$k_{OH} = k_{obs}/[OH^-]$$

Measurements with the phosphorus ester PNPDEP were made at four temperatures 25, 30, 35 and 40°C, using sodium hydroxide solutions 0.0238 to 0.1024 mol dm^{-3}. The kinetic data obtained for the 4-nitrophenyl ester are summerised in Table 2.1, and the activation parameters are listed in Table 2.2.

DNPDEP and DNPEMP aquation and hydrolysis rates

When species other than H_2O and OH^- are excluded from the reaction medium, with the exception of KNO_3 which must be included to maintain ionic strength (KNO_3 itself does not contribute to the reaction), equation (2.1) simplifies to,

$$k_{obs} = k_{aq} + k_{OH}[OH^-]$$

Thus a plot of k_{obs} versus $[OH^-]$ is linear of slope k_{OH} and

TABLE 2.3 Hydrolysis of 2,4-DNPDEP at 30°C and I = 0.1 (KNO_3), monitored by pH-stat

pH	$10^6 x[OH^-]$ mol dm^{-3}	10^6 k_{obs} s^{-1}
8.00	1.91	2.51
8.25	3.39	3.12
8.75	10.73	5.64
9.00	19.07	9.66
9.30	38.06	17.58

TABLE 2.4 Hydrolysis of 2,4-DNPEMP at 30°C and I = 0.1 (KNO_3), monitored by pH-stat

pH	$10^6 x[OH^-]$ mol dm^{-3}	10^6 k_{obs} s^{-1}
8.00	1.91	1.83
8.25	3.39	2.28
8.50	6.98	3.05
8.75	10.73	3.95
9.00	19.07	6.16

Figure 2.5 Plot of first-order rate constants (k_{obs}) versus [OH^-] for the base hydrolysis of DNPDEP at 30°C by pH-stat, I=0.1(KNO_3).

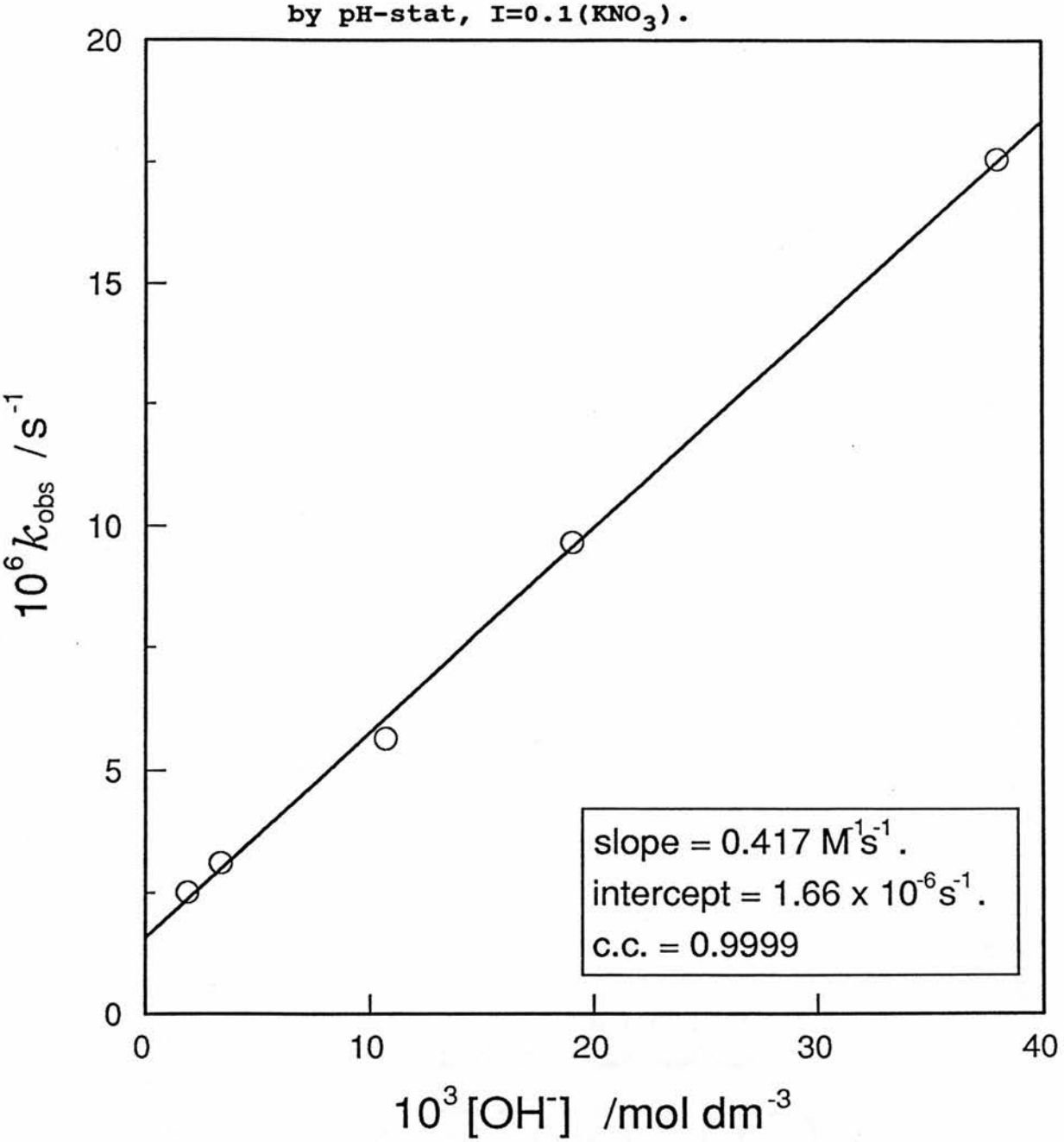

Figure 2.6 Plot of first-order rate constants (k_{obs}) versus $[OH^-]$ for the base hydrolysis of DNPEMP at 30°C by pH-stat, I=0.1(KNO_3).

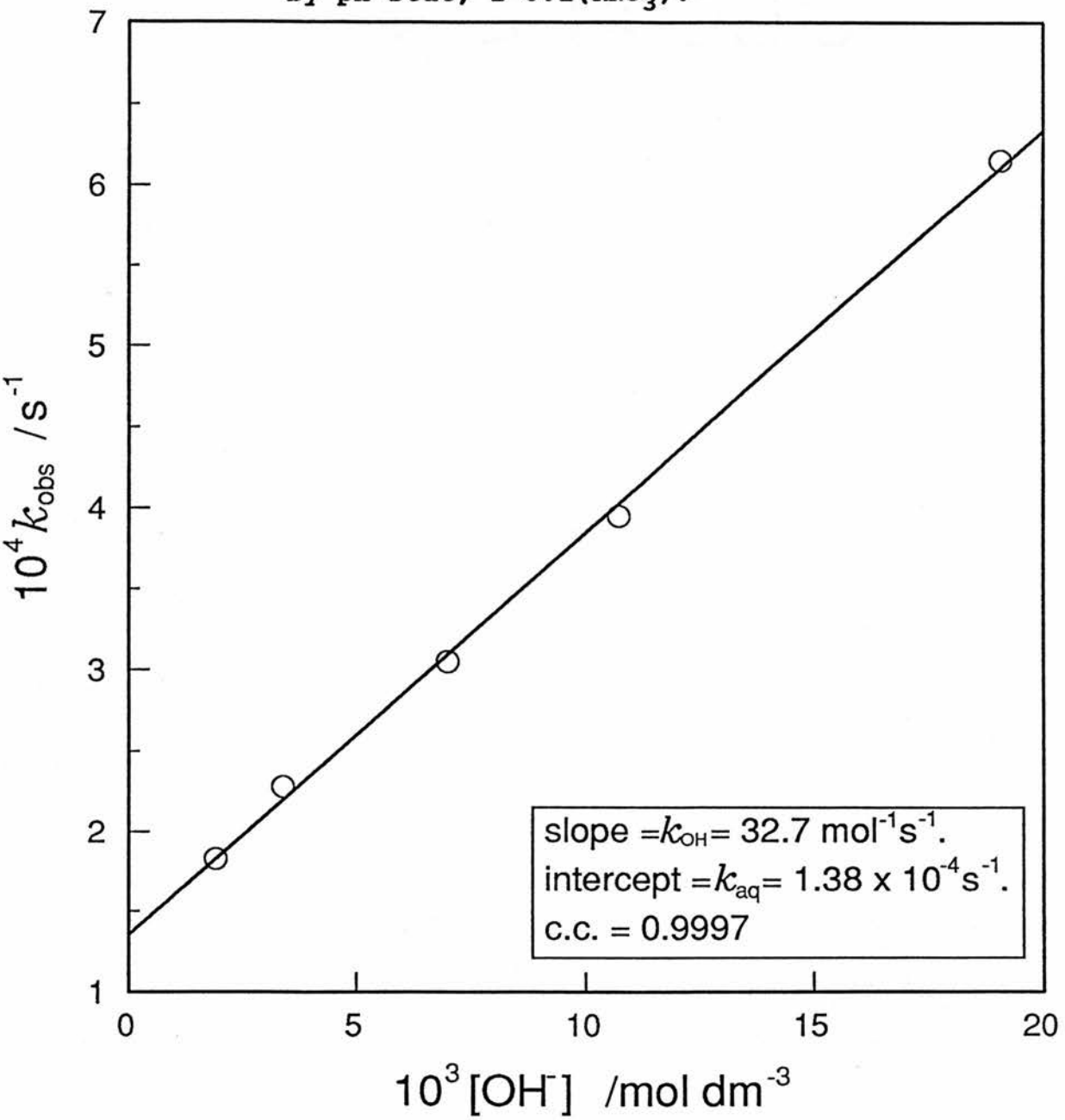

intercept k_{aq}. Examples of such plots for the hydrolysis of DNPDEP and DNPEMP are given in Figure 2.5 and Figure 2.6 respectively. The slope of the plot gives a value of k_{OH} = 0.42 $mol^{-1}s^{-1}$ and k_{aq} = 1.67 x $10^{-6}s^{-1}$ for DNPDEP and k_{OH} = 37.2 $mol^{-1}s^{-1}$ and k_{aq} = 1.37 x $10^{-4}s^{-1}$ for DNPEMP. The data obtained from similar pH stat experiments at various temperatures are summarized in Tables 2.5 and 2.6 for the phosphate and phosphonate esters respectively. Hydroxide ion concentrations were derived from the pH using the appropriate value of pK_w and activity coefficient calculated from the Davies equation[5]. Also included in Table 2.5 and Table 2.6 is data derived from the stop-flow experiments using more concentrated sodium hydroxide ion concentrations (0.01 - 0.05 M).

As can be seen from Figure 2.6, the data observed in Table 2.4, are self consistent and gives a linear plot over a 14 fold change in hydroxide ion concentration. For this reason the value of the intercept derived from the pH-stat data was regarded as a reasonably accurate measure of the aquation rate (k_{aq}), which is difficult to determine independently. Good data was obtained using the pH stat technique at other temperatures. The excellent agreement between pH stat and stop-flow measurements, Tables 2.5 and 2.6, lends confidence to the assigned rate constants. The stop-flow technique is unsuitable for assessment of k_{aq}, as the very small intercepts found on the large ordinate

TABLE 2.5 **Summary of hydrolysis and aquation rates for 2,4-DNPDEP, over the temperature range 10-45°C, I = 0.1 (KNO_3), monitored by pH stat and stop-flow**

Temp/°C	pH - stat		Stop-flow
	$10^6 k_{aq}/s^{-1}$	$10^2 k_{OH}/M^{-1}s^{-1}$	$10^2 k_{OH}/M^{-1}s^{-1}$
10.0	-	-	11.75
15.0	-	-	16.94
20.0	-	-	22.19
25.0	1.22	30.50	29.18
30.0	1.71	41.72	39.64
35.0	2.26	56.53	57.78
40.0	3.03	75.77	80.21
45.0	4.10	99.98	101.00

TABLE 2.6 **Summary of hydrolysis and aquation rates for 2,4-DNPEMP, over the temperature range 10-40°C, I = 0.1 (KNO_3), monitored by pH stat and stop-flow**

Temp/°C	pH - stat		Stop-flow
	$10^4 k_{aq}/s^{-1}$	$k_{OH}/M^{-1}s^{-1}$	$k_{OH}/M^{-1}s^{-1}$
10.0	-	-	10.0
15.0	-	-	13.3
20.0	-	-	18.0
25.0	0.99	26.4	24.2
30.0	1.38	32.7	31.6
35.0	2.30	41.8	43.0
40.0	2.90	53.7	55.6

values leads to large errors. Typical results of stop-flow experiments are shown in Figures 2.7 and 2.8 for the 2,4-dinitrophenoxide phosphate and phosphonate esters respectively.

Figure 2.7 Plot of first-order rate constants (k_{obs}) versus [OH^-] for the base hydrolysis of DNPDEP at 40°C by stopped-flow, I=0.1(KNO_3).

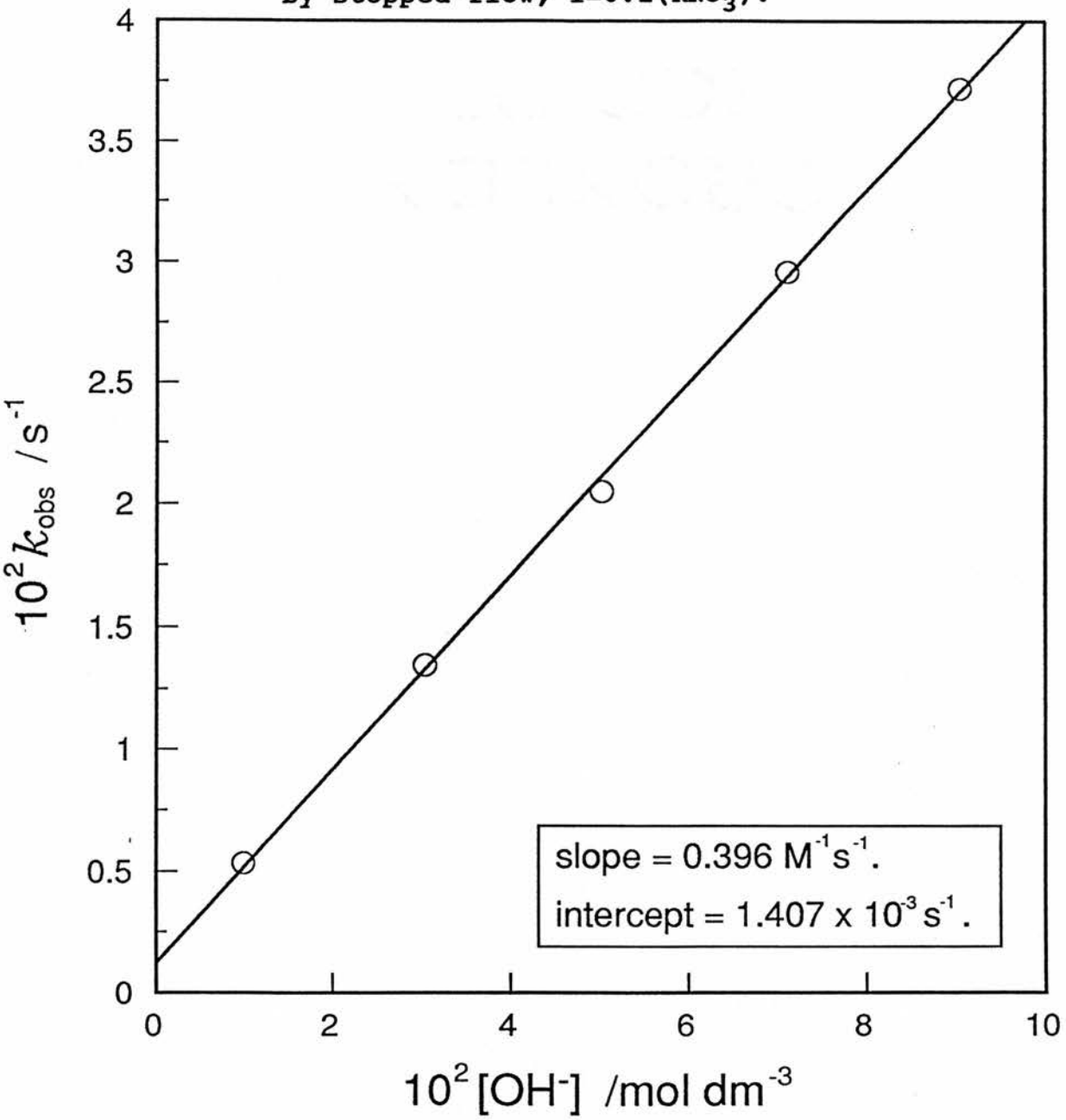

Figure 2.8 Plot of first-order rate constants (k_{obs}) versus $[OH^-]$ for the base hydrolysis of DNPEMP at 40°C by stopped-flow, I=0.1(KNO_3).

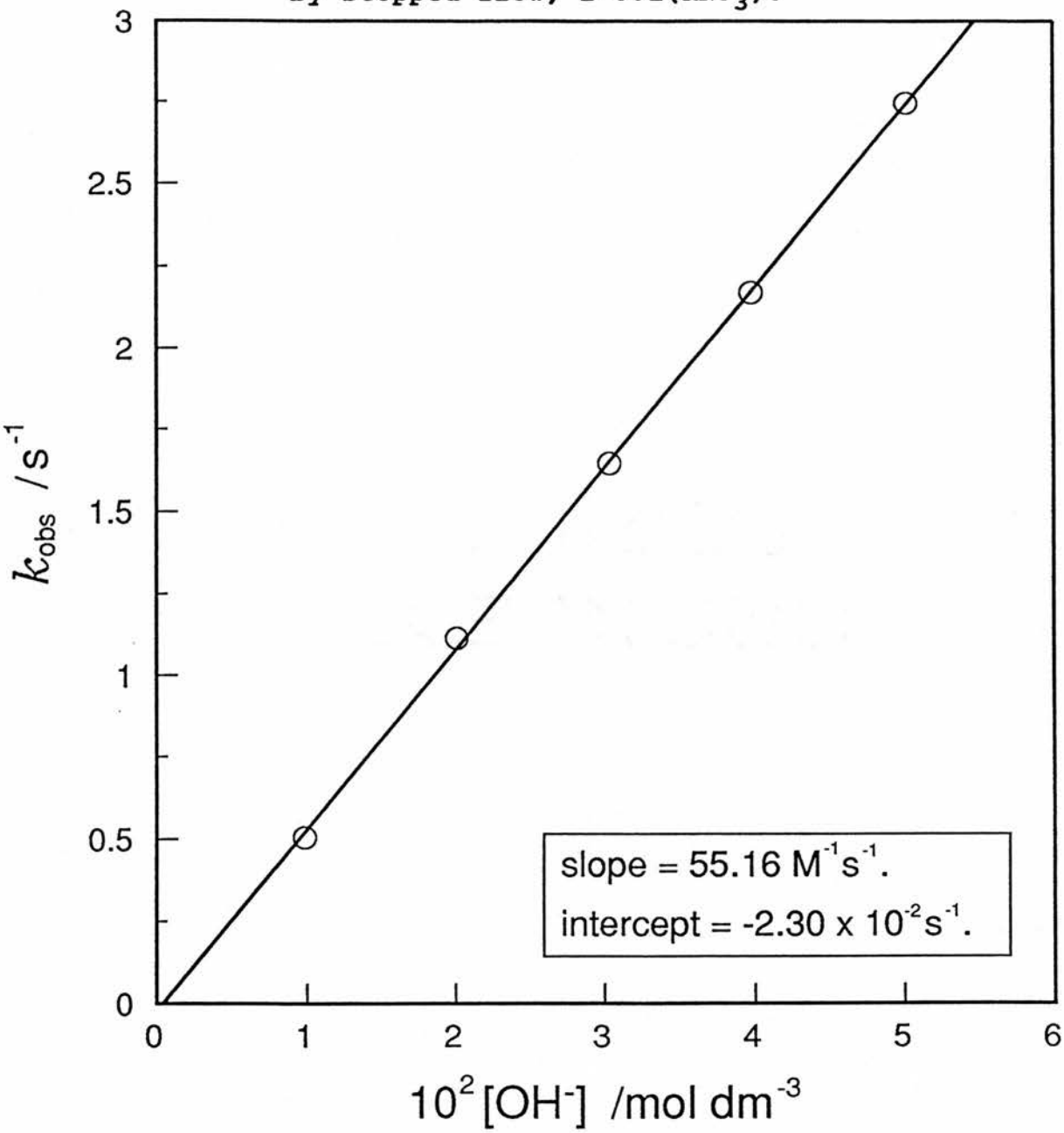

2.5.3 ACTIVATION PARAMETERS FOR DNPDEP AND DNPEMP

The kinetic data in Tables 2.5 and 2.6 is of adequate quality to enable thermodynamic parameters for the hydrolysis of DNPDEP and DNPEMP to be determined. Using the expression

$$A + B \overset{K_C^{\neq}}{\rightleftharpoons} X^{\neq} \longrightarrow \text{Products}$$

where the activated complex $X^{\neq}$ is in equilibrium with reactants A and B and the rate of the reaction $\underline{V}$ is the product of the equilibrium concentration $X^{\neq}$ and the specific rate with which it decomposes. Then from transition state theory[6] the specific rate can be shown to be KT/h where, T = absolute temperature, K = Boltzman constant and h = Plank's constant.

$$\therefore \quad \underline{V} = \frac{KT[X^{\neq}]}{h} = \frac{KTK_C^{\neq}[A][B]}{h}$$

Thus the experimentally determined second order rate constant k is given by the expression

$$k = \frac{KTK_C^{\neq}}{h}$$

From simple thermodynamics,

$$\Delta F^{\ddagger} = -RT \ln K_c^{\ddagger} = \Delta H - T\Delta S$$

then

$$k = \frac{KT}{h} . \exp - \frac{\Delta F^{\ddagger}}{RT} = \frac{KT}{h} . \exp - \frac{\Delta H^{\ddagger}}{RT} . \exp \frac{\Delta S^{\ddagger}}{R}$$

$$\therefore \quad \ln(k/T) = \ln \frac{K}{h} + \frac{\Delta S^{\ddagger}}{R} - \frac{\Delta H^{\ddagger}}{RT} \qquad \text{eq2.2}$$

thus from eq2.2 a plot of ln (k/T) versus 1/T should be linear of slope $-\Delta H^{\ddagger}/R$ and intercept ln (K/h) $+ \Delta S^{\ddagger}/R$. Since ln (K/h) = 23.76, a value of S can be deduced.

The data given in Tables 2.5 and 2.6 can be replotted in this manner (see Figures 2.9 and 2.10) to give activation parameters for the hydroxide reaction and the water reaction for 2,4-DNPEMP and 2,4-DNPDEP. These parameters together with the activation parameters for PNPDEP are shown in Table 2.7.

Figure 2.9 Eyring plot for DNPDEP hydrolysis.

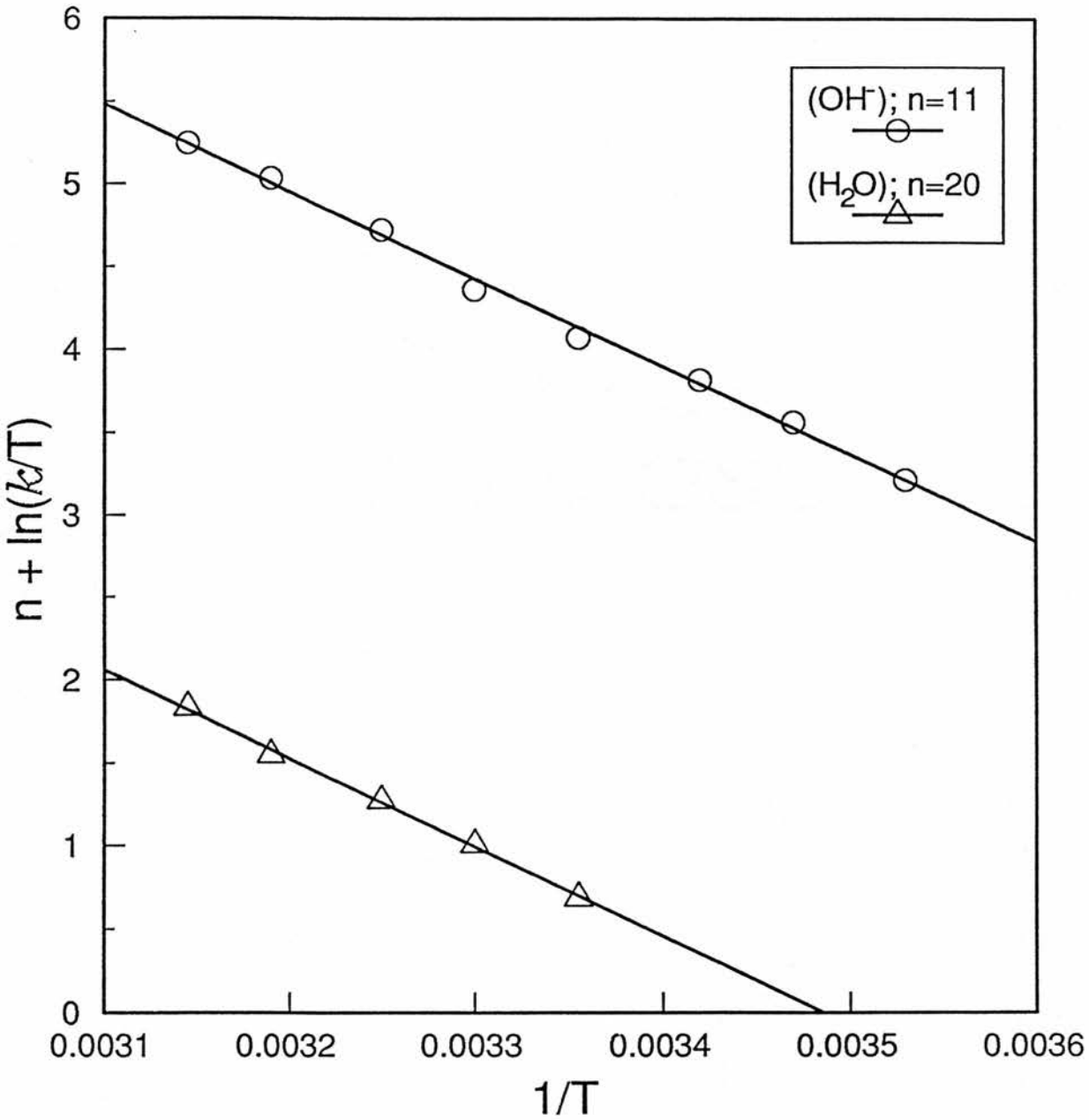

Figure 2.10 Eyring plot for DNPEMP hydrolysis.

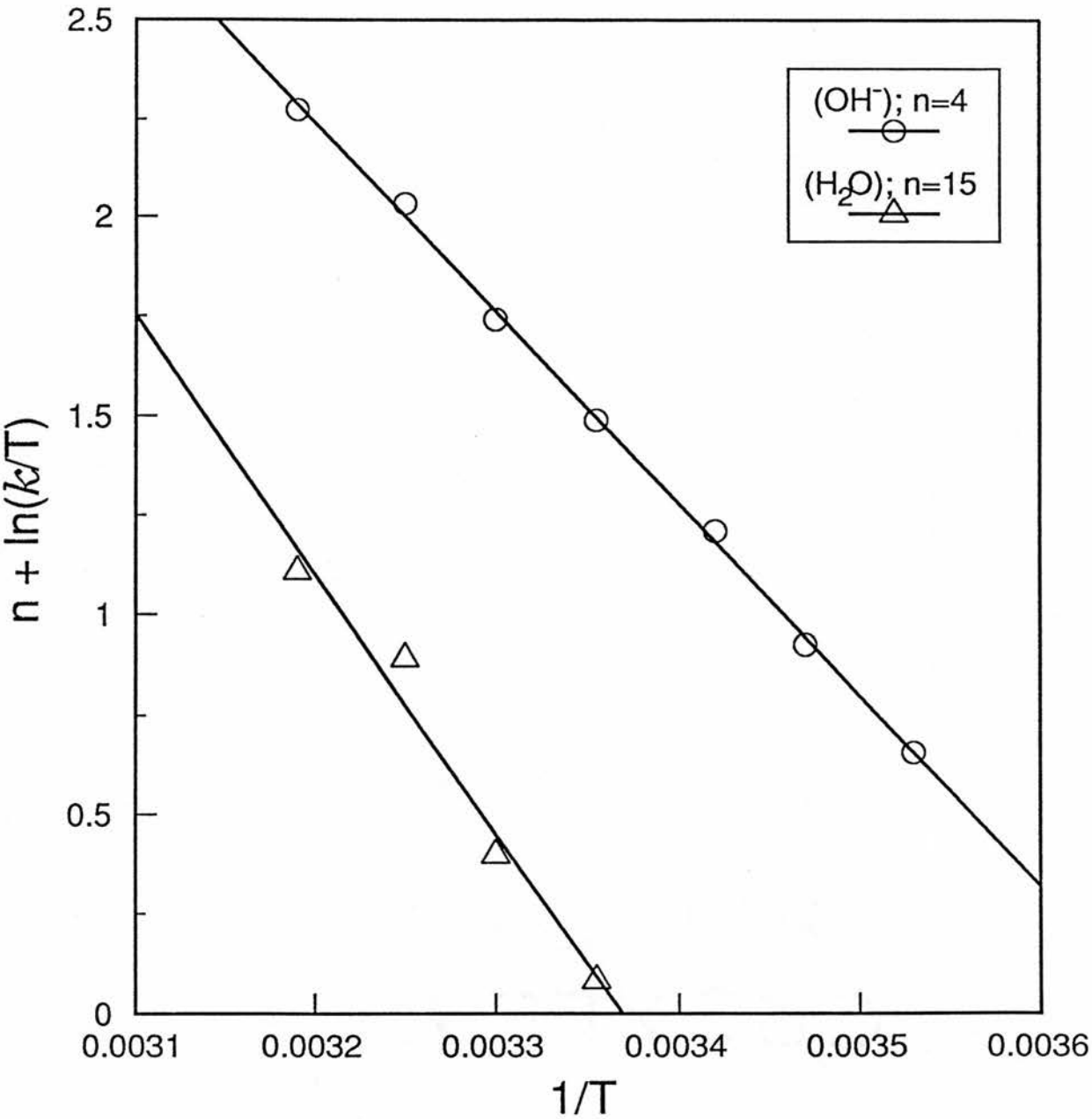

TABLE 2.7 Summary of activation parameters for release of substituted phenoxide ion from PNPDEP, 2,4-DNPDEP and 2,4-DNPEMP

phosphorus ester	k_{OH}		k_{aq}	
	$\Delta H^{\neq}$ /KJmol^{-1}	$\Delta S^{\neq}$ /Jmol^{-1}K^{-1}	$\Delta H^{\neq}$ /KJmol^{-1}	$\Delta S^{\neq}$ /Jmol^{-1}K^{-1}
PNPDEP	50.6	-113	-	-
2,4-DNPDEP	44.4	-105	-	-
2,4-DNPEMP	39.9	-84	55.4	-135

2.6 REFERENCES

1. W.M. Gulick and D.H. Geske, J.Am.Chem.Soc., 38, 2928, (1966).
2. H. Gamp, Talanta, 27, 1037, (1980).
3. S.H. Gellman, R. Petter and R. Breslow, J. Am.Chem.Soc., 108, 2388, (1986).
4. J. Epstein, Phosphorus, 4, 157, (1974).
5. C.W. Davies, J.Chem.Soc., 2093, (1938).
6. A.A. Frost, "Kinetics and Mechanism", Chapt. 5, Wiley, (1961).

CHAPTER THREE

MONO-AQUA METAL COMPLEX PROMOTED HYDROLYSIS OF PHOSPHORUS ESTERS

3.1 INTRODUCTION

The ability of metal ions and metal ion complexes to enhance rates of nucleophilic displacement reactions at neutral phosphorus(V) centres has been well known for a considerable time. Copper(II) chelates have been shown to be effective in assisting the displacement of fluoride ion from both di-isopropyl fluorophosphate[1] (DFP) [3.1] and iso-propylmethyl fluorophosphonate[2] (Sarin) [3.2]. Further screening procedures[3,4]

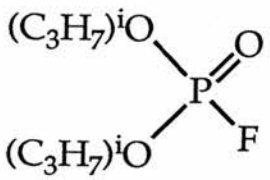

[3.1]

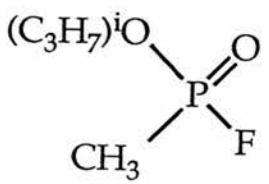

[3.2]

have demonstrated that UO_2(VI), Zr(IV), Th(IV), MoO_2, Y(III) and Al(III) also enhance the degradation rates of similar phosphorus esters. More recently, both Co(III)[5] and Zn(II) species[6,7] have shown to be effective in assisting the hydrolysis of neutral phosphate and phosphonate esters. However, despite the numerous publications that demonstrate the ability of metal complexes to catalyse the hydrolysis reactions at neutral tetrahedral

phosphorus(V) centres, there is little data on the mechanism of these reactions. In view of the potential that metal complexes possess to catalytically degrade such toxic materials, initial studies were carried out to elucidate the interactions of metal ions and phosphorus esters. In order to probe these interactions, the hydrolysis reactions of the phosphate ester 2,4-dinitrophenyl diethylphosphate (DNPDEP) [2.2] and the phosphonate ester 2,4-dinitrophenyl ethyl methylphosphonate (DNPEMP) [2.3] where studied in aqueous solution with a variety of metallo and non-metallo reagents. Earlier studies have shown aqua complexes to be important in the hydrolysis of these reactions. In this section the relationship between the rate of degradation of the phosphate ester and the pK of the attacking agent is examined in order to ascertain whether general base catalysis or direct nucleophilic displacement is the mode of interaction of metal complexes with toxic phosphorus esters. Such data is essential if the value of metal complexes as catalysts in aqueous based decontamination system for toxic phosphorus esters is to be assessed.

3.2 EXPERIMENTAL

3.2.1 MATERIALS AND METHODS

All reagents used were the purest available, the synthesis of metal complexes and their precursors which were not available commercially is described in section (3.2.2). Standard hydrochloric acid and sodium hydroxide solutions were made from BDH"Convol" ampoules adjusted to the desired concentration and standardized against potassium hydrogen phthalate immediately before use. Standard inorganic solutions were made by dissolving weighed amounts of metal salt in appropriate volumes of distilled water, passing known aliquots of these solutions down a cation exchange column (Dowex 50W-8X, H^+ form) and titrating liberated protons with standard base. "Good" buffers (HEPES, TAPS, CHES) were used as supplied by Sigma. Ionic strength for kinetic studies was maintained at 0.1 mol dm^{-3} by either $LiC1O_4$ or KNO_3 depending upon the metal complex under study.

Kinetic measurements were carried out as described in section (2.4). In general, reactions with nucleophiles with a pK greater than 9 where carried out by stop-flow spectrophotometry while reactions of nucleophiles with a pK less than 9 were carried out using the pH-stat technique.

^{1}H NMR spectra were run on a Joel FX100 spectrophotometer while ^{13}C measurements were made on a Joel FX60 FT instrument. Samples were dissolved in the appropriate solvent (d_6-DMSO or d_3-nitromethane for metal complexes) and chemical shifts measured versus TMS. IR spectra were run on a Perkin Elmer 1750FT IR spectrophotometer and UV/VIS spectra were determined with a Perkin Elmer Lamda 5 spectrophotometer. Microanalysis were carried out on a Carlo-Erba CHN analyser. Potentiometeric titrations were carried out using a Radiometer Titra-Lab system. Conductivity measurements were made at 25^{o}C on 1.0mM solutions using a AGB 1000 conductivity meter.

3.2.2 SYNTHESIS OF METAL COMPLEXES

Preparation of $[Co(NH_3)_5(OH_2)](NO_3)_3$ [8]

A solution of cobalt(II) nitrate (30g, 0.103 mol) in 15 cm^3 of water was thoroughly mixed with a solution of (45g, 0.468 mol) ammonium carbonate in 45 cm^3 of water and 75 cm^3 of concentrated aqueous ammonia. A stream of air was bubbled slowly through the mixture for 6 hours. After the mixture had been cooled in an ice-salt bath overnight, the product was collected on a filter washed with 5 ml of ice-cold water, alcohol and ether and dried under vacuo at 50°C. The crude $[Co(NH_3)_5CO_3](NO_3)$ (18g, 64% yield) was purified by recrystallization from water.

Two grams of carbonatopentamine cobalt(III) nitrate (7.2 mmol) was dissolved in 30 cm^3 of 1.0M nitric acid and warmed on a steam bath for 10 minutes. The solution was filtered and, on cooling in the refrigerator overnight, bright red crystals of the product (1.2g,70.7% yield) were obtained. The crystals were washed with 5 cm^3 of propan-2-ol and dried under vacuum. Spectral data (in IM HNO_3) was in agreement with the literature valves (λ max = 492 nm, E = 49 $dm^3\ mol^{-1}\ cm^{-1}$). The complex is a 3:1 electrolyte in aqueous solution (Λ_M = 325 S $cm^2\ mol^{-1}$ at 25°C).

Preparation of $[Cr(NH_3)_5(OH_2)](NO_3)_3.NH_4NO_3$

Potassium chromic sulphate docecahydrate (50g) was finely powdered and mixed with 120 cm^3 of 0.88 ammonia solution. Ammonium nitrate (125g) was added and the flask was warmed in a fume hood at 55°C for one hour with occassional shaking. The mixture was cooled to 20°C and a rapid stream of air was passed through it for 2 hours. The solution was then poured onto a mixture of 50 g of crushed ice and 125 cm^3 of conc nitric acid. The reaction temperature was maintained at less than 25°C by means of an ice bath. The red suspension was then kept at 0°C for 1 hour. The resulting orange crystals were filtered and redissolved in 100 cm^3 water and refiltered. To the filtrate was added 100g ammonium nitrate in 100 cm^3 water. On cooling overnight, orange crystals of the product were obtained (5g, 70%). The crystals were washed with ethanol staturated with ammonium nitrate and finally with a mixture of 1:1 ethanol/diethyl ether and dried under vacuum. The orange crystals were stored below 0°C and had a visible spectrum in good agreement with the literature valves (λ_{max} = 480 nm, E = 35 $dm^3\ mol^{-1}\ cm^{-1}$; 358 nm, E = 31 $dm^3\ mol^{-1}\ cm^{-1}$). The complex is a 3:1 electrolyte in aqueous solution (Λ_M336 S $cm^2\ mol^{-1}$ at 25°C).

Preparation of $[Co([15]aneN_5)(OH_2)](C10_4)_3$

The macrocyclic ligand 1,4,7,10,13-pentaazacyclopentadecane hydrochloride ([15]aneN$_5$) [3.3] was prepared as follows. Tetratosyl-1,8-diamino-3,6-diazaoctane[9] (48g, 0.075 mol) was dissolved in dry (molecular sieves) NN-dimethylformamide (500 cm^3). Sodium hydride (60% in parafin oil, 24g) was added under a stream of nitrogen. When effervescence ceased (ca. 2 hours) the solution was warmed on a water bath (ca. 45 minutes). The solution was cooled to room temperature and the excess sodium hydride filtered off. (At all stages the solution was kept under N_2 with the minimum exposure to the atmosphere). The filtrate was transfered to a flask equipped with a thermometer, double-surface condenser, drying tube, N_2 inlet and magnetic stirrer. NOO'-Tritosyldiethanolamine[9] (35g, 0.075 mol) dissolved in dry NN-dimethylformamide (300 cm^3) was added dropwise and the mixture heated on an oil bath for ca. 10 hours at 110-120^{o}C with continuous stirring. The solution was cooled to room temperature and water (1500 cm^3) added slowly with vigorous stirring. The solid product (which contained unreacted tosylates in addition to the required product) was washed with water and heated with formic acid. The pentatosylate of the macrocycle is more soluble in formic acid than the reactants. Initial fractions were monitored by i.r.

spectroscopy until the γ (NH) band at 3280 cm^{-1} (due to the tetratosylate of 1,8-diamino -3,6-diazaoctane) was absent. Some 30g of the required tosylate m.p. 278-280 (lit[10] 278-280°C) were obtained. The pentatosylate was hydrolysed with concentrated H_2SO_4 using a previously described procedure,[9] then converted to the free base, and finally to the pentahydrochloride. The ^1H NMR spectrum of the amine pentahydrochloride in D_2O solution [sodium 4,4-dimethyl-4-silapentanesulphonate (dss) reference] showed the complete absence of tosyl groups and a single signal at δ 3.58 due to the equivalent CH_2 groups, m.p. 245-260°C (decomp.)

Anal. Calcd. for $C_{10}H_{30}N_5Cl_5$: C, 30.20; H, 7.60; N, 17.60. Found: C, 30.50; H, 7.55; N, 17.60%.

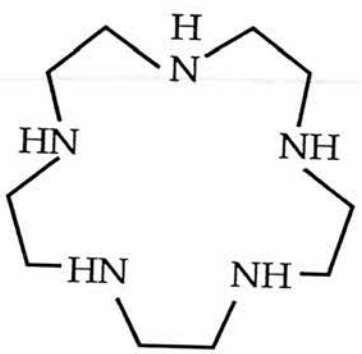

[3.3]

Chloro (1,4,7,10,13-penta-azacydo-pentadecane) cobalt (III) Diperchlorate, [Co([15]aneN_5)Cl] $(ClO_4)_2$, a precursor to the aqua-complex was preprepared as follows. The macrocycle pentahydrochloride (0.30g) was dissolved in water (15 cm^3) and treated with freshly prepared $Na_3[Co(CO_3)_3]$.

$3H_2O$[11] (0.30g). The mixture was heated on a steam bath for 1 hour and filtered hot. To the deep red filtrate was added $NaClO_4$ (0.15g). On standing for 1-2 days the solution deposited reddish brown crystals which were filtered off, washed with propan-2-ol, then diethyl ether, and dried in vacuo.

Anal. Calcd. for $C_{10}H_{25}Cl_3CoN_5O_8$: C, 23.60; H, 4.95; N, 13.75. Found: C, 24.15; H, 5.10; N, 13.50%.

Aqua (1,4,7,10,13-penta-azacyclo-pentadecane) cobalt (III) Triperchlorate, $[Co([15]aneN_5)(OH_2)](ClO_4)_3$, was prepared by dissolving the chloro complex (0.51g) in water (20 cm^3) and treating with $AgClO_4$ (0.22g). The solution was warmed to ca. 60°C and maintained at this temperature for 1 hour and then cooled. The precipitated AgCl was filtered off and the excess Ag(I) removed as AgCl by the careful addition of very dilute HCl. The solution was allowed to stand in the dark overnight and then filtered. The filtrate was evaporated to ca. 5cm^3 on a steam-bath, cooled and the reddish brown complex precipitated by careful addition of ethanol. The complex was filtered off, and further purified by dissolving in the minimum volume of water, cooling in ice, and precipitating with ethanol.

Anal. Calcd. for $C_{10}H_{27}Cl_3CoN_5O_{13}$: C, 20.35; H, 4.60; N, 11.85. Found: C, 20.55; H, 4.35; N, 11.35%. UV/VIS: λ_{max} 220 nm, 19400 dm^3 mol^{-1} cm^{-1}, λ_{max} 450, = 350

$dm^3\ mol^{-1}\ cm^{-1}$. The complex is a 3:1 electrolyte in aqueous solution (Λ_M = 312 S $cm^2\ mol^{-1}$ at 25°C).

Preparation of $[(Zn(CR))_2OH.(OH_2)](C10_4)_3$ (12)

The zinc(II) complex of the ligand 2,12-dimethyl-3,7,11,17-tetraazabicyclo [11.3.1]-septadec-1(17)-13,15-pentaene, (CR) [3.6] was made by "template" synthesis as follows.

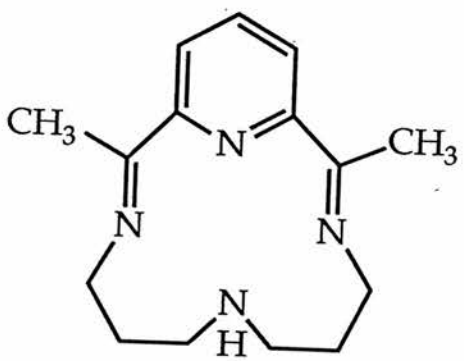

[3.4]

Hydrated zinc(II) perchlorate (8.0g, 30 mmol) was dissolved in 150 cm^3 of ethanol/water (1:1) together with (4.9g, 30 mmol) of 2,6-diacetylpyridine. To this was added dropwise with stirring (4.6g, 60 mmol) of 1, 3-diamino-propane dissolved in 25 cm^3 of the same solvent. The solution was refluxed for four hours and then reduced to half volume under vacuum. The pH was raised to $\sim$ 10 by addition of 1M NaOH, then 15 cm^3 of saturated $NaClO_4$ solution was added and on cooling the crude product crystallised. Purification was achieved by recrystallisation from the minimum of hot ethanol/H_2O(2:1) containing activated charcoal and the

product was finally obtained as off white crystals (9.8g, 34% yield).

Anal. Cald. for $C_{30}H_{46}N_8Zn_2Cl_3O_{14}$: C, 36.77; H, 4.73; N, 11.44. Found: C, 36.49; H, 4.64; N, 11.33%. ^1H NMR; (CD_3NO_2,TMS): 8.2-8.6 (3H); 3.2-4.2 (12H); 2.4(6H). IR: (KBr disk); 3410-3500 (OH); 3120 (NH); 1645 (imine, C=N); 1100, 625 (ClO_4) cm^{-1}. UV/VIS.(H_2O): 296 (E = 18 x 10^3), 245 (E = 5 x 10^3), 215 (E = 8 x 10^3) λ_{max}, nm (E, dm^3 mol^{-1} cm^{-1}).

3.3 RESULTS

3.3.1 REACTIONS WITH INERT METAL COMPLEXES

Having characterised the water and hydroxide rates (Chapter 2), closer detail can be paid to the metal based reactions. Kinetic results for the hydrolysis of DNPDEP by $[Co(NH_3)_5H_2O]^{3+}$ and $[Zn(CR)(OH_2)]^{2+}$ are given in Table 3.1 and shown graphically as pH rate profiles in Figure 3.1. The cobalt complex can be titrated at 35°C (I = 0.1M) to yield a pK for the equilibrium.

$$[Co(NH_3)_5(OH_2)]^{3+} \overset{K}{\rightleftharpoons} [Co(NH_3)_5OH]^{2+} + H^+$$

The pK under these conditions has a value of 6.3. The macrocyclic zinc complex is stable in aqueous solution over the required pH and also shows a single hydrolytic deprotonation with a pK value of 8.1. From examination of the pH dependency of the reactions illustrated in Figure 3.1 it is apparent that deprotonation of the co-ordinated water molecule is a key step in the rate acceleration of the hydrolysis reaction.

Under the conditions of the experiment, the following equation should hold true.

TABLE 3.1 Hydrolysis of DNPDEP by mono-aqua metal complexes at 40°C and varying pH, I=0.1(KNO_3)

pH	$10^5 k_{obs}/s^{-1}$	pH	$10^5 k_{obs}/s^{-1}$
	$[Co(NH_3)_5H_2O]^{3+}$		$[Zn(CR)H_2O]^{2+}$
5.42	2.66	4.90	1.83
5.80	6.68	6.12	4.93
6.10	10.55	6.64	7.87
6.37	17.66	7.70	26.69
6.90	26.83	8.17	38.67
7.45	28.83	8.21	48.13
		8.85	79.68
		9.17	99.61
		9.55	100.10

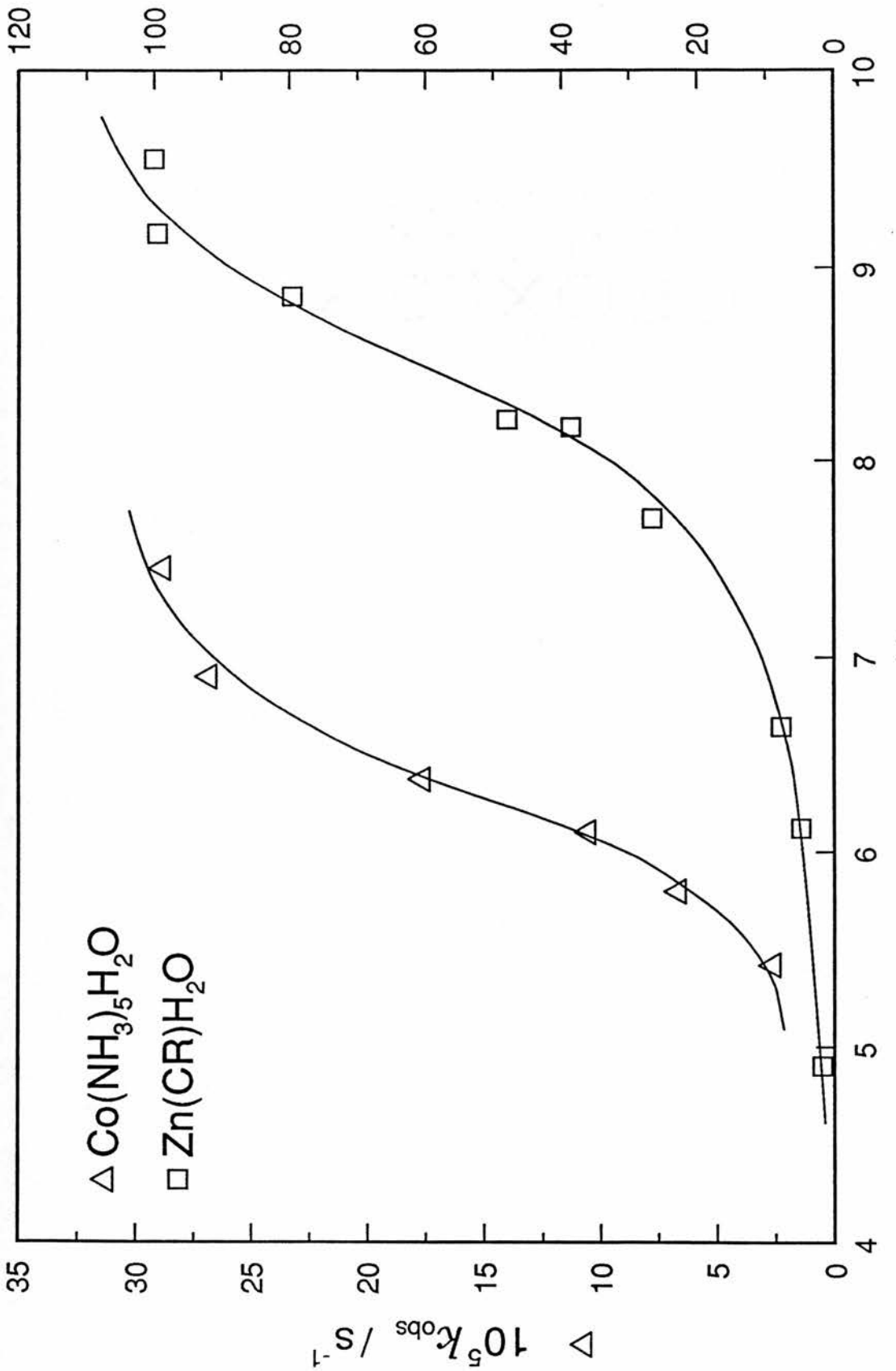

Figure 3.1 pH-rate for the hydrolysis of DNPDEP by mono-aqua metal complexes at 40°C, I=0.1(KNO_3).

TABLE 3.2 Observed-first-order rate constants for the $[Co(NH_3)_5(OH_2)]^{3+}$ promoted hydrolysis of DNPEMP as a function of metal complex concentration at 35°C pH 7.7 and I=0.1(KNO_3)

10^3[cobalt complex] /mol dm^{-3}	$10^4 k_{obs}$ /s^{-1}
1.98	4.76
4.00	7.77
5.99	10.49
7.98	13.42
10.01	16.14
12.00	19.45

Figure 3.2 Observed-first-order rate constants for the $[Co(NH_3)_5OH]^{2+}$ promoted hydrolysis of DNPEMP as a function of metal complex concentration at 35°C and pH 7.7, I=0.1(KNO_3)

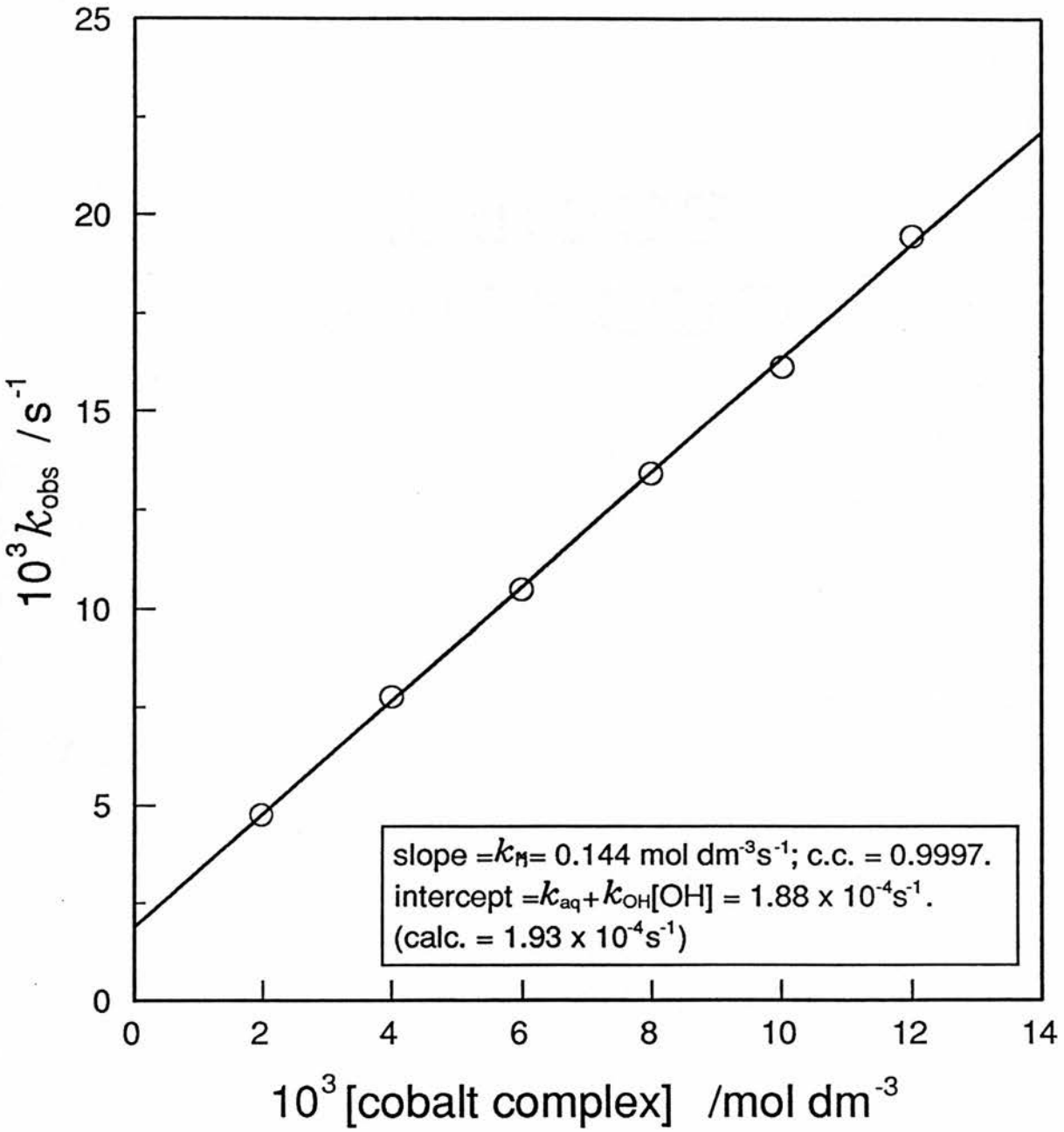

$$k_{obs} = k_{aq} + k_{OH}\ [OH^-] + k_M\ [M\text{-}OH] \qquad eq3.1$$

where

k_{obs} - experimentally observed rate

k_{OH} - second order rate constant for hydroxide reaction

k_m - second order rate constant for attack by metal species.

[M-OH]- concentration of deprotonated metal complex.

k_{aq} - spontaneous first order reaction with water.

Thus, a plot of k_{obs} versus [M-OH] should be a straight line of slope k_m and intercept $k_{aq} + k_{OH}[OH]$, provided that all other parameters (i.e. temperature and pH) are kept constant. When the maintained pH is such that the concentration of deprotonated metal complex equates to the total analytical concentration of cobalt (i.e. pH > pK + 1.4), a value of k_m can be deduced. The rate of hydrolysis of DNPEMP increases linearly with the deprotonated complex $[Co(NH_3)_5OH]^{2+}$ concentration, Table 3.1. A typical plot is shown in Figure 3.2. The intercept of $1.88 \times 10^{-4}\ s^{-1}$ is in good agreement with the calculated value of $1.93 \times 10^{-4}\ s^{-1}$.

The derived values of k_m for the metal complexes under study in this section reacting with DNPDEP and DNPEMP are given in Tables 3.3 and 3.4 respectively together with k_{nuc} values for other nucleophiles.

3.3.2 REACTIONS WITH OTHER NUCLEOPHILES

It is pertinent to the study of reactions with metal complexes to investigate the effects of other nucleophiles and bases. Accordingly, values of k_{nuc} for a variety of compounds were determined by use of equation (2.1). When the pH is maintained at a constant value, a plot of k_{obs} versus [nuc^-] should yield a straight line of slope k_{nuc} and intercept $k_{aq} + k_{OH}$ [OH^-]. This is well supported in practice, where the slope of the graph, k_{nuc} for phenate ion reacting with DNPEMP at 35°C, I = 0.1(KNO_3), is 4.7 mol^{-1} sec^{-1}. The intercept of 4.02 x 10^{-2} sec^{-1} is in good agreement with the calculated value of 4.4 x 10^{-2} sec^{-1} based on a pK value of 10.7 (the pH of the phenate reaction). A complete list of bases and nucleophiles investigated at 35°C, I = 0.1 (KNO_3), for the phosphate ester DNPDEP is given in Table 3.3 and the relevant Bronsted plot shown graphically in Figure 3.3. A corresponding list for the phosphonate ester DNPEMP is given in Table 3.4 and the resulting Bronsted plot is shown in Figure 3.4. Where possible, pK values were taken from the literature and as such may be slightly in error where temperature effects had to be interpolated. The magnitude of these errors is not great and is insignificant in the context in which they are applied. The sources of the pK data are referenced in Table 3.3. Interpretation of the results will be considered later in the discussion.

TABLE 3.3 k_{nuc} **values for bases and nucleophiles reacting DNPDEP at 35.0°C, I=0.1**

	pK	k_{nuc} /$M^{-1}s^{-1}$	$\log_{10}(k_{nuc})$
hydroxide ion(1)	15.7	0.565	-0.25
peroxide ion(2)	11.8	-	-
triethylamine(3)	10.7	0.398	-0.40
2-aminopropane(4)	10.4	0.178	-0.75
DBU(5)	10.1	0.445	-0.35
phenol(6)	10.0	0.170	-0.64
DBN(7)	9.6	0.229	-0.77
cyanide ion(8)	9.2	0.129	-0.89
$[Zn(CR)(H_2O)]^{2+}$(9)	8.1	0.089	-1.05
2-iodobenzoate(10)	7.4	0.553	-0.27
$[Cu(tmen)(H_2O)_2]^{2+}$(11)	7.3	2.452	0.39
$[Co([15]aneN_5)(H_2O)]^{3+}$(12)	6.3	0.028	-1.55
$[Co(NH_3)_5(H_2O)]^{3+}$(13)	6.3	0.017	-1.76
$[Cr(NH_3)_5(H_2O)]^{3+}$(14)	5.2	8.91×10^{-3}	-2.05
acetate ion(15)	4.7	5.89×10^{-3}	-2.23
fluoride ion(16)	3.5	0.211	-0.69
chloroacetate(17)	2.9	1.23×10^{-3}	-2.91
water(18)	-1.7	2.26×10^{-6}	-5.65

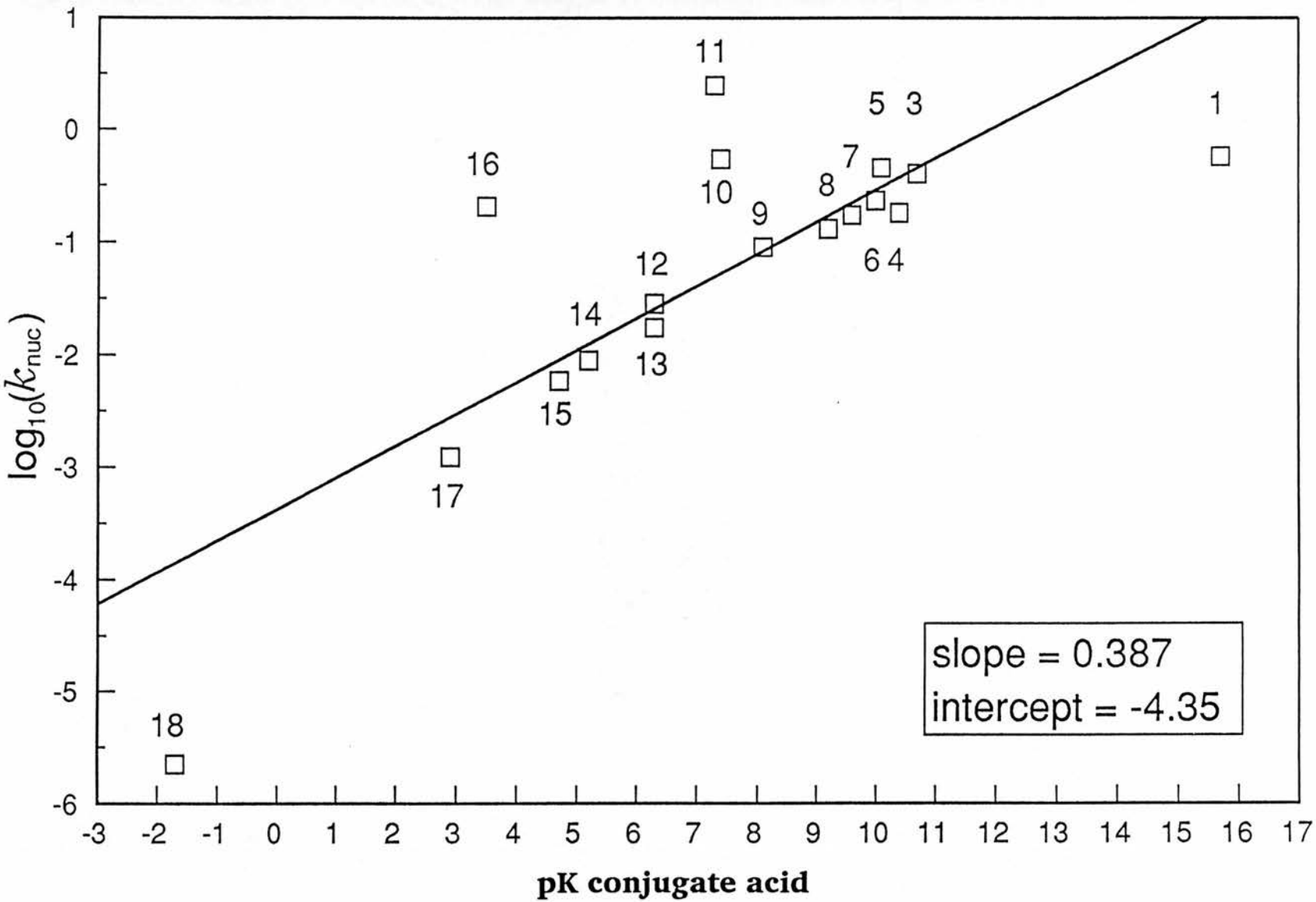

Figure 3.3 Bronsted plot for the hydrolysis of DNPDEP at 35°C, I=0.1(KNO_3).

TABLE 3.4 k_{nuc} **values for bases and nucleophiles reacting DNPEMP at 35.0°C, I=0.1**

	pK	k_{nuc} /$M^{-1}s^{-1}$	$\log_{10}(k_{nuc})$
hydroxide ion(1)	15.7	43.00	1.63
peroxide ion(2)	11.8	2172.0	3.34
triethylamine(3)	10.7	11.43	1.06
2-aminopropane(4)	10.4	6.82	0.83
DBU(5)	10.1	26.88	1.43
phenol(6)	10.0	4.70	0.67
DBN(7)	9.6	12.73	1.10
cyanide(8)	9.2	1.37	0.14
$[Zn(CR)(H_2O)]^{2+}$(9)	8.1	1.21	0.08
2-iodobenzoate ion(10)	7.4	61.66	1.79
$[Cu(tmen)(H_2O)_2]^{2+}$(11)	7.3	49.76	1.70
$[Co([15]aneN_5)(H_2O)]^{3+}$(12)	6.3	0.407	-0.39
$[Co(NH_3)_5(H_2O)]^{3+}$(13)	6.3	0.143	-0.85
$[Cr(NH_3)_5(H_2O)]^{3+}$(14)	5.2	0.065	-1.19
acetate ion(15)	4.7	0.017	-1.77
azide ion(16)	4.7	0.015	-1.82
fluoride ion(17)	3.5	12.92	1.11
chloroacetate(18)	2.9	2.13×10^{-3}	-2.67
water(19)	-1.7	4.16×10^{-6}	-5.38

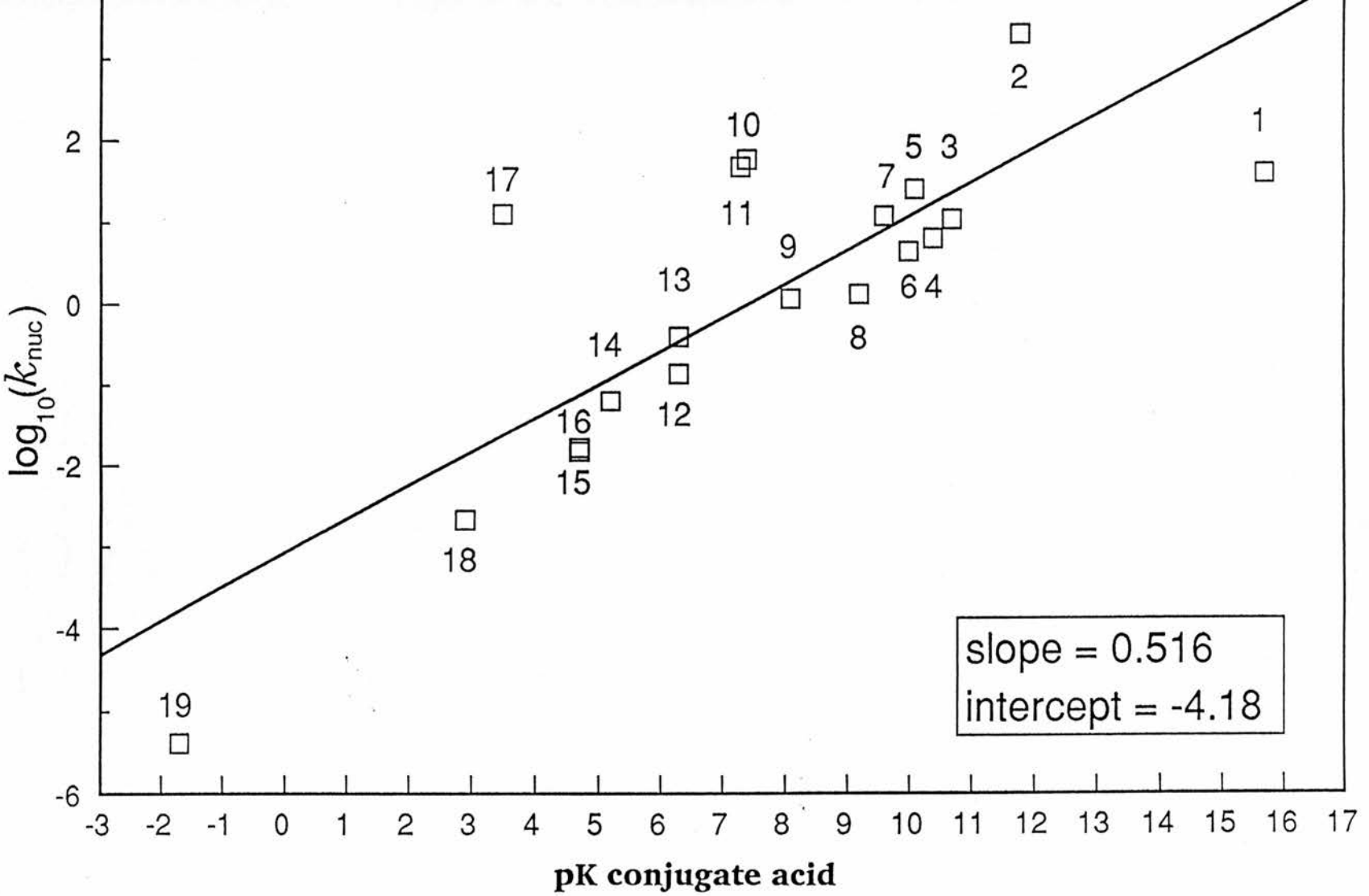

Figure 3.4 Bronsted plot for the hydrolysis of DNPEMP at 35°C, I=0.1(KNO_3).

3.3.3 REACTIONS IN DEUTERIUM OXIDE

The reactions of two bases, fluoride and triethylamine were investigated further to ascertain whether any deuterium isotope effects were evident and if so, whether or not any conclusions could be drawn about the possible mechanism of reaction. The results obtained for DNPDEP reacting with triethylamine are outlined in Table 3.5 and plotted in Figure 3.5. The results for the phosphonate ester reacting with triethylamine are given in Table 3.6 and plotted in Figure 3.6. At 35°C and I = 0.1 (KNO_3), the values for k_{nuc} for triethylamine reacting with DNPDEP in water and deuterium oxide solvents were 0.42 $M^{-1}s^{-1}$ and 0.33 $M^{-1}s^{-1}$ respectively. This gives a value of k_{H2O}/k_{D2O} of 1.27. For the phosphonate ester DNPEMP a similar deuterium isotope effect k_{H2O}/k_{D2O} of 1.30 was obtained.

Studies of fluoride ion reacting with DNPEMP in water and deuterium oxide gave an unexpected k_{H2O}/k_{D2O} of 0.46 from values of 12.92 $M^{-1}s^{-1}$ in H_2O and 27.63 $M^{-1}s^{-1}$ in D_2O. This unusually high rate of reaction observed with fluoride ion in D_2O prompted a further analysis of the system to ascertain the activation parameters for the reaction. The kinetic plot for the fluoride reaction is given in Figure 3.7 with the Eyring plot in Figure 3.8. The data for these reactions of F^- are summarised in Tables 3.7 and 3.8.

TABLE 3.5 Reaction of DNPDEP with triethylamine in aqueous solvents at 35°C, I=0.1(KNO_3)

[Triethylamine] /mol dm^{-3}	$10^2 k_{obs}/s^{-1}$	
	H_2O	D_2O
0.05	2.41	2.10
0.10	4.40	-
0.15	6.35	5.30
0.20	8.20	-
0.25	11.00	8.62
k_{nuc}	0.42 $M^{-1}s^{-1}$	0.325 $M^{-1}s^{-1}$

Figure 3.5 Observed-first-order rate constants for the triethylamine promoted hydrolysis of DNPDEP as a function of triethylamine concentration in H_2O and D_2O at 35°C, I=0.1(KNO_3)

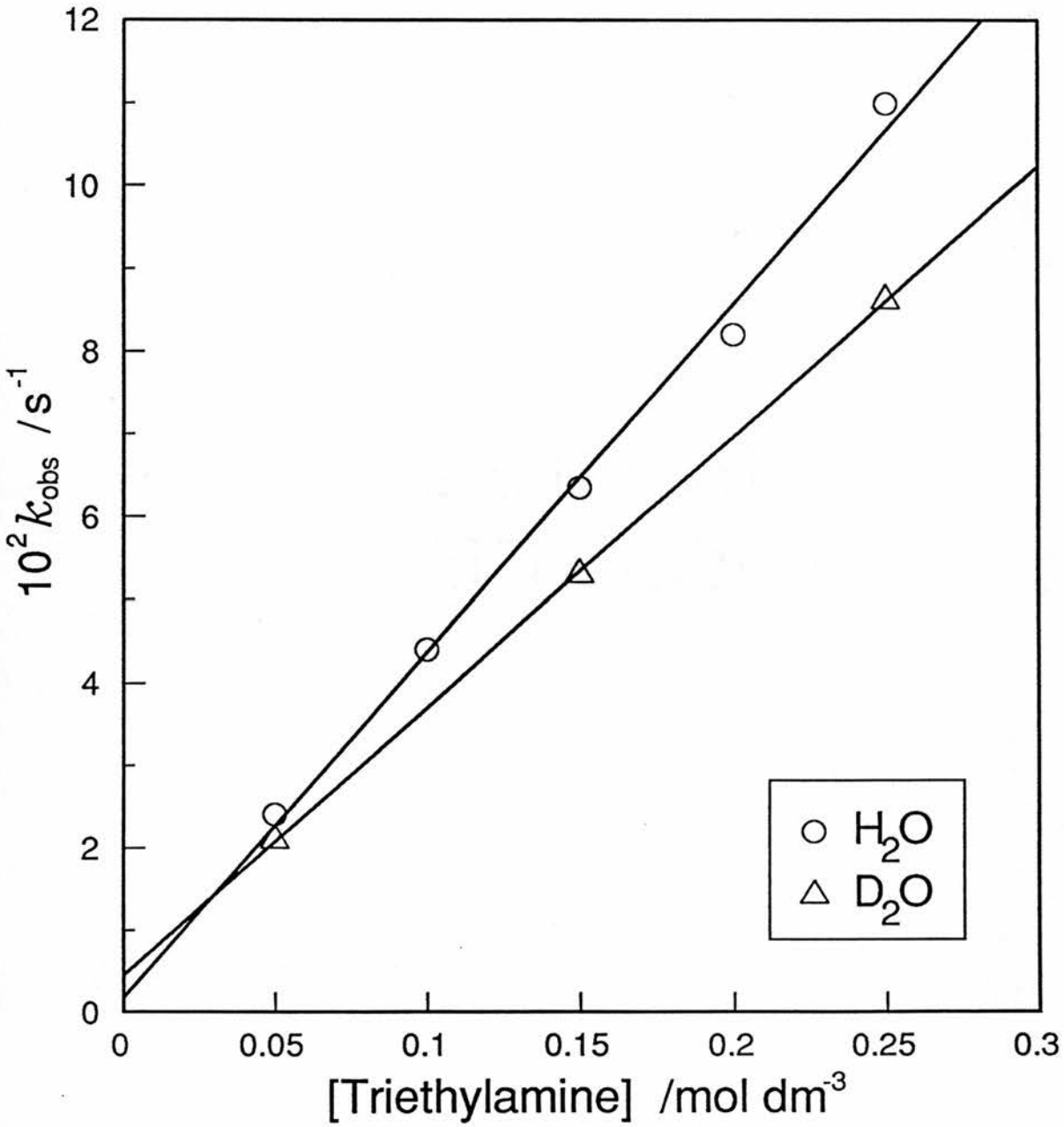

TABLE 3.6 Reaction of 2,4- DNPEMP with triethylamine in aqueous solvents at 35°C, I=0.1(KNO_3)

10^3[Triethylamine] /mol dm^{-3}	k_{obs}/s^{-1}	
	H_2O	D_2O
10	0.287	0.247
20	0.383	-
25	-	0.373
30	0.499	-
40	0.584	-
50	0.757	0.598
k_{nuc}	11.43 $M^{-1}s^{-1}$	8.79 $M^{-1}s^{-1}$

Figure 3.6 Observed-first-order rate constants for the triethylamine promoted hydrolysis of DNPEMP as a function of triethylamine concentration in H_2O and D_2O at 35°C, I=0.1(KNO_3)

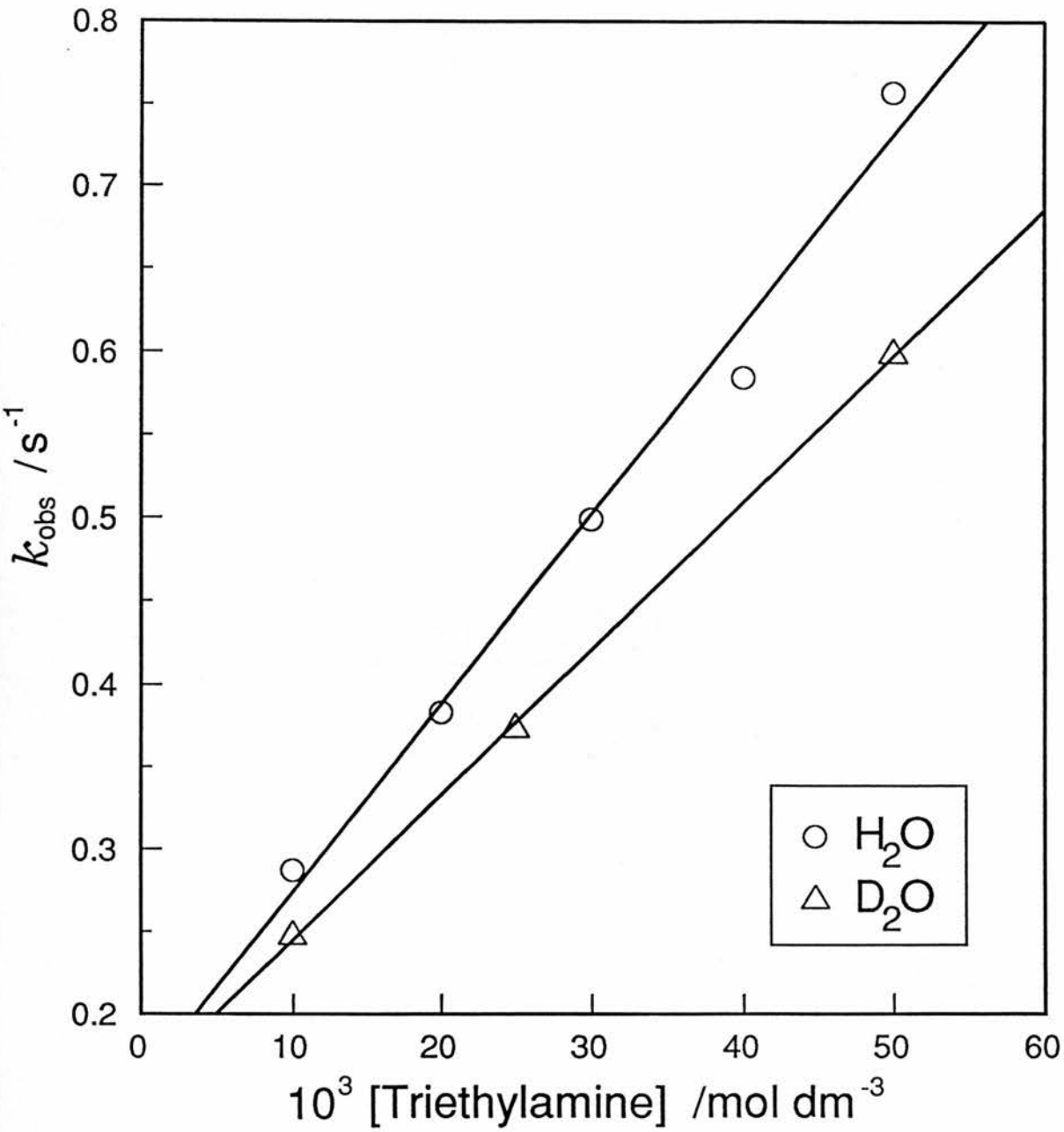

TABLE 3.7 Reaction of 2,4- DNPEMP with F^- in aqueous solutions at 35°C, I=0.1(KNO_3)

$10^3[F^-]$ /mol dm^{-3}	k_{obs}/s^{-1}	
	H_2O	D_2O
10	0.124	0.287
20	0.269	
25	-	0.688
30	0.381	
50	0.647	1.392
k_{nuc}	12.92 $M^{-1}s^{-1}$	27.63 $M^{-1}s^{-1}$

Figure 3.7 Observed-first-order rate constants for the fluoride promoted hydrolysis of DNPEMP as at function of fluoride concentration in H_2O and D_2O at 35°C, I=0.1(KNO_3)

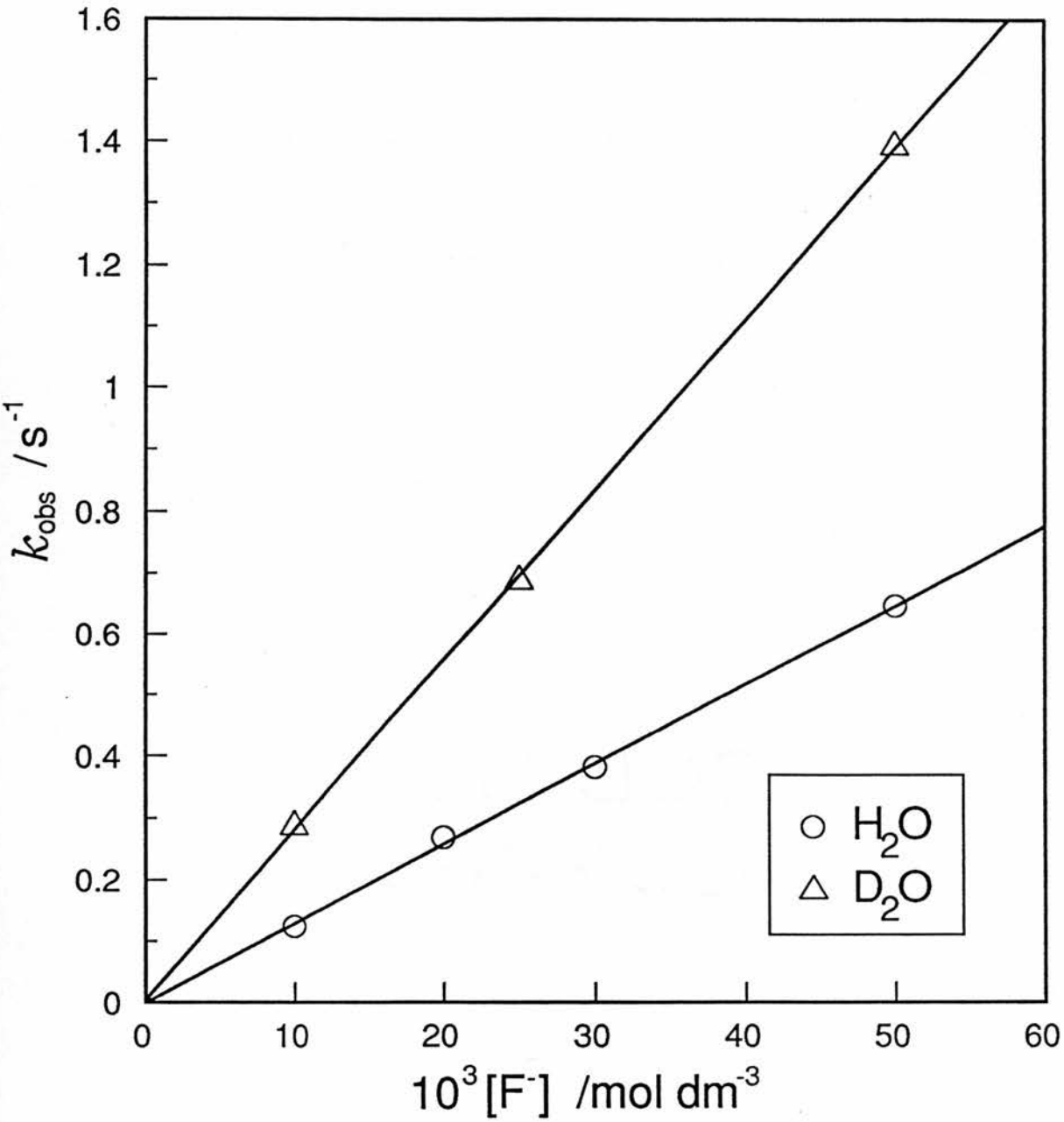

TABLE 3.8 Effect of Temperature on the Reaction of F^- with 2,4- DNPEMP

Temp/^oC	$k_F/M^{-1}s^{-1}$	Temp/^oC	$k_F/M^{-1}s^{-1}$
	H_2O		D_2O
10.05	2.89	10.7	4.86
15.5	4.92	15.8	6.72
20.3	6.65	22.5	11.12
25.2	9.87	27.3	14.74
35.0	12.68	35.0	27.63
40.0	22.58		

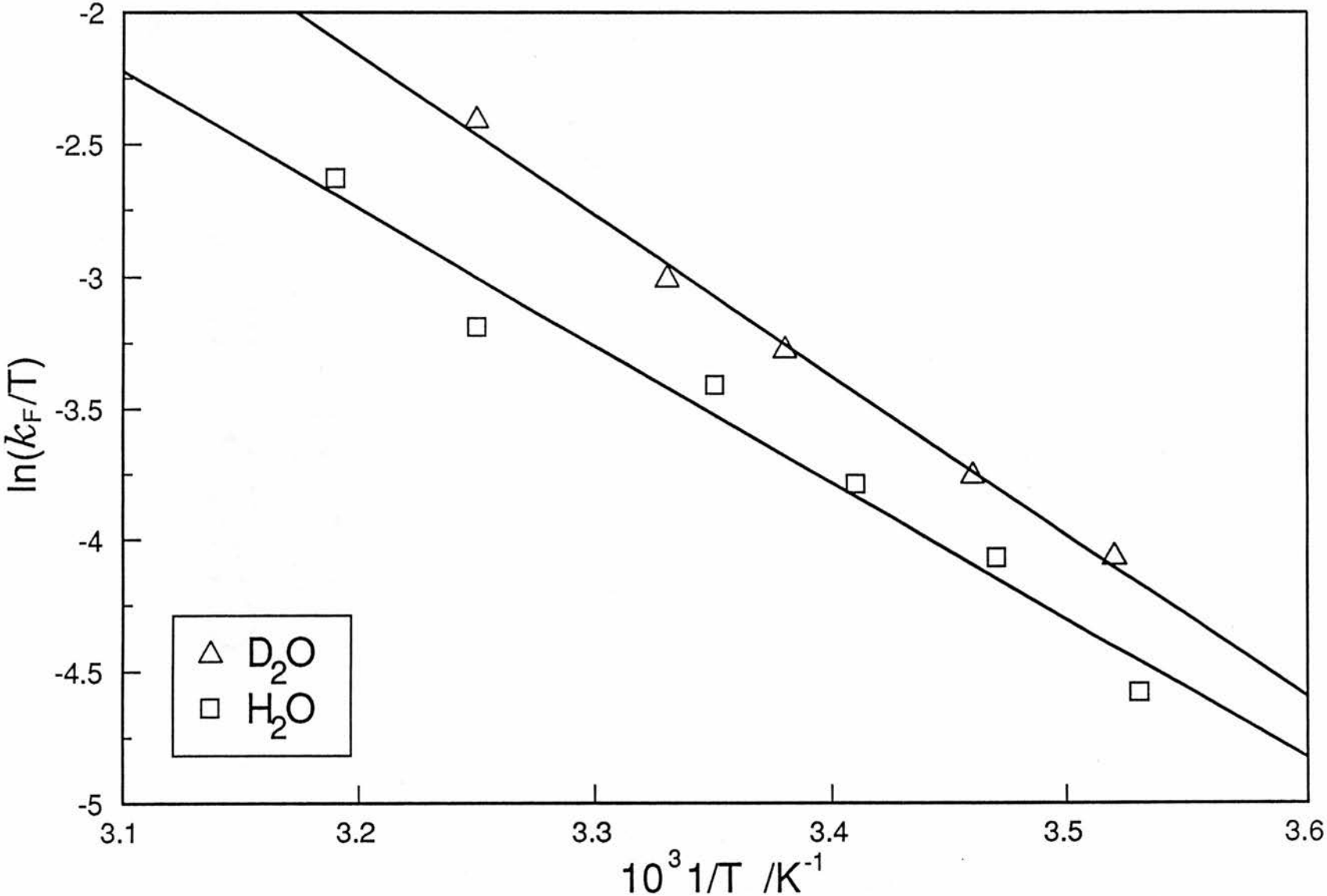

Figure 3.8 Eyring plot for the reaction of fluoride with DNPEMP in H_2O and D_2O.

3.3.4 **ACTIVATION PARAMETERS**

A summary of all activation parameters determined for DNPEMP are given in Table 3.9.

TABLE 3.9 Activation Parameters for the Hydrolysis of 2,4- DNPEMP by various Nucleophiles

Nucleophile	$\triangle H^{\ddagger}$ K J mol^{-1}	$\triangle S^{\ddagger}$ J $mol^{-1}K^{-1}$
H_2O	55.4	-135
OH^-	39.9	-84
$N(C_2H_5)_3$	43.5	-110
F^-	47.1	-115
$F^-/(D_2O)$	49.3	-57
OCI^-	38.5	-124

3.4 DISCUSSION

3.4.1 REACTIONS INVOLVING "INERT" MONO-AQUA METAL COMPLEXES

Studies of metal catalysed hydrolysis of phosphate esters carried out to date have concentrated on the kinetics of copper(II) systems.[1,13,14] A drawback with this system is that the extreme kinetic lability of copper(II) and its complexes makes interpretation of kinetic results difficult. A solution of copper(II) in solution with other ions and ligands can exist as numerous different species in a complex matrix of equilibria. Computer programs such as MINIQUAD[15] are available to deconvolute these complex equilibria in solution but require large amounts of data (usually potentiometric) to solve the many different parameters. This process is known as "Chemical Speciation" analysis and is employed in later sections. In order to avoid such complexity in the early stages of this work, it was decided to initially study systems which are much better characterised such as the kinetically inert chromium(III) and cobalt(III) ions and the "established" 5 co-ordinate aqua-zinc ion $[Zn(CR)H_2O]^{2+}$.[12] Aqua complexes were chosen since earlier studies revealed that co-ordinated water was important in such hydrolyses. In practice,

experiments with poly-aqua cobalt(III) species gave kinetically complex results indicating that some co-operative effects occur with poly-aqua ions, (Chapter 5). Initial experiments were, therefore, centred on reactions of well defined mono-aqua complexes such as $[Co(NH_3)_5(H_2O)]^{3+}$ and $[Cr(NH_3)_5(H_2O)]^{3+}$. For comparative purposes the macrocyclic complex $[Co([15]aneN_5)(H_2O)]^{3+}$ (where $([15]aneN_5)$ = 1,4,7,10,13- penta-azacyclopenta decane [3.4]) and the labile $[(Cu(tmen)(H_2O)_2]^{2+}$ (where (tmen) = tetramethylethylenediamine) were included.

The important conclusion of these preliminary investigations is that for mono-aqua metal ions, a deprotonation of a co-ordinated water molecule is necessary to significantly enhance the rate of hyrdolysis of a phosphate or phosphonate ester. No marked increase in rate was observed below the apparent pK of each coordinated water molecule. Indeed, for the $[Co(NH_3)_5(OH)]^{2+}$ based systems, rates calculated on the basis of a known k_m and pK in conjunction with equation (3.1) can be superimposed with accuracy on the experimentally observed rates. The simulated curve has a best fit at pK 6.28. This value is in excellent agreement with the practical pKa of 6.32, determined titrimetrically. Thus, one of the prime functions of the metal ion in simple non-labile mono-aqua systems is to provide a high concentration of potential nucleophile at low pH. In effect this means that the metal

lowers the pK of water molecules through an inductive effect. It is of interest to compare the role of the inert ligand system of both cobalt(III) complexes in these reactions. The penta-aza macrocyclic ligand [3.5] is a stronger sigma-donor than NH_3 which is expected to affect Lewis acidity of the cobalt(III) centre and hence the pKa and nucleophilicity of the hydroxo-ligand. The practical pKa value of $[Co([15]aneN_5)OH_2]^{3+}$, was determined by potentiometric titration at 35°C and I = 0.1 ($NaClO_4$) to be 6.1. In effect, this constant is not markedly different from that observed for $[Co(NH_3)_5(OH_2)]^{3+}$ where under similar experimental conditions a pK of 6.3 is reported[10]. Comparison of the reaction rates of the two complexes towards DNPDEP (Table 3.3) shows only a slight increase in reactivity of the macrocyclic complex over that of the pentamine complex. This observation is in agreement with other results, discussed later, that suggest a non-nucleophilic pathway for the interaction of inert mono-aqua complexes with the phosphorus esters under study.

These initial studies show that metal complexes can catalyse the degradation of both phosphonate and phosphate esters with deprotonation of a co-ordinated water nucleophile a key initial step. Subsequent reactions are more varied but for simple mono-aqua non-labile complexes, a general base catalysed displacement of the leaving group

would seem likely. Poly-aqua and highly labile complexes of copper(II) and zinc(II) offer some potentially very attractive catalyst systems since their observed rates of reaction can be several orders of magnitude above those predicted by general base catalysis theory.

A study of these labile systems utilising computer programs to determine the active species in solution is reported in later sections. It is not until the nature of the active species is identified that the mechanisms of their very fast reactions can be understood. Future studies should not incorporate buffers as they themselves can contribute to hydrolysis rates.

3.4.2 REACTION WITH OTHER NUCLEOPHILES

An important question to be answered, both from a mechanistic and from a practical viewpoint, in considering the viability of metal based systems is whether or not the presence of water is essential for the catalytic system to function. This will have considerable bearing on the mode of use of possible metal complex systems both in the field of decontamination and analysis of CW agents. At a molecular level, the problem reduces to a consideration of the various mechanisms by which CW agent may be degraded. Together with the inert metal complexes outlined it was decided to investigate a series of simple bases in order to facilitate the assignment of mechanisms. Two possible mechanisms open for consideration for the attack of phosphorus esters by such nucleophiles are shown below.

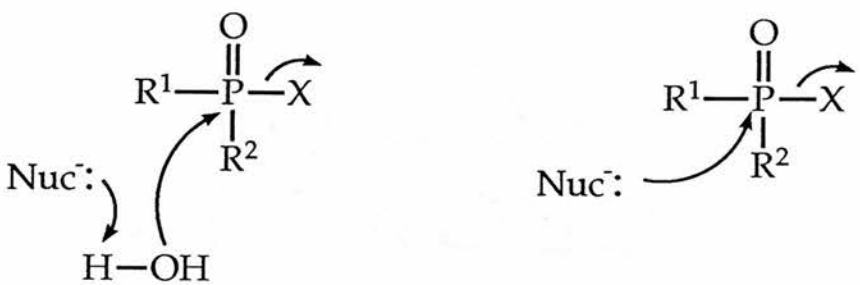

a) general base catalysis

b) nucleophilic catalysis

[Scheme 3.1]

When, (a) general base catalysis (GBC) takes place water plays an important role in the mechanism of the reaction where as the solvent is not necessarily involved in any reaction involving, (b) direct nucleophilic displacement (Scheme 3.1). There is much data in the literature[16,17] concerning the kinetics of degradation of phosphorus esters which offers conflicting evidence as to wether GBC or nucleophilic attack occurs. For instance, heterocylic amines such as pyridine and imidazole as well as ionic nucleophiles such as acetate, bicarbonate and phosphate have been demonstrated to react with phosphonyl phosphorus[18,19]; these reactions have been regarded as general base catalysis since they failed to demonstrate any steric hindrance effects. Thus, 2-methyl pyridine has the same reactivity as pyridine.[20]. From these and other studies lack of steric effect has come to be regarded as diagnostic of general base catalysis. There is, however, also experimental evidence for direct nucleophilic attack on phosphorus. Ashbolt and Rydon[21] have demonstrated that if tyrosine is reacted with di-isopropylfluorophosphate at pH 7.8 in aqueous solution, di-isopropylphosphonylation of the phenolic hydroxyl group occurs. There are also reports that phosphonylated phenols can be obtained from reactions of Sarin with phenols[22].

In considering the possibility that GBC is the preferred mechanistic pathway of the reactions examined in this section, it is benefical to relate the structure of a catalyst to its catalytic activity by means of its pKa. The general form of this relationship which is known as the Bronsted Catalysis Law is given by

$$k_B = G_B(1/K_a)^B$$

where k_B is a rate constant, G_B is a constant for a particular reaction, B is the Bronsted slope and K_a is the dissociation constant for the conjugate acid of the base. This can be rearranged to give,

$$\log(k_B) = BpK_a + \text{constant}$$

Hence, a plot of $\log(k_B)$ versus pK_a will yield a straight line for a series of nucleophiles operating by a similar GBC mechanism.

The evidence available from the present research for both phosphorus esters (Table 3.3, Figure 3.5 and Table 3.4, Figure 3.4) clearly shows that the majority of nucleophiles investigated lie on a fairly good GBC Bronsted plot. The noticeable exceptions are O_2H^-(2), 2-iodosobenzoate (10), F^- (16) and [Cu(tmen)$(OH_2)_2$](11) which will be discussed later. However, care should be taken in immediately assigning a GBC

mechanism solely on the criterion of a single Bronsted plot. A group of similarly related reactions occurring by way of direct nucleophilic attack will also yield a linear Bronsted plot. These processes can be distinguished by examining the data obtained for bases which because of steric hindrance, are known to be non-nucleophilic in character. If such bases behave in a manner predicted by the given Bronsted plot, it is good evidence for GBC rather than direct nucleophilic attack. Several such non-coordinating bases were included amongst the compounds examined, (triethylamine(3), DBU(5), DBN(7)). As these hindered bases lie on the same Bronsted plot as all the other bases investigated, including the inert mono-aqua metal complexes, is reasonable to presume that all the reactions are proceeding via general base catalysis.

Additional support for a GBC mechanism is given by the values of 1.3 and 1.2 (for DNPEMP and DNPDEP respectively) for the deuterium isotope effect in the triethylamine reactions. Nucleophilic reactions in this case do not involve proton transfer in the rate determining step and a value of k_H/k_D close to unity would be expected, as observed for the imidazole catalysed hydrolysis of p-nitrophenylacetate[23] which is recognised to take place via a nucleophilic displacement.

The criterion of a positive deuterium isotope effect also should only be used in conjunction with other evidence since other effects such as solvation can contribute to the result. When the slope of the plots in Figures 3.2, and 3.3 are determined (excluding points obviously above the lines, i.e. numbers 2,10,11 and 16), a Bronsted slope can be determined for the GBC hydrolysis for 2,4-DNPDEP and 2,4-DNPEMP. The values obtained from these slopes are 0.52 and 0.38 respectively. These values are fairly typical for other phosphate esters such as DFP[20], GB[24], and GD[25] which yield values at 25°C of 0.42, 0.49 and 0.52 respectively.

A comparison of the activation parameters for the G-agents and the simulant esters (Table 3.10) indicates their worth as suitable simulants to facilitate studies of metal catalysed hydrolysis. It is also of interest to note that the absolute rates of hydrolysis of GB and DNPEMP are very similar with values of 25.8 mol sec^{-1} and 24.2 mol sec^{-1} respectively at 25°C. This means that a Bronsted plot for GB would almost superimpose the plot obtained for DNPEMP. The reported data thus serves to confirm the choice of DNPEMP as an excellent simulant for G-agent hydrolysis studies.

The construction of a Bronsted plot as illustrated in Figure 3.3, provides a very useful procedure for comparison of the performance of potential catalysts under the

TABLE 3.10 Summary of activitation parameters for G-agent and simulant hydrolysis

phosphorus ester	$\Delta H^{\neq}$ /KJ mol^{-1}	$\Delta S^{\neq}$ /J $mol^{-1}K^{-1}$
GB	37.8	-100
GD	41.6	-92
DNPEMP	39.8	-84
DNPDEP	44.4	-105

practical reaction conditions required for there utility. For example, many compounds, especially amines, function well as a result of the high pK values of there conjugate base, a property which unfortunately means that extreme conditions of pH are required for there use. At more neutral pH values, hydrolysis still occurs but at a much reduced rate. In contrast the mono-aqua metal complexes studied here which show small enhancements from general base rates operate close to neutrality. (In the case of the copper-(tmen) complex the enhancement is significantly larger and further study is warranted. These complexes and other poly-aquo species show great promise as potential catalysts and a more detailed study of their interaction with phosphorus esters is undertaken in later sections). In general, an order of magnitude enhancement in hydrolysis rates was obtained by the use of the mono-aqua metal complexes. An improvement which in view of their catalytic properties, is of particular interest for the development of a non-corrosive decontamination system. Figure 3.3 shows also that much more marked rate enhancements were obtained for species such as F^-(16), HO_2^-(2) and 2-iodosobenzoate (10). Similar enhancements with these ions have been noted previously [26,27].

The high reactivity to these compounds and others such as oxines, has been attributed to bifunctionality as exampled illustrated below,

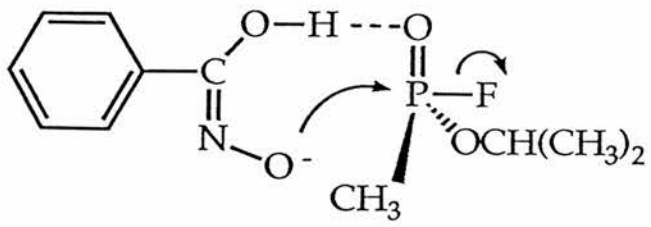

[Scheme 3.2]

or to the α - effect described by Edwards.[28] The origin of the α - effect rate enhancement is postulated to result from the juxtaposition of two atoms with unshared electrons. In this category are HO_2^-, OCl^- and iodosobenzoate with electron rich O, Cl and I atoms immediately adjacent to the nucleophilic oxygen atom.

The reaction with fluoride presents an interesting anomally. Comparison of activation parameters given in Table 3.9 shows that large differences exist in $\Delta S^{\neq}$ for the reaction of fluoride in water and D_2O. Thus a large entropic term would appear to be involved and solvation of the small fluoride ion would appear on first inspection to play an important part in the chemistry of displacement at P(V) by F^- in aqueous systems. Studies on the reactions of 2- iodosobenzoate have been carried out by several

groups[27,29] in view of its obvious potential as a decontaminant. Much of the work has been in surfactant media and a mechanism involving nucleophilic displacement has been proposed.

In addition to their catalytic activity, a major advantage in the utilisation of metal complexes in general purpose CW decontamination systems is their potential ability to confer stability upon highly reactive chemical species. By this means it is hoped to overcome practical difficulties encountered in the use of currently available decontamination mixtures, namely their corrosive action against construction materials and the logistics of field deployment. In the present study a comparison of the reactivity of a number of complexes of Co, Cr, Cu and Zn with two commonly encountered CW agent decontaminants, diethylenetriamine and hypochlorite ion has been carried out. Diethylenetriamine is the major constituent of the primary in-service decontaminant for the USA and several NATO armies, whilst hypochlorite bleaches are utilised by virtually all nations. The studies reported here, Figure 3.3, show that the rates of hydrolysis achieved by the Cu complex are comparable with those exhibited by hypochlorite ion and greater than those achieved by diethylenetriamine. A further advantage of the Cu complex species is that it is expected to offer a greatly enhanced longevity in solution over the highly unstable hypochlorite ion, and has a very

useful reduction in basicity (ca. two pH units) below that of diethylenetrimine.

3.5 CONCLUSIONS

1. Deprotonation of a co-ordinated water molecule, is the important initial step in the metal complex catalysed hydrolysis of phosphate and phosphonate esters.
2. General base catalysis is the likely operative mechanism by which most nucleophiles, including substitutionally inert mono-aqua metal complexes, catalyse the hydrolysis of the phosphorus esters described.
3. Millimolar concentrations of the copper(II) complex of tetramethylethylenediamine dramatically enhance the rates of hydrolysis around neutral pH. A more detailed knowledge of the species in solution is required before the high reaction rates can be fully understood.
4. DNPEMP is an excellent simulant for hydrolysis studies on G-type CW agents.
5. The Bronsted plot provides a good datum line by which potential metal complex catalysts can be related to existing decontaminant species.

3.6 REFERENCES

1. T. Wagner-Jauregg, B.E. Hackley, T.A. Lies, O.O. Owens and R. Roper, J. Am. Chem. Soc., 77, 922 (1955).
2. R.L. Gustafson and A.E. Martell, J. Am. Chem. Soc., 84, 2309 (1962).
3. R.C. Courtney. R.L. Gustafson, S.J. Westerback, H. Hyytiainen, S.C. Chaberek Jr. and A.E. Martell, J. Am. Chem. Soc., 79, 3030 (1957).
4. F.Mc.C. Blewett and P. Watts, J. Chem. Soc. B, 881 (1971).
5. R.A. Kenley, R.H. Fleming, R.M. Laine, D.S. Tse and J.S. Winterle, Inorg. Chem., 23, 1870 (1984).
6. S.N. Gellman, R. Petter and R. Breslow, J. Am. Chem. Soc., 108, 2388 (1986).
7. P.R. Norman, Inorg. Chim. Acta, 130, 1 (1987).
8. F. Baslo, Inorg. Synth. 4, 171, (1953).
9. R.W. Hay and P.R. Norman, J. Chem. Soc., Dalton Frans., 1441, (1979).
10. J.E. Richman and T.J. Atkins, J. Am. Chem. Soc., 96, 2268, (1974).
11. H.F. Baver and W.C. Drinkard, J. Am. Chem. Soc., 82, 5031, (1960).
12. P. Woolley, J.Chem.Soc., Perkin Trans 2, 318, (1977).

13. J. Epstein and D.H. Rosenblatt, J. Am. Chem. Soc., 80, 3596, 1958.

14. R.L. Gustafson and A.E. Martell, J. A.M. Chem. Soc., 84, 2309, 1962.

15. A. Sabatine, et al, Talanta, 21, 53, (1974).

16. J.R. Cox, Chemical Reviews, 64, 317, (1964).

17. T.C. Bruice, "Bio organic Mechanisms" V2, Chapt 6, Benjamin (1966).

18. T. Wagner - Jauregg and B.E. Hackley, J.Am.Chem.Soc., 75, 2125, (1975).

19. F.H. Westheimer, Special Publication No. 8, The Chemical Society, London, (1957).

20. M. Kilpatrick, J.Phys.Chem., 53, 1371, (1949).

21. R.F. Ashbolt and N.H. Rydon, J. Biochem., 66, 273, (1957).

22. MOD Report.

23. W.P. Jencks, "Catalysis in Chemistry and Enzymology", Chapt.3, McGraw-Hill, (1969).

24. C.A. Bunton, J.Am.Chem.Soc., 83, 3214, (1961).

25. MOD Report.

26. J. Epstein, J.Am.Chem.Soc., 78, 4068, (1956).

27. L. Larsson, Acta.Chem.Scand., 12, 723, (1958).

28. J.O. Edwards and R.G. Pearson, J.Am.Chem.Soc., 84, 16, (1962).

29. R.A. Moss, K.W. Alwis and J.S. Shin, J.Am.Chem.Soc., 106, 2651, (1984).

CHAPTER FOUR

COPPER(II) COMPLEX CATALYSED HYDROLYSIS OF PHOSPHORUS ESTERS

4.1 INTRODUCTION

The detoxification of phosphorus(V) pesticides and nerve gases is a challenging problem in catalytic hydrolysis chemistry and has received considerable attention due to the possible significance for enzymic catalysis of phosphoryl transfer.

E.coli alkaline phosphatase[1] is a dimeric enzyme that catalyzes the nonspecific hydrolysis of phosphate monoesters. Each active site contains three M^{2+} ions, of which two are Zn^{2+} separated by 3.9A and which are required for enzymatic phosphorylation and dephosphorylation. One Zn^{2+} is co-ordinated to three histidine imidazole groups and the other one to one histidine imidazole and two aspartate carbozylate groups. Also present at the active site is an essential serine. The mechanism of hydrolysis (illustrated in Scheme 4.1), involves nucleophilic displacement by the serine hydroxyl group of a phosphate monoester to form a phosphoryl serine intermediate. This is followed by a second displacement at phosphorus by a zinc bound hydroxide for overall retention of configuration. In addition to activating a co-ordinated H_2O, the co-operative roles of the Zn^{2+} ions are thought to: (i) neutralize the negative charge of the phosphate monoester; (ii) reduce the pKa of the attacking ser-OH group; (iii) assist by co-ordination the departure of the leaving group.

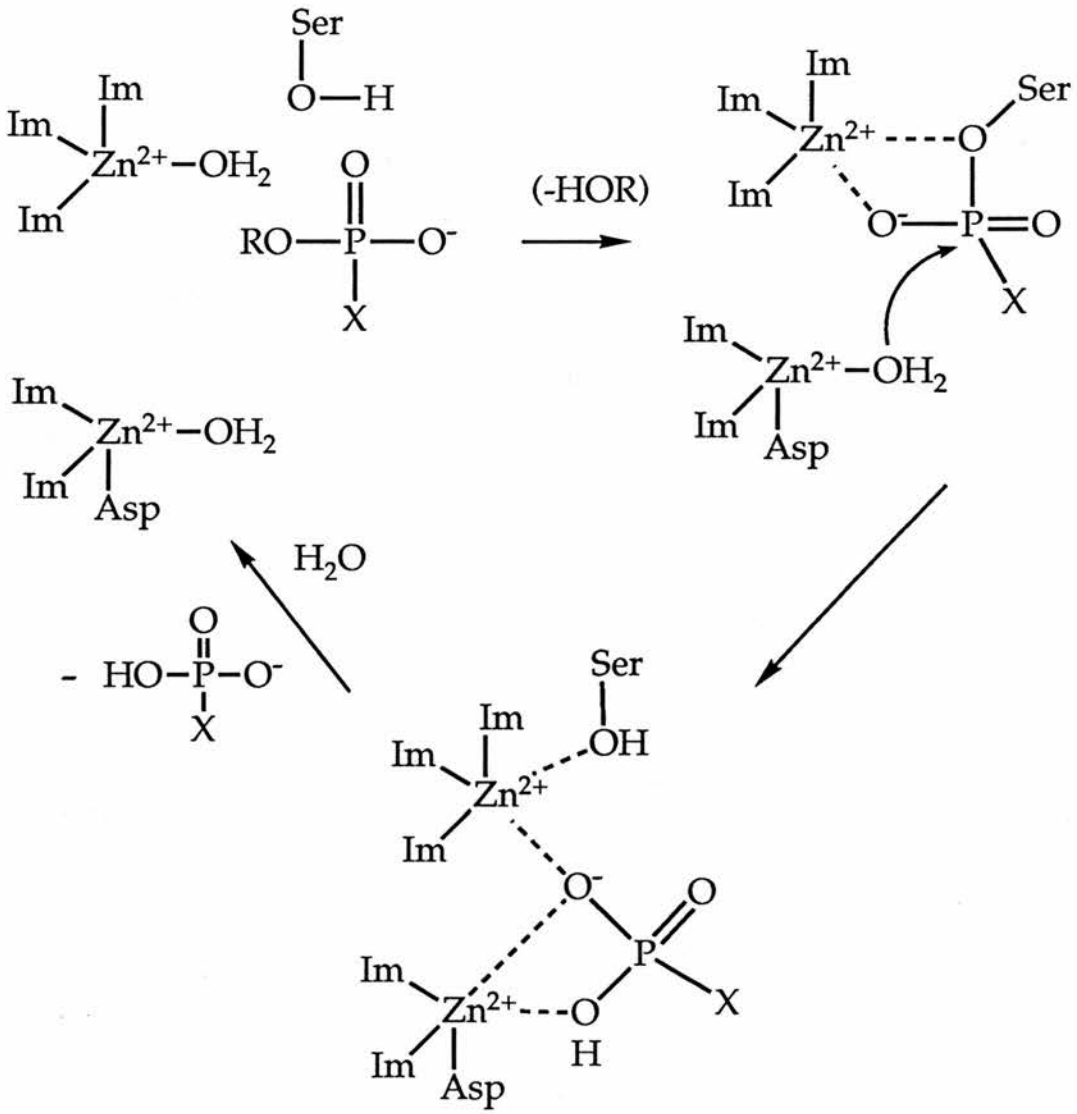

Scheme 4.1 Mechanism of alkaline phosphatase enzyme hydrolysis of phosphate monoester:X=O$^-$,OH.

Divalent metal ions are required in most enzyme catalysed nucleophilic displacement reactions at phosphorus(V) and are therefore a logical choice in the search for catalysts to promote hydrolysis of man-made phosphorus(V) toxins. It should be noted that phosphate triesters are apparently not prominent naturally occurring substances, and enzymes that catalyse phosphoryl transfers in living systems typically act upon anionic substrates. As part of our attempt to design metal complexes which are highly catalytic in the hydrolysis of phosphate esters we have investigated the mechanism of hydrolysis of the phosphate triester 2,4-DNPDEP [2.2] with a series of copper(II) complexes.

Of particular interest as catalysts are the 1:1 copper(II) chelate complexes, which are sufficiently stable in solution at pH values much higher than that at which the aquo metal ion would precipitate as the hydroxide and thus become unavailable for homogeneous catalysis. Such a metal chelate would be particularly effective as a catalyst for the activation of a substrate which can co-ordinate to the metal ion in the chelate compound (e.g. via the phosphoryl oxygen in 2,4-DNPDEP). The interaction of the substrate with the metal ion would increase its reactivity toward potential nucleophilic reagents such as solvent molecules, hydroxyl ions or other co-ordinated species in accordance with the following scheme 4.2.

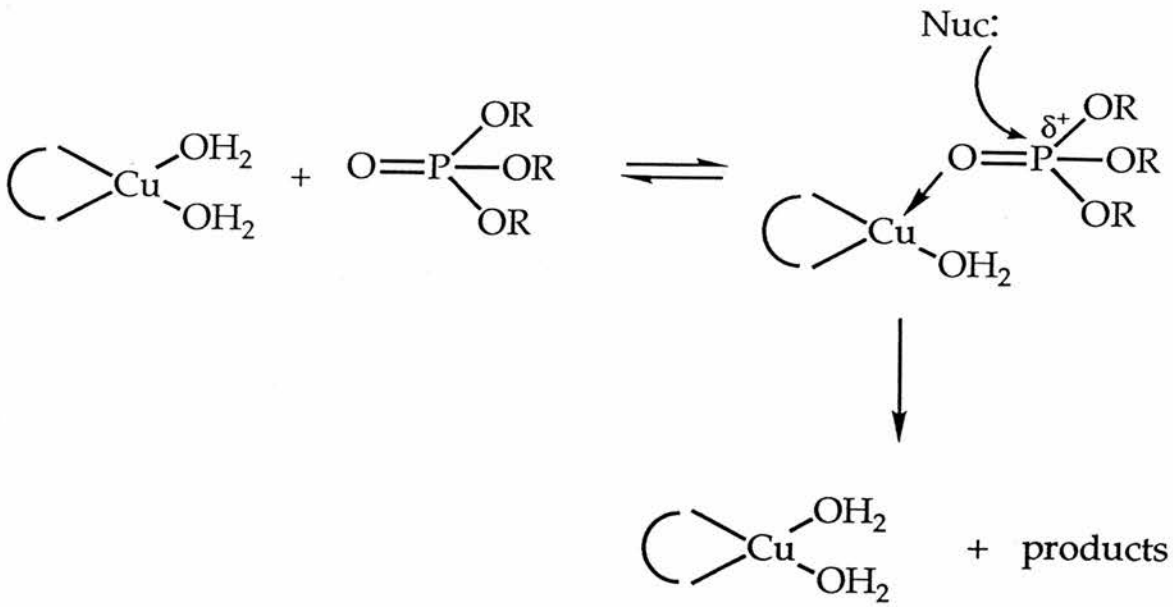

[Scheme 4.2]

Because the electronic interaction of the metal ion with the substrate is considerably less than that of the hydrogen ion, the metal ion can be looked upon as a "sub-proton" in these catalytic reactions. Thus, the catalytic activity of the hydrogen ion, if available at the same concentration (and conditions) as the metal chelate, would be expected to be much greater. Although the metal chelate is an extremely weak Lewis acid, it has some special properties not possessed by the proton. By virtue of its co-ordination number, size, and the steric requirements of its co-ordinate bonds, it would be expected to have high degree of specifity with respect to both the nature of the substrate with which it combines and the selectivity of interaction of the specific groups within the ligand. The hydrolysis of fluorophosphates such as methylisopropylphosphonofluoridate (Sarin) and

diisopropylphosphonofluoridate (DFP) has been found to be promoted by a number of metal ions and metal chelate complexes, [Scheme 4.3][2]. The hydrolysis reactions are generally first order in metal chelate concentration, in substrate concentration, and in hydroxyl ion.

As is suggested by these examples, the catalytic activity decreases as the negative charge of the ligand increases, and as the number of co-ordination positions on the metal ion which are satisfied by the ligand increase. For a completely co-ordinated and stable metal chelate, such as copper(II)-trien, there is very little activity. The aquo metal ion is generally the most effective catalyst, but its pH range of solubility is so low that very little free Cu^{2+} ion is in solution in the pH range (7 or higher) where the hydroxide ion is available in sufficient concentrations to give a reasonably high rate of hydrolysis. For metal chelates and complexes of copper(II), it was seen to be necessary to have at least a bidentate donor co-ordinated to the metal ion to achieve reasonable stability in dilute solutions, so that the most effective copper(II) complexes were those having a 1 to 1 molar ratio of bidentate ligand to metal ion.

Other early studies[3-5] have also demonstrated that divalent metal complexes contribute to impressive rate enhancements in neutral phosphorus ester hydrolysis. However the divalent metal ion complexes, as a class, are

Scheme 4.3 Observed-first-order reaction half-lives of the hydrolysis of Sarin by copper(II) chelate complexes at 25°C and pH 7.0. [Sarin] = [complex] = 10^{-3}M

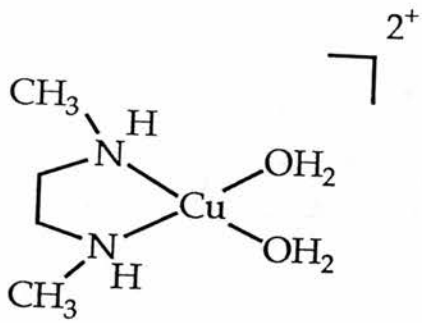

N',N'-Dimethylethylenediamine-Cu(II) complex; t.5 = 3.5 min.

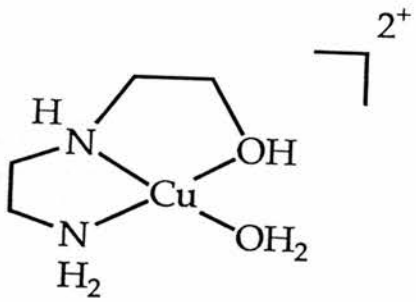

N-Hydroxyethylethylenediamine Cu(II) complex; t.5 = 15 min.

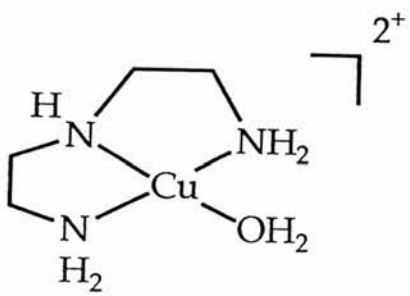

Diethylenetriamine - Cu(II) complex; t.5 - 25 min.

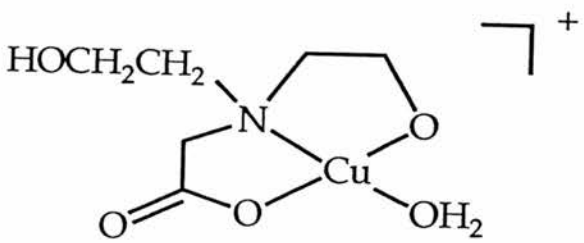

N,N-Dihydroxyethylglycino-Cu(II) complex; t.5 = 25 min.

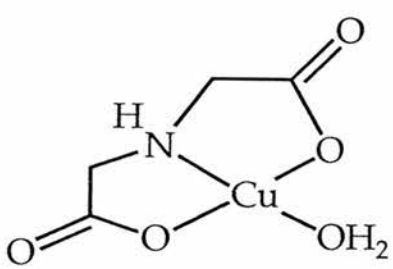

N-Hydroxyethyliminodiacetato-Cu(II) complex; t.5 = 57 min.

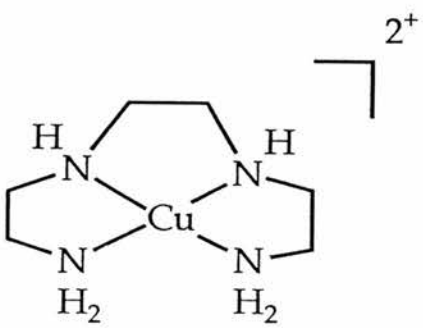

Triethylenetetramine-Cu(II) complex; t.5 = 65 min.

extremely labile toward solvolytic ligand displacement and the simultaneous presence in aqueous solution of monomeric, dimeric, and hydrated complexes seriously complicates reliable identification of the species actually involved in the ester hydrolysis. Thus, despite numerous publications that demonstrate the ability of metal complexes to accelerate hydrolysis reactions at neutral phophorus(V) centres the precise mechanism of these reactions remains unclear.

More recent investigations have shown that M-OH species are the likely active compounds in the hydrolysis of phosphate esters[6-8] (see also Chapter 2). Deprotonation of a co-ordinated water molecule,

$$M - OH_2^{2+} \rightleftharpoons M - OH^{+} + H^{+} \qquad pK_a$$

to give a hydroxo complex is required for catalysis to occur.

In view of the foregoing, a series of copper(II) complexes have been prepared and characterised as potential catalysts. A number of these complexes involve the use of bulky ligands (e.g. tetramethylethylenediamine, (tmen)) which inhibit the formation of bis complexes and so provide two sites for the formation of an aqua complex. The d^9 copper(II) ion has tetragonal stereochemistry due to John Teller distortion in which there are only weak interactions

Scheme 4.4 Structure of copper catalysts in solution.

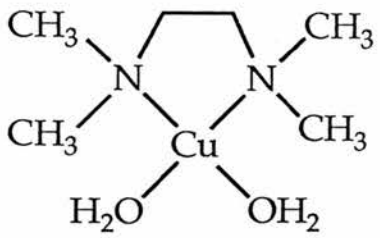

$[Cu(tmen)(OH_2)_2]^{2+}$

[4.1]

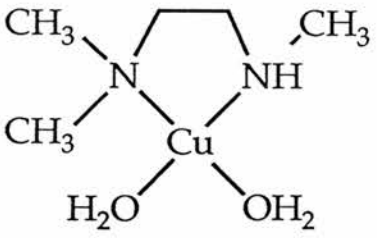

$[Cu(trimen)(OH_2)_2]^{2+}$

[4.2]

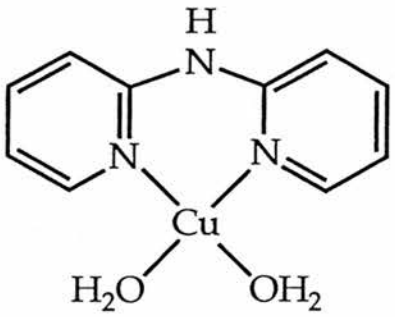

$[Cu(dpa)(OH_2)_2]^{2+}$

[4.3]

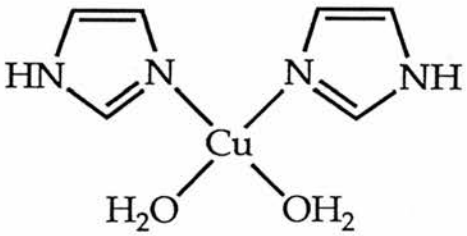

$[Cu(imid)_2(OH_2)_2]^{2+}$

[4.4]

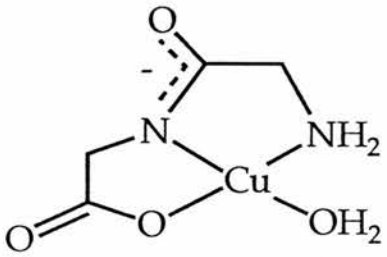

$[Cu(glygly\text{-}2H)(OH_2)]^{2+}$

[4.5]

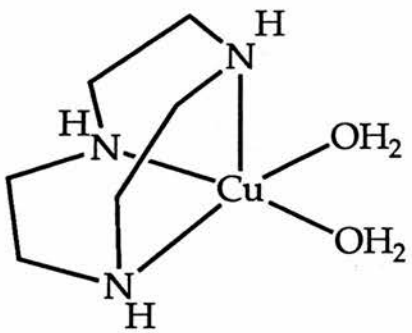

$[\,Cu([9]aneN_3)(OH_2)_2\,]^{2+}$

[4.6]

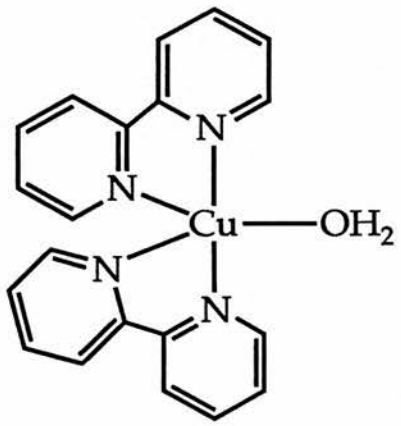

$[\,Cu(bipy)_2(OH_2)\,]^{2+}$

[4.7]

in the axial sites. The complexes prepared are summarised in Scheme 4.4. The complexes were employed as catalysts for the hydrolysis of 2,4-DNPDEP. Several of these complexes greatly accelerated liberation of 2,4-dinitrophenolate (DNP). Moreover, the reactions are truly catalytic with respect to the copper(II) complex, i.e. DNP yields are greater than the stoichiometeric amount on the basis of complex as limiting reagent.

In a effort to determine the "active catalytic species", in the hydrolysis of this phosphate triester, the speciation of copper(II) in the presence of the respective ligands has been studied. The speciation, i.e. the concentration and composition of each of these species, is dependent on the pH and the total copper(II) and ligand concentrations. The study into the possible correlation between the speciation and kinetics confirmed there is a direct correlation between the rate of hydrolysis and the concentration of a particular copper species, i.e. the mono-hydroxoaqua chelate $[Cu(L)(OH)(OH_2)]^+$.

4.2 EXPERIMENTAL

4.2.1 POTENTIOMETERIC TITRATIONS

In a typical titration, an aqueous solution of the metal complex (15 cm^3 of 2.5 x 10^{-3} mol dm^{-3}) was titrated with 0.1 mol dm^{-3} sodium hydroxide solution under a nitrogen atmosphere. Sufficient potassium nitrate was added to maintain the ionic strength at 0.1 mol dm^{-3}. Potentiometeric titrations were carried out using a Radiometer high performance Titra-lab system which employed G202B glass and K401 calomel electrodes. The electrode system was standardised before and after each titration with Radiometer standard buffer solution (pH 4.01 and 9.18). The temperature of the solutions was controlled at the desired temperature $\pm 0.1^{o}C$ by circulating water from a Haake FE thermostat.

4.2.2 KINETICS

The copper(II) complex catalysed hydrolysis of the phosphorus esters 2,4-DNPDEP and 2,4-DNPEMP was monitored using a Gilford spectrophotometer interfaced to an Apple II computing system. The initial release of 2,4-dinitrophenolate was measured at 400 nm, plots of log ($A_\infty - A_t$) versus time were linear for at least three half-lives. First-order rate constants (k_{obs}) were calculated from the slopes of the linear plots. Temperature was controlled by means of circulating water through the cell block from a Heto thermostat (35.0 $\pm$ 0.1^{o}C). In order to avoid complications due to buffer catalysis the metal complex was employed as the buffer system. Reactions were initiated by adding 50 µl of 5×10^{-3} mol dm^{-3} solution of phosphorus ester in CH_3CN to the spectrophotometer cell containing millimolar concentrations of metal complex previously adjusted to the desired pH. The reactions were first-order in phosphorus ester and excellent pseudo-first order kinetics were observed. Reaction rates were verified using the pH-stat technique described earlier (section 2.2.2). Allowing for experimental error a good correlation between rate constants derived from these different techniques was observed (see Table 4.1 for a typical comparison). All experiments were run in duplicate or triplicate, and tabulated data represent the average of these experiments.

Standard deviations were in the range 2 - 5%. Errors in rate constants was conservatively estimated from uncertainties introduced by temperature, pH, and stock concentrations fluctuations since least squares fitting errors were negligible. Generally, second-order rate constants were obtained from plots of observed first order rate constants against catalyst concentration.

4.2.3 SYNTHESIS OF COPPER(II) CATALYSTS

Preparation of [Cu(glygly-2H)H_2O]

To a stirred solution of $Cu(ClO_4)_2.6H_2O$ (3.71g, 10 mmol) in water (30 cm^3) was added glycylglycine (1.32g, 10 mmol) in water (30 cm^3). The solution was neutralised by the addition of ca 1M sodium hydroxide to pH7, and then dimethyl formamide was added (30 cm^3). The mixture was reduced to half volume on a rotary evaporator. On standing overnight, the complex crystalised as dark blue crystals which were filtered off, washed with ethanol, then diethyl ether and dried in vacuo.

Anal. Calcd. for $C_4H_8N_2O_4Cu$: C, 22.72; H, 3.92; N, 13.20. Found : C, 22.51; H, 3.74; N, 13.09%. The complex has a λ_{max} 638 (E = 68 $dm^3\ mol^{-1}\ cm^{-1}$) in water solvent. The complex is a non electrolyte in water with Λ_M = 2 5 $cm^2\ mol^{-1}$ at 25°C.

Preparation of $[Cu(bipy)_2](ClO_4)_2$

To a filtered solution of $Cu(ClO_4)_2.6H_2O$ (1.85g, 5 mmol) dissolved in the minimum volume of ethanol a solution of bipyridyl (1.55g, 10 mmol) in ethanol (50 cm^3) was added dropwise with stirring. The resulting blue precipitate was filtered off washed with successive portions of ethanol then diethyl ether and dried in vacuo.

Anal. Calcd. for $C_{20}H_{16}N_4CuCl_2O_8$: C, 41.79; H, 2.81; N, 9.75. Found : C, 41.65; H, 2.73; N, 9.36%. The complex has a λ_{max} 730 nm (E = 90 dm^3 mol^{-1} cm^{-1}) in water solvent. The complex is a 2:1 electrolyte in water with Λ_M = 188 S cm^2 mol^{-1} at 25°C.

Preparation of $[Cu(imid)_2Cl_2]$

In a typical preparation 1.0 cm^3 of 1 mol dm^{-3} $CuCl_2$ solution was added to 1 mol dm^{-3} imidazole solution (both aqueous solutions) and the pH adjusted to ca 5 by the addition of 0.1 mol dm^{-3} hydrochloric acid. Slow evaporation over a period of several days gave green needle like crystals which were collected by filtration, washed with ethanol and dried in vacuo.

Anal. Calcd. for $C_6H_8N_4CuCl_2$: C, 26.63; H, 2.98; N, 20.70. Found : C, 26.32; H, 2.92; N, 20.93%. The complex has a λ_{max} 682 nm (E = 75 dm^3 mol^{-1} cm^{-1}) in water solvent. The complex is a 2:1 electrolyte in water with Λ_M = 213 S cm^2 mol^{-1} at 25°C.

Preparation of $[Cu(tmen)Cl_2]$

A solution of N,N,N',N'-tetramethylethylenediamine (1.45g, 12.5 mmol) in ethanol (40 cm^3) was added dropwise with stirring to a filtered solution of $CuCl_2.2H_2O$ (2.55g,

15 mmol) in methanol (100 cm^3). The mixture was rotary evaporated to half volume. On standing overnight, the dark blue complex crystallised and was filtered off and recrystallised from methanol-ether and dried in vacuo.

Anal. Calcd. for $C_6H_{16}N_2CuCl_2$: C, 28.75; H, 6.43; N, 11.19. Found : C, 28.26; H, 6.42; N, 10.90%. This has λ_{max} 655 nm (E = 55 dm^3 mol^{-1} cm^{-1}). The complex is a 2:1 electrolyte in water with Λ_M = 202 5 cm^2 mol^{-1} at 25°C.

Preparation of [Cu(trimen)Cl_2]

A solution of N,N,N'-Trimethylethylenediamine (1.28 g, 12.5 mmol) in ethanol (40 cm^3) was added dropwise with stirring to a filtered solution of $CuCl_2.2H_2O$ (2.55g, 15 mmol) in methanol (100 cm^3). The mixture was rotary evaporated to half volume. The resulting blue precipitate was filtered off, washed with ethanol, recrystallised from methanol ether and dried in vacuo.

Anal. Calcd. for $C_5H_{14}N_2CuCl_2$: C, 25.35; H, 5.96; N, 11.84. Found : C, 25.59; H, 5.98; N, 12.01%. The complex has a λ_{max} 645 nm (E = 77 dm^3 mol^{-1} cm^{-1}). The complex is a 2:1 electrolyte in water with Λ_M = 222 S cm^2 mol^{-1} at 25°C.

Preparation of $[Cu(dpa)(H_2O)_2]^{2+}$ (in solution)

The ligand 2,2'dipyridylamine (dpa) was recrystallized twice from hexane and dried in vacuo. Concentrations of $Cu(NO_3)_2$ were determined by titration against ethylenediaminetetraacetic acid with murexide as indicator. An aqueous solution of 5×10^{-2} mol dm^{-3} $Cu(NO_3)_2$ and 2,2'dipyridylamine was prepared by stoicheiometric proportions and used as stock for the described experiments.

The complex has a λ_{max} 690 nm ($E = 94$ dm^3 mol^{-1} cm^{-1}) and behaves as a 2:1 electrolyte in water with 232 Λ_M = S cm^2 mol^{-1} at 25°C.

Preparation of $[Cu([9]aneN_3)Cl_2]$

The ligand, 1,4,7-triazacyclononane, was synthesized by a modification of the method described by Atkins[9], which utilizes the high degree of cyclization achieved by the reaction of the disodium salt of N,N',N"-tritozyldiethylenetriamine with the ditosyl derivative of 1,2-ethanediol (tosyl=Ts=p-toluenesulfonyl) [Scheme 4.5]. All reactions were carried out under a stream of dry N_2.

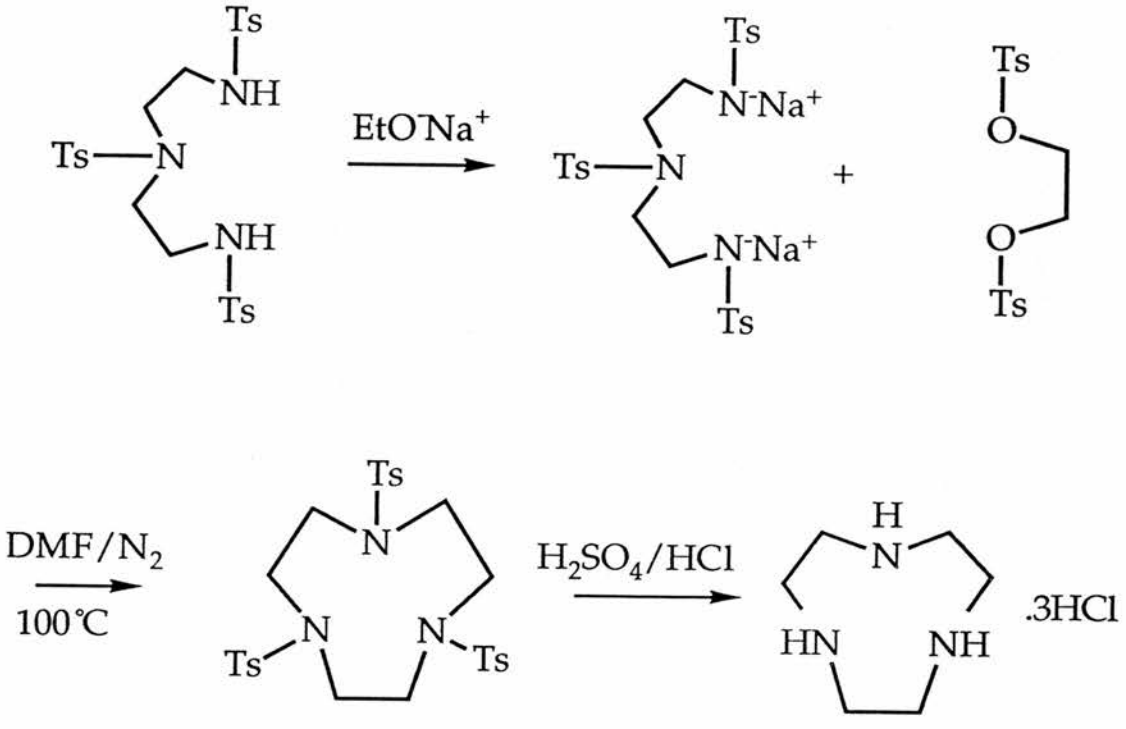

[Scheme 4.5]

1,4,7-Triazacyclcononane N,N',N"-Tritosylate

Disodium tritosyldiethylenetriaminate[10] (53 g, 0.086 mol) was dissolved in 350 cm^3 of dry DMF under a stream of N_2 in a flask (three necked) equipped with a mechanical stirrer. The solution was heated to 90°C, and a solution of (32 g, 0.09 mol) of 1,2-ethanediol ditosylate[10] in 180 cm^3 of dry DMF was added over a 45 min period. Initially the solution turned turbid, but on further heating 105°C (4 hours) the contents of the flask turned a clear golden yellow. The solution was allowed to cool to room temperature. The product was precipitated as a white powder by slow addition of the DMF solution to 2 dm^3 of rapidly stirred water. After filtration and washing with 500 cm^3 of water, the product was recrystallized from EtOH/H_2O and dried in a vacuum oven at 80°C, yield 38 g (74%):mp 220-223°C. ^1H NMR (TMS, $CDCl_3$) : 2.60 (q, 12H phenyl), 3.45 (s, 12H, methyl), 2.40 (s, 9H ethylene).

1,4,7-Triazacyclononane Trihydrochloride [4.8]

Twenty-five grams of the crude tritosyl derivative was dissolved in 120 cm^3 of concentrated H_2SO_4, and the mixture heated with stirring at 130°C for 48 hours. After cooling the solution was neutralized by slow addition of 300 g of NaOH dissolved in 600 cm^3 of water. The resulting solution

was allowed to cool at 0°C overnight to allow Na_2SO_4 to precipitate out. The supernatant was decanted into a continuous - extraction apparatus and extracted with 400 cm^3 $CHCl_3$ over a 3 day period. The solid sulphate was washed with 200 cm^3 of $CHCl_3$, the slurry formed being filtered through Whatman phase-separation paper to remove excess inorganic solid. The chloroform fractions were combined and taken to dryness on a rotary evaporator. Following dissolution in 25 cm^3 of ethanol and filtration, the ligand trihydrochloride was precipitated by addition of 10 cm^3 of concentrated HCl. The product was filtered washed with ethanol and diethyl ether, and air dried, yield 9 g (%). ^1H NMR (TMS, D_2O) : 4.00 (s), no aromatics. The ligand was used without further purification to synthesis of the copper(II) complex.

The macrocylic copper(II) complex [Cu([9]aneN_3)Cl_2] was prepared as follows. To an ethanolic slurry (15 cm^3) of [9]aneN_3 (1.24 g, 5 mmol) was added KOH (0.82, 15 mmol) and the solution was then heated at 60°C for 20 minutes. After cooling the solution was filtered into 10 cm^3 of and ethanolic solution $CuCl_2$ (0.85 g, 5 mmol). Blue crystals of the complex formed on slow evaporation of the solvent.

Anal. Calcd. for $C_6H_{15}N_3CuCl_2$: C, 27.33; H, 5.73; N, 15.94. Found : C, 27.23; H, 6.01; N, 15.88%. The complex has λ max 656 nm (E= 47 dm^3 mol^{-1} cm^{-1}) in water. The complex is a 2:1 electrolyte in solution with Λ_M = 235 S cm^2 mol^{-1} at 25°C.

4.3 RESULTS

The complex $[Cu(tmen)Cl_2]$ was readily characterised as dark blue crystals. On dissolution in water, the chloride ligands are displaced to give $[Cu(tmen)(OH_2)_2]^{2+}$ according to the equilibrium

$$[Cu(tmen)Cl_2] + 2H_2O \longrightarrow [Cu(tmen)(OH_2)]^{2+} + 2Cl^-$$

Thus the complex behaves as a 2:1 electrolyte and has a λ max 655 nm consistent with a CuN_2O_2 chromophore. Generally all the copper(II) catalysts described were characterised as crystals and the respective cationic species generated in solution. However, the complex $[Cu(dpa)Cl_2]$ was not isolated as a solid but the diaquo complex was prepared directly in solution as previously described.

4.3.1 POTENTIOMETERIC TITRATIONS OF COPPER(II) COMPLEXES

Potentiometric titration of $[Cu(tmen)(OH_2)]^{2+}$ with standard base leads to a well defined end point after addition of one equivalent of base, Figure 4.1. This end-point can be attributed to the ionisation,

Figure 4.1 Potentiometeric titration curve for $[Cu(tmen)(OH_2)_2]^{2+}$, (2.48 mM) with standard base (0.10 M) at 35°C, I=0.1(KNO_3).

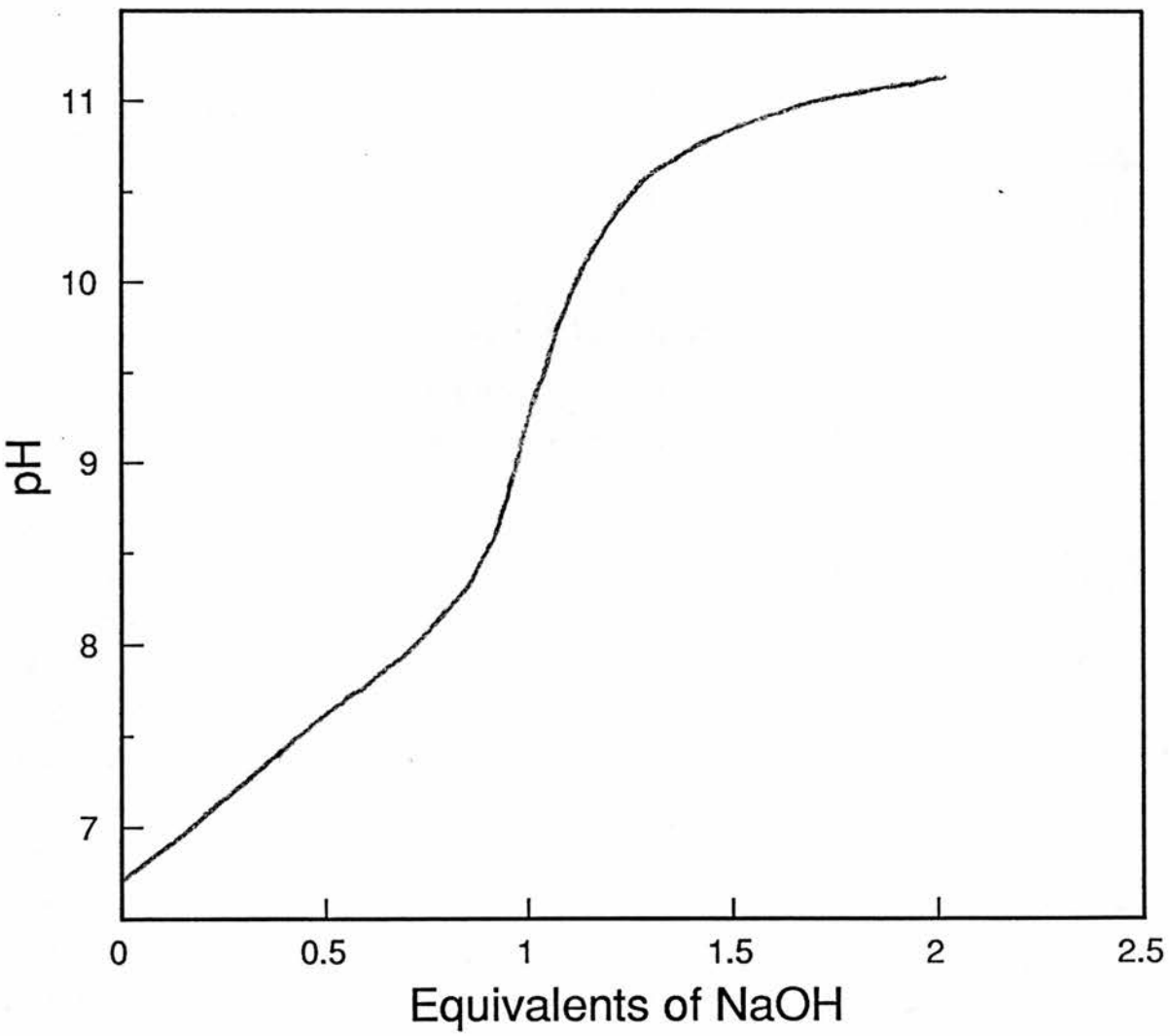

TABLE 4.1 The pK, values for $[Cu(tmen)(OH_2)_2]^{2+}$ at 35°C and I = 0.1 (KNO_3)

Volume NaOH 1 cm^3	pH	pK_1
0.04	6.85	7.58
0.06	7.06	7.57
0.08	7.23	7.57
0.10	7.39	7.58
0.12	7.53	7.58
0.14	7.67	7.58
0.16	7.82	7.58
0.18	7.96	7.59

* End point 0.255 cm^3 of 0.985 dm^{-3} sodium hydroxide

$$[Cu(tmen)(OH_2)_2]^{2+} \overset{K_1}{\rightleftharpoons} [Cu(tmen)(OH)(OH_2)]^{+} + H^{+}$$

to give the hydroxoaqua complex.

The pK values were calculated from the relationship

$$pH = pK + \log \frac{[A^-]}{[HA]}$$

and are thus practical ionisation constants involving the hydrogen ion activity and the concentrations of the other species. Such practical ionisation constants are required for interpretation of the kinetic data. A representative set of data for $[Cu(tmen)(OH_2)_2]^{2+}$ is given in Table 4.1. Analysis of the potentiometeric data gives $pK_1 = 7.58 \pm 0.02$ at 25°C and $pK_1 = 7.40$ at 35°C. The N-permethylated ethylenediamine sterically hinders the formation of bis complexes in solution and the 1:1 complex is predominately formed at 1:1 ligand ratios.

Potentiometric titrations of $[Cu(trimen)(OH_2)_2]^{2+}$, $[Cu(dpa)(OH_2)_2]^{2+}$, $[Cu([9]aneN_3)(OH_2)_2]^{2+}$ and $[Cu([9]aneN_3)(OH_2]^{2+}$ gave well defined end points after the addition of one equivalent of base. The pH titration curves for these complexes are shown in Figures 4.2, 4.3 and 4.4 respectively. The practical pKa values for the complexes determined at 25°C and 35°C from the titration data and are summarised in Tables 4.2 and 4.3 respectively.

Figure 4.2 Potentiometeric titration curve for $[Cu(trimen)(OH_2)_2]^{2+}$, (2.49 mM) with standard base (0.098M) at 35°C, I=0.1(KNO_3)

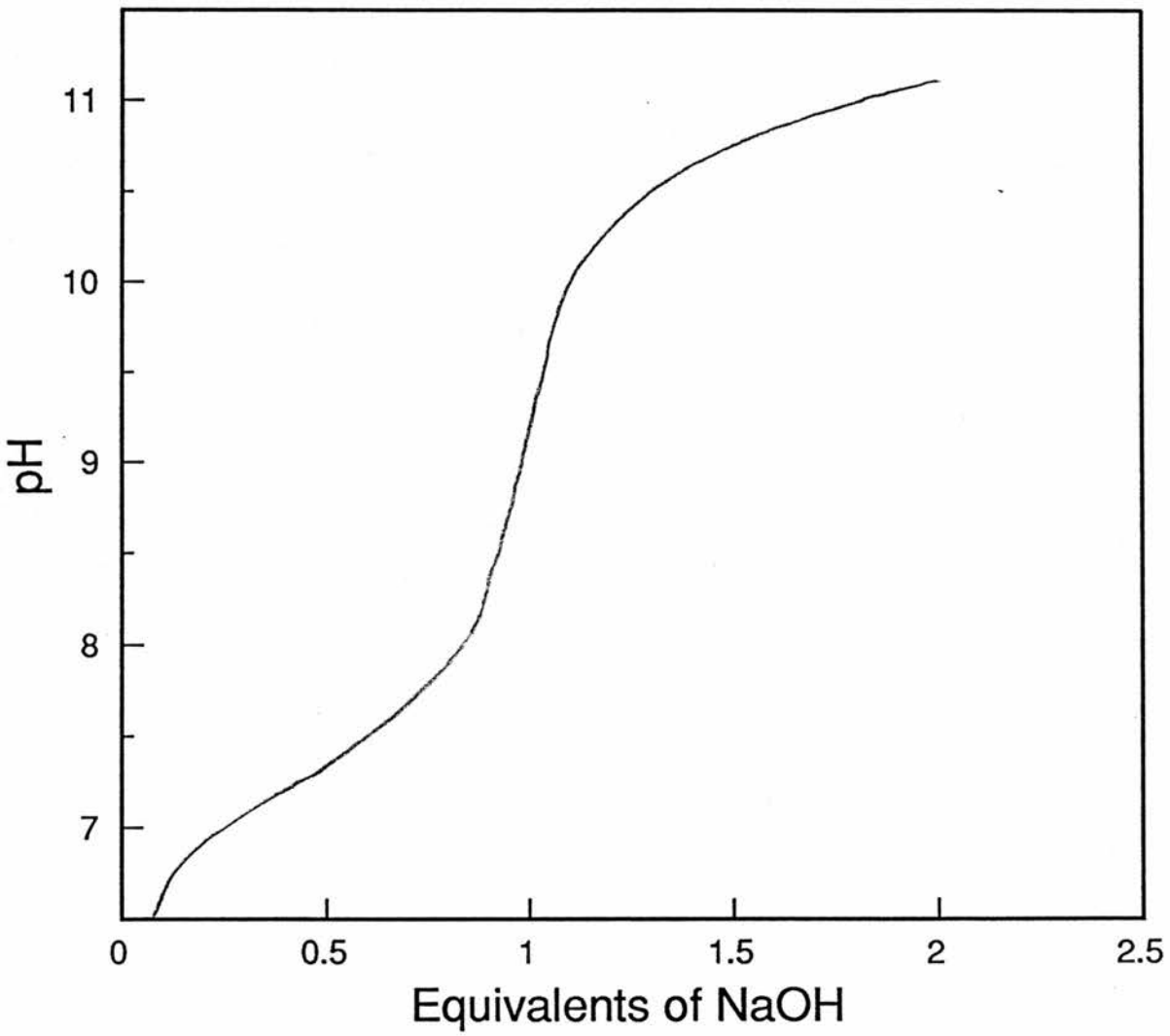

Figure 4.3 Potentiometeric titration curve for $[Cu(dpa)(OH_2)_2]^{2+}$, (0.54 mM) with standard base (0.102 M) at 35°C, I=0.1(KNO_3).

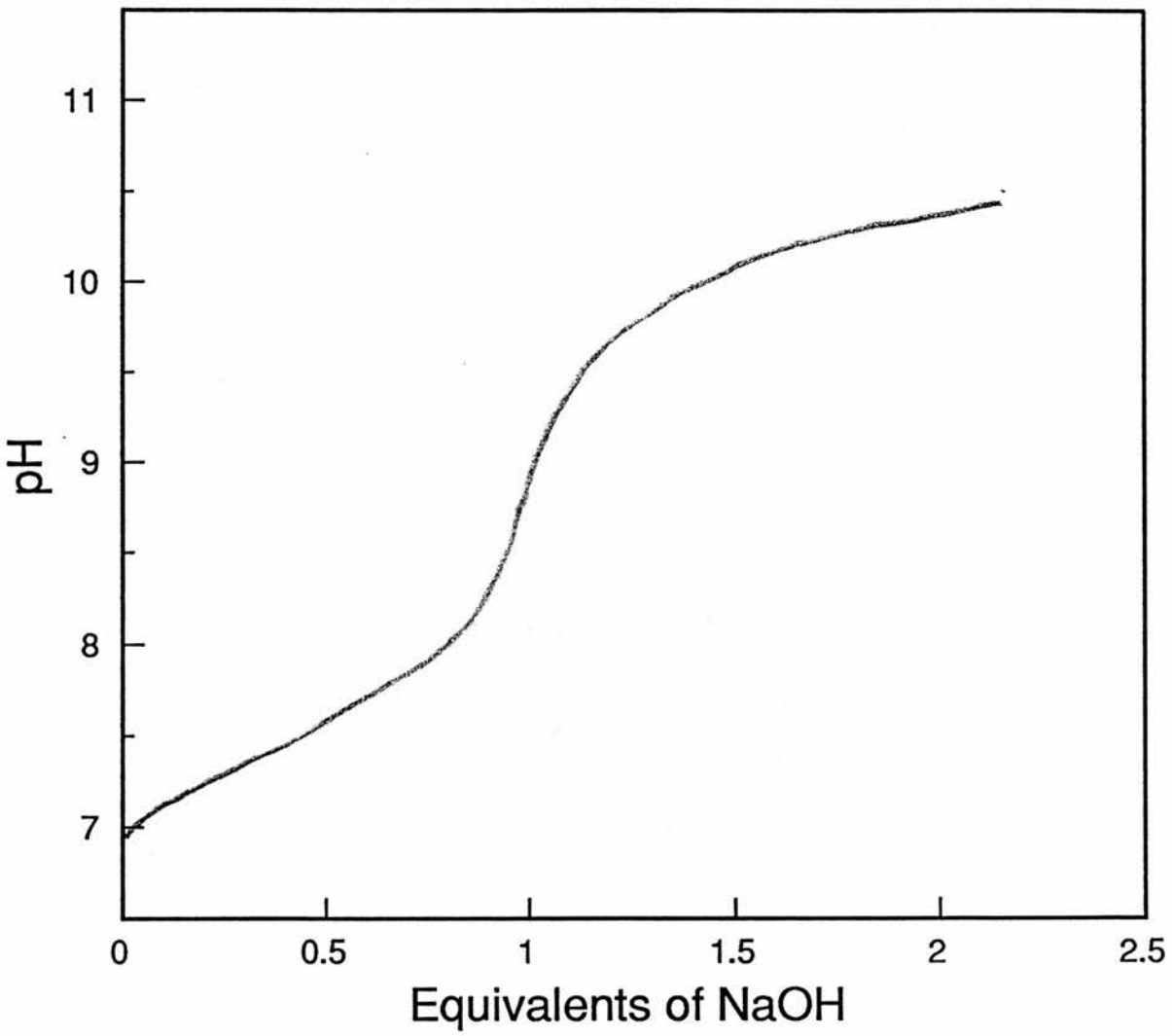

Figure 4.4 Potentiometeric titration curve for $[Cu([9]aneN_3)(OH_2)_2]^{2+}$, (2.49 mM) with standard base (0.099M) at 35°C, I=0.1(KNO_3).

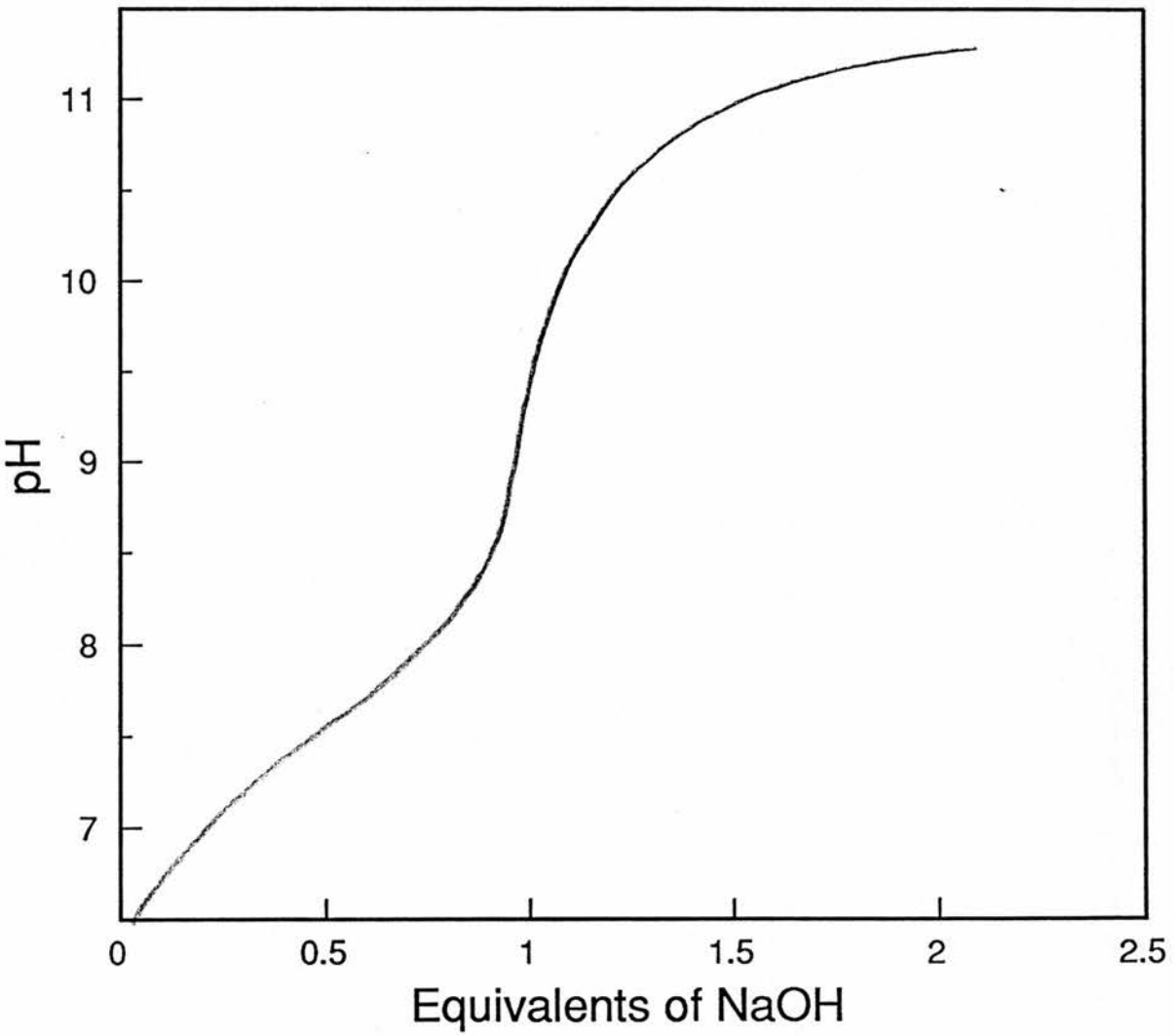

Conductivity data indicates that the bis-imidazole complex $[Cu(imid)_2Cl_2]$, behaves as a 2:1 electrolyte in water, according to the reaction

$$[Cu(imid)_2Cl_2] + 2H_2O \longrightarrow [Cu(imid)_2(OH_2)_2]^{2+} + 2Cl^-$$

Figure 4.5 shows the potentiometeric titration of the di-aqua complex (15 cm^3 of 2.49 x 10^{-3}M complex) with 0.1M NaOH. A definite end-point occurs after addition of two equivalents of base (0.748 cm^3 0.1H NaOH). The data can be interpretated on terms of two ionisation equilibria

$$[Cu(imid)_2(OH_2)_2]^{2+} \overset{K_1}{\rightleftharpoons} [Cu(imid)_2(OH)(OH_2)]^{+} + H^{+}$$

$$[Cu(imid)_2(OH)(OH_2)]^{+} \overset{K_2}{\rightleftharpoons} [Cu(imid)_2(OH)_2] + H^{+}$$

From this potentiometeric data it was possible to calculate pK_1 = 7.33 and pK_2 = 8.21 at 25°C and I = 0.1 M, Tables 4.2, 4.3.

The potentiometeric titrations of the copper(II) complex with glycylglycine is shown in Figure 4.6; two relatively flat zones were found. The first buffer region around pH4 indicates formation of $[Cu(glygly-2H)(OH_2)]$ with

Figure 4.5 Potentiometeric titration curve for $[Cu(imid)_2(OH_2)_2]^{2+}$, (2.49 mM) with standard base (0.10 M) at 35°C, I=0.1(KNO_3).

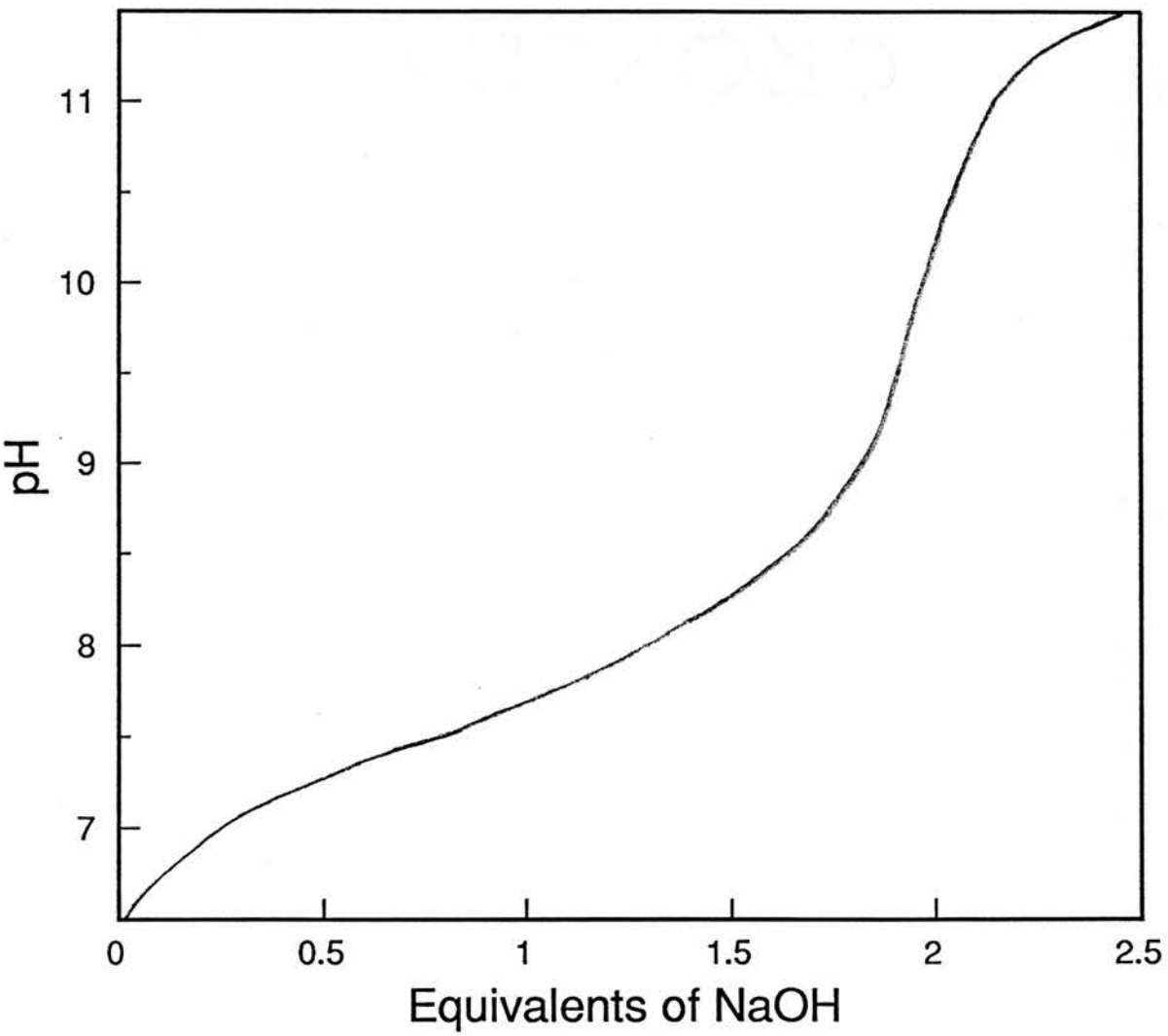

Figure 4.6 Potentiometeric titration curve for $[Cu(glygly)(OH_2)]^{2+}$, (5.0 mM) with standard base (0.10 M) at 5°C, I=0.1(KNO_3).

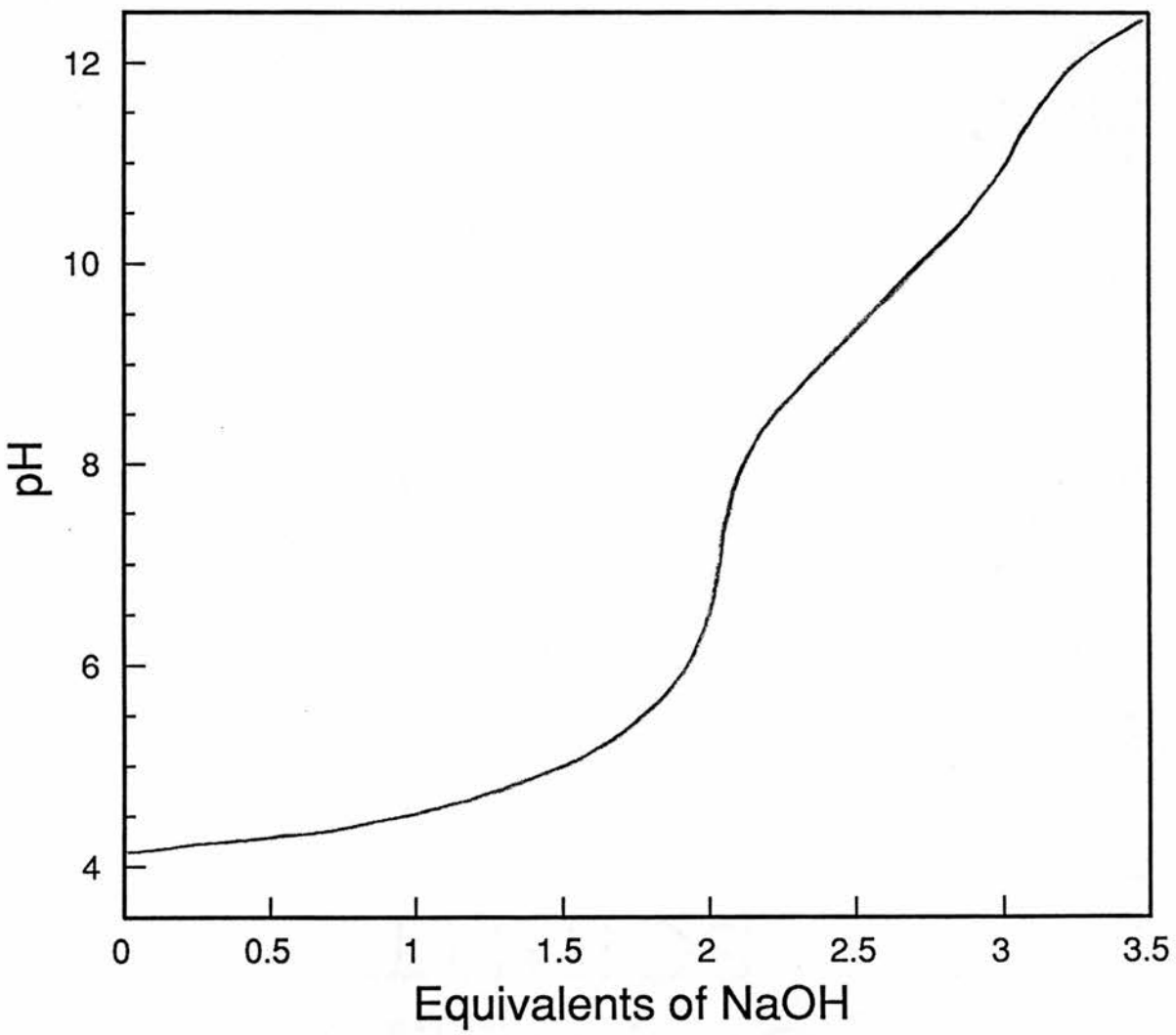

release of two protons, which agrees well with results already in the literature[11,12]. The second relatively flat buffer region shows a weak inflection in the higher pH region where the deprotonation of the co-ordinated water takes place. The various equilibrium involved in this system are summarised in Scheme 4.6.

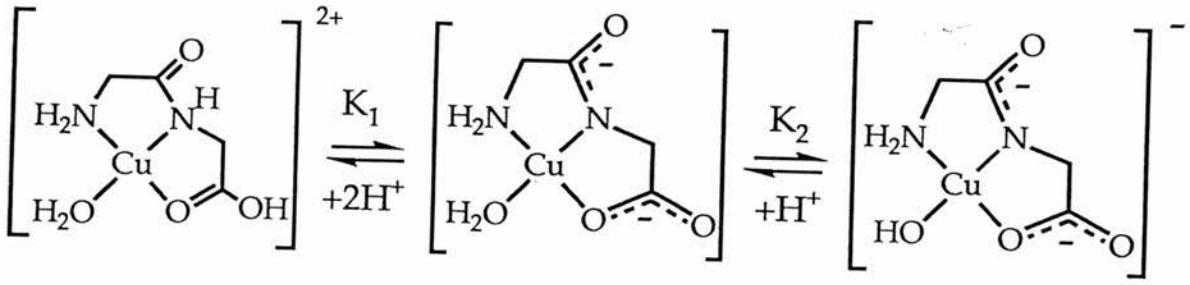

[Scheme 4.6]

From the titration results pK_1 and pK_2 were calculated to be 5.06 and 9.31 respectively. The pK_1 and pK_2 constants show that the fully deprotonated complex becomes the major species present in solution above pH 9.0. At pH 10 more than 95% of the complex is present as the deprotonated species.

Potentiometeric titration of $[Cu(bipy)_2OH_2]^{2+}$ did not lead to straight forward behaviour. In this case 0.5 moles of base was consumed per mole of complex. Polymeric reactions of $Cu(bipy)^{2+}$ forming hydroxo bridged dimers in significant concentrations and the presence of mono (bipy) hydroxo complexes is thought to significantly complicate the titration data.

TABLE 4.2 Summary of pK values determined for the copper (II) complexes at 25°C and I = 0.1 (KNO_3)

copper complex	pK_1[a]	pK_2[a]
$[Cu(tmen)(OH_2)_2]^{2+}$	7.50	
$[Cu(trimen)(OH_2)_2]^{2+}$	7.57	
$[Cu(dpa)(OH_2)_2]^{2+}$	7.26	
$[Cu(imid)_2(OH_2)_2]^{2+}$	7.33	8.21
$[Cu(bipy)_2(OH_2)_2]^{2+}$	-	
$[Cu([9]aneN_3)(OH_2)_2]^{2+}$	7.68	
$[Cu(glygly2H)(OH_2)_2]^{2+}$	9.23	

a) practical ionisation constants

TABLE 4.3 Summary of pK values determined for the copper (II) complexes at 35°C and I = 0.1 (KNO_3)

copper complex	pK_1[a]	pK_2[a]
$[Cu(tmen)(OH_2)_2]^{2+}$	7.35	
$[Cu(trimen)(OH_2)_2]^{2+}$	7.40	
$[Cu(dpa)(OH_2)_2]^{2+}$	7.13	
$[Cu(imid)_2(OH_2)_2]^{2+}$	7.19	8.06
$[Cu(bipy)_2(OH_2)_2]^{2+}$	-	
$[Cu([9]aneN_3)(OH_2)_2]^{2+}$	7.52	
$[Cu(glygly2H)(OH_2)_2]^{2+}$	9.08	

a) practical ionisation constants

4.3.2 SPECIES DISTRIBUTION PROFILES

Copper(II) in the presence of ligand (L) will form many different chemical species, such as $[CuL]^{2+}$, $[CuL_2]^{2+}$, $[Cu\ L\ OH]^{+}$, $[CuL(OH_2)]^{o}$. The speciation (i.e. concentrations and compositions) of each of these species at equilibrium conditions, depends on the pH and the total copper(II) and total ligand concentrations. In order to determine whether one particular species is solely responsible for the catalytic effect, the speciation of copper(II) in the presence of amine ligand over the pH range of interest was studied. The ligands tmen, trimen and glygly were selected for study and the speciation of their copper(II) complexes were determined by computer simulation.

The computer program used for this simulation is called ESTA 1 which is one of a suite of programs used at UWIST. This program used the theory described below to set up the mass balance equations for a multi-equilibria system and then solves them to calculate the concentration of all species present.

Equations 1 - 6 describe the interaction between a metal ion (M) and a protonated ligand (H_2L). The charges on the complexes have been omitted for the sake of simplicity.

$$H_2O \rightleftharpoons H + OH \quad ; \quad K_w = [H][OH] \qquad (1)$$

$$L + H \rightleftharpoons HL \quad ; \quad \beta_{011} = \frac{[HL]}{[L][H]} \qquad (2)$$

$$L + 2H \rightleftharpoons H_2L \quad ; \quad \beta_{012} = \frac{[H_2L]}{[L][H]^2} \tag{3}$$

$$M + L \rightleftharpoons ML \quad ; \quad \beta_{110} = \frac{[ML]}{[M][L]} \tag{4}$$

$$M + 2L \rightleftharpoons ML_2 \quad ; \quad \beta_{120} = \frac{[ML_2]}{[M][L]^2} \tag{5}$$

$$M + H_2O \rightleftharpoons MOH + H \quad ; \quad \beta_{10-1} = \frac{[MOH][H]}{[M]} \tag{6}$$

In these expressions, B is a formation constant and the square bracket denotes concentration.

In general for a metal complex $M_pL_qH_r$, we have a formation constant given by equation (7)

$$pM + qL + rH \rightleftharpoons M_pL_qH_r \quad ; \quad \beta_{pqr} = \frac{[MpLqHr]}{[M]^p[L]^q[H]^r} \tag{7}$$

Hence, the mass balance equations for the total proton (T_H), ligand (T_L) and metal (T_M) concentrations can be set up.

$$T_H = [H] + [HL] + 2[H_2L]$$

$$= [H] + \beta_{011}[L][H] + 2\beta_{012}[L][H]^2 \tag{8}$$

$$T_L = [L] + [HL] + [H_2L] + [ML] + 2[ML]$$

$$= [L] + B_{011}[L][H] + 2B_{012}[L][H]^2$$

$$+ B_{110}[M][L] + 2B_{120}[M][L]^2 \quad (9)$$

$$T_M = [M] + [MOH] + [ML] + [ML_2]$$

$$= [M] + B_{10-1}[M][H]^{-1} + B_{110}[M][L]$$

$$+ B[M][L]^2 \quad (10)$$

If the total component concentrations are known along with the relevant formation constants, it is possible to solve for [M] and [L] and obtain the equilibrium distribution of all species present.

The input parameters required for the program are given below:

1. The initial concentration of copper and ligand.
2. The formation constants of all species present, e.g. CuL^{2+}, $CuLOH^{+}$, $CuOH^{+}$ and others.
3. The background ionic strength.
4. The free acid concentration.

The ESTA program allows the operator to simulate the variation in concentration of all aqueous species with changing pH. A typical species distribution profile for the

copper(II) - N,N,N',N'-tetramethylethylene diamine system is shown in Figure 4.7. The vertical axis represents the percentage of total copper present as each of the species. Similar species distribution profiles have been determined for copper(II)-N,N,N'-trimethylethylenediamine Figure 4.8 and copper(II)-glycylylycine Figure 4.9.

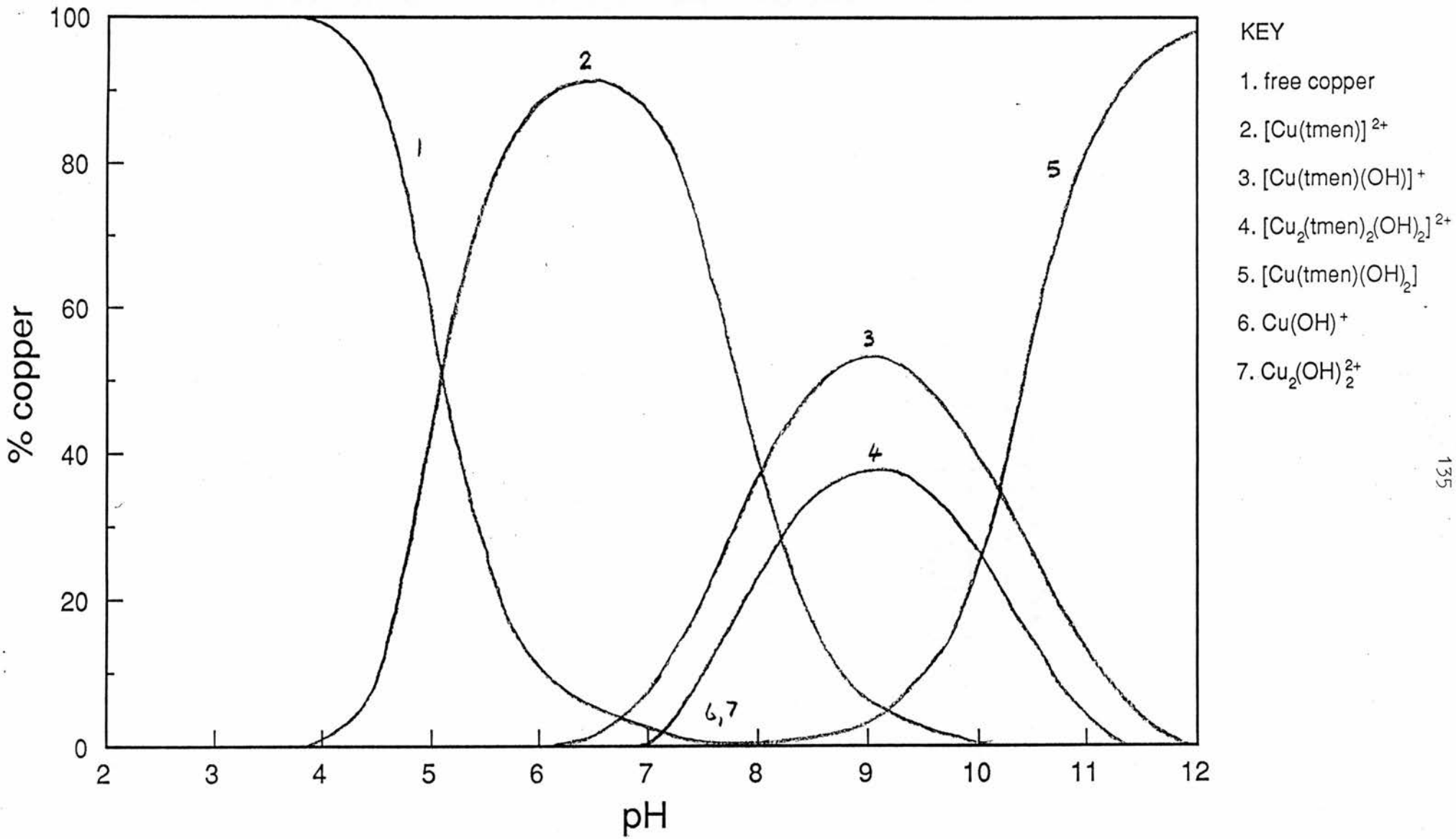

Figure 4.7 **Species Distribution Profile, expressed as a percentage of total copper against pH for the copper-tmen system. $[Cu^{2+}]$ = [tmen] = 2.5mM**

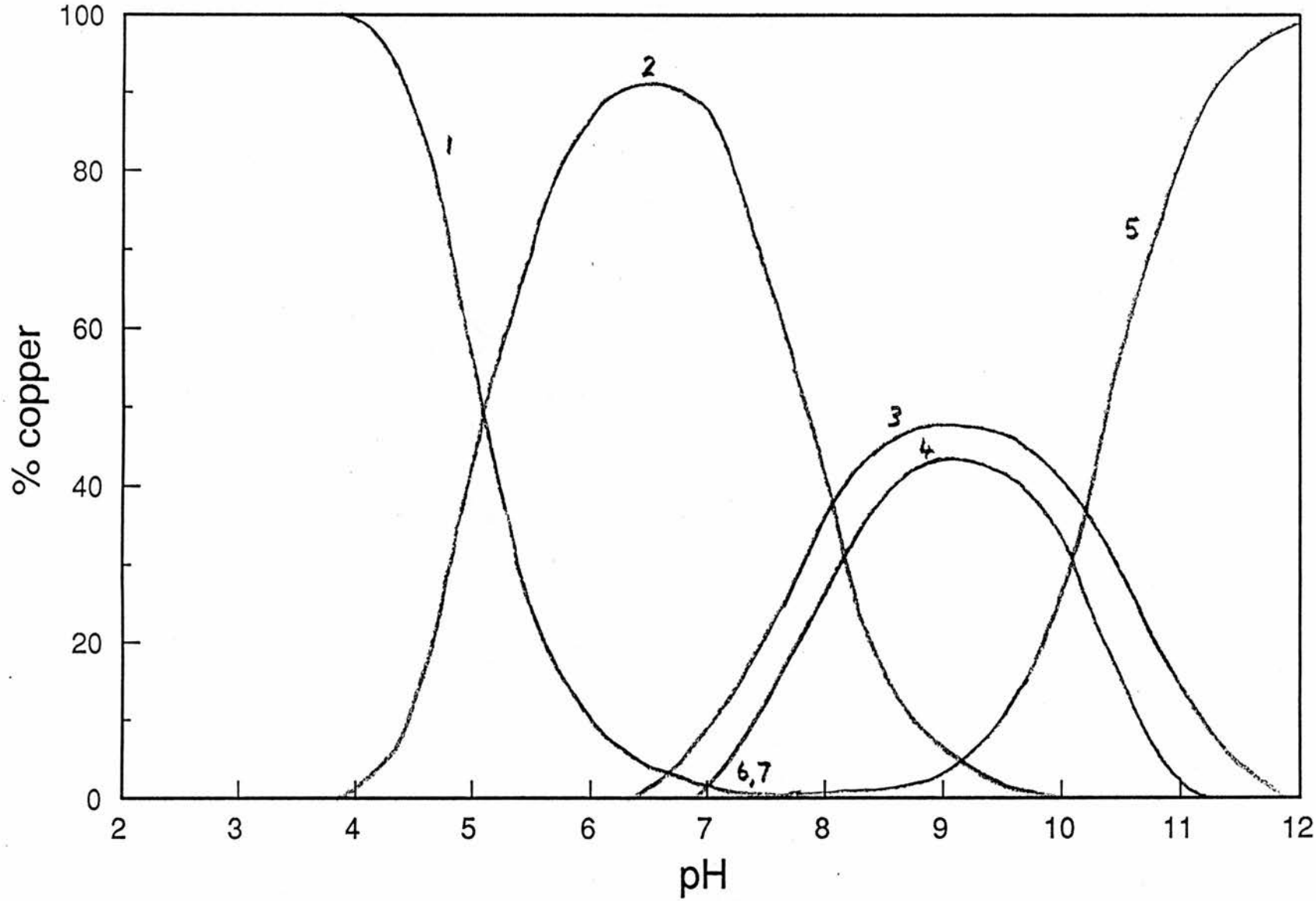

Figure 4.8 Species Distribution Profile, expressed as a percentage of total copper against pH for the copper-trimen system. $[Cu^{2+}]$ = [trimen] = 2.5mM

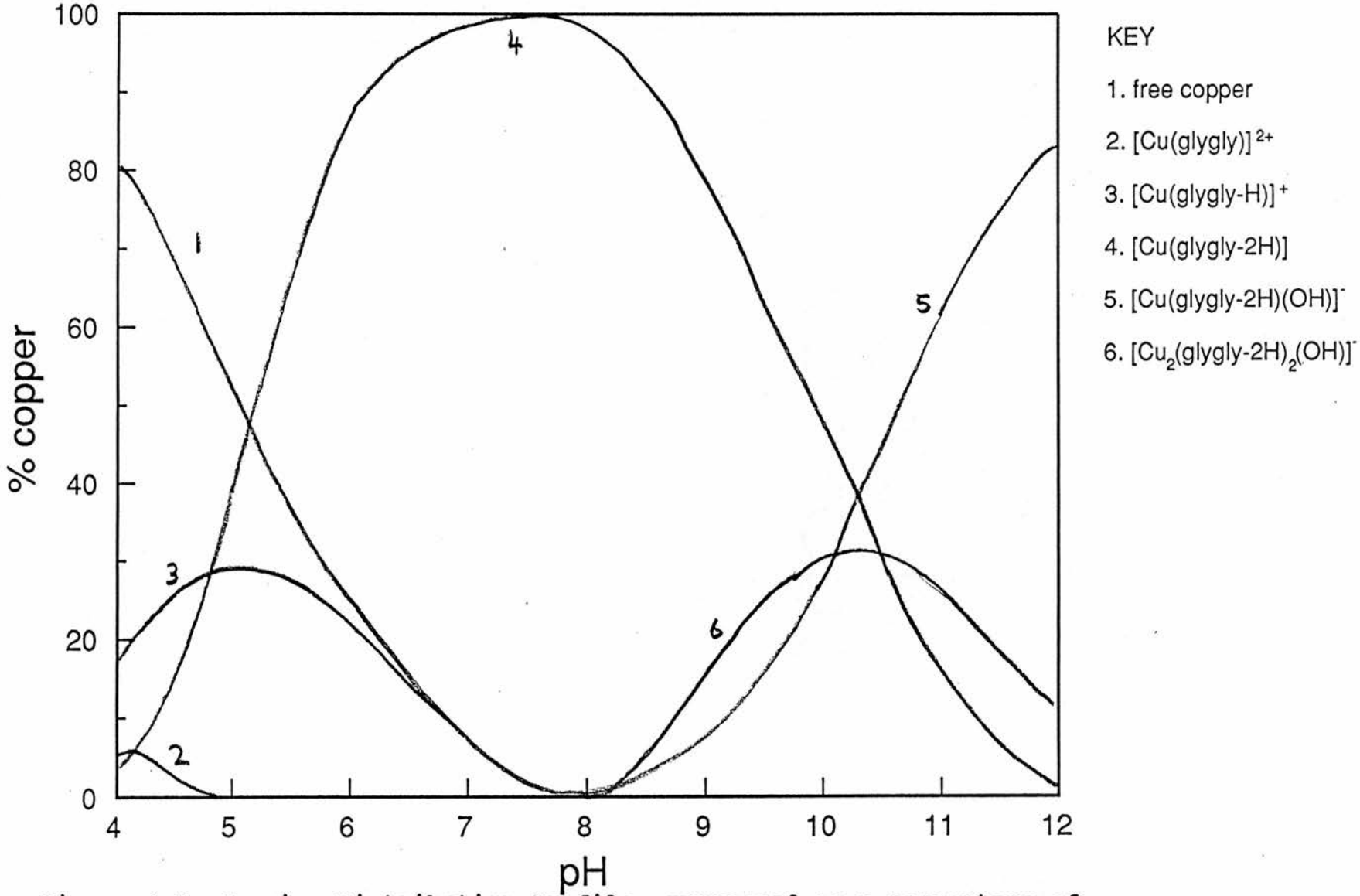

Figure 4.9 Species Distribution Profile, expressed as a percentage of total copper against pH for the copper-glygly system. $[Cu^{2+}]$ = [glygly] = 5.0mM

4.3.3 KINETICS

Representative pseudo-first-order rate constants for the hydrolysis of the simulant phosphorus ester DNPDEP in water at pH 7 by the series of copper(II) complexes at 35°C are shown in Table 4.4. Typically, pH-rate profiles for the copper(II) complex catalysed hydrolysis of the phosphate ester shows two pH independent plateaus and an intermediate pH range (corresponding to the pK of a co-ordinated water molecule) where the rate of hydrolysis depends on the pH, Figures 4.10 to 4.15.

For example, in the pH range 6.6 - 7.8 the hydrolysis of 2,4-DNPDEP is markedly catalysed by [Cu(tmen)(OH)(OH_2)], Figure 4.10. The reactions were studied using a greater than ten fold excess of the copper(II) complex over the phosphate ester. Values of the observed first order rate constants (k_{obs}) for the hyrolysis of 2,4-DNPDEP, which involves loss of 2,4-dinitrophenolate ion, are listed in Table 4.11 as a function of copper complex concentration and the pH. At pH 6.53 no evidence was obtained for saturation kinetics even when the copper(II) complex was in ca. 40 fold excess. At constant pH the reactions display a linear dependence on the concentration of the copper complex, Figures 4.16. Values of the second order rate constant $k_{cat} = k_{obs}/[Complex]_{total}$ were obtained from the least squares slope of the plots of k_{obs} versus the total copper

TABLE 4.4 Representative pseudo-first-order rate constants for 2,4-DNPDEP hydrolysis at 34°C, I = 0.1 (KNO_3)

copper complex	pH	kobs /s^{-1}	$t_{0.5}$ /min
$[Cu(tmen)(OH_2)_2]^{2+}$	7.0	4.48×10^{-3}	2.6
$[Cu(trimen)(OH_2)_2]^{2+}$	7.0	1.88×10^{-3}	6.1
$[Cu(dpa)(OH_2)_2]^{2+}$	7.0	9.21×10^{-3}	1.2
$[Cu(imid)_2(OH_2)_2]^{2+}$	7.0	4.89×10^{-4}	23.6
$[Cu(bipy)_2(OH_2)_2]^{2+}$	7.0	1.51×10^{-4}	76.5
$[Cu([9]aneN_3)(OH_2)_2]^{2+}$	7.0	3.36×10^{-4}	34.4
$[Cu(glygly2H)(OH_2)_2]^{2+}$	8.5	5.51×10^{-5}	209.6
control	7.0	1.55×10^{-7}	52 days

TABLE 4.5 Observed-first-order rate constants for the $[Cu(tmen)(H_2O)_2]^{2+}$ catalysed hydrolysis of 2,4-DNPDEP as a function of pH at 35°C, I = 0.1 (KNO_3)[a]

pH	$10^3 k_{obs}$[b] /s^{-1}	pH	$10^3 k_{obs}$[b] /s^{-1}
5.90	0.45	7.30	5.16
6.23	0.90	7.52	5.55
6.53	1.57	7.71	6.62
6.72	2.25	8.12	6.99
6.92	3.18		
7.12	4.25		

a) All reactions were monitored spectrophotometrically at 400 nm for the production of 2,4-dinitrophenolate from an initial [DNPDEP] = 0.08 mM. Concentration of $[Cu(tmen)(H_2O)_2]^{2+}$ employed = 1.98 mM. Temperature was maintained at 35.0 ± 0.2°C.

b) Average of at least 3 kinetic runs.

Figure 4.10 pH-rate profile for the $[Cu(tmen)(H_2O)_2]^{2+}$ catalysed hydrolysis of 2,4-DNPDEP at 35°C, I=0.1(KNO_3).
$[catalyst]_{total}$= 2.5mM

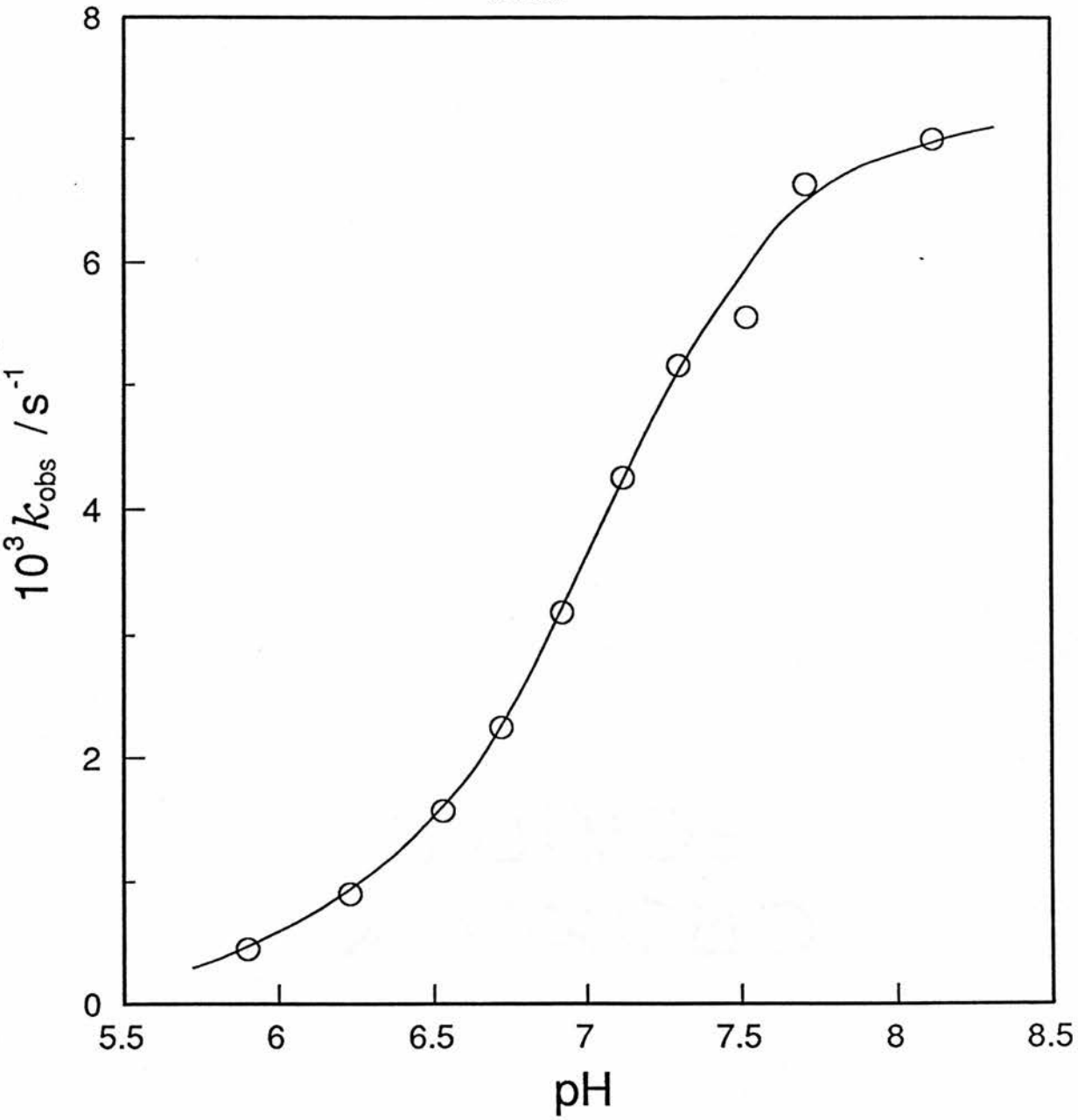

TABLE 4.6 **Observed-first-order rate constants for the $[Cu(trimen)(H_2O)_2]^{2+}$ catalysed hydrolysis of 2,4-DNPDEP as a function of pH at 35°C, I = 0.1 (KNO_3)[a]**

pH	$10^3 k_{obs}$[b]	pH	$10^3 k_{obs}$[b]
5.99	0.25	7.40	4.05 (4.42[c])
6.54	0.69	7.61	4.37
6.75	1.05 (1.12[c])	8.05	4.52
6.94	1.65	8.53	4.88
7.10	1.88 (2.02[c])		
7.24	3.41		

a) All reactions were monitored spectrophotometrically at 400 mm for the production of 2,4-dinitrophenolate from an initial [DNPDEP] = 0.08 mM. Concentration of $[Cu(trimen)(H_2O)_2]^{2+}$ employed = 2.00 mM. Temperature was maintained at 35.0 ± 0.2°C.

b) Average of at least 3 kinetic runs.

c) Observed rates obtained by pH stat method.

Figure 4.11 pH-rate profile for the $[Cu(trimen)(H_2O)_2]^{2+}$ catalysed hydrolysis of 2,4-DNPDEP at 35°C, I=0.1(KNO_3).

$[catalyst]_{total}$= 2.5mM

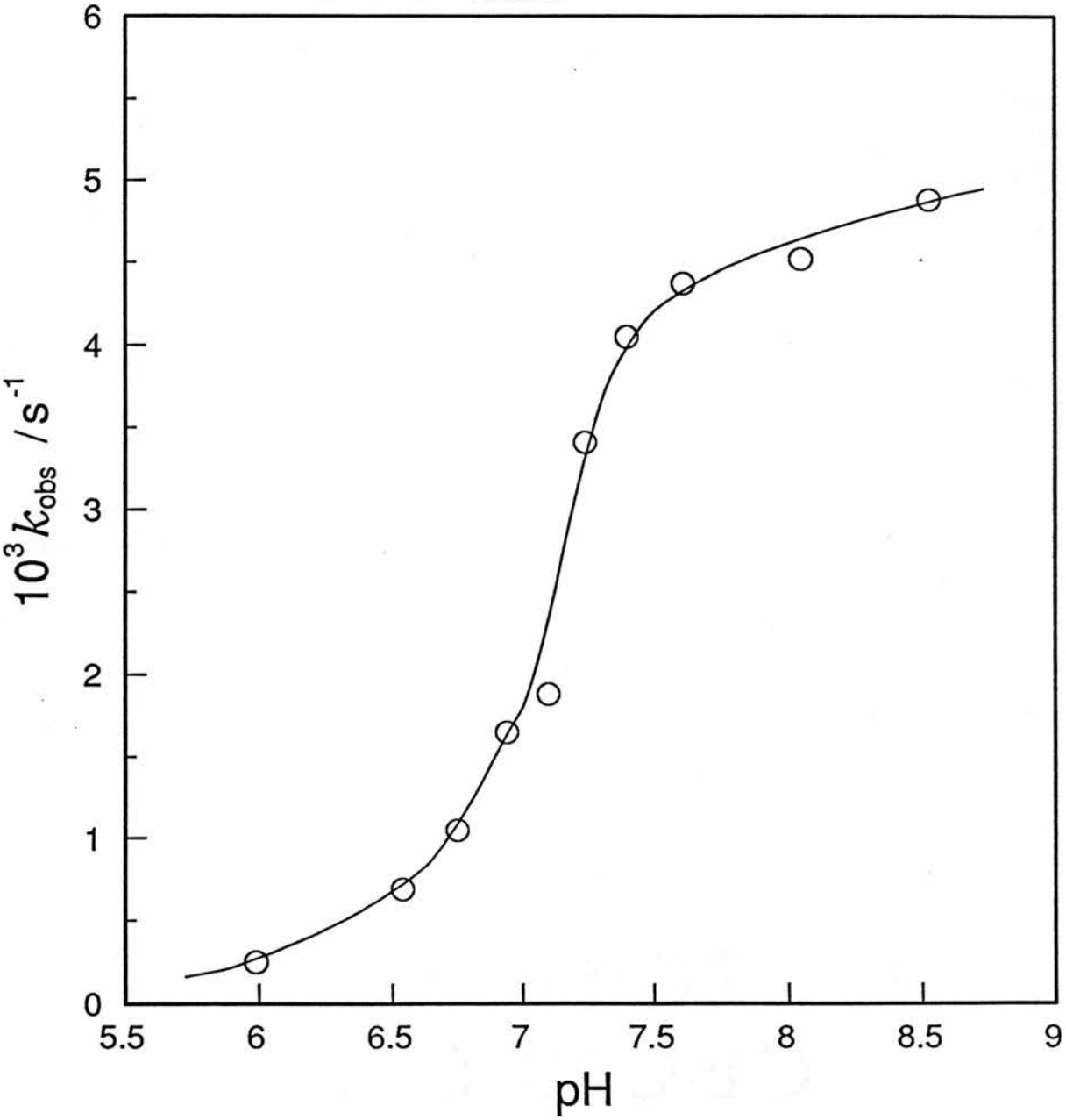

TABLE 4.7 Observed-first-order rate constants for the $[Cu(dpa)(H_2O)_2]^{2+}$ catalysed hydrolysis of 2,4-DNPDEP as a function of pH at 35°C, I = 0.1 (KNO_3)[a]

pH	$10^3 k_{obs}$[b] /s^{-1}	pH	$10^3 k_{obs}$[b] /s^{-1}
5.50	0.40	7.22	7.05
5.82	0.76	7.5	8.11
6.20	1.60	-	opalescense > pH 7.5
6.49	2.52		
6.80	4.15		
7.05	5.68		

a) as Table 4.6

b) as Table 4.6

Figure 4.12 pH-rate profile for the $[Cu(dpa)(H_2O)_2]^{2+}$ catalysed hydrolysis of 2,4-DNPDEP at 35°C, I=0.1(KNO_3).

$[catalyst]_{total}$= 2.5mM

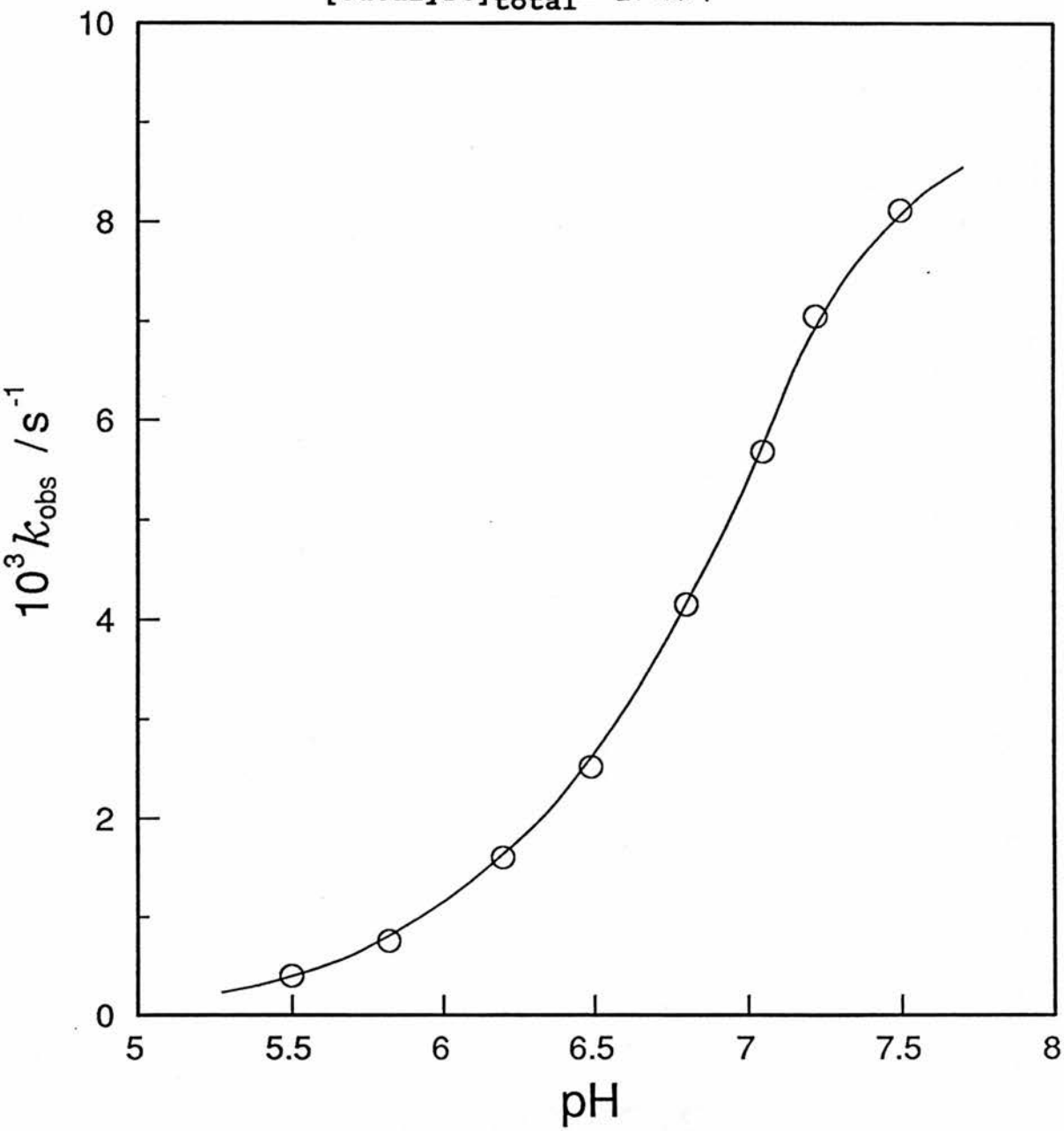

TABLE 4.8 **Observed-first-order rate constants for the $[Cu(imid)_2(H_2O)_2]^{2+}$ catalysed hydrolysis of 2,4-DNPDEP as a function of pH at 35°C, I = 0.1 (KNO_3)[a]**

pH	$10^4 k_{obs}$[b] /s^{-1}	pH	$10^4 k_{obs}$[b] /s^{-1}
6.28	2.30	7.66	12.30
6.50	3.01	7.80	13.00
6.70	4.16		
7.05	7.00		
7.20	8.10		
7.40	10.40		

a) as Table 4.6

b) as Table 4.6

Figure 4.13 pH-rate profile for the $[Cu(imid)_2(H_2O)_2]^{2+}$ catalysed hydrolysis of 2,4-DNPDEP at 35°C, I=0.1(KNO_3).

$[catalyst]_{total}$= 2.5 mM

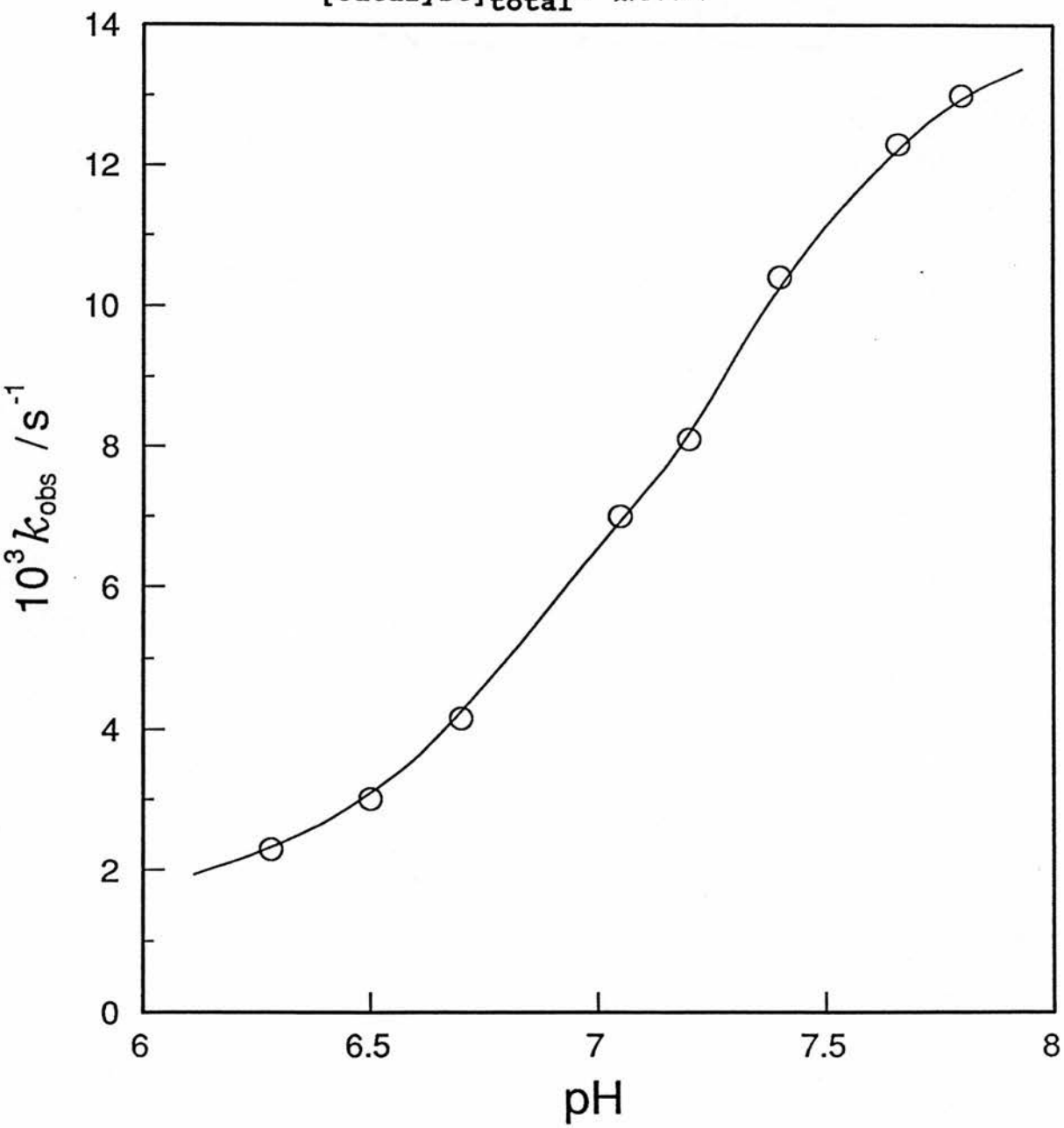

TABLE 4.9 **Observed-first-order rate constants for the $[Cu([9]aneN_3)(H_2O)_2]^{2+}$ catalysed hydrolysis of 2,4-DNPDEP as a function of pH at 35°C, I = 0.1 (KNO_3)[a]**

pH	$10^4 k_{obs}$[b] /s^{-1}	pH	$10^4 k_{obs}$[b] /s^{-1}
6.20	1.98	7.85	14.90
6.51	3.02	8.13	16.68
6.67	3.86	8.38	15.82
6.93	4.34	8.71	16.10
7.21	7.62		
7.53	11.90		

a) as Table 4.6

b) as Table 4.6

Figure 4.14 pH-rate profile for the $[Cu([9]aneN_3)(H_2O)_2]^{2+}$ catalysed hydrolysis of 2,4-DNPDEP at 35°C, I=0.1(KNO_3). $[catalyst]_{total}$= 2.5mM

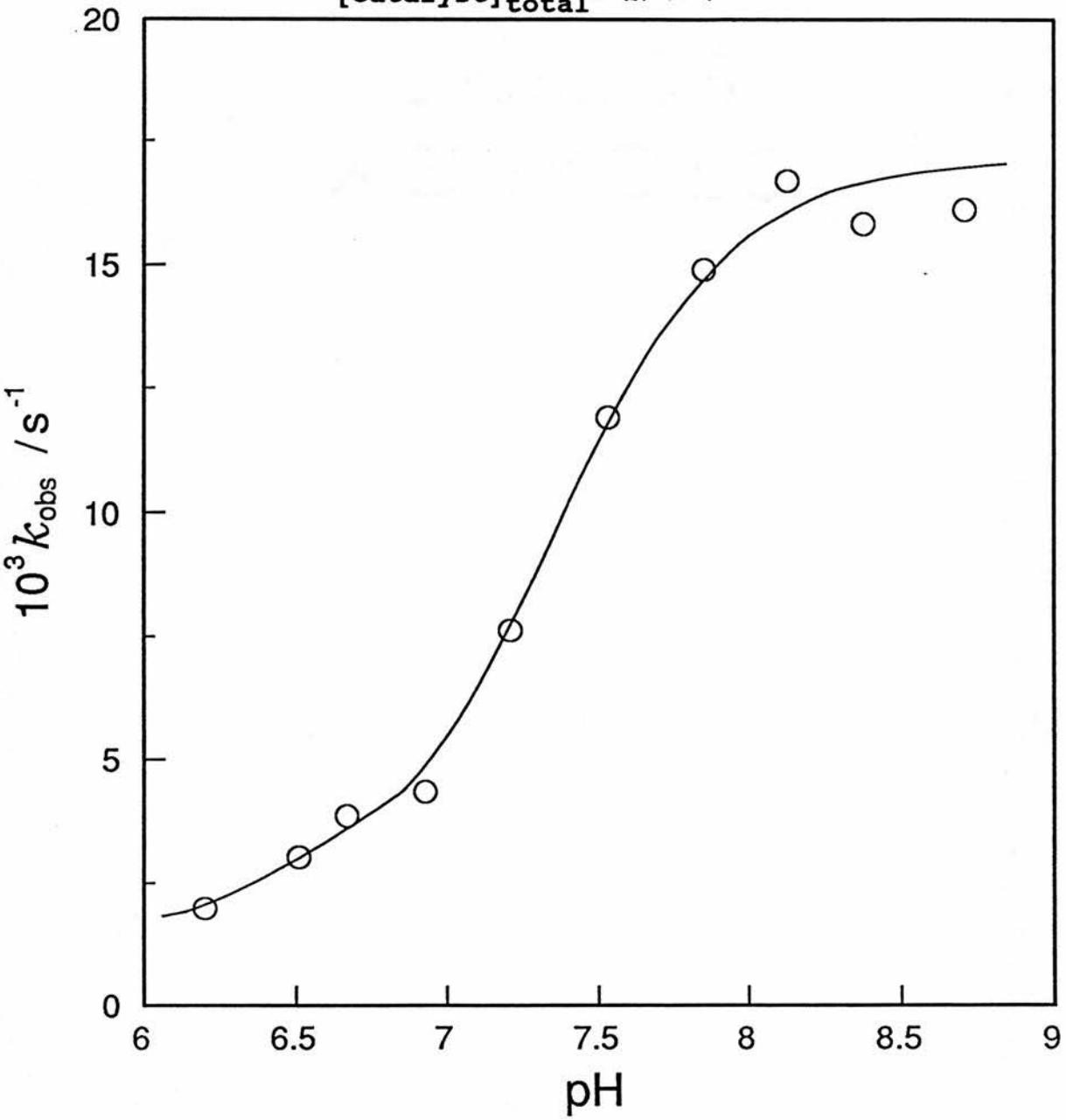

TABLE 4.10 Observed-first-order rate constants for the $[Cu(glygly\text{-}2H)(OH_2)_2)]^{2+}$ promoted hydrolysis of 2,4-DNPDEP as a function of pH at 35°C, I = 0.1 (KNO_3)[a]

pH	$10^4 k_{obs}$[b] /s^{-1}	pH	$10^4 k_{obs}$[b] /s^{-1}
8.01	0.06	9.99	3.40
8.55	0.15	10.50	opalescense > pH 10
8.80	0.49		
9.00	1.25		
9.21	1.58		
9.50	2.61		

a) as Table 4.6

b) as Table 4.6

Figure 4.15 pH-rate profile for the [Cu(gly-2H)(OH_2)] catalysed hydrolysis of 2,4-DNPDEP at 35°C, I=0.1(KNO_3).
$[catalyst]_{total}$= 2.5mM

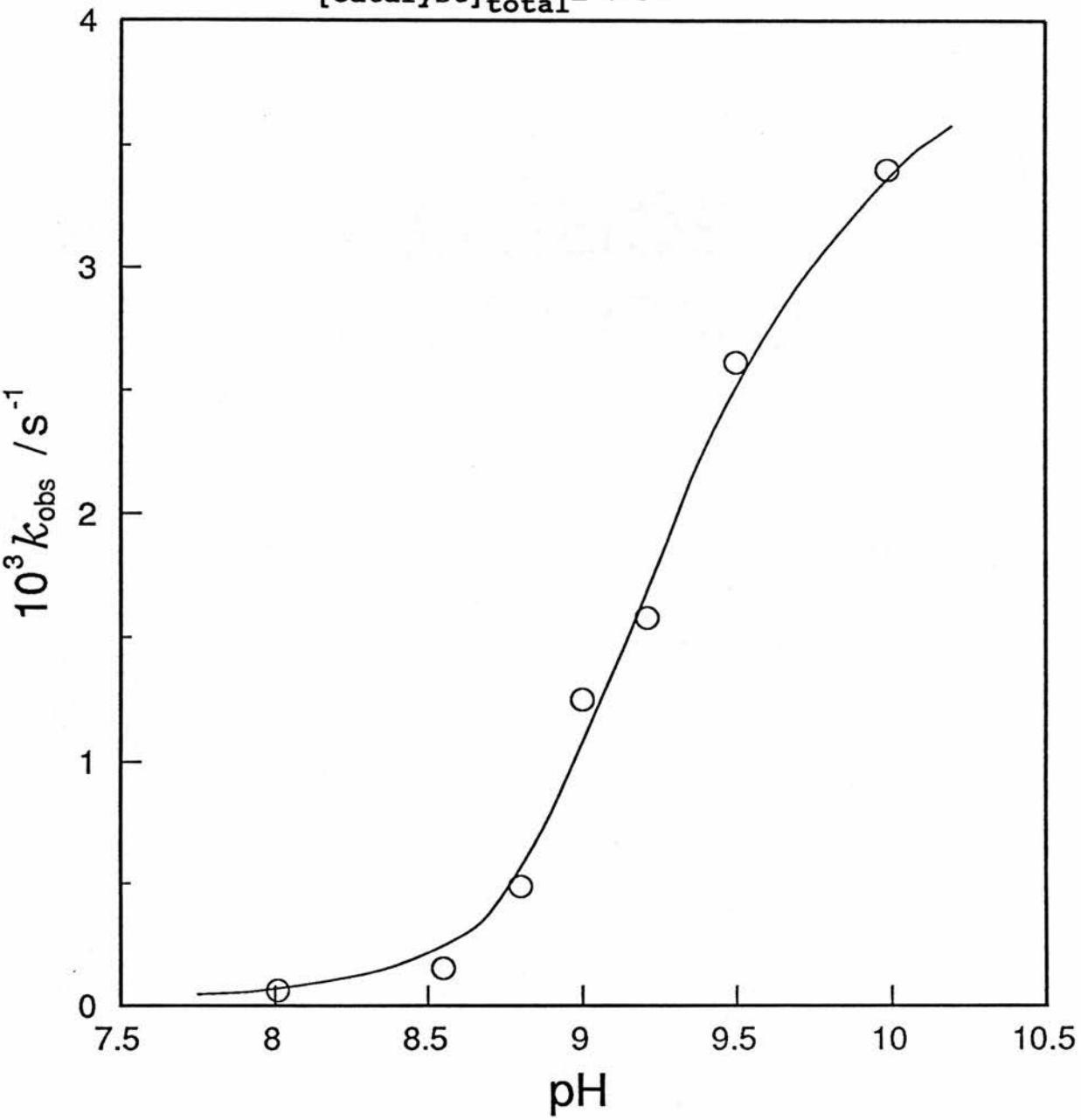

(II) concentration, Table 4.12. Values of k_{cat} increase with pH in a sigmoidal manner over the pH range under study, Figure 4.17, consistent with the complex $[Cu(tmen)(OH)(OH_2)]^+$ being the active species in the reaction. If this is the case, values of k_{cat}/α where α is the fraction of the total complex ionised to the hydroxoaqua complex should be effectively constant.

$$\alpha = [Cu(tmen)(OH)(OH_2)]^+/[Complex]_{total}$$

Values of α were calculated from the determined ionisation constant at 35°C. Values of k_{cat}/α are reasonably constant, Table 4.12, giving an average value for $k_m = k_{cat}/\alpha = 5.7\ dm^3\ mol^{-1}\ s^{-1}$ at 35°C and I = 0.1 mol dm^{-3}.

The rate of hydrolysis of DNPDEP showed good first order dependence on copper(II) complex concentrations for all the catalysts studied. The kinetic data obtained for the series of copper(II) complexes was treated in a similar manner to that outlined for the copper(II) tetramethylethylenediamine system. Again, values of k_{cat} increased with pH in a sigmoidal manner over the pH range corresponding to the ionisation of the first co-ordinated water molecule. This observation is consistant with $[Cu(L)(OH)(OH_2)]^+$ being the active catalytic species. Typical pH versus k_{cat} rate profiles for the hydrolysis

TABLE 4.11 Observed-first-order for the $[Cu(tmen)(OH_2)_2]^{2+}$ catalysed hydrolysis of 2,4-DNPDEP as a function of pH at 35°C and I = 0.1 (KNO_3)

pH	$10^3[Cu(tmen)]^{2+a}$ /mol dm^{-3}	$10^3 k_{obs}{}^b$ /s^{-1}
6.53	0.50	0.44
	1.00	0.84
	1.50	1.15
	2.00	1.52
	2.50	1.95
	3.00	2.32
6.73	0.50	0.60
	1.00	1.18
	1.50	1.73
	2.00	2.27
	2.50	2.83
6.93	0.50	0.80
	1.00	1.59
	1.50	2.56
	2.00	3.17
	2.50	4.11

TABLE 4.11 Continued

pH	10^3[Cu(tmen)]$^{2+a}$ /mol dm^{-3}	$10^3 k_{obs}{}^b$ /s^{-1}
7.13	0.50	1.10
	1.00	2.10
	1.50	3.27
	2.00	4.25
	2.50	5.38
7.33	0.50	1.15
	1.00	2.50
	1.50	4.25
	2.00	4.95
	2.50	6.05
7.53	0.50	1.31
	1.00	2.94
	1.50	4.40
	2.00	5.55
	2.50	6.93

TABLE 4.11 Continued

pH	10^3[Cu(tmen)]$^{2+a}$ /mol dm^{-3}	$10^3 k_{obs}{}^b$ /s^{-1}
7.73	0.50	1.14
	1.00	3.45
	1.50	4.99
	2.00	6.60
	2.50	7.93

a) The total catalyst concentration i.e ($[Cu(tmen)(OH_2)_2]^{2+}$ + $[Cu(tmen)(OH)(OH_2)]^{+}$, reactions were monitored spectrophotometerically at 400 nm for the production of 2,4-dinitrophenolate from initial [DNPDEP] = 0.08 mM.

b) Average of at least 3 kinetic runs

Figure 4.16 Dependence of K_{obs} for the $[Cu(tmen)(OH)(OH_2)]^+$ hyrdolysis of 2,4-DNPDEP on catalyst concentration at 35°C and varying pH, I=0.1(KNO_3).

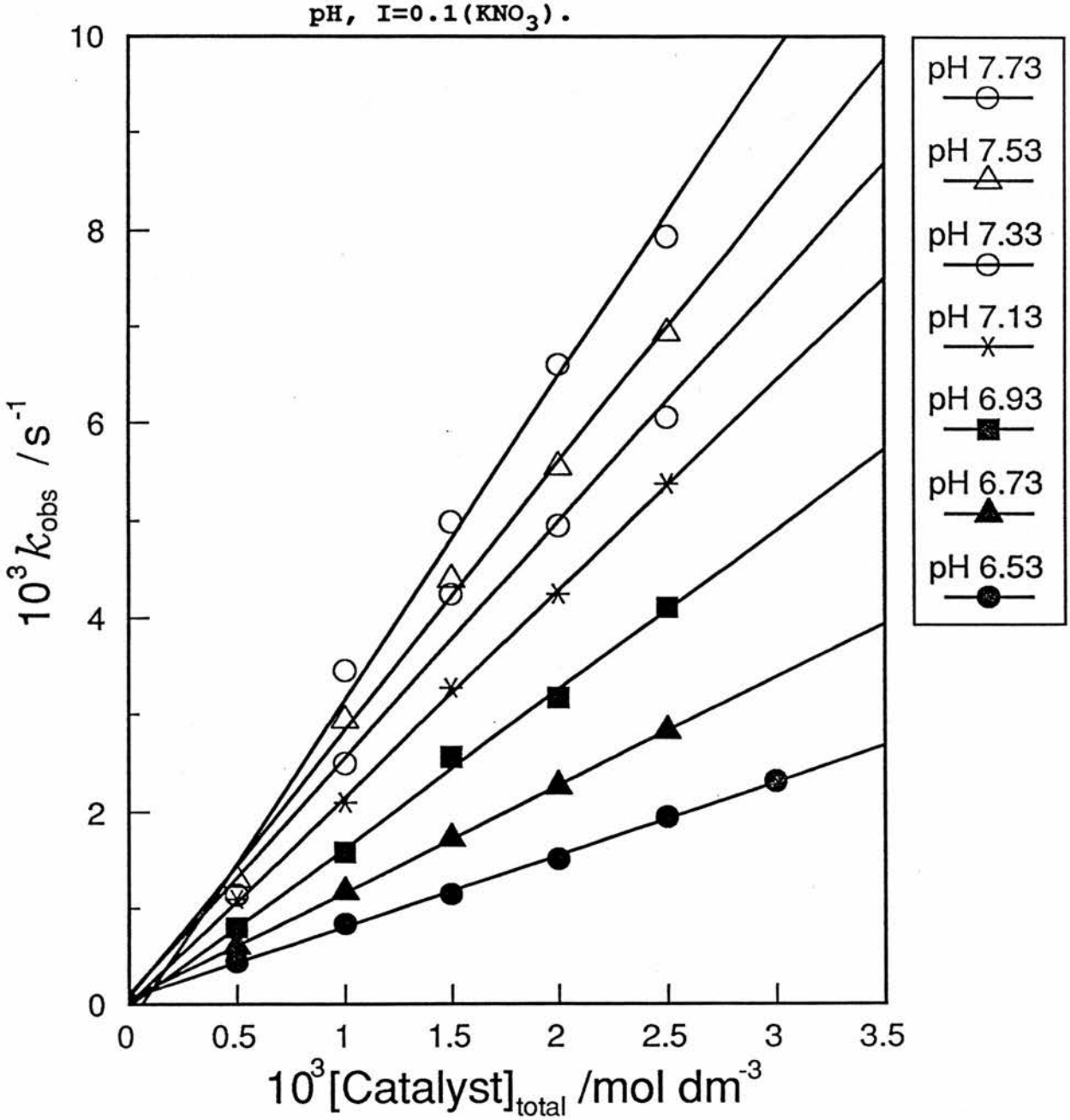

of the phosphate ester by the Cu(II)-(trimen) and Cu(II)-(dpa) systems are shown in Figures 4.18 and 4.19 respectively. Second order rate constants k_m for the hydrolysis of DNPDEP by the various copper(II) complexes studied [4.1] - [4.7] are summarised in Table 4.15, the k_m values shown represent constant values of k_{cat}/α determined for each individual catalytic system.

A true catalytic system should exhibit turnover. Turnover experiments were carried out by pH stat using a Radiometer Titra-Lab system interfaced with an Apple IIe computer. In a typical catalytic run a solution of 7.25 x 10^{-4} mol dm^{-3} DNPDEP and 5 x 10^{-5} mol dm^{-3} copper complex, (ratio 15:1) was adjusted to pH 7.6 at 35°C and the release of H^+ due to ester hydrolysis monitored by automatic addition of 0.01 mol dm^{-3} sodium hydroxide. Figure 4.20 shows the pH stat trace obtained for the Cu(II)-dpa system from a typical turnover experiment. The observation of pseudo-zeroth-order kinetics for at least three turnovers of $Cu(dpa)^{2+}$ in solutions containing an excess of phosphate triester confirmed that the copper complex was functioning catalytically. At pH 7.6 and 35°C complete hydrolysis of the phosphate ester (15 moles) is hydrolysed by one mole of catalyst in ca. 90 minutes. At this pH the half life of the free ester is 71 hours. The initial slope of the plot gives a release rate for H^+ of 2.61 x 10^{-5} mol min^{-1}, with a turnover of 31.2 turnovers $hours^{-1}$. The catalytic

TABLE 4.12 **The pH dependence of the second order rate constants, k_{cat}, for the $[Cu(tmen)(OH)(OH_2)]^+$ catalysed hydrolysis of 2,4-DNPDEP at 35°C, I = 0.1 (KNO_3)**

pH	k_{cat} $dm^3\ mol^{-1}\ s^{-1}$	α	k_{cat}/α $dm^3\ mol^{-1}\ s^{-1}$
6.53	0.75	0.12	6.3
6.73	1.10	0.18	6.1
6.93	1.64	0.25	6.6
7.13	2.14	0.35	6.1
7.33	2.45	0.46	5.3
7.53	2.77	0.57	4.9
7.73	3.24	0.68	4.8

Figure 4.17 Dependence of the second-order rate constant, k_{cat}, on pH for the $[Cu(tmen)(OH)(OH_2)]^+$ catalysed hyrdolysis of 2,4-DNPDEP at 35°C, I=0.1(KNO_3).

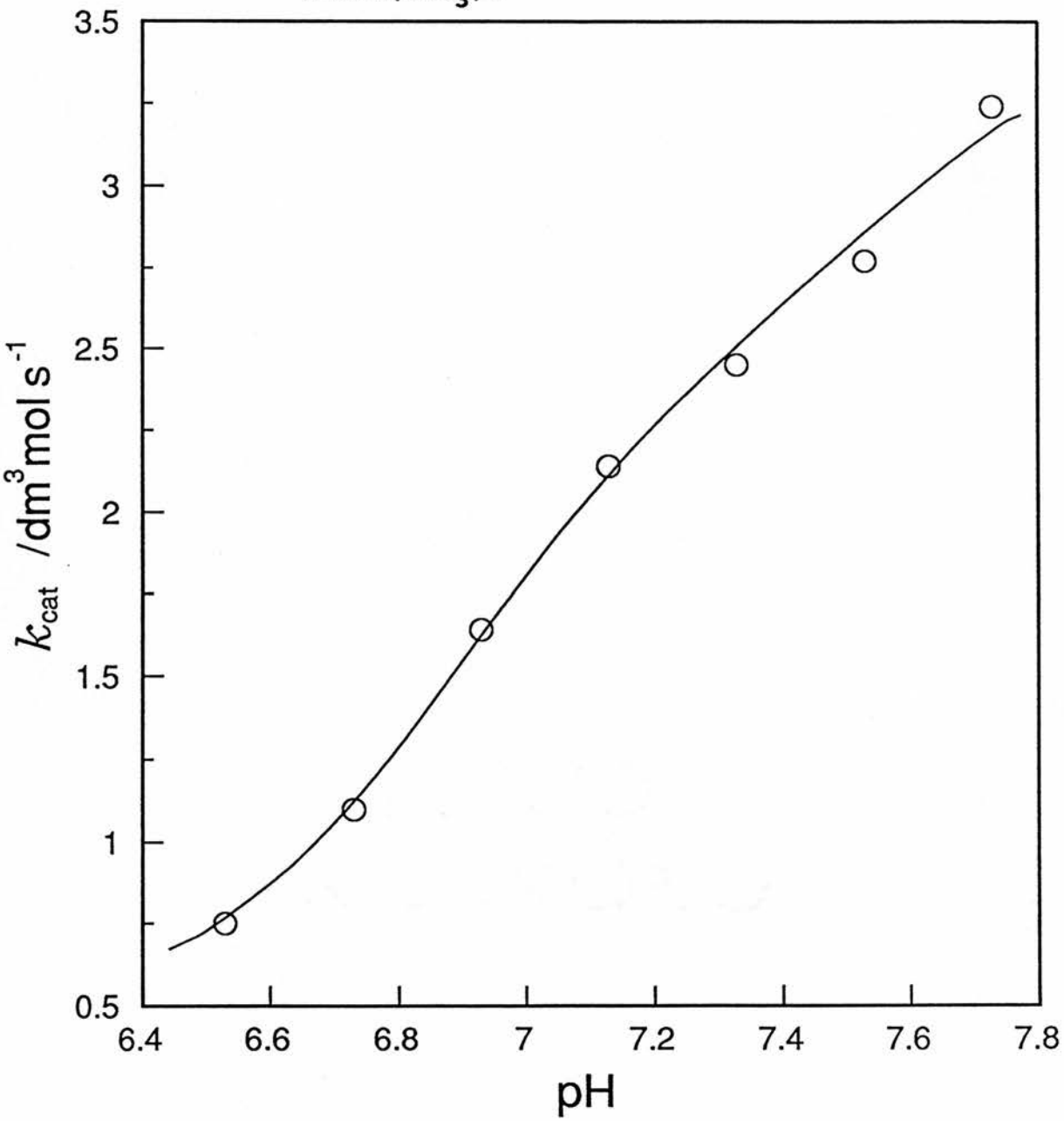

TABLE 4.13 The pH dependence of the second order rate constants, k_{cat}, for the $[Cu(trimen)(OH)(OH_2)]^+$ catalysed hydrolysis of 2,4-DNPDEP at 35°C, I = 0.1 (KNO_3)

pH	k_{cat} $dm^3\ mol^{-1}\ s^{-1}$	α	k_{cat}/α $dm^3\ mol^{-1}\ s^{-1}$
6.55	0.38	0.14	2.7
6.75	0.59	0.20	2.9
6.95	0.81	0.29	2.8
7.15	0.97	0.38	2.6
7.35	1.38	0.50	2.8
7.55	1.54	0.61	2.5
7.75	1.74	0.71	2.5

Figure 4.18 Dependence of the second-order rate constant, k_{cat}, on pH for the $[Cu(trimen)(OH)(OH_2)]^+$ catalysed hyrdolysis of 2,4-DNPDEP at 35°C, I=0.1(KNO_3).

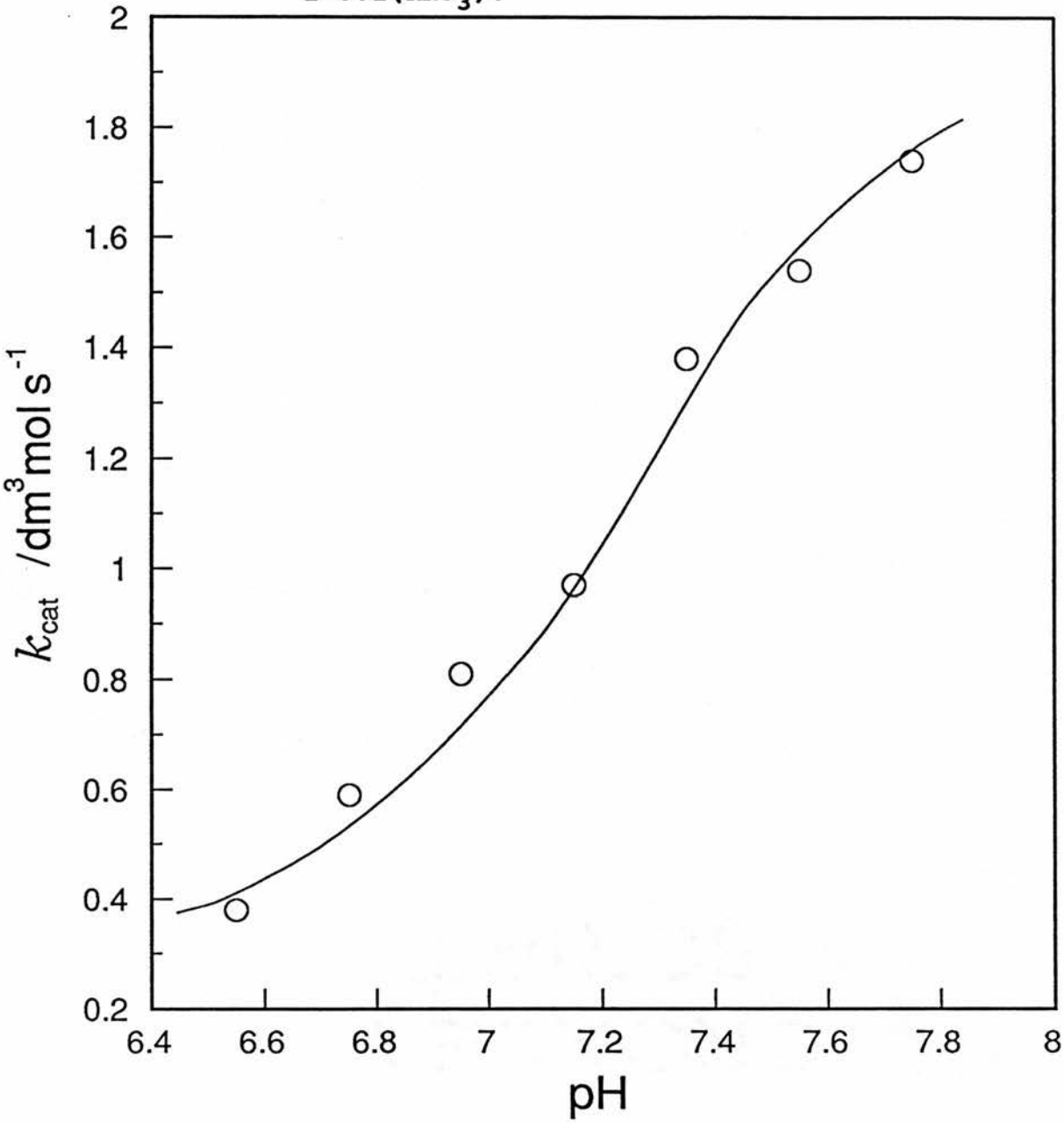

TABLE 4.14 **The pH dependence of the second order rate constants, k_{cat}, for the $[Cu(dpa)(OH)(OH_2)]^+$ catalysed hydrolysis of 2,4-DNPDEP at 35°C, I = 0.1 (KNO_3)**

pH	k_{cat} / $dm^3\ mol^{-1}\ s^{-1}$	α	k_{cat}/ $dm^3\ mol^{-1}\ s_{-1}$
5.82	0.46	0.05	9.3
6.20	0.99	0.11	9.4
6.49	1.74	0.19	9.3
6.80	2.91	0.32	9.1
7.05	4.13	0.45	9.1
7.22	5.02	0.55	9.1
7.50	6.24	0.70	8.9

Figure 4.19 Dependence of the second-order rate constant, k_{cat}, on pH for the $[Cu(dpa)(OH)(OH_2)]^+$ catalysed hyrdolysis of 2,4-DNPDEP at 35°C, I=0.1(KNO_3).

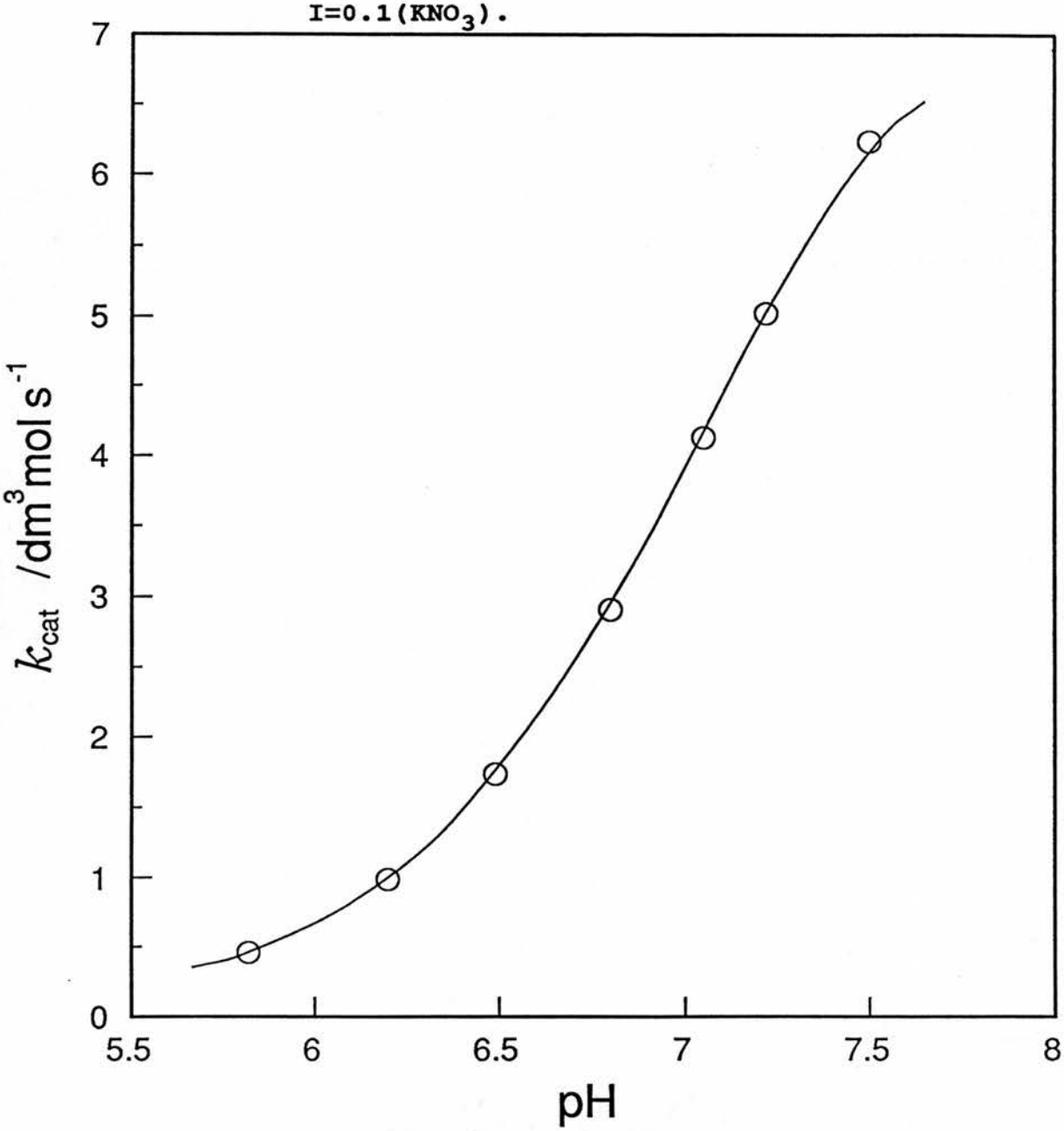

efficiency of the series of copper(II) complexes towards hydrolyses of 2,4-DNPDEP was examined, the results obtained are summarised in Table 4.16.

A few Cu(II)-$(tmen)^{2+}$ hydrolysis experiments were monitored periodically by removal of catalyst and analysis by ^{31}P nmr spectroscopy. Analysis of the catalytic hydrolysis experiments at pH 7.6, stopped before one equivalent of 2,4-dinitrophenalate was produced showed only resonances attributed to the unreacted starting material 2,4-dinitrophenyldiethylphosphate and diethylphosphate. Note that the rate constants from the spectrophotometric kinetic experiments for the appearance of 2,4-dinitrophenolate are valid, since no unseen concurrent competitive reactions such as the liberation of $^{-}OCH_2CH_3$ producing ethyl 2,4-dinitrophenyl phosphate is observed.

TABLE 4.15 Summary of second order rate constants for the hydrolysis of 2,4-dinitrophenyl diethylphosphate in aqueous at 35°C, by various copper(II) catalysts

copper complex	k_m /dm^3 mol^{-1} s^{-1}
$[Cu(tmen)(OH)(OH_2)]^{2+}$	5.73
$[Cu(trimen)(OH)(OH_2)]^{+}$	2.69
$[Cu(dpa)(OH)(OH_2)]^{+}$	9.17
$[Cu(imid)_2(OH)(OH_2)]^{+}$	0.52
$[Cu([9]aneN_3)(OH)(OH_2)]^{+}$	0.56
$[Cu(glygly-2H)(OH)]^{-}$	0.11

Figure 4.20 Typical turnover experiment showing consumption of NaOH (0.01M) for $[Cu(dpa)(OH)(OH_2)]^+$ (50 μM) catalysed hyrdolysis of DNPDEP (750 μM) at pH 7.0 and 25°C.

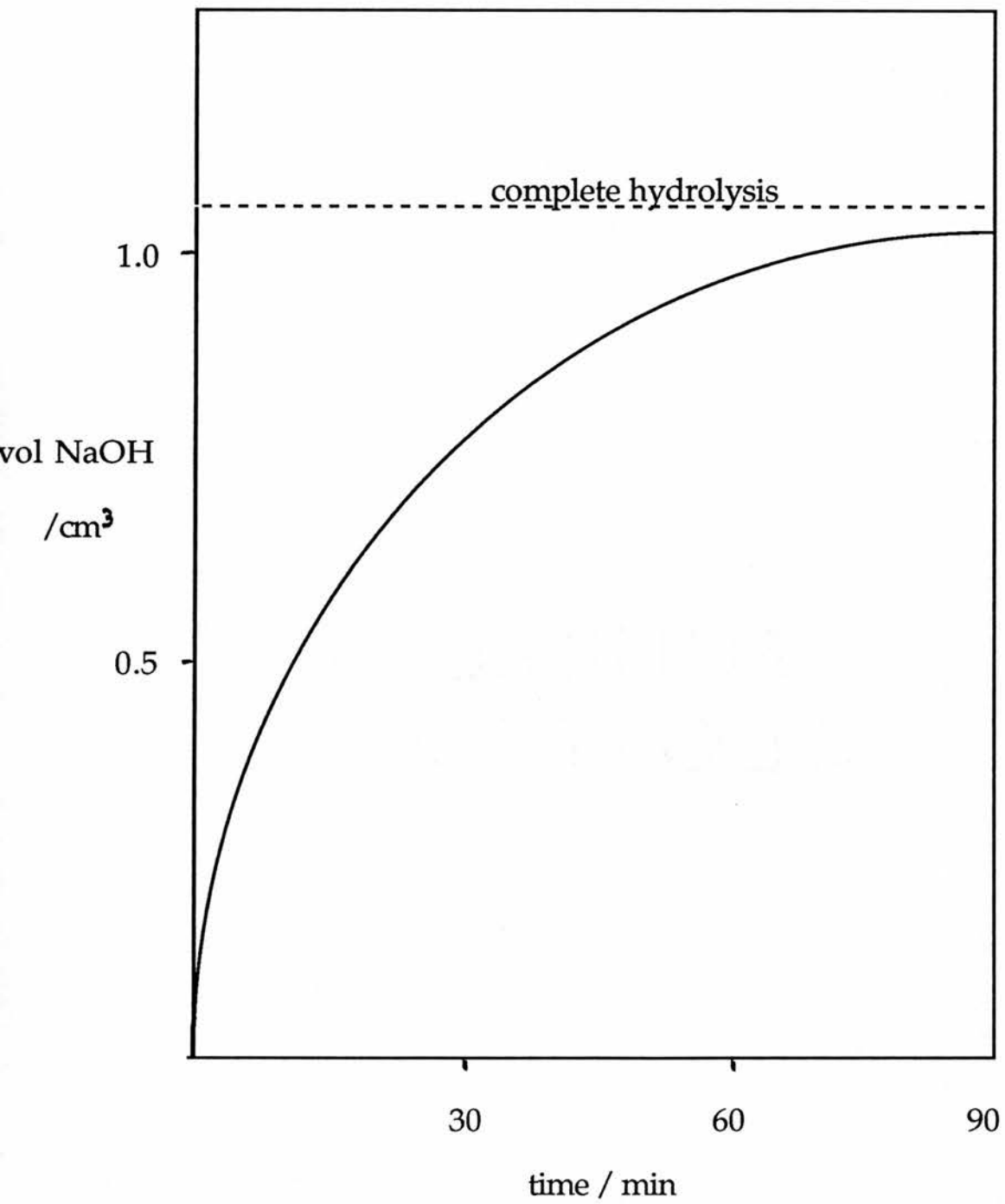

TABLE 4.16 Summary of catalytic activity for the hydrolysis of 2,4-dinitrophenyl diethylphosphate in aqueous at 25°C, by various copper(II) catalysts

copper complex	turnover/hr
$[Cu(tmen)(OH)(OH_2)]^{2+}$	20.6
$[Cu(dpa)(OH)(OH_2)]^{+}$	31.2
$[Cu([9]aneN_3)(OH)(OH_2)]^{+}$	2.2
$[Cu(glygly-2H)(OH)]^{-}$	stoicheiometric

4.4 DISCUSSION

The mechansim by which copper(II) complexes exert their catalytic effects is of considerable interest in the development of catalytic systems for the detoxification of nerve agents and as rudimentary phosphatases. It is clear from our data that all the copper(II) complexes studied with the exception of $[Cu(glygly-2H)(OH)]^-$ are true catalysts for the hydrolysis of the phosphate triester 2,4-DNPDEP under neutral and mildly alkaline conditions. The sigmoidal variation of the observed rate constants with pH, Figures 4.5 - 4.10, suggest that formation of the catalytically active species requires removal of a relatively acidic proton. This observation implicates $Cu(L)(OH)^+$ (or its kinetic equivalent), $Cu(L)^{2+}$ with free hydroxide as the active species.

Figure 4.7 shows a typical species distribution profile for the copper(II)-tmen system. From this profile it can be seen that two species are increasing in concentration over the pH range of interest (i.e. pH = 6.0-8.9), the monohydroxo chelate $Cu(L)(OH)^+$ and its dimer ($Cu_2(L)_2(OH)_2^{2+}$). There is only a very low concentration of the dihydroxo chelate $Cu(L)(OH)_2$, even at pH 8.9. Martel[5] has shown that the dimer possesses no catalytic activity and the present study also found no correlation between the

kinetic rate (Figure 4.17) and the concentration of this species. Further, we found no correlation between the rate and concentration of dihydroxo chelate. However this does not entirely eliminate the species as being active because its concentration in the pH range of interest is extremely low as it only becomes a major species above pH = 9.0. These observations confirm $Cu(L)(OH)^+$ as the active species in solution for this system. Similar correlations were found in the Cu-trimen and Cu-(glygly-2H) speciation profiles. Comparison of the speciation profiles, (Figures 4.8 and 4.9) with the rate data in Figures 4.18 and 4.15, similarly define the monohydroxo chelate as the active species in these systems.

There are four mechanistic possibilities for a catalytic species involving $Cu(L)(OH)^+$.

1. General base catalysis, which has been observed to be the predominant pathway for the "inert" monohydroxo metal complex catalysed hydrolysis of 2,4-DNPDEP and 2,4-DNPEMP, Chapter 3. In these cases a good Bronsted relationship was determined between values of k_m and the pK_a of the conjugate acid.
2. A nucleophilic process involving attack on a phosphorus atom by a metal bound hydroxide.
3. An electrophilic activation of the phosphoryl P=O bond, by co-ordiation to the metal centre, towards attack by free hydroxide.

4. A "hybrid" mechanism where the metal centre delivers a co-ordinated hydroxide nucleophilically to a DNPDEP molecule, while simultaneously drawing electron density away from the phosphorus atom by interacting with the phosphoryl oxygen [4.9].

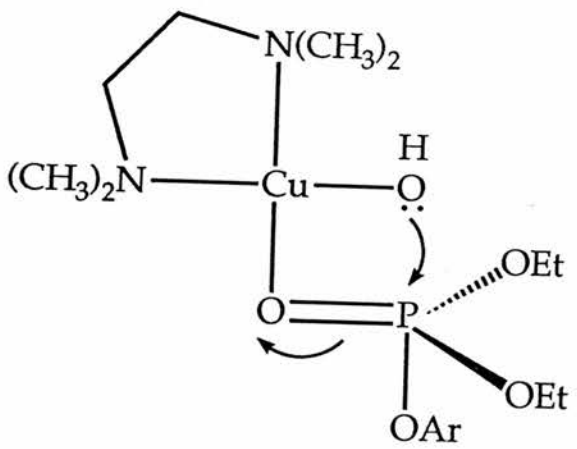

[4.9]

Some version of the "hybrid" mechanism seems to be operative in our system. Values of the second order rate constants k_m attack by the monohydroxoaqua complex on the triester 2,4-DNPDEP are summarised in Table 4.15. An interesting feature of the reaction is that k_m is considerably greater than the measured second order rate constant k_{OH} for base hydrolysis of the substrate, Table 2.5. For example, in the most efficient system involving $[Cu(dpa)(OH)(OH_2)]^+$, k_m (10.85 $dm^3\ mol^{-1}\ s^{-1}$) is nearly 20-fold greater than k_{OH} (0.58 $dm^{-3}\ mol^{-1}\ s^{-1}$) at 35°C. Since free hydroxide ion is more than a million times stronger as a base than $[Cu(dpa)(OH)(OH_2)]^+$ this observation effectively

excludes the copper complex acting as a general base catalysts in the reaction. Remarkable polarizability effects would be required to make the monohydroxo complex a better simple nucleophile. If, however, copper acts as a Lewis acid, the resulting bifunctional mechanism could well be better than simple nucleophilic attack by free hydroxide. This argument does not exclude the kinetically equivalent possibility that the substrate forms a complex with the metal which is then attached by free hydroxide ion, but a purely Lewis acid mechanism would require extremely strong bonding and electrophilic catalysis to make up for the low concentration of hydroxide ion in solution. Lewis acid facilitation of nucleophilic reactions at phosphorus(V) centres has been observed[13]. The apparent second order rate constants for hydroxide ion attack on trimethyl phosphate is increased 400-fold when the phosphonyl moiety is co-ordinated to iridium(III) in the complex [4.10]. However this mode of catalysis alone does not seem capable of more than modest rate enhancements.

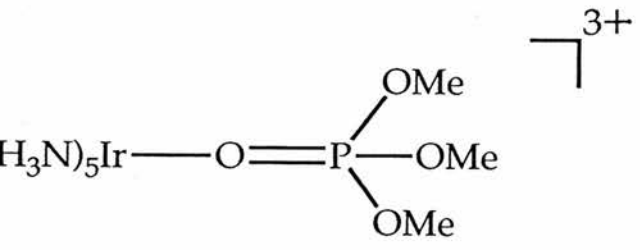

[4.10]

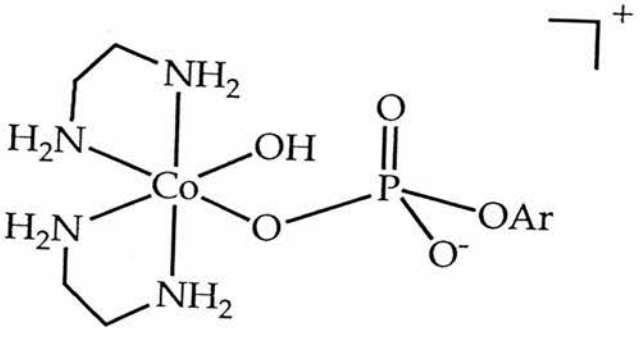

[4.11]

Similar bifunctional or "push-pull" mechanisms have been invoked for metal chelate-mediated hydrolysis of isopropyl methylphosphonofluoridate[4]. The hydrolysis of 4-nitrophenyl phosphate by the cobalt(III) complex [4.11] has been shown to occur by intramolecular attack by co-ordinated hydroxide at phosphorus to give an initially five co-ordinate phosphorane, which decays to $[Co(en)_2PO_4]$ containing bidentate phosphate and 4-nitrophenol[14]. The present results are also consistent with the observations of Breslow[8] on the $[Zn(CR)OH]^+$ [4.12] catalysed hydrolysis of 2,4-dinitrophenyl diphenyl phosphate and of Trogler[15] on the $[Cu(bipy)(OH)(OH)_2]+$ catalysed hydrolysis of 4-nitrophenyl diethylphosphate.

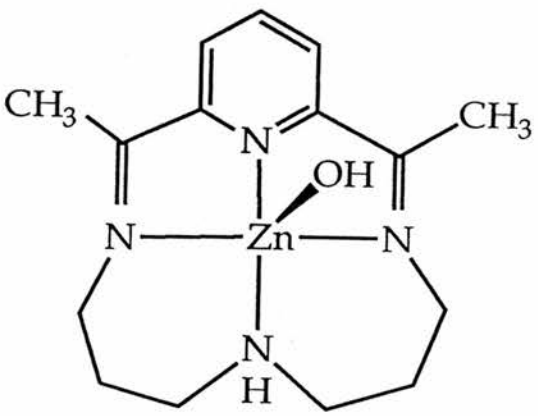

[4.12]

Pure nucleophilic mechanisms have been invoked for some metal complex mediated reactions of non-phosphate substrates. In his studies of ZnCR as a catalyst for acetaldehyde hydration, Woolley concluded that ZnCR-OH was

acting as a simple nucleophile[16]. Free hydroxide had a much larger second order rate constant for reaction with acetaldehyde than did the metal bound hydroxide. The contrast probably reflects differing geometric requirements at a trigonal-bipyramidal phosphorus and at a tetrahedral carbon. In the hybrid mechanism at phosphorus all four atoms of the transient ring have almost normal valence angles; for such a four membered ring containing carbon, there would be significant angle strain.

Representative pseudo-first-order rate constants for the hydrolysis of 2,4-DNPDEP at pH = 7 by the series of copper(II) complexes investigated are shown in Table 4.4. All the copper(II) complexes with mono or polydentate ligands (2 and 1 equivalents respectively) exhibit rate acceleration. Our detailed studies of the copper(II) chelate catalysed reactions demonstrate that it is the square planar cis-diaquo complexes that exhibit the greatest rate acceleration. Hydrolysis of 2,4-DNPDEP proceeds 6×10^4 fold more rapidly with 2.5 mM $Cu(dpa)^{2+}$ at pH = 7 and $35^{o}C$ than without catalyst.

The catalytic cycle proposed in Scheme 4.5 is consistent with the pH-rate profile, the first-order-dependence on catalyst and phosphate ester concentrations and the absence of saturation kinetics. A concerted mechanism via a five-co-ordinate phosphorane intermediate state is proposed. A reasonable formulation for the complex

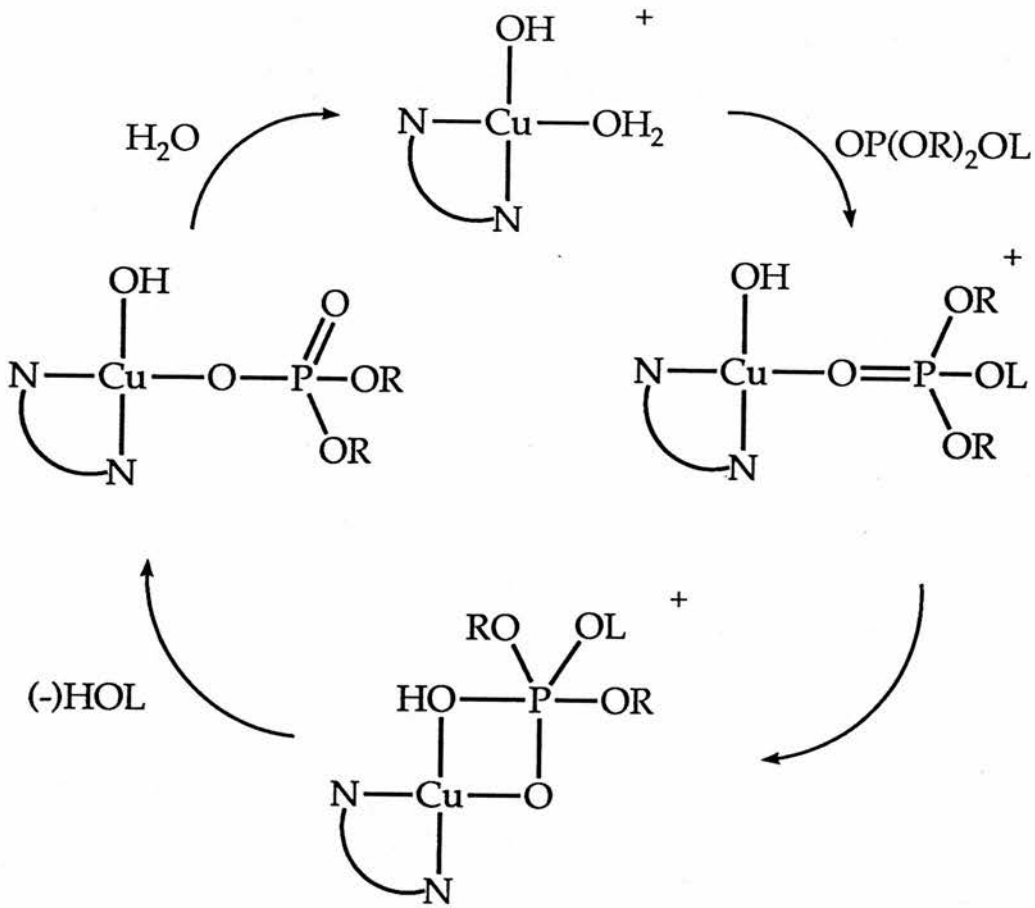
OH
+
N—Cu—OH2
H2O
OP(OR)2OL
OH
O
N—Cu—O—P—OR
OR
N
OH
OR
+
N—Cu—O=P—OL
OR
N
RO
OL
+
HO—P—OR
(-)HOL
N—Cu—O
N

[Scheme 4.5]

(Scheme 4.7) has hydroxyl and phosphate ester ligands bound cis to $Cu(L)^{2+}$. The copper(II) complex plays a bifunctional role effecting hydrolysis by electrophilic activation of the co-ordinated phosphate ester and providing a cis hydroxide nucleophile in a position to undergo intra-molecular attack at phosphorus. In support of this mechanism it was found that copper(II) complexes with one less available co-ordination site, such as Cu(terpyridine)$^{2+}$ or Cu(diethylenetriamine)$^{2+}$, promote hydrolysis of the phosphate triester much less effectively than the bidentate cis- diaquo chelates.

A comparison of the phosphate triester hydrolysis rates by the copper(II) complexes with various ligand systems leads to the following.

Reactivity patterns for copper(II) complex catalysed hydrolysis of 2,4-DNPDEP, $[Cu(dpa)(OH)(OH_2)]^+$ > $[Cu(tmen)(OH)(OH_2)]^+$ > $[Cu(trimen)(OH)(OH_2)]^+$ > $[Cu(imid)_2(OH)(OH_2)]^+$ > $[Cu([9]aneN_3)(OH)(OH_2)]^+$ > $[Cu(bipy)_2(OH)]^+$ > $[Cu(glygly\text{-}2H)(OH)]^-$. The structure of the amine ligand on the copper(II) complex has a significant effect on the rate of hydrolysis of the phosphate triester. The difference in the reactivity can be rationalised in terms of,

1. the availability of cis aqua sites on the complex, which facilitate the "push-pull" mechanism.

2. the ability of the ligand to inhibit dimer formation i.e. ligand bulk.
3. the pK_a of the bound water molecule.

Hydrolysis of the phosphonate ester 2,4-DNPEMP by copper(II) complexes resembles that of the phosphate triester 2,4-DNPDEP in the observed first-order dependence on phosphonate ester and copper(II) complex concentrations. The pH-rate profiles are also similar. However, hydrolysis of 2,4-DNPEMP occurs more than six times faster with $[Cu(trimen)(OH)(OH_2)]^+$ than with 2,4-DNPDEP at 35°C (Table 4.15). It is unlikely that the phosphonate ester binds more effectively than the phosphate ester, to the metal complex. Therefore, the large rate increase may be attributed to more favourable substituent effects. The replacement of an ethoxy grouping ($-OCHCH_3$) by a methyl group ($-CH_3$) on the phosphonate ester results in enhanced intramolecular attack on the more positive phosphorus by bound hydroxide.

4.5 REFERENCES

1. J.E. Coleman and P. Gettins, Adv.Enzymol., 55, 381, (1983), and references therein.
2. R.C. Courtney, R.L. Gustafson, S. Westerback, H. Hyytiainen, S.C. Chaberek and A.E. Martell, J.Am.Chem.Soc., 79, 3030, (1957).
3. T. Wagner - Jauregg, B.E. Hackley, T.A. Lies, O.O. Owens and R. Roper, J.Am.Chem.Soc., 77, 922, (1955).
4. J. Epstein and D.H. Rosenblatt, J.Am.Chem.Soc., 80, 3596, (1958).
5. R.L. Gustafson and A.E. Martell, J.Am.Chem.Soc., 84, 2309, (1962).
6. P.R. Norman and G. Williams, MOD report No. 469.
7. P.R. Norman, Inorg.Chimi.Acta., 130 (1987).
8. S.H. Gellman, R. Petter and R. Breslow, J.Am.Chem.Soc., 108, 2388, (1986).
9. T.J. Atkins and J.E. Richman, Org.Synth., 58, 86, (1978).
10. R.W. Hay and P.R. Norman, J.Chem.Soc., Dalton Trans., 1441, (1979).
11. M. Sato, S. Matsuki, M. Ikeda and J - I. Nakaya, Inorg.Chimi.Acta., 125, 49, (1986).
12. M.B. Hursthouse, S.A.A. Jayaseera, H. Milburn and A. Quick, J.Chem.Soc. Dalton Trans., 2569 (1975).

13. P. Hendry and A.M. Sargeson, J.Chem.Soc., Chem. Commun., 164, (1982).

14. D.R. Jones, L.F. Lindoy and A.M. Sargeson, J.Am. Chem.Soc., 105, 7327, (1983).

15. J. Morrow and W.C. Trogler, Inorg.Chem., 2330, (1989).

16. P. Woolley, J.Chem.Soc., Perkin Trans. 2, 318, (1977).

17. F.M. Menger, L.H. Gan, E. Johnson, D.H. Dust, J.Am. Soc., 2800, 109, (1987).

18. J. Chin and X. Zou, J.Am.Chem.Soc., 110, 223, (1988).

CHAPTER FIVE

COBALT(III) COMPLEX CATALYSED HYDROLYSIS OF PHOSPHORUS ESTERS

5.1 INTRODUCTION

Organophosphorus compounds as a class are ubiquitous in nature and in modern society. To fully understand these compounds, it is important to establish mechanisms for their transformations in biological systems. Essentially all biological phosphorus chemistry is enzyme mediated, and their relevant enzymes require metal ions for activity or the activities depend strongly on the metal ion content of the reaction media[1].

To better characterize the role of metal ions in biological phosphorus chemistry, many investigators have examined metal ion complexes that model the activitiy of specific enzymes[2]. Early work[3-6] demonstrated that divalent metal complexes contribute to impressive rate enhancements in neutral phosphorus ester hydrolysis. However, as discussed in chapter four, divalent metal complexes, are extremely labile towards solvolytic ligand displacement and the simultaneous presence of monomeric, dimeric and hydrated complexes seriously complicates reliable identification of the species actually involved in ester hydrolysis.

More recently attention has focused the effects of (tetraamine)cobalt(III) complexes on the hydrolysis of anionic phosphates such as pyrophosphate[7] adenosine di-

and tri-phosphate[8], p-nitrophenyl phosphate[9] and triphosphate[10]. Currently there is considerable interest in developing catalysts that can cleave DNA sequence specifically. Due to the stability of the DNA phosphate diester backbone toward hydrolytic cleavage emphasis to date has mainly focused on oxidative cleavage of DNA[11]. A major challenge remains in developing catalysts that can cleave DNA hydrolytically. It has recently been demonstrated that cobalt(III) complexes are efficient in promoting the hydrolysis of phosphate diesters[12]. Compared with divalent metal ion complexes, tetraamine chelates of cobalt(III) offer two important advantages. First, the cobalt(III) complexes are simply prepared and are kinetically robust, thereby permitting characterization of all species present in solution. Secondly, the kinetics and mechanisms of cobalt(III) complex substitution reactions are well understood[13] and this knowledge should facilitate identifying mechanism involved in complex-promoted phosphorus ester hydrolysis.

Interestingly, the activity of the cobalt complexes is sensitive to the tetramine ligand structure. For example, $[Co(trien)(OH)(OH_2)]^{2+}$ is more reactive than $[Co(en)_2(OH)(OH_2)]^{2+}$ towards phosphate diesters[12]. However, it is difficult to evaluate the structure-reactivity relationship in this system because both cobalt complexes undergo rapid <u>cis</u>-<u>trans</u> equilibration with <u>trans</u> forms being inactive.

In view of the foregoing we have investigated reactions of the aquohydroxo(tetramine)cobalt(III) complexes [5.1], [5.2] and [5.3] with the phosphate triester 2,4-DNPDEP and the corresponding phosphonate ester 2,4-DNPEMP. The cobalt (III) complexes are ideal for evaluating the structure-reactivity relationship since they are held rigidly in the cis form[14] and cannot undergo cis-trans or other similar isomerisation processes. These complexes greatly accelerate 2,4-dinitrophenolate liberation from the respective phosphorus esters. Moreover, with [5.3] the reactions are truly catalytic with respect to cobalt chelate; i.e. 2,4-DNP yields are greater than the stoichiometeric amounts on the basis of complex as limiting reagent. These observations are of importance in the development of metal complex decontamination system for CW agents and in the search for compounds that model phosphatase activity.

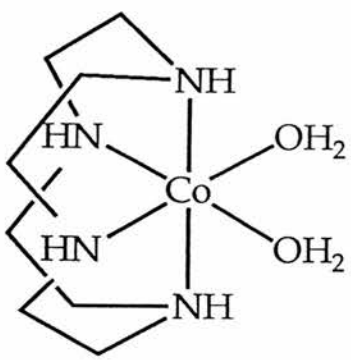

$[Co(cyclen)(OH_2)_2]^{3+}$

[5.1]

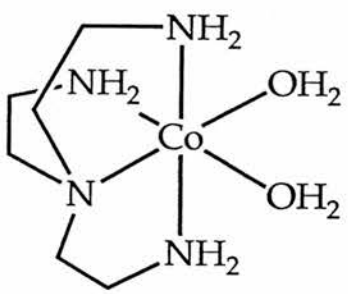

$[Co(tren)(OH_2)_2]^{3+}$

[5.2]

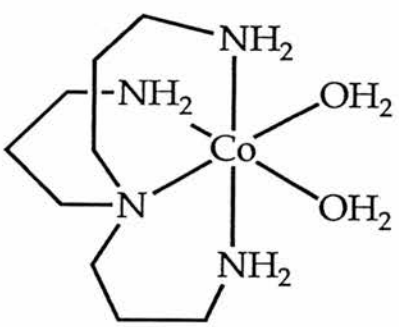

$[Co(trpn)(OH_2)_2]^{3+}$

[5.3]

5.2 EXPERIMENTAL

5.2.1 KINETICS

The cobalt(III) complex promoted hyrolysis of the phosphorus esters 2,4-DNPDEP and 2,4-DNPEMP was monitored using a Hewlett-Packard Lambda-5 multi-cell spectophotometer fitted with a water cooled thermostat. The reactions were carried out under pseudo-first-order conditions with a large excess of the cobalt complex over the phosphorus ester. Initial release of 2,4-dinitrophenolate was measured at 400 nm, plots of log (A_∞ - A_t) versus time were linear for at least three half-lives. First-order rate constants (k_{obs}) were calculated from the slopes of the linear plots (correlation co-efficient > 0.998). In a typical kinetic experiment, 0.01 mol dm^{-3} $[Co(trpn)(OH)(OH_2)]^{2+}$/ $[Co(trpn)(OH_2)_2]^{3+}$ solution in water was prepared by adding 1.5 equivalents of sodium hydroxide to $[Co(trpn)Cl_2]Cl$. After 5 minutes (1 hour for $[Co(tren)Cl_2]Cl$) the solution pH was adjusted to 7.0. The rate of aquation of $[Co(N_4)Cl_2]Cl$ is sensitive to the tetramine ligand structure[13]. Completion of aquation was confirmed by visible adsorption spectra (Table 5.1). Alternatively, where the hydoxy-aqua complex could be isolated as described for $[Co(tren)(OH)(OH_2)]$ the complex was prepared directly in .PA solution and the pH adjusted accordingly. The hydrolysis

solution and the pH adjusted accordingly. The hydrolysis were initiated by addition of 50 µl of 5 x 10^{-3} mol dm^{-3} stock solution in CH_3CN to 3 ml the freshly prepared 0.01 M cobalt complex previously adjusted to the desired pH and temperature. The pH of the reaction solution did not change appreciably (pH 7.0 $\pm$ 0.1) during the course of the hydrolysis reaction due to the buffering effect of the cobalt complex in solution. All experiments were run in duplicate or triplicate, and the tabulated data represent an average of these experiments. Second-order rate constants where obtained from plots of first-order rate constants against cobalt complex concentration.

5.2.2 POTENTIOMETERIC TITRATIONS

Titration of the cobalt complexes with standard base were carried out using the procedures described earlier (Section 4.2).

5.2.3 PREPARATION OF COBALT COMPLEXES

Preparation of $[Co(cyclen)Cl_2]Cl$

The macrocyclic ligand 1,4,7,10-tetra-azacyclododecane (cyclen) was synthesised as described in the literature[20] by reacting the disodium salt of the tritosylate of diethylene triamine with the tritosylate of diethanolamine.

Tritosyldiethylenetriamine (28 g, 0.05 mol) was dissolved in dry NN-dimethylformamide (300 cm^3). Sodium hydride (80% in paraffin oil, 12 g) was added in small portions and kept under a stream of nitrogen. When effervescence ceased the solution was warmed in a water bath (ca. 1 hour). The solution was cooled to room temperature and the excess of sodium hydride filtered off. The filtrate was transferred to a flask equipped with a thermometer, double-surface condenser, drying tube, N_2 inlet and magnetic stirrer. NOO'-tritosyldiethanolamine (28 g, 0.05 mol) dissolved in NN-dimethylformamide (200 cm^3) was added dropwise and the mixture heated on an oil-bath for ca. 2 hours at 110-120°C with continuous stirring. The solid product was filtered off, washed thoroughly with water, and dried in a vacuum oven at 60°C (yield 32 g). The tosyl derivative was recrystallised from formic acid m.p. 269-272°C (lit., 273°C[21]).

Anal. Calcd. for $C_{36}H_{44}N_4O_8S_4$: C, 54.80; H, 5.60; N, 7.10. Found: C, 54.70; H, 5.40; N, 7.10%.

The tetratosyl derivative was hydrolysed as follows. Thirty two grams of the crude product were dissolved in concentrated sulphuric acid (150 cm^3) and the solution heated on an oil-bath with continuous stirring at 110-120°C for 48 hours. The black solution was cooled to room temperature. The reaction mixture was then slowly added with stirring to sodium hydroxide solution (1 dm^3, 8 mol dm^{-3}) cooled in an ice-bath. On completion of the addition the pH was checked to ensure that pH > 14 (pK_a values of cyclen are[16] pK, <1, pK_2 1.15, pK_3 9.60 and pK_4 10.53). The mixture was allowed to stand at room temperature for ca. 2 hours to complete the precipitation of sodium sulphate, which was then filtered off. The filtrate was extracted with portions of chloroform (4 x 200 cm^3) and the chloroform removed on the rotary evaporator. The oily product was dissolved in methanol (20 cm^3) and concentrated hydrochloric acid (2.5 cm^3) added. The precipitated tetrahydrochloride was filtered off and recrystallised from 50% hydrochloric acid. Yield 4.5 g (35%).

Anal. Calcd. for $C_8H_{24}Cl_4N_4$: C, 30.20; H, 17.60; N, 7.60. Found: C, 30.20; H, 17.50; N, 7.50%.

The ^1H n.m.r. spectrum of the amine tetrahydrochloride (D_2O solution) showed the complete absence of tosyl groups and a single signal at δ 3.34 due to the CH_2 groups.

The cobalt(III) complex cis-[Co(cyclen)Cl_2]Cl was prepared via the cis-[Co[cyclen$(NO_2)_2$]Cl compound by the method of Collman and Schneider[17] as follows. A stream of CO_2 free air was passed for 12 hours through a solution containing cyclen.4HCl (635 mg, 2 mmol), lithium hydroxide (145 mg, 6 mmol), cobalt(II) chloride hexahydrate (475 mg, 2 mmol) and sodium nitrite (145 mg, 2.1 mmol) is 150 cm^3 of water. Yellow-brown crystals were obtained after concentration of the solution to about 15 cm^3. These were recrytallized from a minimum amount of hot water, yield 450 mg (62%).

Anal. Calcd. for $C_8H_{10}N_6O_4CoCl$: C, 26.80; H, 5.60; N, 23.50. Found: C, 26.70; H, 5.90; N, 22.30%.

A mixture of the cis-[Co(cyclen)$(NO_2)_2$]Cl (450 mg, 1.25 mmol) and 10 cm^3 of concentrated hydrochloric acid was evapourated to dryness on a steam bath, and the violet residue was then recrystallized from concentrated hydrchloric acid, yield 330 mg, (72%).

Anal. Calcd. for $C_8H_{20}N_4CoCl_3.1.5H_2O$: C, 26.30; H, 6.40; N, 15.30. Found: C, 26.20; H, 6.30; N, 15.60%.

Preparation of [Co(tren)Cl_2]Cl.H_2O[18]

2,2',2"-Triaminotriethylamine (tren) (7.31 g, 0.05 mol) was dissolved in 100 cm^3 of water containing sodium perchlorate monohydrate (24.58 g, 0.175 mol). To this was

added cobalt(II) perchlorate hexahydrate (18.30 g, 0.05 mol) in 50 cm^3 of water immediately followed by sodium nitrite (5.18 g, 0.075 mol) in 50 cm^3 of water. A brown solution containing some greenish precipitate formed, but on vigorous passage of air for ca. 1 hour the precipitate dissolved and a khaki-coloured solid was deposited. This was washed on the filter with ice cold water then ethanol, yield 32 g (95%) presuming a constitution of $[Co_2(tren)(NO_2)_2O_2](ClO_4)_2$.

The khaki-brown peroxo dimer (16 g, 0.028 mol) was added in portions to hot concentrated hydrochloric acid (100 cm^3) and heating was continued on a steam bath for 10 minutes after the final addition. Ethanol (150 cm^3) was mixed into the deep blue solution and on cooling a nearly quantitive yield (91%) of violet crystals (8.2 g, 0.025 mol) were collected and recrystallized from concentrated hydrochloric acid.

Anal. Calcd. for $C_6H_{18}N_4CoCl_3.H_2O$: C, 21.87; H, 6.12; N, 17.00. Found: C, 22.11; H, 5.95; N, 17.52%.

Preparation of $[Co(tren)(OH)(OH_2)](ClO_4)_2$

To a solution containing excess sodium carbonate (1.58 g, 0.015 mol) in 10 cm^3 of water, $[Co(tren)Cl_2]Cl$ (3.1 g, 0.01 mol) was added and heated on a steam bath for ca. 1 hour. Sodium perchlorate (2.11 g, 0.015 mol) was then added to the wine red solution and perchloric acid was added

dropwise until evolution of CO_2 had ceased and pH < 1 was obtained. Nitrogen was then bubbled through the solution to expel dissolved CO_2 and the pH of the solution was adjusted to pH 6.5 by the careful addition of 5 mol dm^{-3} sodium hydroxide solution. On standing mauve $[Co(tren)(OH)(OH_2)](ClO_4)_2$ crystallized readily as needles which were collected washed with ethanol and ether and dried under vacuum, yield 2.89 g (66%).

Anal. Calcd. $C_6H_{21}N_4CoCl_2O_{10}$: C, 16.41; H, 4.82; N, 12.76. Found: C, 16.11; H, 4.66; N, 12.51%.

Preparation of $[Co(trpn)Cl_2]Cl$

The quadridentate tripod ligand 3,3',3"-triaminotripropylamine (trpn) was prepared by catalytic hydrogenation of the readily prepared trinitrile devivative tris(2-cyanoethyl)amine as follows.

Tris (2-cyanoethyl)amine

Acrylonitrile (110 g, 2 mol) was added dropwise to a stirred solution of ammonia (61 g, mol) at 30°C at such a rate that little or no second phase was present at any time. Stirring was continued for ca. 2 hours and then water and (350 cm^3) and more acrylonitrile (110 g, 2 mol) were added. After the mixture had been stirred at 75-80°C for approximately 60 hours, water and excess acrylonitrile were removed by distillation under reduced pressure. The residual liquid (122 g, 71% yield) crystallized on standing. Recrystallization from ethanol gave white needles m.p. 58-59°C.

Anal. Calcd. for $C_9H_{12}N_4$: C, 61.34; H, 6.86; N, 31.79. Found: C, 61.29; H, 6.63; N, 31.80%.

3,3',3"-Triaminotripropylamine (trpn)

This compound has been synthesized previously in 40%

yield[19]. The following procedure gave quantitative yield of trpn. Tris (2-cyanoethyl)amine (6.13 g, 0.03 mol) and 6.6 g of 50% Raney nickel slurry were added to a 250 cm^3 glass hydrogenation vessel containing a solution of sodium hydroxide (2.33 g, 0.06 mol) and 85 cm^3 of 95% ethanol. The mixture was placed under hydrogen (40 psi) and the mixture was stirred until the uptake of hydrogen was complete, approximately 8 hours. The catalyst was vacuum filtered and rinsed with 95% ethanol. Ethanol was evaporated, and the residue was extracted with methylene chloride. The organic layer was dried over NaOH, filtered through anhydrous aluminium oxide, and evaporated. The crude product was distilled (b.p. 118°C, 0.1 mm) on a Kugelrohr apparatus, yield 4.71 g (72%).

Anal. Calcd. for $C_9H_{24}N_4$: C, 57.40; H, 12.85; N, 29.75. Found: C, 57.21; H, 12.61; N, 29.60%.

^1H NMR ($CDCl_3$,TMS) : 1.15 (6H,s), 1.59(6H,q), 2.45 (6H,t), 2.72 (6H,t).

The tripodal cobalt(III) complex $[Co(trpn)Cl_2]Cl$ was prepared as follows. To a methanolic solution of cobalt chloride hexahydrate (0.47 g, 2.0 mmol), a solution of 3,3',3"-triaminotriproplyamine (0.37 g, 2.0 mmol) in methanol (20 cm^3) was added dropwise. The solution mixture was aerated with CO_2 free, dry air for ca. 2 hours followed by slow addition of HCl gas until some green precipitate formed. On cooling the mixture in a refrigerator overnight,

the precipitate was filtered and washed with absolute ethanol then ether and vacuum dried, yield 0.31 g (42%).

Anal. Calcd. $C_9H_{24}N_4CoCl_3.H_2O$: C, 29.09; H, 7.05; N, 15.08. Found: C, 28.64; H, 6.63; N, 14.73%.

Preparation of $[Co(NH_3)_5(DEP)](CF_3SO_3)_2$

The cobalt complex $[Co(NH_3)_5OSO_2CF_3](CF_3SO_3)_2$ was synthesized as described in the literature[20]. Dissolution of the triflato complex in diethylphosphoric acid generated the desired product using the following procedure.

$[Co(NH_3)_5(OSO_2CF_3)](CF_3SO_2)$ (2.72 g, 4.6 mmol) and diethylphosphoric acid (0.71 g, 4.6 mmol) were dissolved in 50 cm^3 absolute ethanol. To this was added 0.5 g of triethylamine, and the whole was refluxed for ca. 30 minutes under dry nitrogen. On cooling, the solution was reduced under vacuum to approximately 2 cm^3, filtered through a no. 3 glass sinter and left for several days under dry nitrogen at -10^oC. Pink microcrystals formed, and were collected by filtration, washed with 0.5 cm^3 ice cold propan-2-ol and vacuum dried over silica-gel. The product was very soluble in water, ethanol and methanol and recrystallisation proved impracticable.

Anal. Calcd. for $C_6H_{25}N_5F_6O_8PS_2Co$: C, 12.79; H, 4.47; N, 12.43. Found: C, 12.30; H, 4.29; N, 11.88%.

TABLE 5.1 Visible absorption maxima of (amine) cobalt(III) complexes

complex	solvent	λ max,nm(εmax,$M^{-1}cm^{-1}$)
$[Co(NH_3)_5(OH_2)]^{3+}$	0.1MHClO_4	492 (48) 345 (45)
$[Co(NH_3)_5(DEP)]^{2+}$	0.1MHClO_4	505 (53) 354 (44)
$[Co([15]aneN_5)Cl]^{2+}$	H_2O	510 (253) 348 (342)
$[Co([15]aneN_5)(OH_2)]^{3+}$	H_2O	450 (305)
$[Co(cyclen)Cl_2]^{+}$	37% HC1	565 (185) 390 (165)
$[Co(cyclen)(OH_2)_2]^{3+}$	0.1MHClO_4	530 (230) 368 (133)
$[Co(tren)Cl_2]^{+}$	37% HC1	560 (125) 385 (120)
$[Co(tren)(OH)(OH_2)]^{2+}$	H_2O,pH6.5	514 (102) 358 (94)
$[Co(tren)(OH_2)_2]^{3+}$	0.1MHClO_4	504 (109) 346 (82)
$[Co(trpn)Cl_2]$	37% HC1	578 (55)
$[Co(trpn)(OH_2)_2]^{3+}$	0.1MHClO_4	530 (57) 366 (92)

5.3 RESULTS

5.3.1 POTENTIOMETERIC TITRATIONS

The diaquo-, aquohydroxo- and dihydroxo (tetraamine) cobalt (III) complexes are related by the acid-base equilibria shown in reactions (1) and (2).

$$(N_4)Co(OH_2)_2 \overset{K_1}{\rightleftharpoons} (N_4)Co(OH)(OH_2) + H^+ \quad (1)$$

$$(N_4)Co(OH)(OH_2) \overset{K_2}{\rightleftharpoons} (N_4)Co(OH)_2 + H^+ \quad (2)$$

The pK_1 and pK_2 values for $[Co(cyclen)(OH_2)_2]^{3+}$, $[Co(tren)(OH_2)_2]^{3+}$ and $[Co(cyclen)(OH_2)_2]^{3+}$ determined by potentiometeric titration are shown in Table 5.2 together with the pK values for the mono aqua complexes $[Co(NH_3)_5(OH_2)]^{3+}$ and $[Co([15]aneN_5)(OH_2)]^{3+}$.

5.3.2 KINETICS

Observed first-order rate constants for the series of cobalt (III) complex promoted hydrolysis reactions of 2,4-DNPDEP and 2,4-DNPEMP as shown in Table 5.3. The pH rate profile for $[Co(cyclen)(OH_2)]^{3+}$, $[Co(tren)(OH_2)]^{3+}$ and

TABLE 5.2 **Summary of practical pKa values of the water molecules co-ordinated to the cobalt (III) complexes, determined by potentiometeric titration at 25°C, (I=0.1)**

cobalt complex	pK_{a1}	pK_{a2}
$[Co(NH_3)_5(OH_2)]^{3+}$	6.21	-
$[Co([15]aneN_5)(OH_2)]^{3+}$	6.30	-
$[Co(cyclen)(OH_2)_2]^{3+}$	5.21	7.71
$[Co(tren)(OH_2)_2]^{3+}$	5.17	7.66
$[Co(trpn)(OH_2)_2]^{3+}$	4.90	7.51

TABLE 5.3 Observed first-order rate constants for cobalt (III) complex (0.01 mol dm^{-3}) promoted hyrolysis of 2,4-DNPDEP and 2,4-DNPEMP at 25°C, pH 7.0

cobalt complex	DNPDEP k_{obs}/s^{-1}	DNPEMP k_{obs}/s^{-1}
$[Co(NH_3)_5(OH)]^{2+}$	1.82×10^{-5}	1.24×10^{-3}
$[Co([15]aneN_5)(OH)]^{2+}$	2.11×10^{-5}	1.58×10^{-3}
$[Co(cyclen)(OH)(OH_2)]^{2+}$	2.98×10^{-4}	-
$[Co(tren)(OH)(0H_2)]^{2+}$	4.25×10^{-5}	-
$[Co(trpn)(OH)(0H_2)]^{2+}$	7.15×10^{-3}	1.01×10^{-2}
control	1.55×10^{-7}	1.03×10^{-4}

TABLE 5.4 **Observed first-order rate constants for the $[Co(cyclen)(OH)(OH_2)]^{2+}$ promoted hyrdolysis of 2,4-DNPDEP as a function of pH at 25°C, I=0.1 (KNO_3)**

pH	$10^4 k_{obs}$[b] /s^{-1}	pH	$10^4 k_{obs}$[b] /s^{-1}
4.00	0.13	6.40	2.63
4.42	0.22	6.80	2.91
4.80	0.27	7.20	3.14
5.22	0.62		
5.60	1.30		
5.98	2.19		

a) All reactions were monitored spectrophotometerically at 400 nm for the production of 2,4-dinitrophenolate from an initial [2,4-DNPDEP] = 0.08 mM. Concentration of cobalt complex employed = 0.1 M. Temperature was maintained at 25.0 ± 0.1°C.

b) Average of at least 3 kinetic runs.

Figure 5.1 pH-rate profile for the $[Co(cyclen)(OH)(OH_2)]^{2+}$ promoted hydrolysis of 2,4-DNPDEP at 25°C, I=0.1(KNO_3)

$[cobalt\ complex]_{total}$ = 0.100 mol dm^{-3}

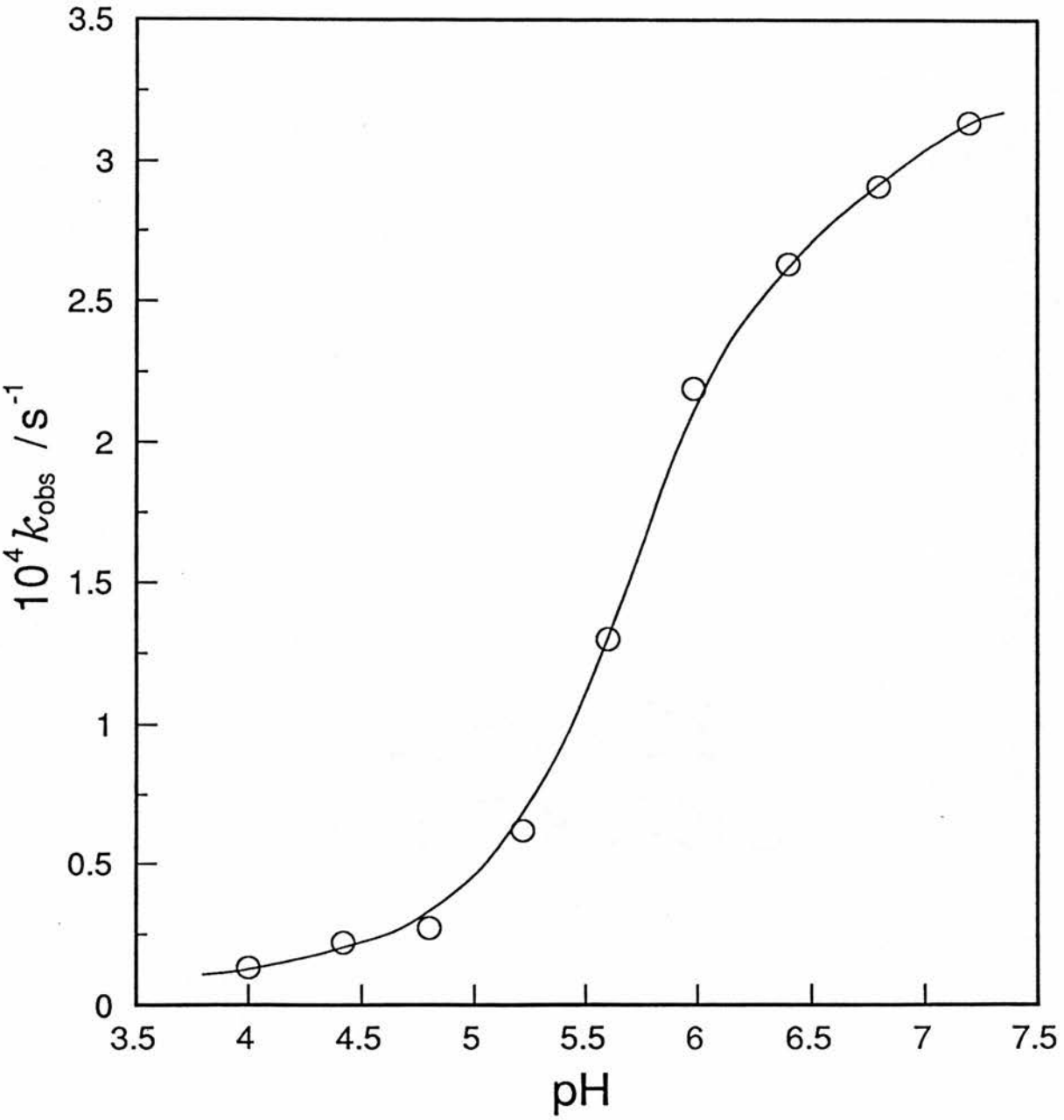

TABLE 5.5 **Observed first-order rate constants for the $[Co(tren)(OH)(OH_2)]^{2+}$ promoted hydrolysis of 2,4-DNPDEP as a function of pH at 25°C, I=0.1 (KNO_3)[a]**

pH	$10^5 k_{obs}$[b] /s^{-1}	pH	$10^5 k_{obs}$[b] /s^{-1}
2.90	0.85	6.00	4.70
3.48	0.95	6.55	5.22
4.00	1.25	7.00	5.50
4.52	1.60		
4.95	2.30		
5.50	3.62		

a) as Table 5.3 except cobalt concentration = 0.101 mol dm^{-3}

b) as Table 5.3

Figure 5.2 pH-rate profile for the $[Co(tren)(OH)(OH_2)]^{2+}$ promoted hydrolysis of 2,4-DNPDEP at 25°C, I=0.1(KNO_3)

$[cobalt\ complex]_{total}$ = 0.101 mol dm^{-3}

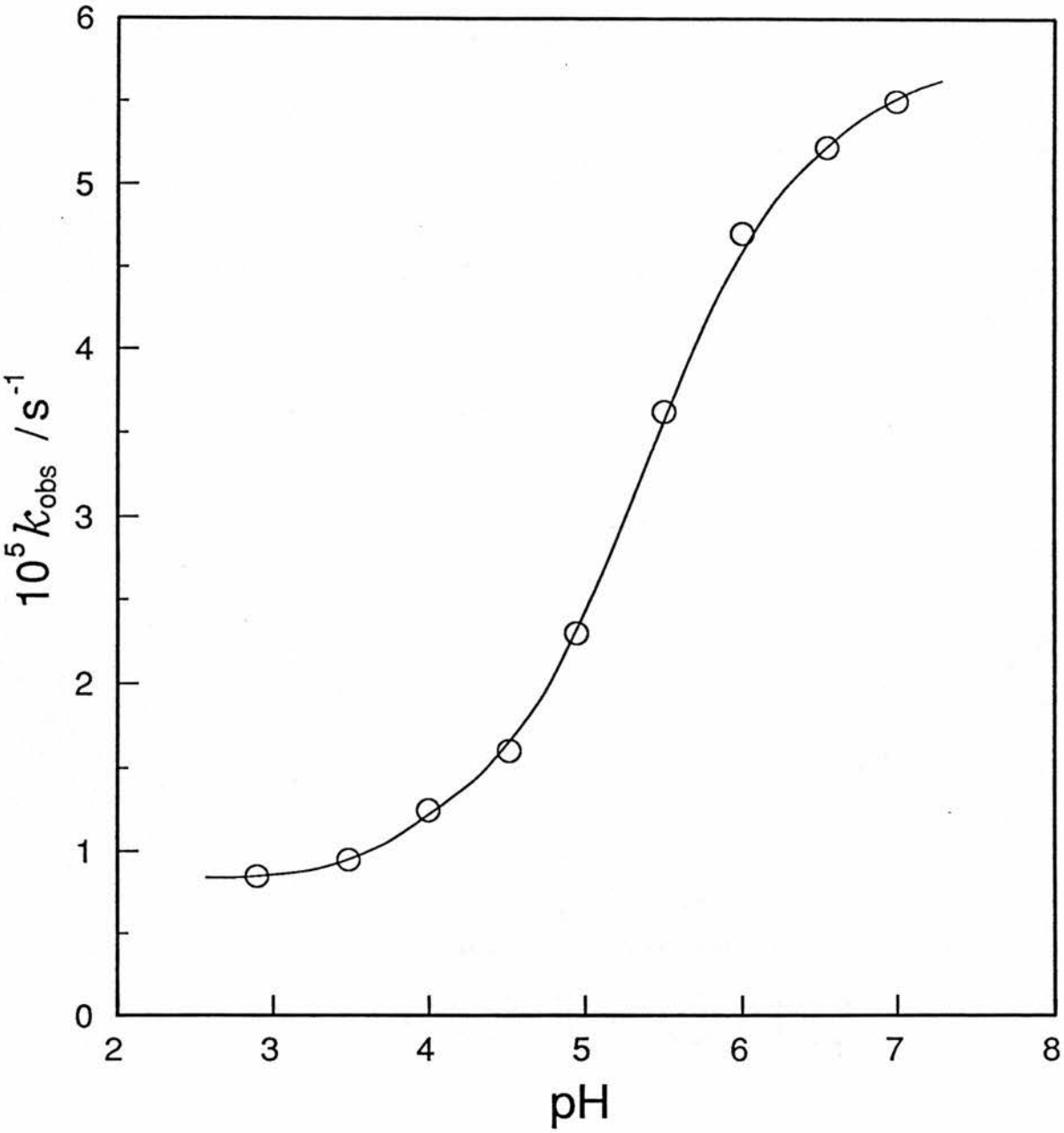

TABLE 5.6 **Observed first-order rate constants for the $[Co(trpn)(OH)(OH_2)]^{2+}$ promoted hydrolysis of 2,4-DNPDEP as a function of pH at 25°C, I=0.1 (KNO_3)[a]**

pH	$10^3 k_{obs}$[b] /s^{-1}	pH	$10^3 k_{obs}$[b] /s^{-1}
3.32	0.05	5.50	5.10
3.80	0.08	5.71	5.62
4.40	0.31	5.99	6.11
4.79	0.70	6.40	6.70
4.99	4.22	7.11	7.22
5.30	4.50		

a) as Table 5.3 except cobalt concentration = 0.0998 mol dm^{-3}

b) as Table 5.3

Figure 5.3 pH-rate profile for the $[Co(trpn)(OH)(OH_2)]^{2+}$ promoted hydrolysis of 2,4-DNPDEP at 25°C, I=0.1(KNO_3)

$[cobalt\ complex]_{total}$ = 0.099 mol dm^{-3}

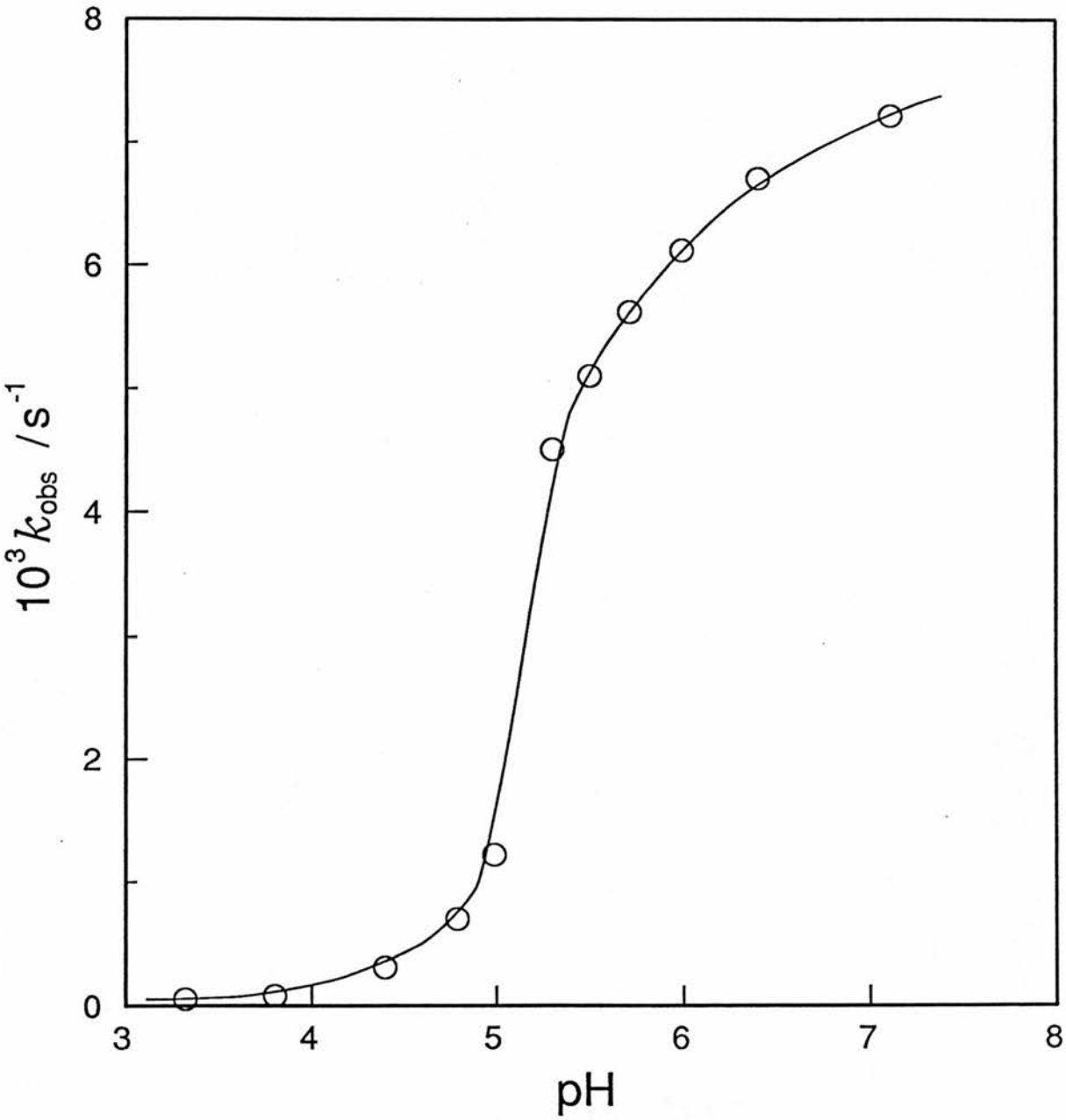

$[Co(trpn)(OH_2)]^{3+}$ promoted hydrolysis of 2,4-DNPDEP (see Tables 5.4, 5.5 and 5.6) are illustrated in Figures 5.1, 5.2 and 5.3 respectively. The rate of hydrolysis of 2,4-DNPDEP increases linearly with increasing cobalt complex concentration for the three chelates under study, Figures 5.4, 5.5 and 5.6. Second-order rate constants obtained from these plots of first-order rate constants versus complex concentration (see Tables 5.7, 5.8 and 5.9) are summarized in Table 5.10. Of the cobalt complexes studied only $[Co(trpn)(OH_2)_2]^{3+}$ demonstrated true catalytic activity. The cobalt(III) complex catalysed hydrolysis of 2,4-DNPDEP was monitored by the pH stat method. In a typical turnover experiment 2,4-DNPDEP (0.01 mol dm^{-3}) and $[Co(trpn)(OH_2)_2]^{3+}$ (0.001 mol dm^{-3}) in 15 cm^3 of water were stirred at 25°C. The pH of the reaction was maintained at 7.0 on a Radiometer Titra-lab system. Figure 5.7 shows a typical acid production versus time trace.

TABLE 5.7 **Observed first-order rate constants for the $[Co(cyclen)(OH)(OH_2)]^{2+}$ promoted hydrolysis of 2,4-DNPDEP as a function of cobalt complex concentration at pH 7.0, 25°C and I=0.1 (KNO_3)**

10^2[cobalt complex] /mol dm^{-3}	10^4 k_{obs} /s^{-1}	$10^2 k_{cat}$[a] /mol $dm^{-3} s^{-1}$
0.18	0.51	2.85
0.41	1.20	2.95
0.60	1.83	3.05
0.81	2.51	3.10
1.00	2.98	2.98
1.18	3.56	3.02

a) average $k_{cat} = 2.99 \times 10^{-2}$ mol $dm^{-3} s^{-1}$

Figure 5.4 Effect of increasing the concentration of $[Co(cyclen)(OH)(OH_2)]^{2+}$ on the rate of cobalt complex promoted hydrolysis of 2,4-DNPDEP at pH 7.0, 25°C and I=0.1(KNO_3)

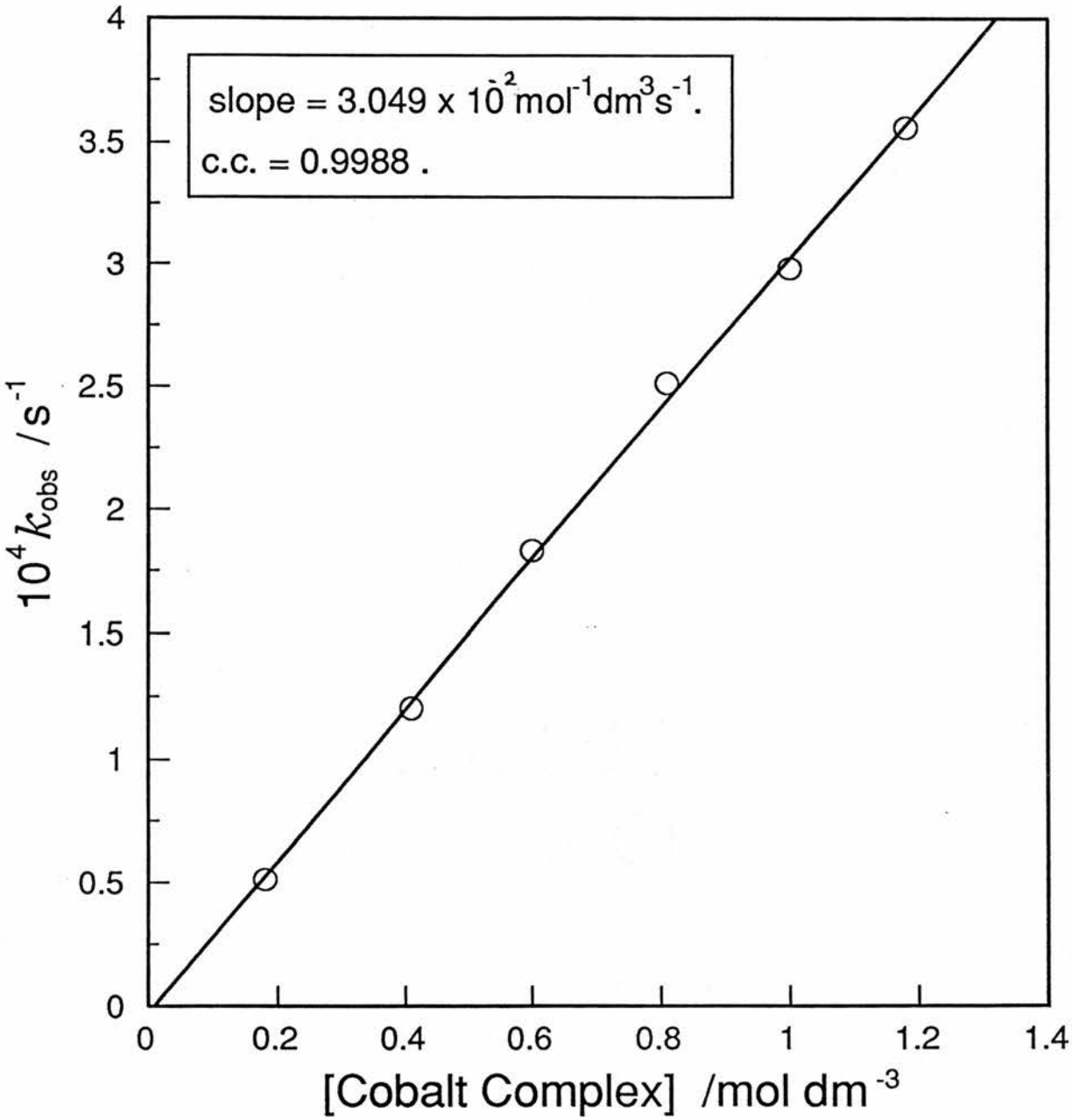

TABLE 5.8 **Observed first-order rate constants for the $[Co(tren)(OH)(OH_2)]^{2+}$ promoted hydrolysis of 2,4-DNPDEP as a function of cobalt complex concentration at pH 7.0, 25°C and I=0.1 (KNO_3)**

10^2[cobalt complex] /mol dm^{-3}	10^5 k_{obs} /s^{-1}	$10^3 k_{cat}$[a] /mol $dm^{-3} s^{-1}$
0.15	0.61	4.10
0.34	1.41	4.15
0.49	2.13	4.18
0.76	3.22	4.24
1.01	4.25	4.21
1.16	4.92	4.24

a) average $k_{cat} = 4.19 \times 10^{-3}$ mol $dm^{-3} s^{-1}$

Figure 5.5 Effect of increasing the concentration of $[Co(tren)(OH)(OH_2)]^{2+}$ on the rate of cobalt complex promoted hydrolysis of 2,4-DNPDEP at pH 7.0, 25°C and I=0.1(KNO_3)

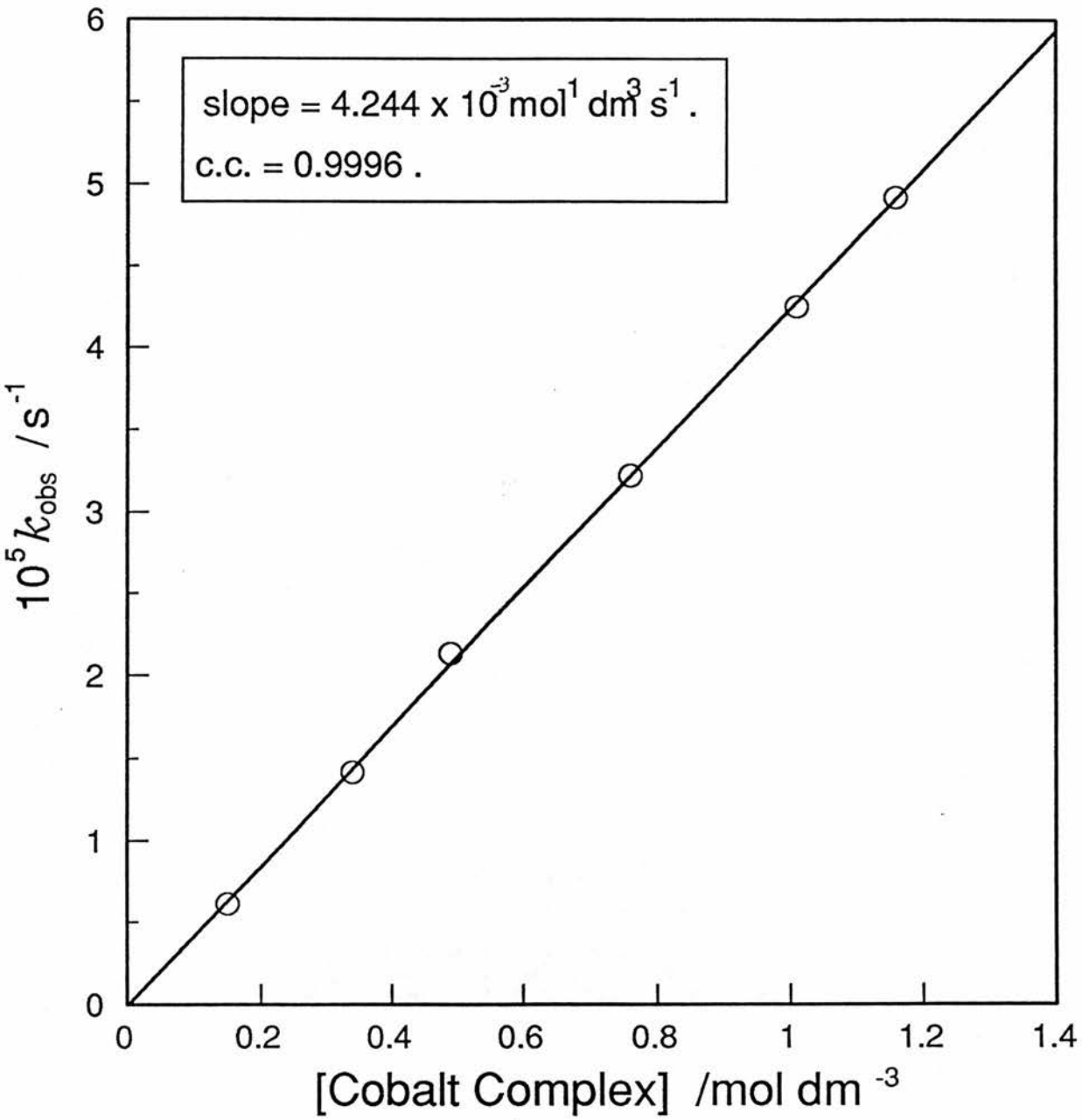

TABLE 5.9 **Observed first-order rate constants for the $[Co(trpn)(OH)(OH_2)]^{2+}$ promoted hydrolysis of 2,4-DNPDEP as a function of cobalt complex concentration at pH 7.0, 25°C and I=0.1 (KNO_3)**

10^2[cobalt complex] /mol dm^{-3}	10^3 k_{obs} /s^{-1}	k_{cat} /mol $dm^{-3}s^{-1}$
0.11	0.71	0.65
0.19	1.42	0.75
0.30	2.04	0.68
0.40	2.76	0.69
0.59	4.25	0.72
0.80	6.16	0.77
0.99	7.15	0.72

a) average k_{cat} = 0.72 mol $dm^{-3}s^{-1}$

Figure 5.6 Effect of increasing the concentration of $[Co(trpn)(OH)(OH_2)]^{2+}$ on the rate of cobalt complex promoted hydrolysis of 2,4-DNPDEP at pH 7.0, 25°C and I=0.1(KNO_3)

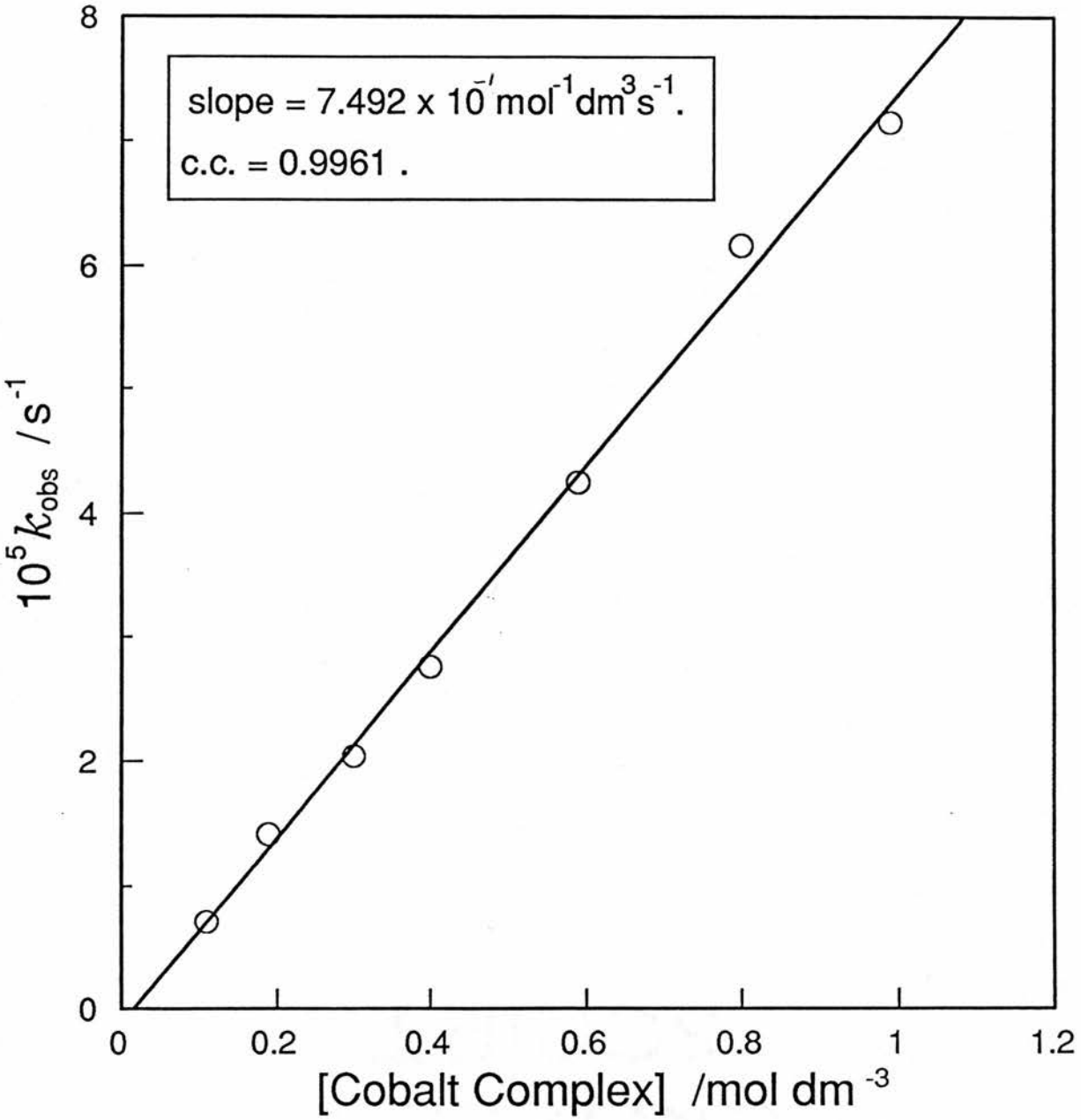

TABLE 5.10 Second-order rate constants for the hydrolysis of 2,4-DNPDEP in aqueous at 25°C by aquahydroxo cobalt(III) tetraamine complexes

cobalt complex	k_m /mol dm^{-3} s^{-1}
$[Co(cyclen)(OH)(OH_2)]^{2+}$	3.09×10^{-2}
$[Co(tren)(OH)(OH_2)]^{2+}$	4.24×10^{-3}
$[Co(trpn)(OH)(0H_2)]^{2+}$	0.749

Figure 5.7 Consumption of NaOH with time in the $[Co(trpn)(OH)(OH_2)]^{2+}$ (5 μM) catalysed hydrolysis of DNPDEP (50 μM) at pH 7.0 and 25°C.

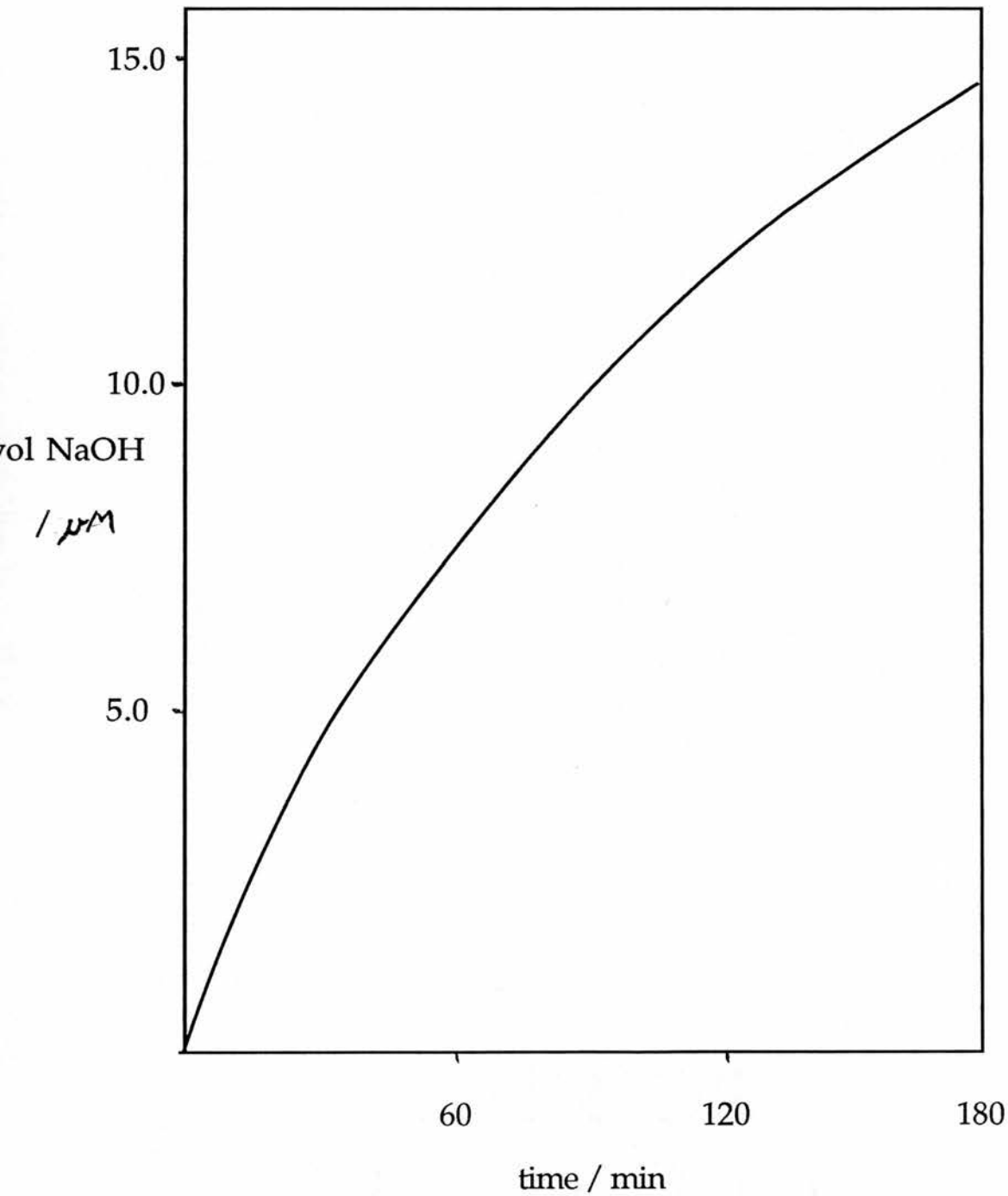

5.4 DISCUSSION

Earlier chapters have demonstrated an accelerating effect when labile positions are available on the metal complex. The most marked effects so far studied are observed when two sites, cis to one another, are available. This observation has been confirmed where cis diaquo cobalt(III) complexes are employed.

The cobalt(III) cyclen species [5.1] is 100% cis by virtue of the fact that the hole size of the macrocycle is too small to accept a cobalt atom in the plane of the four nitrogen donor atoms, so the ligand must fold slightly to accommodate the metal atom[17]. The complexes of cobalt(III) with the tripodal tetraamine, 2',2',2"-triaminotriethylamine [tren = $N(CH_2CH_2NH_2)_3$] [5.2] have been extensively studied[21]. The addition of another CH_2 group into each ethylene bridge of tren produces the more flexible quadridentate tripodal ligand 3,3',3"-triaminotripropylamine [trpn=$N(CH_2CH_2CH_2NH_2)_3$], which allows the formation of trigonal-bipyramidal or octahedral complexes[22]. The cobalt(III) complex of trpn [5.3] has been shown to dramatically enhance the rate of hydrolysis of ATP[23]. In many octahedral cobalt(III) tetraamine complexes cis/trans isomerisation complicates their reactivitiy. In this study

isomerisation is avoided by using tripodal ligands, in which the fifth and sixth co-ordination sites are fixed and forced into the cis-position.

It is well known that the rate of anation of cobalt (III) complexes is highly sensitive to the structure of the tetraamine ligand. Limited studies on the effect of tetraamine ligand structure on the efficiency of cobalt(III) complexes in the hydrolysis of phosphorus esters have been reported[23].

The first and second acid dissociations of the complexes are shown in Scheme 5.1.

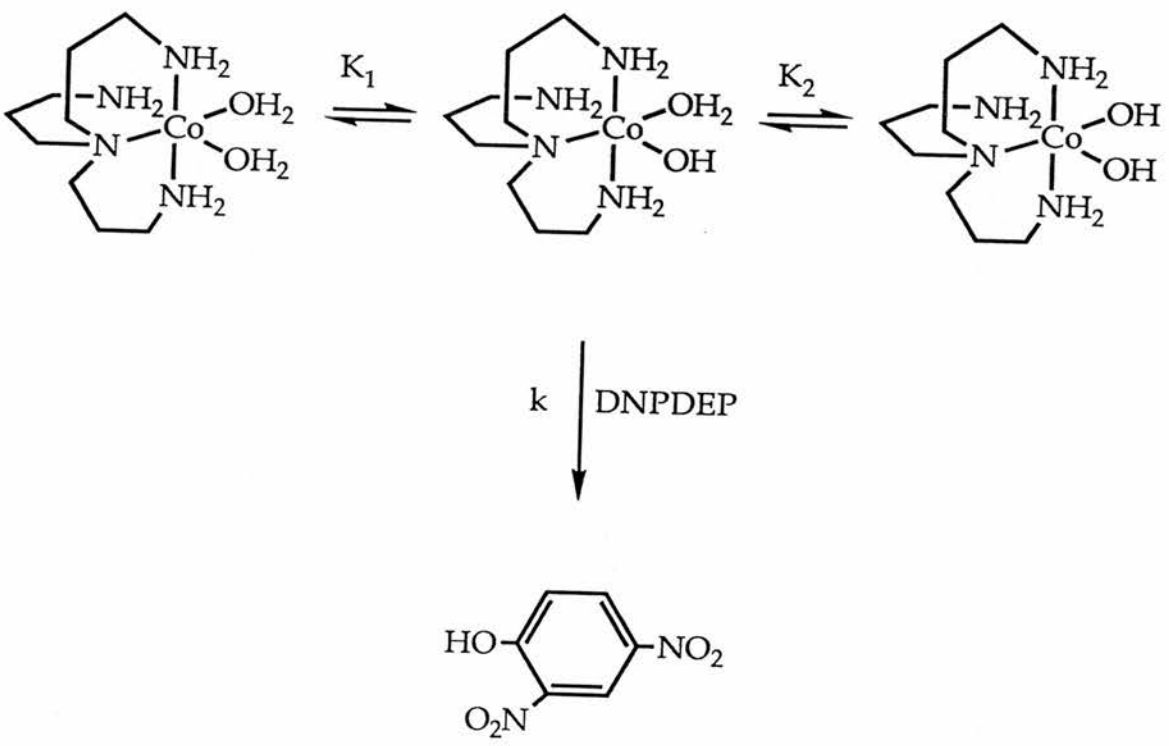

[Scheme 5.1]

The constants (K_{a1},K_{a2}) are listed in Table 5.2. The pH-rate profiles for the three $N_4Co(aq)$ DNPDEP systems are shown in Figures 5.1, 5.2 and 5.3. The curves closely resemble a titration curve for a weak acid. The acid dissociation constants obtained from the pH-rate curves are in good agreement to those obtained by direct titration considering the differing experimental conditions. It is apparant from these sigmodial shaped pH-rate profiles that the cobalt aquohydroxo form is the active species that promotes the hydrolysis of 2,4-DNPDEP.

The hydrolysis reactions are first order in the cobalt complex and rates are seen to increase linearly with the concentration of the aquohydroxo cobalt(III) tetraamine complex Figures 5.4, 5.5 and 5.6. These observations would suggest there is only one cobalt species involved in the hydrolyses reactions.

A mechanism for the cobalt aquohydroxo-complex promoted hydrolysis of 2,4-DNPDEP is outlined in Scheme 5.2.

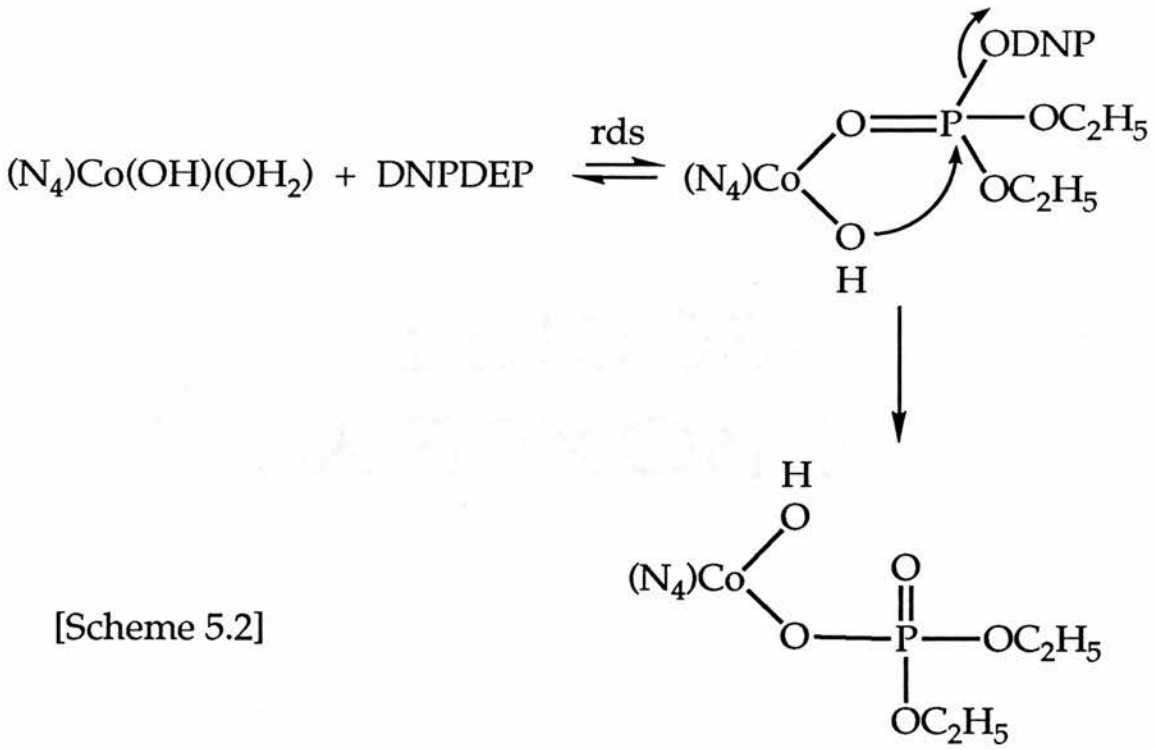
(N4)Co(OH)(OH2) + DNPDEP
rds
(N4)Co
O
P
ODNP
OC2H5
OC2H5
O
H
H
O
(N4)Co
O
O
P
OC2H5
OC2H5

[Scheme 5.2]

The reaction of the aquohydroxo-complex (the major species and the most reactive towards substitution) and the phosphorus ester proceeds via rate-limiting formation of the mono-dentate species. The hydroxo (dinitrophenyldiethylphosphonato) (tetraamine)cobalt(III) complex reacts intramolecularly liberating 2,4-dinitrophenolate and gives the bidentate (diethylphosphonato)(tetraamine)cobalt(III) complex which rapidly hydrolyses.

In support of this scheme a number of experimental results and literature comparisons can be cited. The overall reactivity order (trpn > cyclen > tren) of the aquohydroxo complexes towards DNPDEP parallels the reactivity order of analogous substitution reactions for cobalt complexes with these ligands. These substitutions proceed via a mechanism that is essentially a rate-limiting, D-type process.

The most plausible reaction pathway would be internal nucleophilic attack at phosphorus by coordinated hydroxide. Entropic effects favour this pathway over the alternative intermolecular attack by solvent water. This type of intramolecular reaction in cobalt(III) amine complexes well established in the cobalt(III) assisted hydrolysis of amino acid esters, amino acid amides and dipeptides[25,26]. Indeed, there is also evidence for internal attack by co-ordinated NH_2 on amino acid esters[27] and phosphate esters[1]

so the effect is not limited to hydroxide ion. The requirements[10] for cis-co-ordinated hydroxide in establishing the reactivity of macrocyclic cobalt(III) complexes towards triphosphate anion hydrolysis is particularly compelling evidence for a similar mechanism in the reactions reported here.

Further evidence that water substitution, by phosphoryl oxygen, is the rate determining step is the observation that aquahydroxo cobalt(III) complexes hydrolyze DNPEMP at comparable rates to those for DNPDEP (Table 5.2). If complexation was not the rate determining step, the rates of cobalt complex promoted hydrolysis of DNPEMP would be significantly larger than those observed for DNPDEP. The water exchange step is probably rate determining.

In neutral water the rate of hydrolysis of 2,4-DNPDEP is 1.55×10^{-7} s^{-1} at 25°C, (Chapter 2). With added cobalt complex (0.01 mol dm^{-3} [5.1], [5.2] and [5.3]) the observed rate constants for hydrolysis of 2,4-DNPDEP is increased 3.5×10^{2} - 4.6×10^{4}-fold depending on the cobalt complex used (Table 5.2). The difference in reactivity of the cobalt complexes is believed to be due primarily to their different water exchange rates. Under our experimental conditions greater than 99% of 2,4-DNPDEP is estimated to be in the free form and less than 1% in the cobalt bound form. It is clear from our concentration dependence studies Figures 5.4, 5.5 and 5.6 that saturation kinetics have not been reached

at 0.01 mol dm^{-3} cobalt complex. The hydrolysis at DNPDEP by $[Co(trpn)(OH)(OH_2)]^{2+}$ is 4.6×10^4 times faster than that of free DNPDEP and some 130 times faster than hydrolysis by $[Co(tren)(OH)(OH_2)]^{2+}$ its close structural analogue.

The high lability of the $Co(trpn)^{3+}$ species towards substitution is believed to be associated, at least in part, with the flexibility of the six membered ring system. Such flexibility is likely to contribute to the ease of forming the dissociative transition state.

Turnover experiments were carried out by the pH-stat method as described earlier. Three turnovers of substrate take place within 180 minutes for the $[Co(trpn)(OH)(OH_2)]^{2+}$ system. Production of diethylphosphate was confirmed by ^{31}P nmr. By contrast turnover experiments employing $[Co(tren)(OH)(OH_2)]^{2+}$ and $[Co(cyclen)(OH)(OH_2)]^{2+}$ as catalysts, failed to produce more than stoichiometeric quantities of acid. The catalytic cycle for $[Co(trpn)(OH)(OH_2)]^{2+}$ catalyzed hydrolysis of 2,4-DNPDEP is outlined in Scheme 5.3.

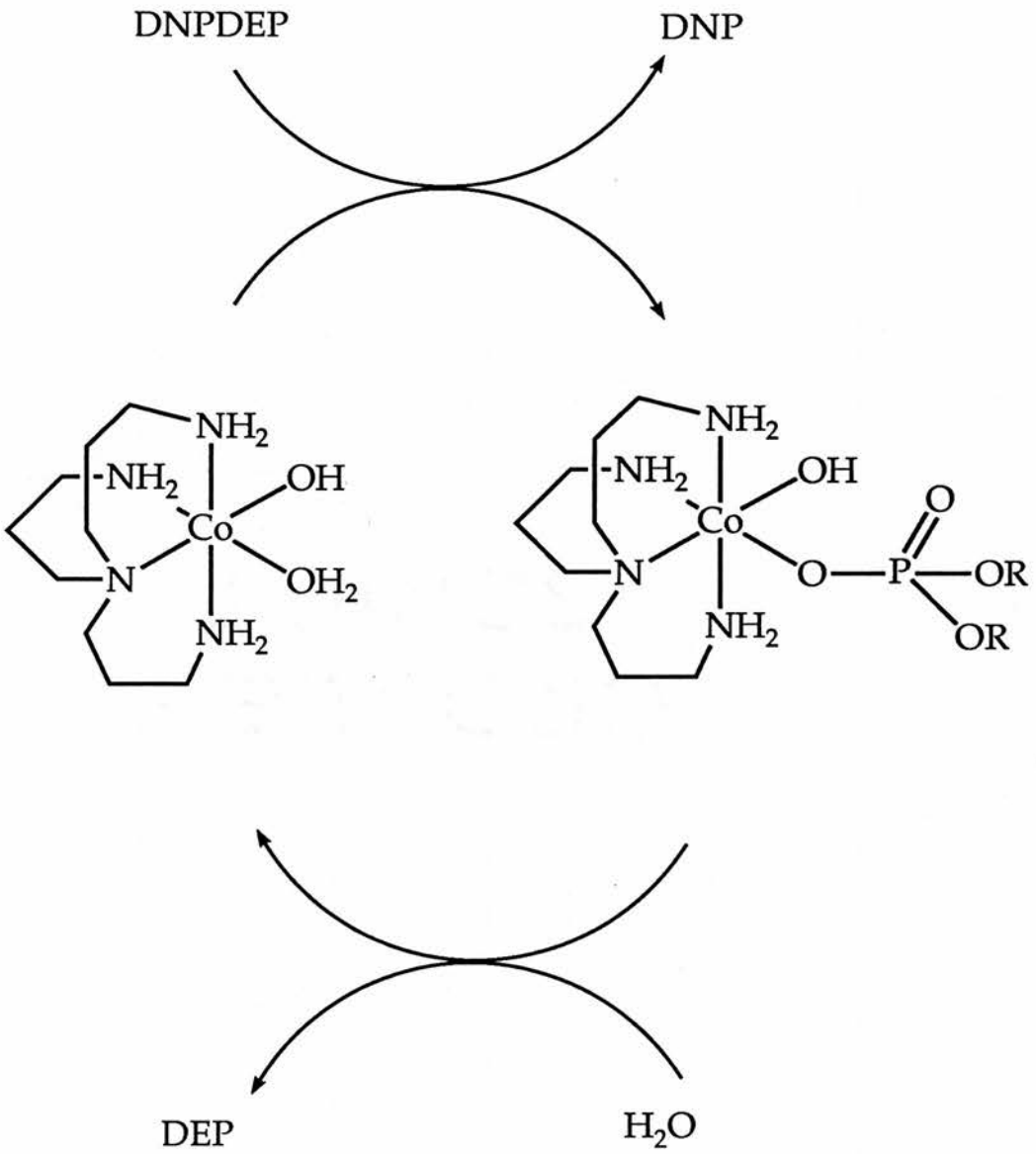
DNPDEP
DNP
NH2
-NH2
OH
Co
N
OH2
NH2
NH2
-NH2
OH
Co
N
O
P
O
OR
OR
NH2
DEP
H2O

[Scheme 5.3]

5.5 CONCLUSIONS

Our observations concerning aquohydroxo (tetraamine) cobalt(III) complex catalyzed hydrolysis of organophosphorus esters have important practical and fundamental ramifications.

In the practical context we have demonstrated that these chelates can provide large accelerations of neutral organophosphorus ester hydrolyses. This suggests that cobalt(III) chelates have potential applications for rapidly degrading hazardous organophosphorus substances. It has been demonstrated that:

1. rigid cis-aquohydroxo (tetramine) cobalt(III) complexes are highly reactive in promoting the hyrolysis of organophosphorus esters;
2. the reactivity of the tetraamine complexes changes dramatically with change in ligand structure.
3. the replacement of the five membered rings (N_4 = cyclen or tren) with the more flexible tripodal ligand trpn causes marked rate enhancements.
4. the reactivity of the aquohydroxo (tetraamine)-cobalt complexes towards organophosphorus ester hydrolysis decreases in the order trpn > cyclen > tren.

Fundamentally, our findings contribute to the understanding the mechanism of metal ion catalyzed organophosphorus ester hydrolysis reactions. This understanding permits us to predict the effect of structural modification on inherent reactivity and to design novel materials with enhanced reactivity. The demonstrated catalytic hydrolysis of 2,4-DNPDEP reveals that the cobalt complex $[Co(trpn)(OH)(OH_2)]^{2+}$ possesses the principle property (i.e. catalytic activity) common to all enzymes. Cobalt (III) complexes in solution are well charaterised species and are, in this regard, considerably superior to similar complexes based on divalent metal ions. Since the factors controlling the activity of cobalt(III) chelates are well established, this class of compounds could serve as a powerful probe to the complex mechanisms involved in metalloenzyme reactions.

5.6 REFERENCES

1. A.S. Mildvan, C.M. Grisham, Struct.Bonding, (Berlin), 20, 1, (1974).
2. P. Woolley, Nature, (London), 258, 677, (1975).
3. T. Wagner - Jauregg, B.E. Hackley, T.A. Lies, O.O. Owens, R. Proper, J.Am.Chem.Soc., 77, 922, (1955).
4. J. Epstein, D.H. Rosenblatt, J.Am.Chem.Soc., 80, 3596, (1958).
5. R.L. Gustafson, S. Chaberek, A.E. Martell, J.Am.Chem, Soc., 85, 589, (1963).
6. F.M. Fowkes, G.S. Ronay, L.B. Ryland, J.Phys.Chem., 62, 867, (1958).
7. R.M. Milburn, P.W.A. Hubner, Inorg.Chem., 19, 1267, (1980).
8. M. Hediger, R.M. Milburn, ACS Symp.Ser., 171, 211, (1981).
9. B. Anderson, R.M. Milburn, J.M. Harrowfield, G.B. Robertson, A.M. Sargeson, J.Am.Chem.Soc., 99, 2652, (1977).
10. P.R. Norman, R.D. Cornelius, J.Am.Chem.Soc., 104, 2356, (1982).
11. D.S. Sigman, Acc.Chem.Res., 19. 180, (1986).
12. J. Chin, X. Zou, J.Am.Chem.Soc., 110, 223, (1988).
13. F. Baslo, R.G. Pearson, "Mechanisms of Inorganic Reactions", 2nd ed., Wiley, New York, (1967).

14. Y. Iitaka, M. Shina and E. Kimura, Inorg.Chem., 13, 2886, (1974).

15. R.W. Hay and P.R. Norman, J.Chem.Soc., Dalton Trans., 1441, (1979).

16. K.C. Chang, E. Grunwald and L.R. Robinson, J.Am.Chem. Soc., 99, 3794, (1977).

17. J.P. Collman and P.W. Schneider, Inorg.Chem., 5, 1380, (1966).

18. D.A. Buckingham, P.J. Cresswell and A.M. Sargeson, Inorg.Chem., 7, 1485, (1975).

19. J.L. van Winkle, J.D. McClure, P.H. Williams, J.Org. Chem., 31, 3300, (1966).

20. N.E. Dixon, W.G. Jackson, M.J. Lancaster, G.A. Lawrence and A.M. Sargeson, Inorg.Chem., 20, 470, (1981).

21. S.G. Zipp, A.P. Zipp and S.K. Madan, Coord.Chem.Rev., 14, 29, (1974).

22. J.L. Shafer and K.N. Raymond, Inorg.Chem., 10, 1799, (1971).

23. F. Tafesse and R.M. Milburn, Inorg.Chem.Acta., 135, 119, (1987).

24. S.S. Massoud and R.M. Milburn, Polyhedron, 8, 275, (1989).

25. D.A. Buckingham, C.E. Davis, D.M. Foster, A.M. Sargeson, J.Am.Chem.Soc., 92, 5571, (1970).

26. D.A. Buckingham, D.M. Foster and A.M. Sargeson, J.Am. Chem.Soc., 91, 4102, (1969).

27. D.A. Buckingham, D.M. Foster and A.M. Sargeson, J.Am. Chem.Soc., 91, 3451, (1969).

28. J.M. Harrowfield, D.R. Jones, L.F. Lindoy, A.M. Sargeson, J.Am.Chem.Soc., 102, 7733, (1980).

CHAPTER SIX

METALLOMICELLE CATALYSED HYDROLYSIS OF PHOSPHORUS ESTERS

6.1 INTRODUCTION

Micelles in water can be described as spherical aggregates of surfactant monomer, and somewhat resemble enzyme proteins in structure and function[1]. Some time ago, Bunton and co-workers found that micellar cetyltrimethylammonium bromide (CTAB) enhanced the reaction of hydroxide and fluoride anions with p-nitrophenyl diphenylyphosphate (PNPDPP)[2]. Subsequent reports from that laboratory showed that even greater enhancements resulted from placing a hydroxyl group on the cationic surfactant, near the quaternary centre[3]. This system was not catalytic, as turnover was demonstrated. Two more recent reports one from Moss et al.[4] and the other from Menger and Whitesell[5], have described micellar systems for hydrolysis of the phosphate triester PNPDPP that offer more dramatic rate enhancements and rapid turnover of the reactive groups. Both systems seem to involve nucleophilic catalysis. The common catalytic strategy for these two non-metallic systems is reminisant of metal cation facilitation of phosphate ester hydrolysis. Metal ions can lower the pKa of a ligated water molecule, generating relatively large concentrations of metal-bound hydroxide near neutral pH.

Although there have been numerous studies of micellar models of enzymes few attempts have been made to model

mettalloenzymes. Tagaki and coworkers[6] have developed micellar models of carboxypeptidase and carbonic anhydrase, but there have been few attempts to develop phosphatase models. We have previously found that the 1:1 complex of N,N,N',N' - tetramethylethylenediamine with copper(II) is an excellent catalyst for the hydrolysis of phosphorus esters (Chapter 4). This chapter discusses the activity of the copper(II) complex of N,N,N' - trimethyl-N'-tetradecylethylenediamine [6.1] towards 2,4-dinitrophenyl diethylphosphate (DNPDEP) and 2,4-dinitrophenyl ethyl methylphosphonate (DNPEMP). When dissolved in water above the critical micelle concentration (CMC), the complex forms metallomicelles having a Stern region filled with copper (II) ion[7].

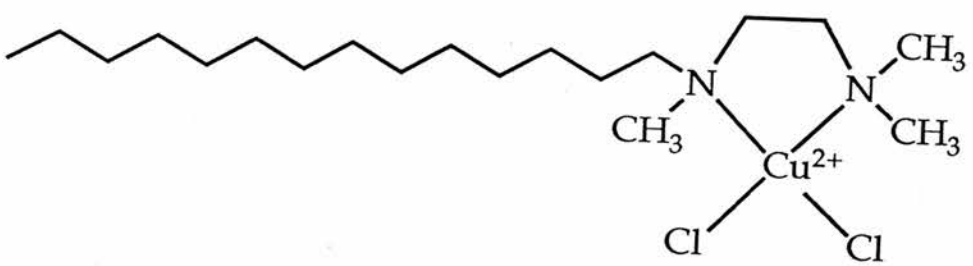

[Cu(tmten)Cl_2]

[6.1]

6.2 EXPERIMENTAL

6.2.1 KINETICS

Hydrolysis rates were determined by the stopped-flow method using the High-Tech Scientific apparatus described earlier (see section 2.4.3). Reaction was achieved by loading the sample syringes with (i) an aqueous solution containing the desired concentration of long chain copper (II) complex and 0.02M HEPES buffer that had been adjusted to pH 8.0 (ii) a freshly prepared 6.5 x 10^{-5}M stock solution of phosphorus ester in 0.02M HEPES buffer adjusted to pH 8.0. The apparatus was thermostated at the desired temperature (LKB 2219 II circulator) and the reaction initiated by pneumatically injecting 100 µl of each reactant into the mixing chamber (Figure 2.4). The effluent from the chamber was used to operate a stopping syringe which in turn, activated the trigger for the data collection. Typically, a pressure of 60 psi on the activating ram yielded a dead time of 2 milliseconds. Data was fed directly into a Hewlett-Packard 310 microcomputer where curve fitting routines based on the algorithm of Gamp[8] were used to calculate desired rate constants. A total of 400 data points were collected during each run irrespective

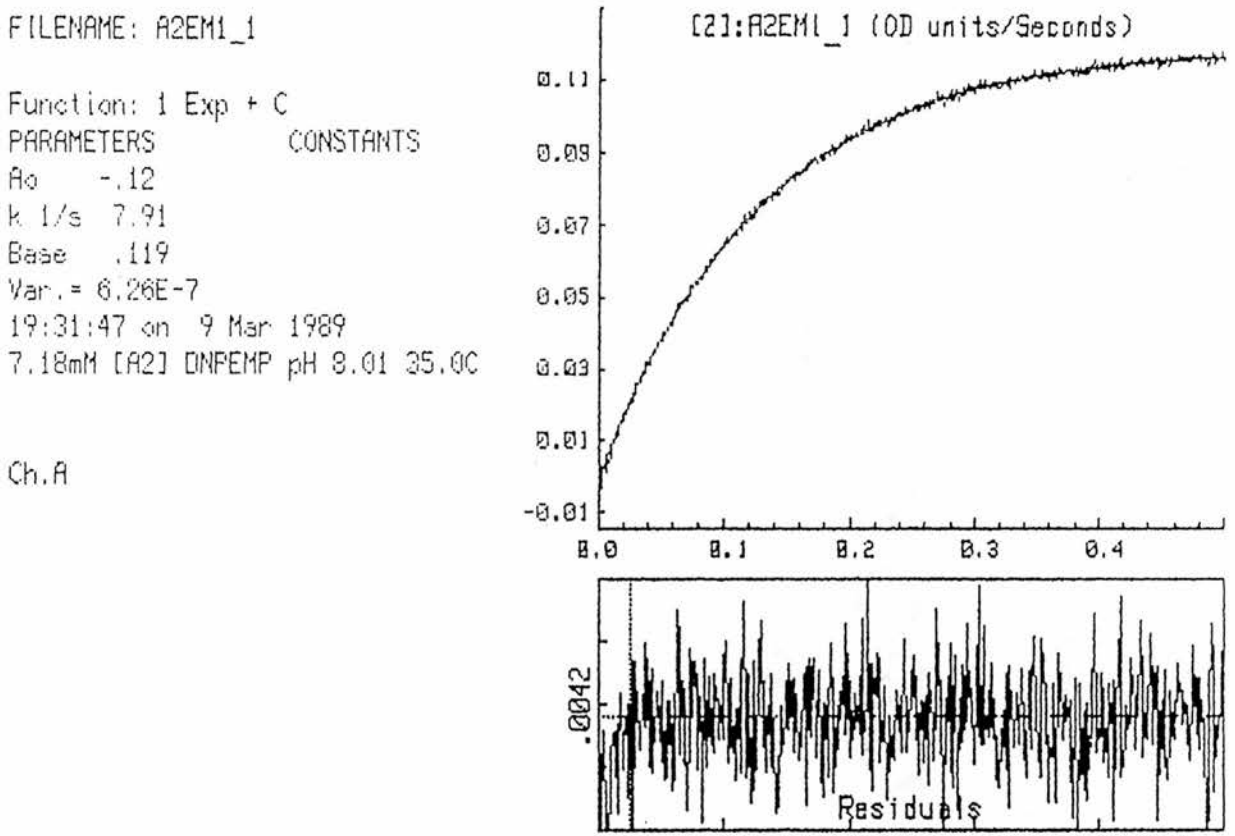

Figure 6.1 Typical stopped-flow trace for a metallomicelle catalysed hydrolysis experiment

of the time base used. A typical stopped-flow trace for the metallomicelle reacting with the phosphorus ester is shown in Figure 6.1.

6.2.2 PHYSICAL MEASUREMENTS

Attempts to detect micelle formation were made using the conductivity method[9]. During the measurements, for which a AGB 1000 conductivity meter was used, the solutions were kept at constant temperature. Plots of equivalent conductance versus the square root of concentration were constructed Figure 6.2. A critical micelle concentration of 1.8×10^{-4}M was estimated for the long chain copper(II) chelate. Interval scan uv/visible spectra were determined using a Perkin Elmer Lambda 5 instrument.

TABLE 6.1 Equivalent conductance versus square root of complex concentration plot.

$10^5 \frac{\text{conductivity}}{[\text{conc}]}$	$10^2/[\text{conc}]$ mol dm^{-3}
12.52	0.67
10.08	0.99
9.24	1.32
8.29	2.32
8.11	2.92
7.79	3.48
7.61	4.00
7.22	4.80
6.89	5.44

Figure 6.2 C.M.C. determination of $[Cu(tmten)(OH_2)_2]^{2+}$, equivalent conductance versus sq. root of concentration plot at 25°C.

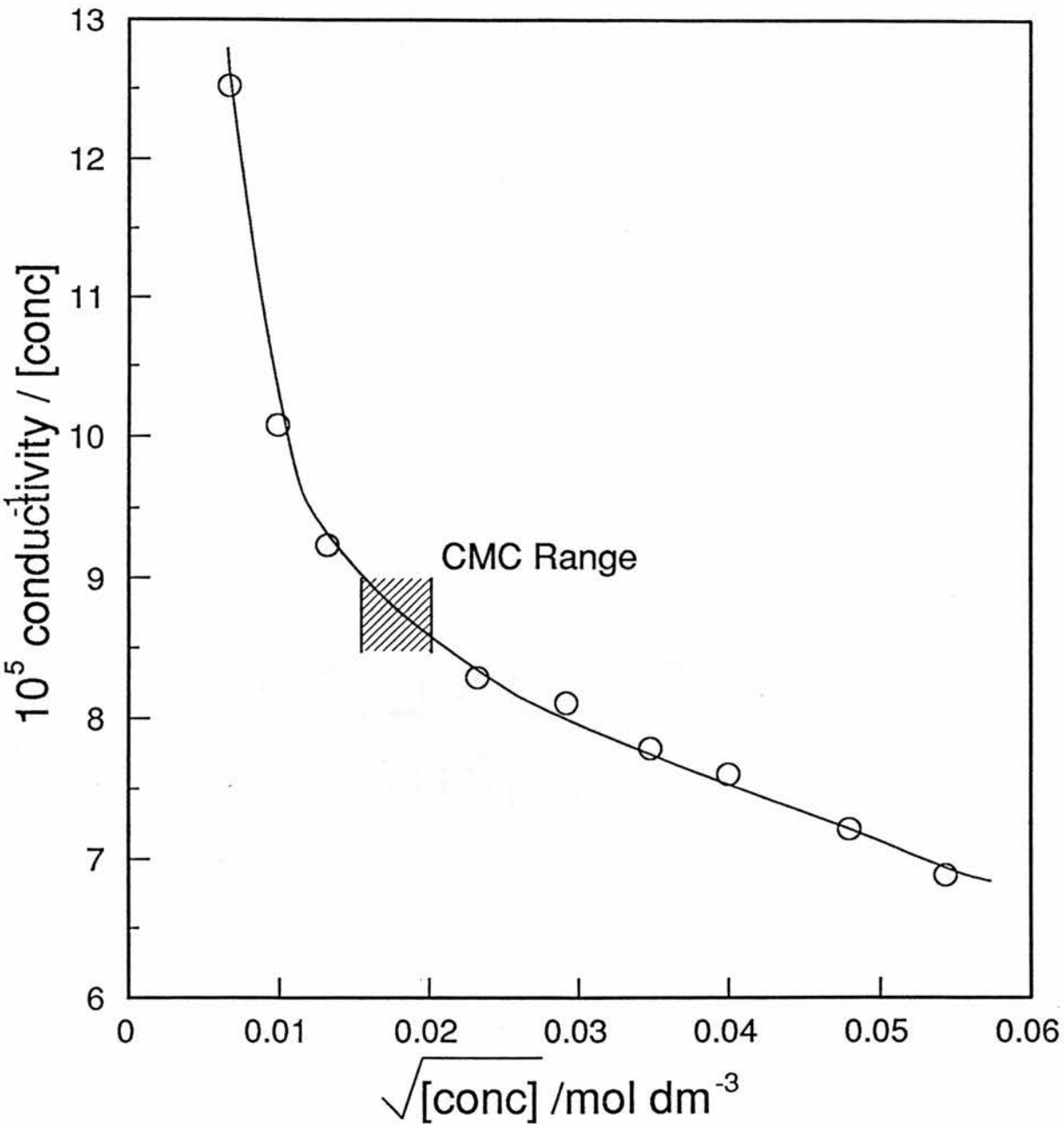

6.2.3 SYNTHESIS OF METALLOMICELLE SURFACTANT MONOMER

N,N',N''-Trimethyl-N'-tetradecylethylenediamine (tmten)

N,N,N' - Trimethylethylenediamine (12.0 g, 0.12 mol) and 1 - bromotetradecane (14.0 g, 0.05 mol) in absolute ethanol (70 cm^3) were refluxed for 10 minutes. A solution of sodium hydroxide (2.4 g in 4 cm^3 of water) was added, and the mixture was further refluxed for 5 hours, cooled, and shaken with a solvent mixture consisting of 20 cm^3 1-butanol, 20 cm^3 of benzene and 100 cm^3 of water. The organic layer was removed and washed with water (120 cm^3) creating an emulsion which required several hours standing to separate. After removing the volatiles from the organic layer on a rotary evaporator, the residue ($\sim$ 10 g) was distilled under reduced pressure on a Kugelrohr apparatus, b.p. 150 - 155^{o}C at 0.25 mm Hg. An initial cut of 3.2 g which contained considerable amounts of alkyl bromide was dissolved in ca. 200 cm^3 of ether and treated with dry HCl gas to generate the hydrochloride salt which precipitated from solution. The salt was collected by filtration and washed with ether. Free amine was isolated by dissolving and adding sodium hydroxide solution, followed by ether extraction (yield $\sim$ 2.0 g) and redistilled on the Kugelrohr distillation apparatus (yield ca. 1.4 g). The second cut from the vacuum distillation was (4.2 g) was virtually pure

amine. The combined yield of the clear viscous oil being 5.4 g (36%). No attempt was made to optimize yields. The ligand structure was confirmed by ^{1}H and ^{13}CNMR spectra.

Anal. Calcd. for $C_{19}H_{42}N_2$: C, 77.44; H, 14.18; N, 9.38. Found: C, 77.60; H, 14.67; N, 9.52%.

Preparation of $[Cu(tmten)Cl_2].H_2O$

A solution of N,N,N'-trimethyl-N'-tetradecyl-ethylenediamine prepared as above (0.99 g, 3.3 mmol) in absolute ethanol (10 cm^3) was slowly added to a filtered solution of anhydrous copper(II) chloride (0.55 g, 4.1 mmol) in absolute ethanol with stirring. The resulting precipitate was collected by filtration, recrystallised from absolute ethanol and dried in vacuo.

Anal. Calcd. for $C_{19}H_{42}Cl_2N_2$ Cu. H_2O : C, 50.60; H, 9.83; N, 6.21. Found : C, 50.84; H, 9.60; N, 5.93%.

The complex has λ max 660 nm (E = 77 $moldm^{-3}cm^{-1}$) in water solvent. The complex is a 2 : 1 electrolyte in water Λ_M = 195 S cm^2mol^{-1} at 25°C.

6.3 RESULTS

Hydrolysis of the phosphorus esters 2,4-DNPDEP and 2,4-DNPEMP where studied at 35°C using HEPES buffers. The reactions were carried out under pseudo-first -order conditions with the metallomicelle in at least 10 fold excess, using an ester concentration of 6.5×10^{-5}M. The reactions were monitored at 400 nm the absorption maximum for 2,4-dinitrophenoxide ion released on hydrolysis of the ester (the pK of 2,4-dinitrophenol is ca. 4.1 at 35°C). Figures 6.3 and 6.4 show pH-rate profiles for the hydrolysis of DNPDEP and DNPEMP in the pH range 6.8 - 8.2 in the presence of metallomicelle. Values of k_{obs} are listed in Tables 6.2 and 6.3 respectively. A plot of k_{obs} for the hydrolysis of DNPDEP versus the concentration of the complex is curved indicating the onset of saturation kinetics at high complex concentration, (Table 6.4, Figure 6.5). With the 2,4-DNPEMP substrate an analogous concentration rate dependence is observed, (Table 6.4, Figure 6.6).

The kinetic data was evaluated using the standard treatments available for micellar catalysis[9],

TABLE 6.2 Observed-first-order rate constants for the metallomicelle $[Cu(tmten)(OH_2)_2]^{2+}$ catalysed hydrolysis of 2,4-DNPDEP at 35°C in HEPES buffer[a].

pH	$10^2 k_{obs}$[b] /s^{-1}	pH	$10^2 k_{obs}$[b] /s^{-1}
6.84	3.50	7.82	4.42
7.01	3.64	8.04	4.36
7.24	4.00	8.25	4.22
7.40	4.23		
7.60	4.49		

a) Reactions were monitored at 400 nm for the production of 2,4-dinitrophenolate from an initial [DNPDEP] = 5 x 10^{-5} mol dm^{-3}. The total concentration of $[Cu(tmten)(OH_2)_2]^{2+}$ was 5 x 10^{-4} mol dm^{-3} and a buffer concentration of 0.02 mol dm^{-3} was employed.

b) Average of at least 3 kinetic runs.

Figure 6.3 pH-rate profile for the metallomicelle $[Cu(tmten)(OH_2)_2]^{2+}$, catalysed hydrolysis of DNPDEP at 35°C in HEPES buffer.

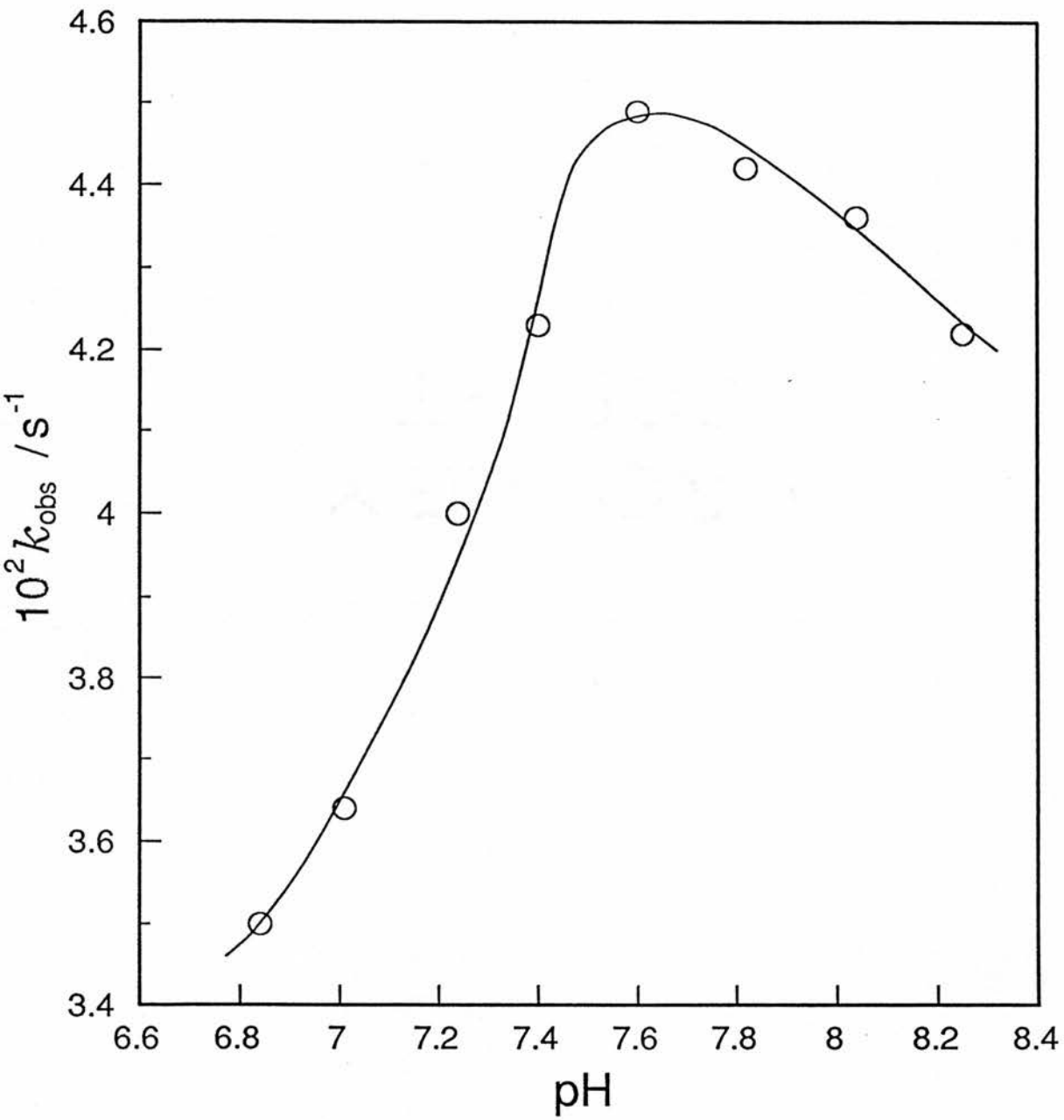

TABLE 6.3 **Observed-first-order rate constants for the metallomicelle $[Cu(tmten)(OH_2)_2]^{2+}$ catalysed hydrolysis of 2,4-DNPEMP at 35°C in HEPES buffer[a].**

pH	k_{obs}[b] /s^{-1}	pH	k_{obs}[b] /s^{-1}
6.84	2.05	7.82	3.37
7.01	2.14	8.04	3.28
7.24	2.45	8.25	3.18
7.40	3.02		
7.60	3.35		

a) as table 6.2

b) as table 6.2

Figure 6.4 pH-rate profile for the metallomicelle $[Cu(tmten)(OH_2)_2]^{2+}$, catalysed hydrolysis of DNPEMP at 35°C in HEPES buffer.

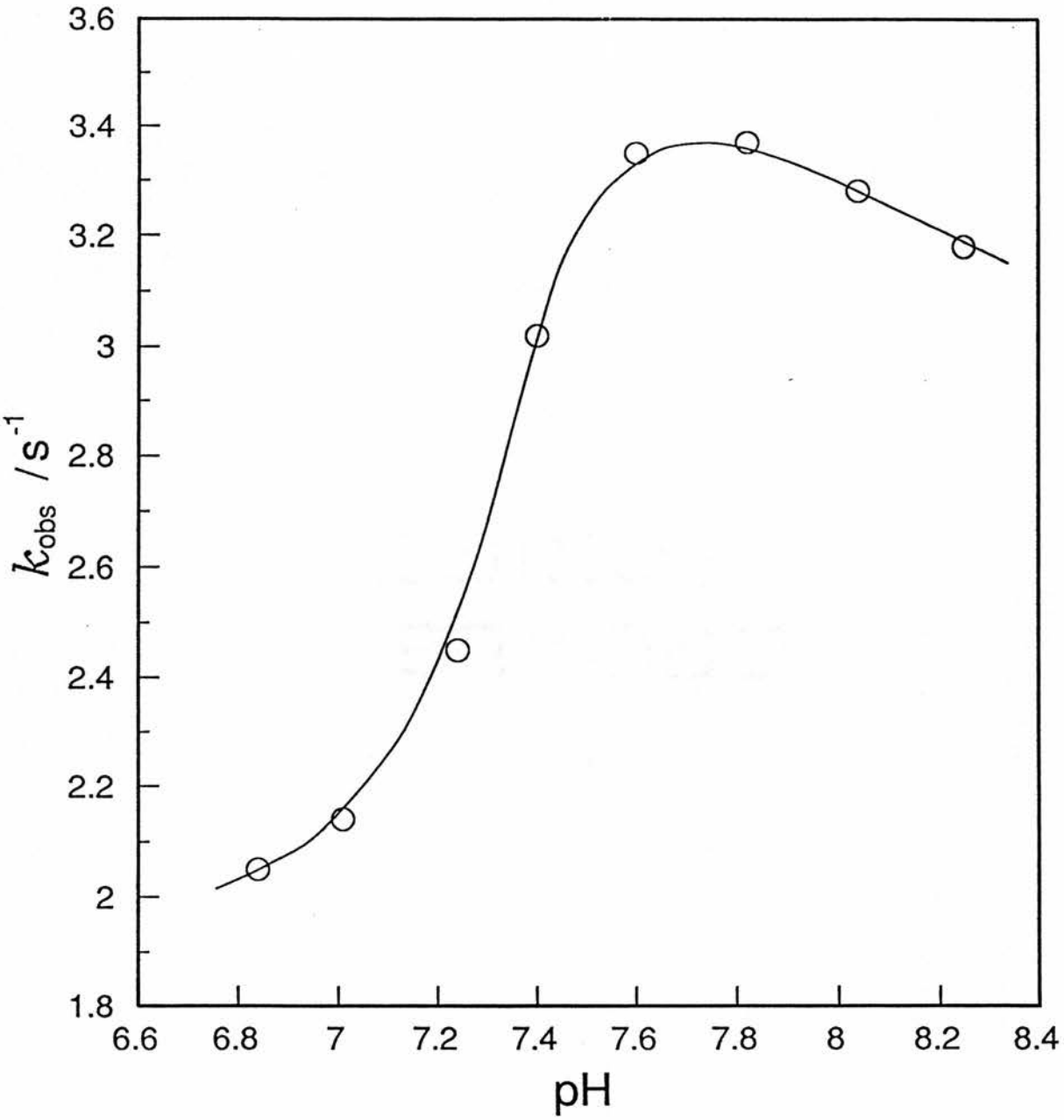

TABLE 6.4 **Observed-first-order rate constants for the metallomicelle catalysed hydrolysis of 2,4-DNPDEP as a function of $[Cu(tmten)(OH_2)_2]^{2+}$ concentration at pH 8.01 in HEPES buffer at 35°C.**

10^4[Complex] /mol dm^{-3}	k_{obs} /s^{-1}	10^4[Complex] /mol dm^{-3}	k_{obs} /s^{-1}
1.25	0.008	25.00	0.181
2.50	0.016	36.09	0.248
5.00	0.036	71.88	0.354
7.50	0.059		
15.00	0.116		
20.00	0.142		

Figure 6.5 Effect of increasing concentration of $[Cu(tmten)(OH_2)_2]^{2+}$ on the rate of metallomicelle catalysed hydrolysis of DNPDEP at pH 8.01 (HEPES) and 35°C.

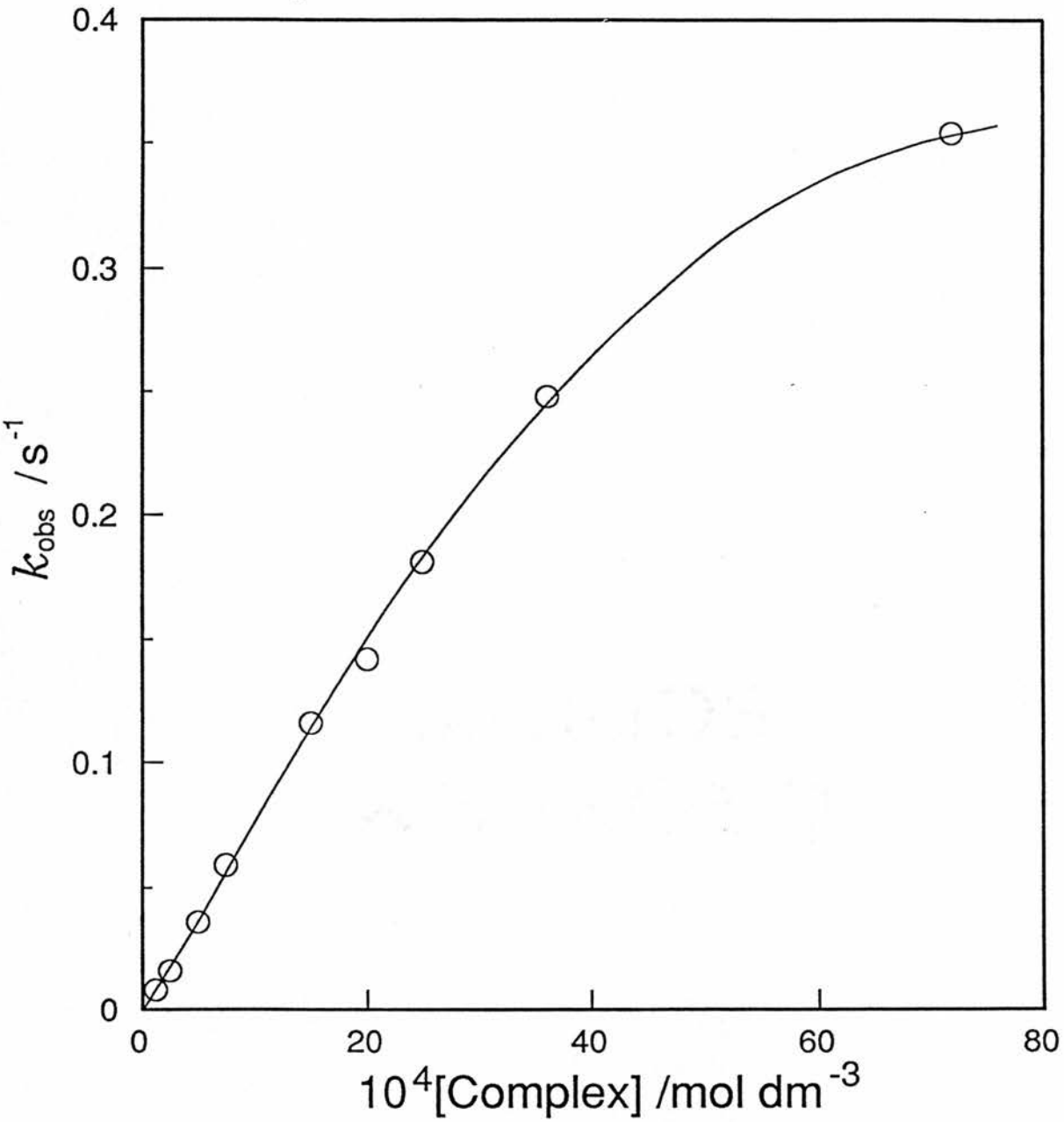

TABLE 6.5 **Observed-first-order rate constants for the metallomicelle catalysed hydrolysis of 2,4-DNPEMP as a function of $[Cu(tmten)(OH_2)_2]^{2+}$ concentration at pH 8.01 in HEPES buffer at 35°C.**

10^4[Complex] /mol dm^{-3}	k_{obs} /s^{-1}	10^4[Complex] /mol dm^{-3}	k_{obs} /s^{-1}
1.25	0.034	25.00	3.42
2.50	0.134	36.09	4.71
5.00	0.335	71.88	7.95
7.50	0.690		
15.00	1.872		
20.00	2.75		

Figure 6.6 Effect of increasing concentration of $[Cu(tmten)(OH_2)_2]^{2+}$ on the rate of metallomicelle catalysed hydrolysis of DNPEMP at pH 8.01 (HEPES) and 35°C.

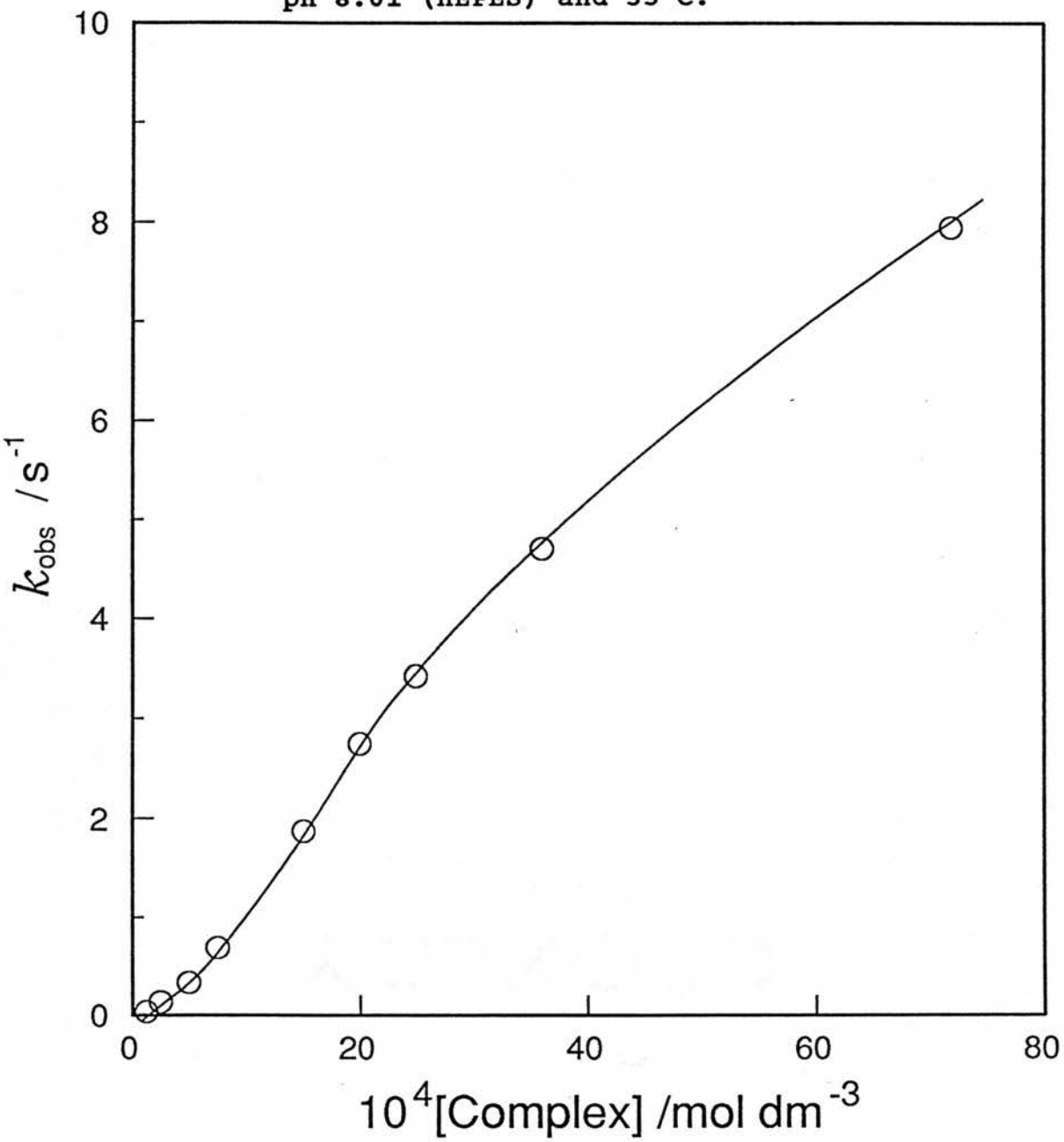

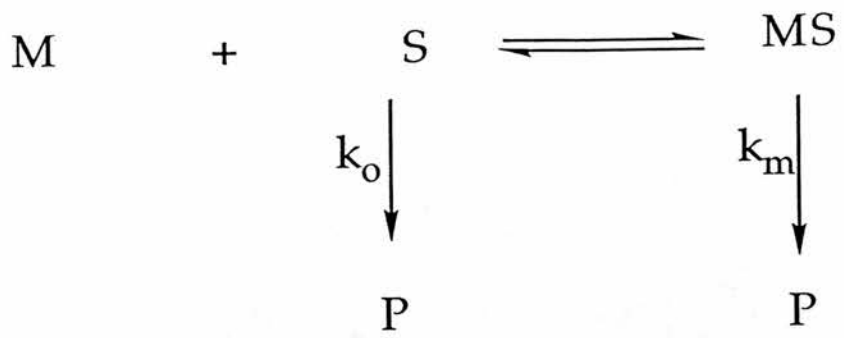

[Scheme 6.1]

where M is the micelle, S the substrate and P the produce. The rate constants k_o and k_m are the rate constants for product formation in the bulk solvent and in the micellar phase respectively. Since k_o is negligible in this system (k_{obs}) for the uncatalysed hydrolysis of 2,4-DNPDEP and 2,4-DNPEMP at pH 8.0 were determined to be $3.8 \times 10^{-6} s^{-1}$ and $2.41 \times 10^{-4} s^{-1}$ at 35°C respectively, (see chapter 2), it can readily be shown that,

$$\frac{1}{k_{obs}} = \frac{1}{k_m} + \frac{1}{k_m K[M]}$$

values of the micelle concentration [M] were evaluated from the expression

$$[M] = (C - CMC)/N$$

where C= the total concentration of the complex, CMC = the critical micelle concentration (1.8×10^{-4}M) and N = the Aggregation Number assumed to be 40[1]. A double reciprocal

plot of $1/k_{obs}$ <u>versus</u> 1/[M] for the metallomicelle catalysed hydrolysis of 2,4-DNPDEP shows excellent linearity (Figure 6.7, correlation coefficient 0.999) giving $k_m = 0.497s^{-1}$ and $K = 9.7 \times 10^{-3}M^{-1}$ at 35^oC. Analogous treatment of the data obtained for metallomicelle catalysed hydrolysis of the substrate ester 2,4-DNPEMP, yields values of $k_m = 22.73s^{-1}$ and $K = 3.0 \times 10^{-3}M^{-1}$ at 35^oC, Figure 6.8.

TABLE 6.6 Relationship between micelle concentration and rate of hydrolysis of 2,4-DNPEMP at pH 8.01 and 35°C

$10^4 1/[\text{micelle}]$ mol dm^{-3}	$1/k^{obs}$ s^{-1}
0.57	0.126
1.14	0.212
1.72	0.292
2.19	0.363

slope = $1/_{kmK}$ = 1.45×10^{-5}; c.c. = 0.999

intercept = $1/_{km}$ = 0.044

Figure 6.7 Double reciprocal plot of micelle concentration versus rate of hydrolysis of DNPDEP at pH 8.01 and 35°C.

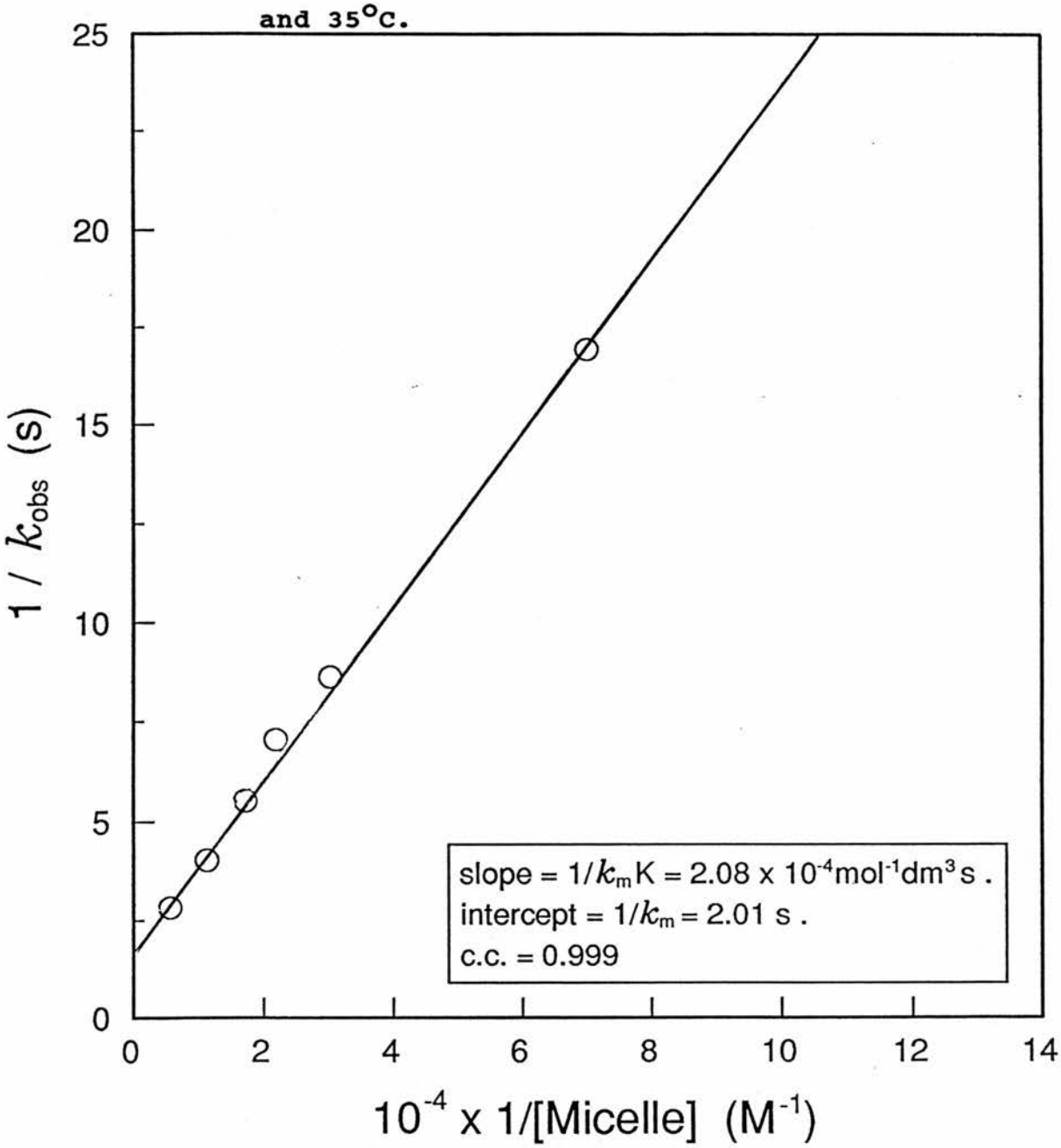

TABLE 6.7 Relationship between micelle concentration and rate of hydrolysis of 2,4-DNPDEP at pH 8.01 and 35°C

$10^4 1/[\text{micelle}]$ mol dm^{-3}	$1/k^{obs}$ s^{-1}
0.57	2.82
1.14	4.03
1.72	5.52
2.19	7.04
3.03	8.62
7.01	16.94
12.50	22.77

slope = $1/_{kmK}$ = 2.08×10^{-4}; c.c. = 0.999

intercept = $1/_{km}$ = 2.01

Figure 6.8 Double reciprocal plot of micelle concentration versus rate of hydrolysis of DNPEMP at pH 8.01 and 35°C.

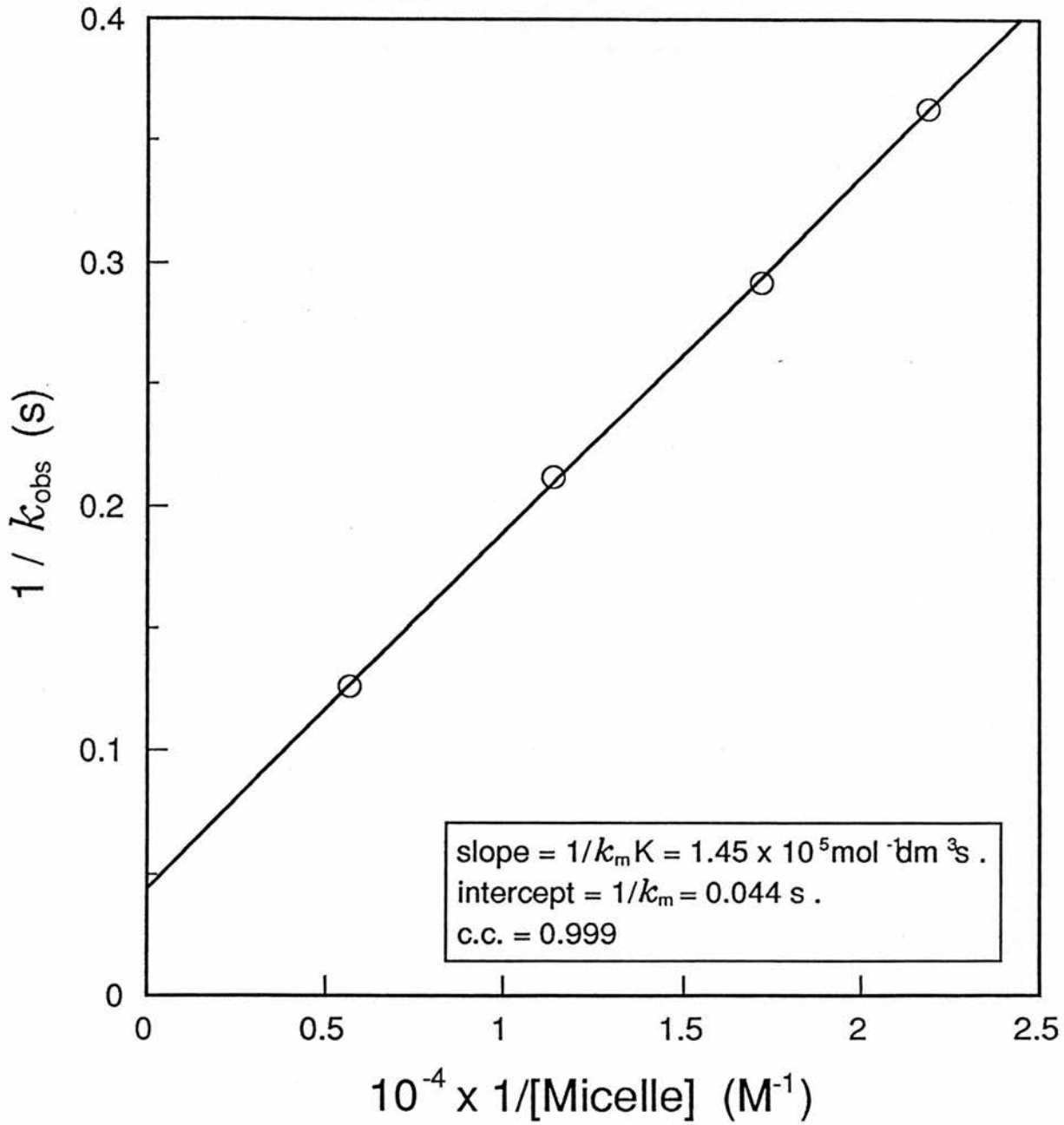

6.4 DISCUSSION

The copper(II) complex of N,N,N' - trimethyl-N'-tetradecylethylenediamine [6.1] is a long chain chelate. The amino groups were deliberately made tertiary to preclude possible irreversible reactions between nitrogens and substrate and to inhibit dimer formation. When dissolved in water above its critical micelle concentration of 1.8×10^{-4}M (determined tensiometerically, see Figure 6.1) the complex forms "metallomicelles" having a Stern region filled with cupric ion. A simplified two dimensional representation of the spherical metallomicelle is shown below [6.2] (taken from reference 9). The counter ions (X), the head groups (O), and hydrocarbon chains (∿∿) are schematically indicated to denote their relative locations.

[6.2]

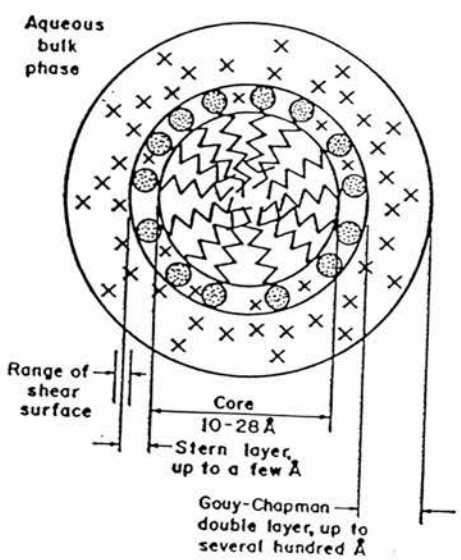

Only a few other examples of copper surfactants are known. Moroi et al.[10] prepared poorly soluble copper(II) alkylsulfonates. Gutsche and Mei[11] found that the copper complex of a tetradentate ligand bearing a hydrocarbon chain catalyzes the hydrolysis of acetyl phosphate by a factor of ten. Gratzel et al.[12] studied copper(II) crown ether surfactants while the group of Kunitake[13] and Fuhrhop[14] synthesized copper-bound vesicles. Catalytically active bolaforms were reported by Tonellato et al[15]. Several groups, including those of Tagaki[6], Breslow[16], and Tonellato[17], examined micelles containing transition metals other than copper.

The metallomicelle formed from $[Cu(tmten)(OH_2)_2]^{2+}$ [6.1] is a potent catalyst for the hydrolysis of DNPDEP and DNPEMP. For the uncatalysed reactions at pH8 the value of k_{obs} for the hydrolysis of DNPDEP is calculated to be $3.8 \times 10^{-6} s^{-1}$. With a micelle concentration of $1.75 \times 10^{-4} M$, the value of $k_{obs} = 0.354\ s^{-1}$ a rate enhancement approaching 1×10^5 fold. The magnitude of the rate enhancement is more clearly understood using half-life criteria. Thus, the half-life of the uncatalysed ester hydrolysis at pH 8.0 is 51 hours which is reduced to 2 seconds with a micelle concentration of $1.75 \times 10^{-4} M$. As the DNPDEP substrate is less reactive towards hydrolysis than the G agents, the metallomicelle certainly meets the famous McKay criterion for useful nerve-agent decontaminant "destruction within a

cigarette break".

Metallomicelle catalysed hydrolysis of DNPDEP is greater than 20 times faster than the reactions catalysed by an equivalent concentration of the 1 : 1 complex of N,N,N',N'- tetramethylethylene diamine with copper(II) [4.1]. Copper(II), known from earlier studies to catalyse phosphate ester hydrolysis, is therefore much more effective when the metal is bound to a micelle surface. The dramatic rate enhancements associated with the long chain copper(II) chelate probably stem from a micellization effect superimposed upon the inherent copper(II) complex catalysis. Among the "phosphotriesterase" models only the micellar o-iodosobenzoates of Moss et al.[18] surpass the long chain chelate $[Cu(tmten)(OH_2)]^{2+}$. From a practical point of view, however, the iodoso compounds possess less than ideal stability. Moreover, it has been demonstrated that the Moss compounds, in contrast to the long chain copper chelate, are inert towards some particularly toxic and persistant phosphorus(V) compounds namely phosphothiolates of which VX is the best known.

The variation of k_{obs} with pH (Figures 6.3 and 6.4) implicates $[Cu(tmten)(OH)(OH_2)]^{+}$ as the catalytically active species within the micelle. It seems likely that catalysis by the metallomicelle is related mechanistically to the process discussed in Chapter 4 for $[Cu(tmen)(OH)(OH_2)]^{2+}$ in aqueous solution. However, the increased reaction rates

observed in the micellar system suggests that $[Cu(tmten)(OH)(OH_2)]^{2+}$ aggregates can perform hydrolysis through some higher order mechanism and that this new mechanism is more effective.

Plots of k_{obs} versus concentration of chelate for DNPDEP and DNPEMP are illustrated in Figures 6.5 and 6.6. On reaching the CMC rates increase sharply with increasing complex concentration and then start to level off a high concentrations of complex as the substrate becomes more fully bound to the micelles. Analysis of the kinetic data by standard treatments for micellar kinetics gave binding constants (K_{assoc}) for DNPDEP and DNPEMP - micelle complexation of 9.6×10^3 and $3.0 \times 10^3 M^{-1}$ respectively. Substrate hydrophobicity and binding of the P=O group to copper(II) probably contribute to the high binding constants which are fairly typical of many micellar promoted reactions where values of K_{assoc} of the order of 10^5 are commonly observed.

Neither buffer (0.2 M HEPES) nor tmen ligand (which was used to model the water insoluble N,N,N' - trimethyl-N'-tetradecylethylenediamine) reacts by itself with DNPEMP. Thus DNPDEP hydrolysis in the presence of metallomicelle is ascribed solely to the long chain copper(II) complex. For solubility reasons reactions were carried out a low ionic strength (< 0.01). Addition of large amounts of KCl had only a minor effect on the rate : k_{obs} = 0.059, 0.051 and

0.047 s^{-1} at 0.00, 0.20 and 0.50 M KCI, respectively ([micelle] = 1.42 x 10^{-5}M, 35.0°C, and pH 8.0).

The observed 10^5 rate enhancements probably arises from multiple effects : (a) DNPDEP binds to the surface of the micelle where the nucleophile, the OH of $Cu(L)(OH)^+$, is located. Thus, attack on the DNPDEP phosphorus simulates an intramolecular reaction (resembling the observed for the monomeric copper(II) complex discussed in Chapter 2) [6.3]. (b) the pKa of the water molecule bound to the micellar copper is lowered, thereby increasing the concentration of available nucleophile at pH values near neutrality (c) Copper(II) ion can polarise the P=O group[19]. Electrophilic catalysis should be greater than that found with the monomeric copper(II) complexes owing to the cationic nature of the Stern region.

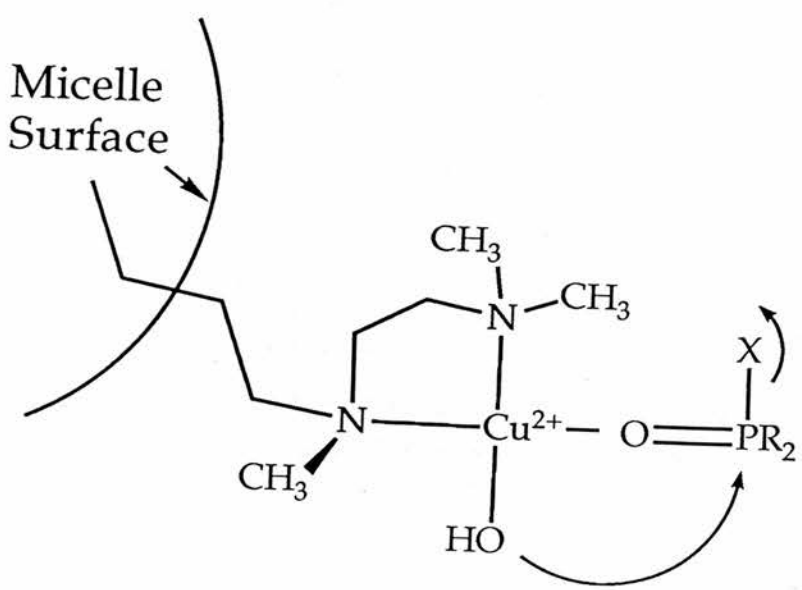

[6.3]

Catalysts must display "turnover" where each catalyst molecule brings about reaction of many substrate molecules. Additional experiments confirm the metallomicelle system is truly catalytic. A 10-fold excess of DNPDEP over catalyst gives a quantitave yield of 2,4-dinitrophenoxide (i.e. 8.1 x 10^{-5}M DNPDEP and an effective micelle concentration of 8.0 x 10^{-6}M in HEPES buffer pH 8.0 at 35^{o}C). The initial slope of the plot gives a release rate of 2.8 x 10^{-5} mol min^{-1}, with a turnover 2.8 x $10^{-5}/8.0 \times 10^{-6}$ = 3.5 turnovers min^{-1}.

6.5 REFERENCES

1. F.M. Menger, Acc.Chem.Res., 12, 111 (1979).
2. C.A. Bunton and L.J. Robinson, J.Am.Chem.Soc., 34, 773 (1969).
3. C.A. Bunton and L.G. Ionescu, J.Am.Chem.Soc., 95, 2912, (1973).
4. R.A. Moss, K.W. Alwis and S.J. Shin, J.Am.Chem.Soc., 106, 2651, (1984).
5. F.M. Menger and L.G. Whitesell, J.Am.Chem.Soc., 107, 707, (1985).
6. For a review see W. Takagi and K. Ogino, Topics Curr. Chem., 128, 143, (1985).
7. F.M. Menger, L.H. Gan, F. Johnson and D.H. Hurst, J.Am. Chem.Soc., 109, 2800, (1987).
8. H. Gamp, Talanta, 27, 1037, (1980).
9. J.H. Fendler and E.J. Fendler, Catalysis in Micellar and Macromolecular Systems, Academic Press, (1975).
10. Y. Moroi, R. Sugii, C. Akine and R. Matuura, J. Colloid, Interface Sci., 108, 180, (1985).
11. C.D. Gutsche, G.C. Mei, J.Am.Chem.Soc., 107, 7964, (1985).
12. R. Humphry-Baker, Y. Moroi, M. Gratzel, E. Pelizzett and P. Tundo, J.Am.Chem.Soc., 102, 3689, (1980).

13. T. Kunitake, Y. Ishikawa and Shimoumura, J.Am.Chem. Soc., 108, 327, (1986).

14. J.H. Furhop, V. Koesling and G. Schonberger, Liebigs Am.Chem., 1634 (1984).

15. R. Fronasier, D. Milani, P. Scrimin and U. Tonellato, J.Chem.Soc., Perkin Trans. 2, 233, (1986).

16. S.H. Gellman, R. Petter and R. Breslow, J.Am.Chem.Soc., 108, 2388, (1986).

17. F. DiFuria, R. Fronasier and U. Tonellato, J. Molo. Catalysis 19, 81, (1983).

18. R.A. Moss, K.Y. Kim and S. Swarup, J.Am.Chem.Soc., 108, 788, (1986).

19. R.C. Courtney, R.L. Gustafson, S.J. Westerback, H. Hytiainen, S.C. Chaberek and A.E. Martell, J.Am. Chem.Soc., 79, 3030, (1957).

CHAPTER SEVEN

A LANTHANUM MACROCYCLE CATALYSED HYDROLYSIS OF A PHOSPHATE TRIESTER

7.1 INTRODUCTION

In recent years there has been a growing interest in the metal ion promoted hydrolysis of phosphate esters as model systems for metallo-phosphatase enzymes and as potential catalysts for the detoxification of anticholinesterase agents used in chemical warfare[1-5]. Early studies by Butcher and Westheimer[6] indicated that lanthanum hydroxide gels promoted the hydrolysis of esters such as B-methoxyethyl and B-aminoethylphosphates at pH 8.5 and 78°C. Bamann[7] also noted that the hydroxides of La^{3+}, Ce^{3+} and Th^{3+} promoted the hydrolysis of -glycerophosphate in the pH range 7 - 10 and suggested that the reaction could be regarded as a model for the metal containing alkaline phosphatases which cleave phosphate esters around pH9. In view of the heterogeneous nature of these reactions it is difficult to come to firm mechanistic conclusions, however, it seems likely that metal bound hydroxide nucleophiles are involved. For this reason we investigated the activity of the lanthanum complex of the macrocycle [7.1] as a potential catalyst for the hydrolysis of the water soluble triester DNPDEP [2.2].

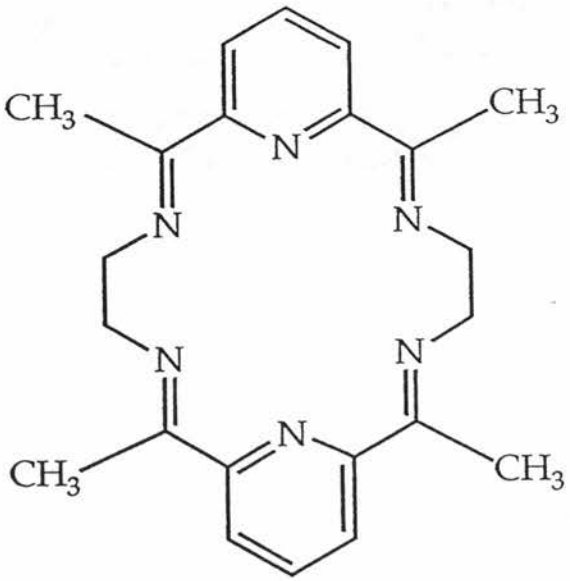

[7.1]

7.2 EXPERIMENTAL

Preparation of the lanthanum macrocyclic complex $[La(L)(NO_3)_3]$

The macrocyclic complex was prepared as previously described[9] by Schiff base condensation of 2,6-diacetylpyridine with ethylenediamine in a template synthesis.

Hydrated lanthanum nitrate ((0.325 g, 0.75 mmol), ethylenediamine (0.09 g, 1.50 mmol), and 2,6-diacetylpyridine (1.5 mmol) were refluxed in methanol (30 cm^3) for ca. 4 hours giving pale pink-brown crystals of the product (0.38 g, 73% yield). The crystals were collected washed with ethanol and diethyl ether and dried under vacuum.

Anal. Calcd. for $C_{22}H_{26}N_9O_9La$: C, 37.78; H, 3.75; N, 18.02. Found : C, 37.58; H, 3.72; N, 18.12%.

^1H nmr (DMSO d_6 ; TMS) : 8.3 (6H), 3.9 (8H), 2.5 (12H) ppm IR (KBr disk) : 1633 (C = N); 1588 (pyridine); 1445, 1421, 1374, 1304 (NO_3); (no NH); (no C = O) cm^{-1}. The complex is a 3:1 electrolyte in solution Λ_M = 354 S cm^2 mol^{-1} at 25°C.

7.3 RESULTS AND DISCUSSION

There has been considerable interest in the synthesis of lanthanide macrocycles and the topic has recently been reviewed;[8] however the catalytic potential of these complexes has not been previously studied. The complex $[La(NO_3)_3L]$ was prepared as previously described[9]. The crystal structure establishes twelve-co-ordination of the metal-ion to the six macrocyclic nitrogen atoms and to three bidentate nitrate ions. Conductivity measurements show that in aqueous solution the complex exists mainly as $[LaL(H_2O)_n]^{3+}$. The macrocylic ligand remains undissociated in water and is kinetically stable to dissociation. Furthermore, the complex gives no precipitation on addition of KF or KOH.

The triester DNPDEP provides a useful water soluble substrate of relatively low toxicity. Hydrolysis to diethylphosphate was readily monitored at 360 nm as described earlier (section 2.4.1). The reaction is first-order in phosphate ester and excellent pseudo-first-order kinetics were observed in the presence of millimollar concentrations of the complex. In order to avoid complications due to buffer catalysis the metal complex was employed as the buffer system and the pH was adjusted by the

dropwise addition of hydrochloric acid. The pH dependence of the catalysis was studied over the pH range 7.00 - 9.50 (Table 7.1). The reactions displays a sigmoidal pH-rate profile of the type discussed in earlier chapters dealing with phosphate ester hydrolysis promoted copper(II) and cobalt(II) complexes (Figure 7.1). Such profiles are indicative of the involvement of metal hydroxo complexes and the data suggests that intermediates of the type [7.2] and [7.3] are probably involved in the reaction.

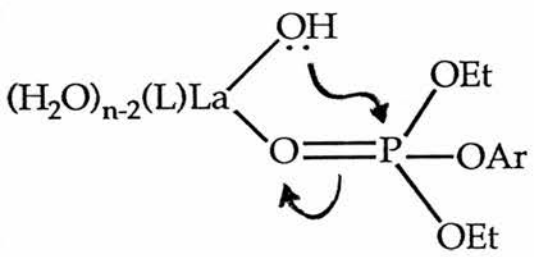

[7.2]

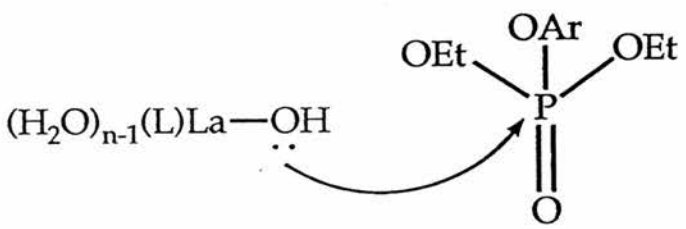

[7.3]

Potentiometeric tiration of $[La(NO_3)_3L]$ in aqueous solution with hydrochloric acid gives the titration curve shown in Figure 7.2. A pronounced end-point is observed after addition of one equivalent of hydrochloric acid consistant with protonation of a La--OH species. The apparent pK of the equilibrium is ca. 7.4.

TABLE 7.1 The lanthanum macrocycle promoted hydrolysis of 2,4-dinitrophenyl diethyl phosphate at 25°C and I=0.1 mol dm^{-3} (KNO_3)[a]

pH	k_{obs}/s^{-1}
7.00	6.25×10^{-5}
7.50	5.22×10^{-4}
8.00	2.45×10^{-3}
8.25	6.30×10^{-3}
8.80	6.70×10^{-3}
9.50	7.28×10^{-3}

a) Hydrolysis monitored spectrophotometrically at 360 nm. Concentration of [$LaL(NO_3)_3$] employed = 2.5×10^{-3} mol dm^{-3}; concentration of 2,4-dinitrophenyl diethyl phosphate = 4×10^{-5} mol dm^{-3}.

Figure 7.1 The pH-rate profile for the lanthanum macrocycle catalysed hydrolysis of 2,4-dinitrophenyl diethyl phosphate at 25°C and I=0.1 mol dm^{-3}.

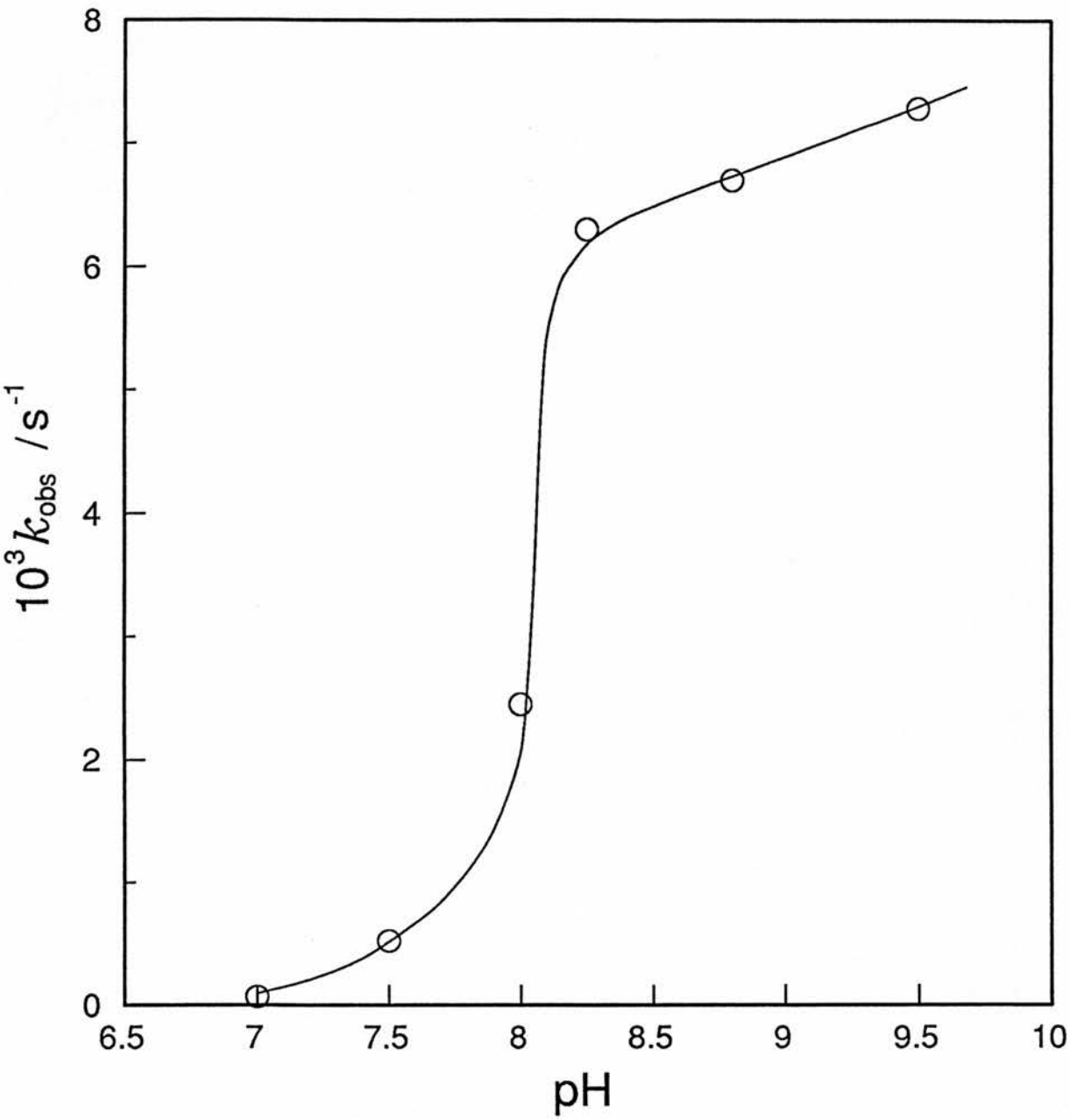

Figure 7.2 Potentiometric titration of $[La(NO_3)_3L]$ in aqueous solution with hydrochloric acid.

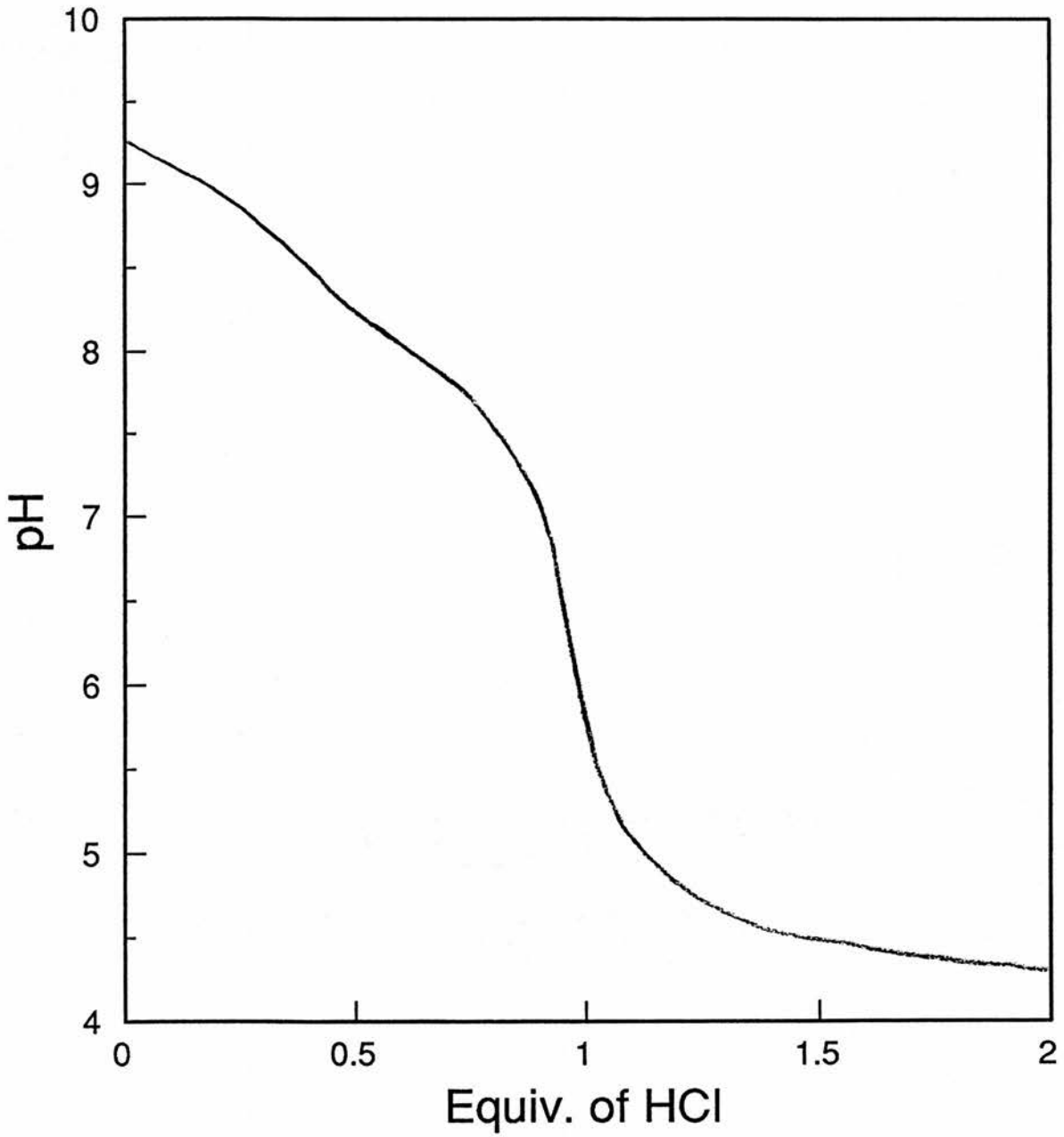

At pH 9 k_{obs} for the base hydrolysis of 2,4-dinitrophenyl diethylphosphate is 9.66 x 10^{-6} s^{-1} (see chapter 2). The rate enhancement at pH 9 is thus ca. 10^3-fold using a catalyst concentration of 2.5 x 10^{-3} mol dm^{-3}.

Turnover experiments were carried out using a Radiometer Titra-Lab system interfaced with an Apple IIe computing system. A solution containing 5 x 10^{-4} mol dm^{-3} 2,4-dinitrophenyl diethylphosphate and 5 x 10^{-5} mol dm^{-3} [$La(NO_3)_3L$] was adjusted to pH 8.50 at 25°C and release of H^+ due to ester hydrolysis monitored by the automaic addition of 0.002 mol dm^{-3} sodium hydroxide solution. The initial slope of the plot (Figure 7.3) gives a release rate of H^+ of 1.9 x 10^{-4} mol min^{-1}, with a turnover of 1.9 x $10^{-4}/5$ x 10^{-5} = 3.8 turnovers min^{-1}. At pH 8.50 and 25°C, ten moles of ester are hydrolysed by one mole of catalyst in ca. 50 min. At this pH the half-life of the free triester is 48.1 hours.

Figure 7.3 A pH-stat trace for the hydrolysis of 2,4-dinitrophenyl diethyl phosphate at pH 8.50 and 25°C. The concentration of 2,4-dinitrophenyl diethyl phosphate was 5 x 10^{-4} mol dm^{-3} and that of the lanthanum macrocycle 5 x 10^{-5} mol dm^{-3}.

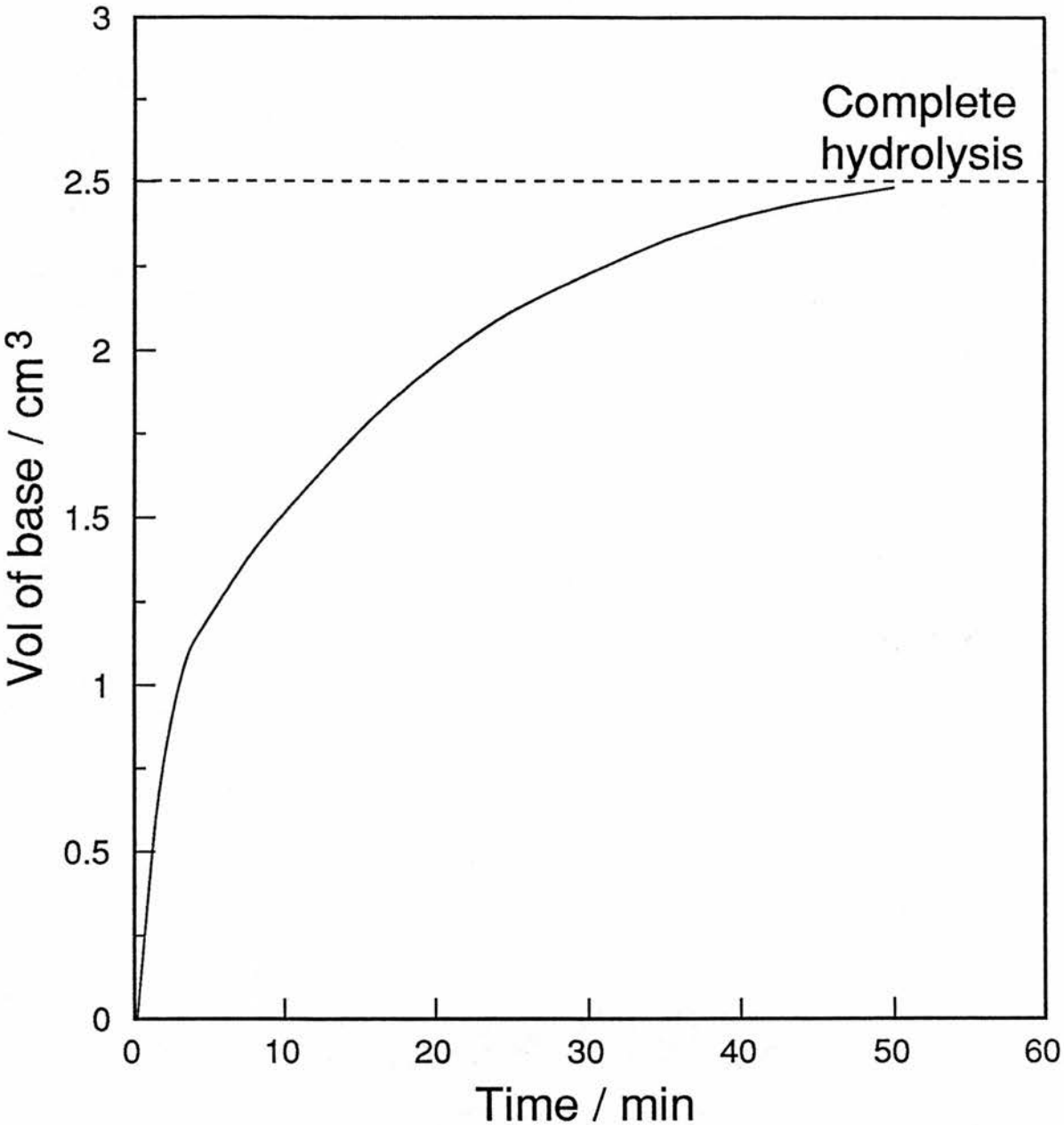

7.4 REFERENCES

1. R.W. Hay 'Reactions of Coordinated Ligands', vol. 2, ed. P.S. Braterman, Plenum, New York, 316, (1989).
2. M.A. De Rosch and W.C. Trogler, Inorg.Chem., 29, 2409, (1990).
3. S.H. Gellman, R. Peter and R. Breslow, J.Am.Chem.Soc., 108, 2388, (1986).
4. R. Hendry and A.M. Sargeson, J.Am.Chem.Soc., 111, 2521, (1989).
5. T.H. Fife and M.P. Pujari, J.Am.Chem.Soc., 110, 7790, (1988).
6. W.W. Butcher and F.H. Westheimer, J.Am.Chem.Soc., 77, 2420, (1955).
7. E. Bamann and M. Meisenheimer, Chem.Ber., 71, 1711, 1980, 2086, 2233, (1938).
8. D.E. Fenton and P.A. Vigato, Chem.Soc.Rev., 17, 69, (1988).
9. J.D.J. Backer-Dirks, G.J. Gray, F.A. Hart, M.B. Hursthouse and B.C. Schoop, J.Chem.Soc., Chem. Commun., 774, (1979).

APPENDIX

APPENDIX

Description and operating procedures for "Interface.V13"

The program "Interface.V13" may be accessed on soft disc "Titra Lab Serial Interface" on which detailed operating procedures are described.

The program was written for an Apple IIe computer in order to collect and analyse pH stat kinetic data down loaded from the Titra Lab VIT 90.

The program was written, tested and debugged on the Apple. When satisfactory operation was achieved the source code was compiled using a TASC MICROSOFT COMPILER. (This would allow the code to run much faster, though the data transmission speed is controlled by the BAUO RATE).

Program Description

Lines 5 to 120 are the initialisation routines. Several subroutines are called these are:

GOSUB 4800:	This routine asks the user whether or not he wishes to Log new or old data.
GOSUB 2500:	Prints introductory messages.
LINES 80-110:	Sets - Up Serial interface card.
GOSUB 3000:	Clears screen and prints that Titra Lab should now be running.

Lines 125 to 210: These lines of code accept the ASCII characters from the Titra Lab and store when a data table. The program knows when the transmission is ended when it detects the EOT character.

Lines 220 to 5560: These lines from the main program. They evaluate the ASCII characters received and combine them to form the required pH and time values which are stored in the array.

Lines 580 to 620: These lines allow the user to store the array of data values on the disk. If he does wish to store the data on the disc.

ALGORITHM

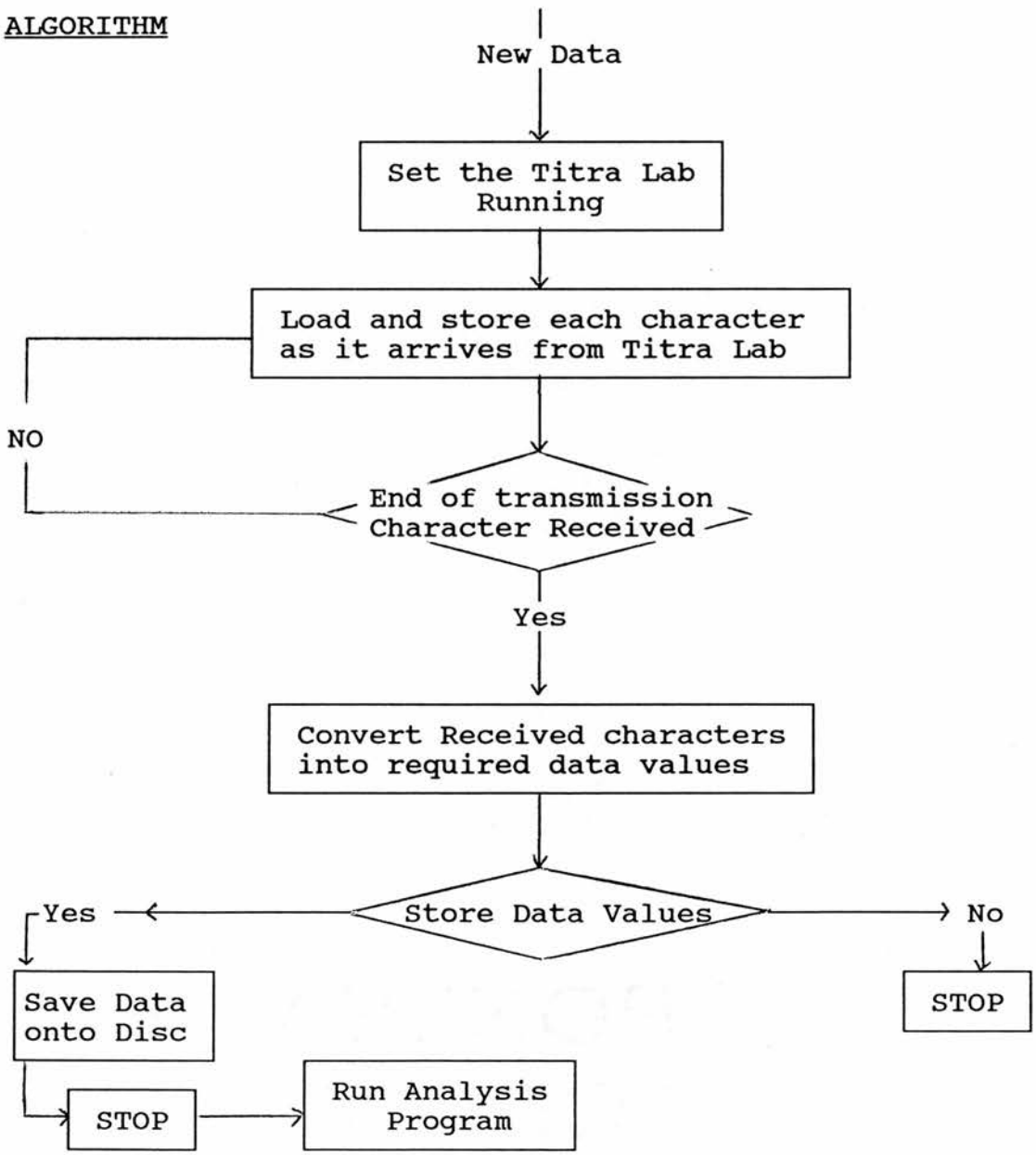

GOSUB 2000 is called. This routine finds out how many drives are being used and also gives the user the opportunity to insert a special data disc.

The user after returning from the GOSUB can also input a special file name. The data is then stored on the disc.

NOTE: IF OLD DATA had been selected the program would have jumped to line 5500 where upon the file name of the data could be loaded in. GOSUB 4500 calls the routine to display the results.

Analysis of Results

After the results have been down loaded to the Apple Computer and saved on disc, the Analysis program may be run. This program was already being used in the chemistry department and only required modification to take its input from the disc file created by the previous program.

In Operation

Both programs worked well together although the data capture program was slow. In an attempt to speed up the operation both programs were compiled. This allowed the BAUO rate to be increased to 1200. The analysis program also worked much more quickly. This was especially noticeable where there were large numbers of results.